Investigating the role of the extracellular matrix (ECM) on pluripotent stem cell differentiation towards retinal lineages

Majed Abdulsamad Felemban

A thesis submitted to Newcastle University for the degree of Doctor of Philosophy (PhD)

Institute of Genetic Medicine

November 2018

Abstract

Human pluripotent stem cells (hPSCs) can be differentiated into retinal organoids to study inherited and age related retinal dystrophies, to screen new drugs and to use them as replacement tissues. Published evidence suggests that retinal pigmented epithelium (RPE) and decellularised extracellular matrix (ECM) from RPE and neural retina contain several ECM molecules that are important for retinal development and synaptic formation between various cell types. To date, there has been limited detailed analysis of ECM components distribution during human retinal ontogenesis and the functional importance of several components is poorly understood. In this study, the expression of key ECM components in adult mouse and monkey retina, developing and adult human retina and hPSC-derived retinal organoids was studied. The results demonstrate that different ECM components have distinct distribution patterns throughout the adult retina of different species and a well conserved expression pattern between adult and developing human retinae. Furthermore, the expression of ECM components examined in retinal organoids was found to recapitulate at large human retinal development *in vivo*. The functional role of ECM on the differentiation of hPSC-derived retinal organoids was investigated either via blocking the action of two ECMs: cluster of differentiation 44 (CD44) and interphotoreceptor matrix proteoglycan 1 (IMPG1) in the organoids or via supplementation of culture media with RPE conditioned medium, decellularised ECM of neural retina or RPE. The findings indicate that IMPG1 and CD44 play an important role on photoreceptor development, their inner and outer segments, connecting cilia and IPM formation; with IMPG1 acting earlier and having more significant effect than CD44. All three supplements enhanced the light response in retinal organoids suggesting a beneficial effect of ECM on the development and function of hPSC-derived retinal organoids. Together, the study highlights a conserved expression of ECMs between human adult and developing retinae and retinal organoids as well as an important role for ECM in retinal development *in vitro*.

Acknowledgements

I would like to express my sincere gratitude to Professor Majlinda Lako and Dr. Birthe Hilgen for their supervision and continuous support during my PhD study. Without their advices, guidance and persistent help this thesis would not have been possible. I am deeply grateful to Professor Majlinda Lako and Professor Lyle Armstrong for giving me the opportunity to join their lab.

My sincere thanks also to Dr. Carla Mellough, Dr. Nicola Hunt, Dr. Joseph Collin, Mr. David Steel, Dr. Yuchun Ding, Professor Evelyne Sernagor, Dr. Helen Phillips, Dr. Gerrit Hilgen, Dr. Darin Zerti, Dr. Lisa Hodgson and the stem cell team for their continued assistance throughout my time at Newcastle University.

I would like to thank our previous lab members Dr. Dean Hallam, Dr. Minjin Jeong, Dr. Taty Kamarudin, Dr. Georgios Anyfantis, and all of my colleagues from the Institute of Genetic Medicine for their support.

I gratefully acknowledge the funding received towards my PhD from King Abdulaziz University, Saudi Arabia. Without their financial support it would not be possible to conduct this PhD study.

My deepest appreciation goes to my wife and son for supporting me spiritually throughout my PhD study.

Finally, this thesis is dedicated to the memory of my mother, Majed Felemban.

Table of Contents

List of Figures

List of Tables

List of Abbreviations

ABPs	Actin binding proteins
ACAN	Aggrecan
aCSF	Artificial cerebrospinal fluid
ADAMs	A disintegrin and metalloproteinase
Akt/PKB	Protein kinase B pathway
AMD	Age-related macular degeneration
bb	Basal body
BCAN	Brevican
bFGF	Basic fibroblastic growth factor
BrM	Bruch's membrane
BSA	Bovine serum albumin
CC	Connecting cilium
CD44	Cluster Of Differentiation 44
cGMP	Cyclic guanosine monophosphate
CM	conditioned medium
CNS	Central nervous tissue
Col4A1	Collagen IV
CSPGs	Chondroitin sulphates
CT	Threshold cycle
CTAB	Cetyltrimethylammonium bromide
DDR	Discoidin domain receptor
decel NR	Decellularised neural retina
decel RPE	Decellularised RPE
DMAB	Dimethylaminobenzaldehyde
Dok1	Docking protein 1
dRetina	Decellularised neural retina
dRPE	Decellularised RPE
DSPGs	Dermatan sulphates
ECM	Extracellular Matrix
EGF	Epidermal growth factor
Erk	Extracellular signal-regulated kinase pathway
ESCs	Embryonic stem cells
FAK	Focal adhesion kinase
FAs	Focal adhesions
FBS	Fetal Bovine Serum
FGF	Fibroblast growth factor
FN1	Fibronectin
GAGs	Glycosaminoglycans
GCL	Ganglion cell layer
GCs	Ganglion cells
GFOGER	Gly-Phe-Hyp-Gly-Glu-Arg
GFR	Growth factor receptors
HA	Hyaluronan/Hyaluronic acid
HDBR	Human Developmental Biology Resource
hESCs	Human embryonic stem cells
HGF	hepatocyte growth factor
hiPSCs	Human induced pluripotent stem cells

Hoe	Hoechst
hPSCs	Human pluripotent stem cells
HRP	Horseradish peroxidase
HSCs	Haematopoietic stem cells
HSPGs	Heparan sulphates
HTA	Human Tissue Authority
iC3b	Inactivated complement component 3b
ICAM	Intracellular-cell adhesion molecules
ICAP1	Integrin-cytoplasmic-domain-associated protein 1
ICM	Inner cell mas
IGF	Insulin growth factor
IHC	Immunohistochemistry
Ihh	Indian hedgehog
ILM	Inner limiting membrane
IMPG1	Interphotoreceptor Matrix Proteoglycan 1
IMPG2	Interphotoreceptor Matrix Proteoglycan 2
INL	Inner nuclear layer
INZ	Inner neuroblastic zone
IPL	Inner plexiform layer
IPM	Interphotoreceptor matrix
IRBP	Interphotoreceptor Retinoid Binding Protein
IS	Inner segment of photoreceptor cells
IVF	*in vitro* fertilisation
KSPGs	Keratan sulphates
MadCaM	Mucosal vascular addressin cell adhesion molecule
MAPK	Mitogen-activated protein kinase
MEA	Multielectrode array
MEM	Minimum Essential Medium
MIDAS	Metal-ion-dependant adhesion site
MMPs	Matrix metalloproteinases
MSCs	Mesenchymal stem cells
NCAN	Neurocan
NGF	Nerve growth factor
NR	Neural retina
OCT	Optimal cutting temperature
OLM	Outer limiting membrane
ONL	Outer nuclear layer
ONZ	Outer neuroblastic zone
OPL	Outer plexiform layer
OS	Outer segment of photoreceptor cells
Pan-HS	Pan Heparan Sulfate
PBS	Phosphate buffered saline
PCW	Weeks of post-conception
PDGF	Platelet-derived growth factor
PFA	Paraformaldehyde
PGs	Proteoglycans
PSCs	Pluripotent stem cells
PTB	Phosphotyrosine binding domain

qRT-PCR	Quantitative Reverse Transcription Polymerase Chain Reaction
RA	Retinoic Acid
RBP3	Retinol Binding Protein 3
Recov	Recoverin
RGD	Arg-Gly-Asp
RhoA/ROCK	Rho associated protein kinase pathway
ROM1	Retinal outer membrane-1
RPCs	Retinal progenitor cells
RPE	Retinal pigmented epithelium
RT	room temperature
SBL	Sustained broad blue light
SEM	Standard errors of all means
siRNA	Small interfering RNA
SLRPs	Small leucine-rich PGs
SPACR	Sialoprotein associated with cones and rods
SPACRCAN	Sialoproteoglycan associated with cones and rods
SPARC	Secreted Protein Acidic And Rich Cysteine
T3	tri-iodothyronine
TER	Trans-epithelial resistance
TGFβ	Transforming growth factor-β
TGF-β-LAP	Transforming growth factor beta- Latency associated peptide
TIMP	Tissue inhibitor of metalloproteinases
VCAM	Vascular- cell adhesion molecules
VCAN	Versican
VEGF	Vascular endothelial growth factor
WG	Weeks of gestations
WLP	White light pulses

Chapter 1

Chapter 1. Introduction

1.1. The extracellular matrix (ECM)

1.1.1. The ECM at a glance

The ECM is the non-cellular component of all tissues and organs. It consists of proteins, water and polysaccharides (Frantz *et al.*, 2010) and each tissue has a distinctive ECM composition (Frantz *et al.*, 2010). The ECM acts as a structural support that facilities cell adhesion via integrins and other adhesion molecules which mediate various signalling pathways such as the serine/threonine kinase pathway known as protein kinase B (Akt/PKB) and the extracellular signal-regulated kinase (Erk) pathway (Streuli, 2009; Moreno-Layseca and Streuli, 2014) that are essential for cell proliferation (Streuli, 2009; Fournier *et al.*, 2012; Moreno-Layseca and Streuli, 2014). More than 150 components have been recognised to interact at integrins adhesion sites, forming an adhesion complex identified as "adhesome" (Harburger and Calderwood, 2009; Moreno-Layseca and Streuli, 2014). Adhesion complex molecules involve cytoskeletal components, adaptor proteins and enzymes that regulate cell behaviour including cell migration, ECM expression, differentiation, apoptosis and proliferation (Humphries *et al.*, 2006; Berrier and Yamada, 2007; Leitinger and Hohenester, 2007; Harburger and Calderwood, 2009; Streuli, 2009; Frantz *et al.*, 2010; Schmidt and Friedl, 2010; Xian *et al.*, 2010; Moreno-Layseca and Streuli, 2014). ECM can regulate cell behaviour through harbouring growth factors or through ECM-cell interaction that mediate signalling pathways and alter the cellular response to growth factors (Streuli, 1999). The ECM is dynamic and changes throughout development (Hausman, 2007). It provides biochemical and biomechanical cues that are essential for tissue morphogenesis (Frantz *et al.*, 2010).

Many reports indicated the important role of different ECM components in animal models (**Table 1-1**). For example, mutation in aggrecan gene (*ACAN*, 7 bp deletion in exon 5) resulted in severely truncated aggrecan molecule which was a major cause of cartilage matrix deficiency in mice suggesting an important role of aggrecan in cartilage formation (Watanabe *et al.*, 1994). Another example, transgene insertion mutation of versican gene inhibited the growth of the heart right ventricle (first segment) in heart defect mouse suggesting important role of versican in the development of the mouse heart (Mjaatvedt *et al.*, 1998). Similarly, disrupting the *Has2* gene, a major source for hyaluronic acid, resulted in sever cardiac defect and death of embryos in $Has2^{-/-}$ mice suggesting that hyaluronic acid plays important role in the migration ant transformation of endothelial-cell in AV canal morphogenesis in mouse

(Camenisch *et al.*, 2000). In addition, mutations in the ECM genes were reported in several human diseases (**Table 1-2**). For example, A splice mutation in the Versican gene (*VCAN*, heterozygous c.9265 + 1G > A nucleotide change in intron 8) was reported in Wagner syndrome patients with retinal detachment (Rothschild *et al.*, 2013). Interphotoreceptor matrix proteoglycan 1 (*IMPG1*) gene mutations were reported in Vitelliform macular dystrophies (characterised by the accumulation of yellow deposits of lipofuscin pigment at the centre of the macula) leading to impaired metabolism of the interphotoreceptor matrix (IPM) and the accumulation of Vitelliform deposits in the sub-retinal space (Manes *et al.*, 2013), whilst mutations in interphotoreceptor matrix proteoglycan 2 gene (*IMPG2*) cause progressive degeneration of the photoreceptors, leading to autosomal dominant retinitis pigmentosa (an inherited retinal dystrophy characterised by progressive degeneration of the photoreceptors (Bandah-Rozenfeld *et al.*, 2010; Manes *et al.*, 2013).

Proteoglycans (PGs) and glycoproteins are the main macromolecules of the ECM (Frantz *et al.*, 2010; Kwan, 2014; Reinhard *et al.*, 2015). There are two main types of ECM that differ according to their location and arrangement: the basement membrane, which separates the epithelium from the surrounding stroma; and the interstitial connective tissue matrix, which surround cells and offers structural scaffolding for tissues (Bonnans *et al.*, 2014).

Table 1-1: Role of different ECM components in animal models

ECM	Phenotypes	References
Aggrecan	Mutation in Aggrecan gene (*ACAN*, 7 bp deletion in exon 5) resulted in severely truncated aggrecan molecule which was a major cause of cartilage matrix deficiency in mice.	(Watanabe *et al.*, 1994; Rozario and DeSimone, 2010)
Brevican	Brevican-null mice displayed alterations in the expression of neurocan and less prominent formation of Perineuronal nets surrounding neurons than in wild-type mice brain suggesting structural and functional roles of Brevican in the development of mouse brain.	(Brakebusch *et al.*, 2002; Rozario and DeSimone, 2010)
Collagen IV	Collagen IV-null mice displayed structural deficiencies (discontinuities or ruptures) in the basement membranes suggesting a fundamental role for collagen IV in for the maintenance of integrity and function of basement membranes in mice.	(Poschl *et al.*, 2004; Rozario and DeSimone, 2010)
Fibronectin	Fibronectin-mutant caused embryonic (E14.5) abnormalities such as deformed heart and embryonic vessels which caused lethality in mice suggesting that fibronectin is required for embryogenesis in mice.	(George *et al.*, 1993; Rozario and DeSimone, 2010)

Table 1-1: Role of different ECM components in animal models, continued.

ECM	Phenotypes	References
Hyaluronan	Hyaluronan synthases, *Has2*$^{-/-}$ mouse embryos lack the characteristic transformation of cardiac endothelial cells into mesenchyme suggesting important role of Hyaluronan in the migration ant transformation of endothelial-cell in AV canal morphogenesis in mouse.	(Camenisch *et al.*, 2000)
Laminin	Disruption of laminin *lambc1* in zebrafish caused the expulsion of retinal cells through the retinal pigment epithelium RPE into the adjacent forebrain and lens and corneal malformations suggesting important role for *lambc1* in eye development in zebrafish.	(Gross *et al.*, 2005; Rozario and DeSimone, 2010)
Neurocan	Mild defects in synaptic plasticity in Neurocan-deficient mice suggesting important function of Neurocan subtle function in the development of mice brain.	(Zhou *et al.*, 2001; Rozario and DeSimone, 2010)
Nidogen	Nidogen-1 knockout mouse displayed interruptions in the inner limiting membrane that result in small retinal ectopias and small holes in the optic nerve suggesting important function for Nidogen-1 in the development of basement membranes.	(May, 2012)
Versican	Transgene insertion mutation of versican gene inhibited the growth of right ventricle of the heart in heart defect mouse suggesting important role of versican in the development of the mouse heart.	(Mjaatvedt *et al.*, 1998; Rozario and DeSimone, 2010)

Table 1-2: Examples of mutations in ECM components reported in human diseases.

ECM	Human Disease	Reference
Aggrecan	Spondyloepiphyseal dysplasia, Kimberley type	(Bateman *et al.*, 2009)
Collagen IV	Axenfeld-Rieger syndrome	(Hausman, 2007)
Collagen XVIII	Knobloch syndrome type I	(Hausman, 2007; Sarrazin *et al.*, 2011)
Fibrillin-1	Marfan's syndrome	(Hausman, 2007)
Perlecan	Schwartz–Jampel syndrome (skeletal dysplasia)	(Sarrazin *et al.*, 2011)
Versican	Wagner syndrome	(Kloeckener-Gruissem *et al.*, 2013)
SPACR (IMPG1)	Vitelliform Macular Dystrophies	(Manes *et al.*, 2013)
SPACRCAN (IMPG2)	Retinitis pigmentosa	(Bandah-Rozenfeld *et al.*, 2010)

1.1.2. Proteoglycans (PGs)

PGs include both ECM molecules and cell-surface PGs such as syndecans and glypicans (**Figure 1-1**) (Schaefer and Schaefer, 2010). PGs consist of one core protein and one or several glycosaminoglycans (GAG) which are long, negatively charged, linear chains of disaccharide repeats with the exception of hyaluronan (HA) which is only polysaccharide and lacks a protein core (Hausman, 2007; Frantz *et al.*, 2010; Clark *et al.*, 2011; Keenan *et al.*, 2012; Mouw *et al.*, 2014; Reinhard *et al.*, 2015).

Based on their sulphated and non-sulphated GAG chains, PGs are classified into heparan sulphates (HSPGs), chondroitin sulphates (CSPGs), dermatan sulphates (DSPGs), keratan sulphates (KSPGs) and HA (Clark *et al.*, 2011; Reinhard *et al.*, 2015). The GAG chains of HSPGs, CSPGs and DSPGs are composed of repeated region of disaccharide that contain acetylated amino sugar moieties (N-acetyl-glucosamine or N-acetylgalactosamine) and mostly uronic acid (L-iduronic acid or D-glucoronic acid) (Schaefer and Schaefer, 2010). HSPGs, CSPGs and DSPGs sulphated chains are connected to their core proteins via serine residues (Schaefer and Schaefer, 2010). In contrast, the GAG chains of KSPGs are made of repeating disaccharide containing galactose (−4 N-acetyl-glucosamine-β1,3-galactose-β1) and have a different linkage regions from other GAGs because their chains can be synthesised on serine/threonine *O*-linked oligosaccharides and on *N*-linked oligosaccharides (Schaefer and Schaefer, 2010). Alternatively, based on their location and binding, PGs can be classified into three main families: 1) small leucine-rich PGs (SLRPs) such as decorin), 2) modular PGs that can be divided into hyalectans (hyaluronan-binding PGs including versican, aggrecan, neurocan, and brevican) and non-hyaluronan-binding PGs of the basement membrane such as agrin and perlecan (both are HSPGs) (Bix and Iozzo, 2008; Schaefer and Schaefer, 2010).

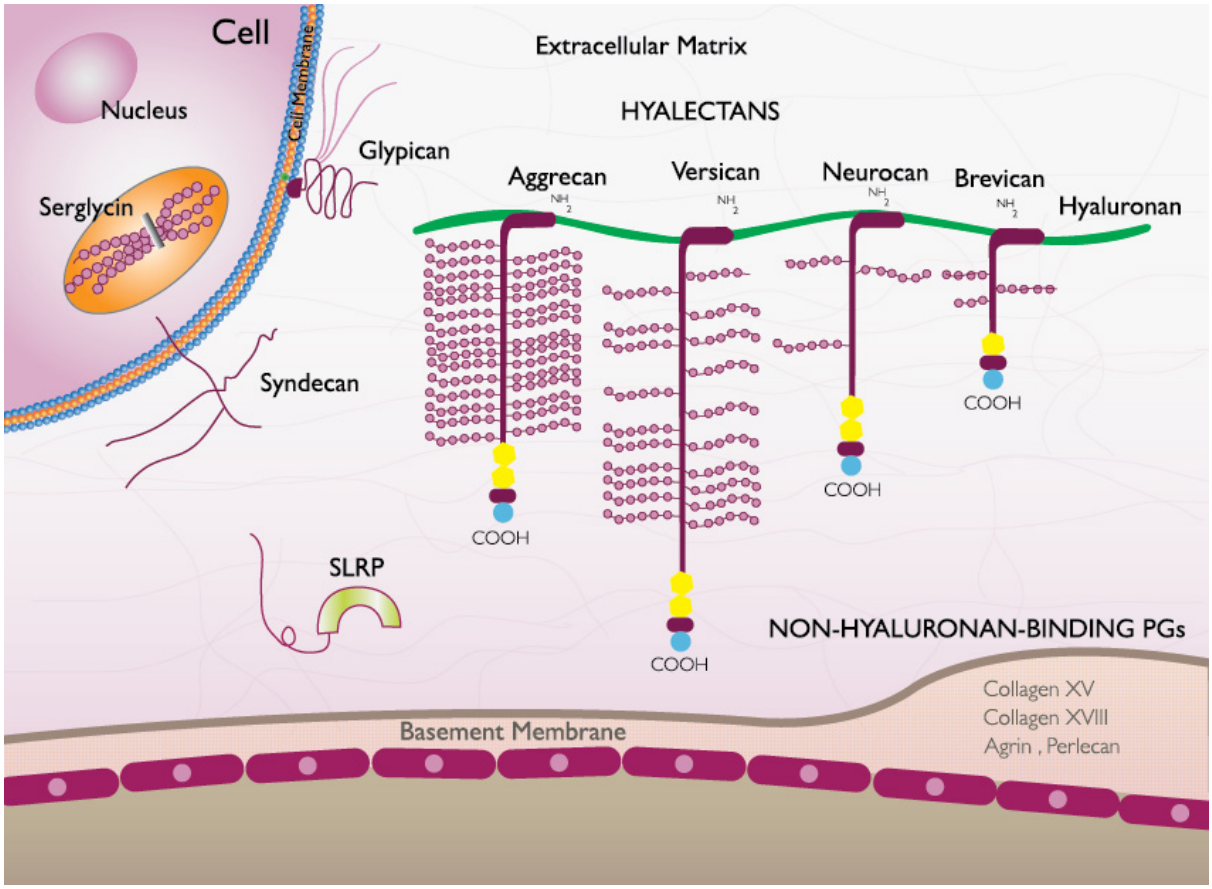

Figure 1-1: Main classification of PGs (adapted from reference (Schaefer and Schaefer, 2010)).
Based on their location and binding, PGs can be classified into three families including SLRPs, modular PGs (hyaluronan- and non-hyaluronan-binding PGs) and cell-surface PGs (Schaefer and Schaefer, 2010).

1.1.3. Glycoproteins

ECM glycoproteins are fibrous proteins that have structural and adhesive functions and include collagens, elastin, tenascins, fibronectins, laminins and entactin (nidogen) (Hausman, 2007; Frantz *et al.*, 2010; Rozario and DeSimone, 2010). ECM glycoproteins contain less sugar residues in the heterosaccharide than PGs (Margolis and Margolis, 1983). Glycoproteins are involved in ECM assembly and act as reservoir of growth factors (Bonnans *et al.*, 2014). For example, the amount of collagen IV in the basement membrane modulates the assembly of fibronectin (FN) via confining cell-FN interaction (Groulx *et al.*, 2011). Collagens are the most abundant proteins in the interstitial ECM (Rozario and DeSimone, 2010) and comprise up to 30% of the total protein mass in animals (Frantz *et al.*, 2010). Collagens form the structural part of the ECM and provide tensile strength to a tissue (Frantz *et al.*, 2010; Rozario and DeSimone, 2010). There are 28 discovered collagens resulting from 49 gene products of collagen α-chain (Gordon and Hahn, 2010). Collagens are mainly

classified into fibril and non-fibril forms that can be arranged into sheets or reticular networks (Rozario and DeSimone, 2010). Elastin fibres allow recoil to tissue that undergo frequent stretch (Frantz *et al.*, 2010) and are mainly covered by fibrillins (glycoprotein microfibrils) that are important for elastin fiber integrity (Wise and Weiss, 2009). FN is a fibrous glycoprotein that mediates cell attachment and function (Frantz *et al.*, 2010). It can stretch various times over its length via cellular traction forces and act as mechano-regulator (Smith *et al.*, 2007; Frantz *et al.*, 2010). Moreover, FN is essential for cell migration during development such as directing the migration of myocardial precursor in zebrafish heart organogenesis (Matsui *et al.*, 2007).

1.1.4. Cellular receptors for ECM

The major receptors for the ECM are the integrins (Hynes and Naba, 2012) but other ECM receptors also exist such as dystroglycan (that binds to laminin, agrin, and perlecan in the basement membrane), CD44 (which binds to hyaluronan), the discoidin domain receptor (DDR) and tyrosine-kinases which are the receptors for collagen (Hynes and Naba, 2012). These ECM receptors act as transmembrane link to the cytoskeleton and to signal transduction pathways (Hynes and Naba, 2012). Integrins regulate the extracellular affinity of other receptors (Hynes and Naba, 2012).

Integrins are widely expressed transmembrane glycoprotein receptors that facilitate cell-cell adhesion and cell-ECM adhesion (Harburger and Calderwood, 2009; Barczyk *et al.*, 2010; Moreno-Layseca and Streuli, 2014; Walters and Gentleman, 2015). Different subunits of integrins are expressed in several layers of the adult human retina (**Table 1-3**) (Brem *et al.*, 1994), and in embryonic and adult stem cells (**Table 1-4**) (Prowse *et al.*, 2011). Integrin heterodimers consist of non-covalently associated α and β subunits (Harburger and Calderwood, 2009; Barczyk *et al.*, 2010).

Table 1-3: Expression of integrins in adult retina of human eyes (Brem *et al.*, 1994).

Integrins	RPE	Rods	Cones	OLM	ONL	OPL	INL	IPL	GCL	NFL	ILM
β1	-	-	-	-	-	-	-	-	-	-	+
β2	+/-	+	+	+	+	+	+/++	+	+	+	+
β3	-	-	-	-	-	-	-	-	-	+/-	-
α2	-	+	+	-	+/++	+	+/++	+	+/++	+	+/-
α3	-	-	-	+/-	+	+	+	+	+	+	+/-
α4	+	+	+	+	+	+	+	+	+	+	-
α5	-	+/-	+/-	+	+/-	+/-	+	+/-	+/-	-	-
α6	-	-	-	-	-	-	-	-	-	-	-
αv	-	-	-	-	-	-	-	-	-	-	-

RPE = retinal pigment epithelial cells; OLM = outer limiting membrane; ONL = outer nuclear layer; OPL = outer plexiform layer; INL = inner nuclear layer; IPL = inner plexiform layer; GCL = ganglion cell layer; NFL = nerve fiber layer; ILM = inner limiting membrane.

Table 1-4: The expression of integrins in embryonic and adult stem cells (Prowse *et al.*, 2011).

Cell Type	Integrin subunit																							
	α 1	**α 2**	**α 3**	**α 4**	**α 5**	**α V**	**α 6**	**α 7**	**α 8**	**α 9**	**α 10**	**α 11**	**α M**	**α X**	**α L**	**α E**	**β 1**	**β 2**	**β 3**	**β 4**	**β 5**	**β 6**	**β 7**	**β 8**
MSC	+/-	+/-	+	+/-	+	+/-	+/-	-			+/-	+	-	+	+	-	+	+/-	+/-	+	+/-	+/-	+	+
hESC	+/-	+/-	+	-	+	+	+	+	-	-	-	+				+	+	+	+/-	-	+	-		
HSC	-	-	-	+	+		+	+	-	+	-	-					+	+						
NSC	-	+/-	+	-	+/-		+	+									+			-				

MSC; mesenchymal stem cell. hESC; human embryonic stem cells. HSC; haematopoietic stem cell or CD34+ haematopoietic progenitor. NSC; neural stem cell. "+" shows an identified integrin (Prowse *et al.*, 2011). "-" shows the integrin subunit was investigated but not detected and "+/-" shows positive and negative testing for the subunit in different publications (Prowse *et al.*, 2011). No information has been found for the remaining stem cells and integrin subunit pairs (Prowse *et al.*, 2011).

In human, there are 18 α and 8 β subunits that can assemble into 24 possible confirmations (**Table 1-5**) (Johnson *et al.*, 2009; Barczyk *et al.*, 2010; Walters and Gentleman, 2015). Each subunit contains a large extracellular domain and short cytoplasmic domain (50aa sequence, except for β4 which has around 1000aa sequence in its cytoplasmic domain), creating a typical type I transmembrane subunit (Hynes, 2002; Prowse *et al.*, 2011). On the extracellular side, integrins bind to various ECM components by recognising specific amino acid sequence such as Arg-Gly-Asp (RGD) in fibronectin, vitronectin and fibrinogen; Gly-Phe-Hyp-Gly-Glu-Arg (GFOGER) in collagens; and Leu-Asp-Val (LDV) in alternatively spliced region of fibronectin (Barczyk *et al.*, 2010; Walters and Gentleman, 2015). Moreover, integrins can bind to surface receptors on other cells by direct interaction with membrane bound proteins including intracellular- or vascular- cell adhesion molecules (ICAM and VCAM), or through linker molecules such as von Willebrand factor (**Figure 1-2**) (Prowse *et al.*, 2011). Inside the cell, integrins attach to the cytoskeleton via several linker proteins (Walters and Gentleman, 2015). As a result, integrins act as mechanosensors and bidirectional signalling receptors that transmit environmental information into the cell (outside-in signalling) and intracellular information to the ECM (inside-out signalling) (Walters and Gentleman, 2015).

Table 1-5: Integrins and their ligands

Integrin	Ligands	Recognition Sequence	References
α1β1	Collagens, semaphoring 7A	GFOGER	(Johnson *et al.*, 2009; Barczyk *et al.*, 2010)
α2β1	Collagens, tenascin C, E-cadherin, endorepellin	GFOGER	
α3β1	Laminins		
α4β1	Fibronectin, VCAM		
α5β1	Fibronectin	RGD	
α6β1	Laminins, ADAMs		
α7β1	Laminins		
α8β1	Fibronectin, vitronectin, tenascin C,	RGD	
α9β1	Tenascin C, osteopontin, ADAMs, factor XIII, VCAM, VEGF-C, VEGF-D		
α10β1	Collagens	GFOGER	
α11β1	Collagens	GFOGER	
αLβ2	ICAM		
αMβ2	ICAM, VCAM, iC3b, factor X, fibrinogen		
αXβ2	Fibrinogen, plasminogen, heparin, iC3b		
αDβ2	ICAM, VCAM		
αIIBβ3	Fibrinogen, fibronectin, vitronectin	RGD	
α6β4	Laminins		
αvβ1	Fibronectin, vitronectin	RGD	
αvβ3	Fibrinogen, fibronectin, vitronectin, tenascin C, tumstatin, MMP-2	RGD	
αvβ5	Vitronectin	RGD	
αvβ6	Fibronectin, TGF-β-LAP	RGD	
αvβ8	Vitronectin, TGF-β-LAP	RGD	
αEβ7	E-cadherin		
α4 β7	Fibronectin, VCAM, MadCaM		

ADAM= a disintegrin and metalloproteinase; **GFOGER**= Gly-Phe-Hyp-Gly-Glu-Arg; **iC3b**= inactivated complement component 3b; **ICAM**= intercellular adhesion molecule; **MadCaM**= mucosal vascular addressin cell adhesion molecule; **MMP-2**= matrix metalloproteinase-2; **RGD**= Arg-Gly-Asp; **TGF-β-LAP**= transforming growth factor beta- Latency associated peptide; **VCAM**= vascular cell adhesion molecule; **VEGF**= vascular endothelial growth factor.

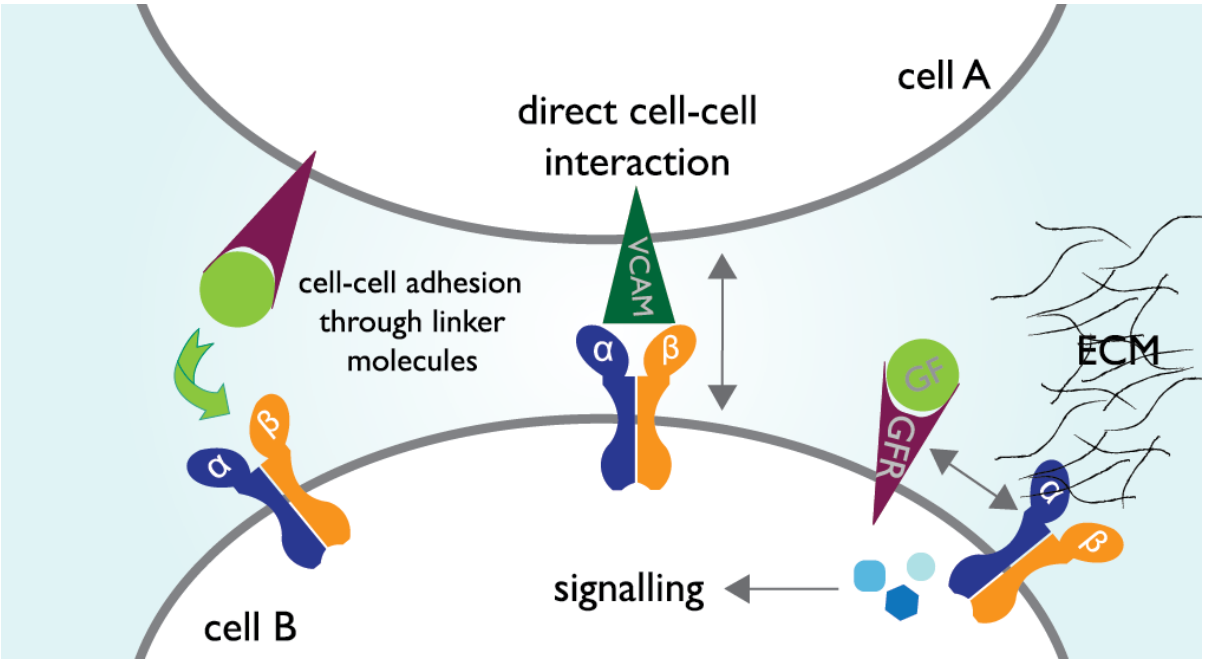

Figure 1-2: Integrins functions (adapted from reference (Prowse *et al.*, 2011)).
A diagram of main integrins interactions in Cell-ECM adhesion, Cell-Cell adhesion and integrins-growth factor cross-talk. **ECM**, extracellular matrix; **GF**, growth factor; **GFR**, growth factor receptor; **VCAM**, vascular cell adhesion molecule.

1.1.5. Integrin activation and inside-out signalling

Integrins exist in a compact bent conformation that represents the inactive form of integrins (Barczyk *et al.*, 2010). Inside-out signalling is initiated by the binding of talin to integrins β cytoplasmic tail via phosphotyrosine binding domain (PTB) (Ginsberg *et al.*, 2005). Talin is one of the actin binding proteins that connect integrins to the actin cytoskeleton (Ginsberg *et al.*, 2005). The head domain of talin disrupts the salt bridge between the α and β cytoplasmic tails causing their separation and the activation of integrins (Ginsberg *et al.*, 2005). Integrin activation can be inhibited by binding of integrins to proteins containing (PTB)-domain such as docking protein 1 (Dok1) and integrin-cytoplasmic-domain-associated protein 1 (ICAP1) that compete with talin binding to β integrin and impair activation (Harburger and Calderwood, 2009).

1.1.6. Outside-in signalling (focal adhesion formation)

On the extracellular side, the binding of the integrin receptors to the ECM ligands initiates cell-ECM interaction (Walters and Gentleman, 2015). The interaction of integrins receptors with the ECM mediate outside-in signalling through the formation of integrin clusters known as focal adhesion sites (Prowse *et al.*, 2011). Several types of adhesion structures are formed due to cell-ECM interaction including focal complexes, focal adhesions and fibrillar adhesions (Berrier and Yamada, 2007). Focal complexes are small and transient

adhesion structures that are formed during early cell attachment to the matrix (Berrier and Yamada, 2007). Focal adhesions (FAs) are large elongated structures in which binding of clustered integrins to the ECM fibrils occurs on the outside of the cell and connect on the inside to the actin cytoskeleton *via* actin binding proteins (ABPs) such as tensin, paxillin, vinculin, talin and zyxin (**Figure 1-3**) (Olberding *et al.*, 2010; Schwartz, 2010; Ciobanasu *et al.*, 2013). If the focal complexes stabilised they will form focal adhesions that can convert into fibrillar adhesion (Berrier and Yamada, 2007).

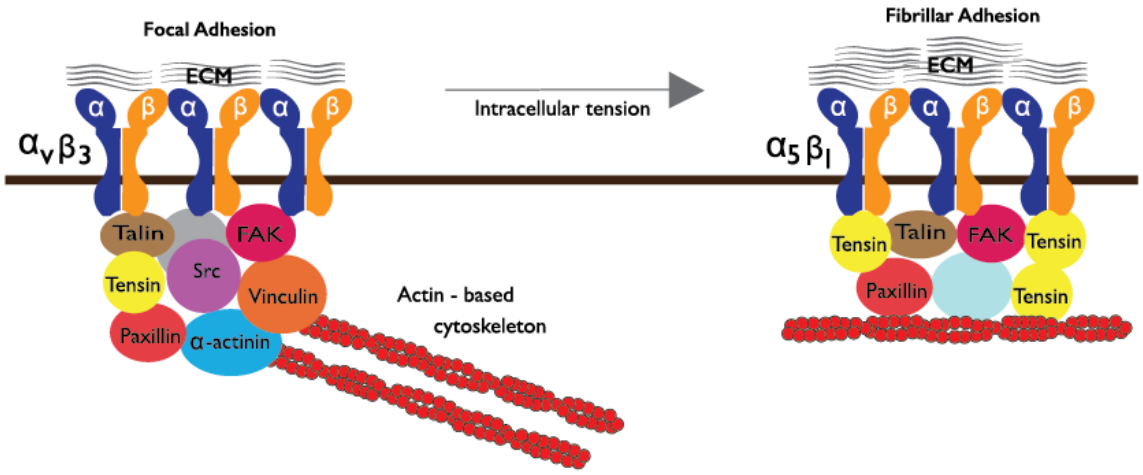

Figure 1-3: Comparison between focal and fibrillar adhesions, adapted from reference (Berrier and Yamada, 2007).

Signalling proteins must be recruited to regulate adhesion-dependant processes due to the lack of intrinsic enzymatic activity in the integrins receptors (Berrier and Yamada, 2007). Three main classes of proteins aggregate to the cell-ECM adhesion: (1) integrin-binding proteins that bind directly to integrin cytoplasmic domains such as talin; (2) adaptors proteins lacking enzymatic activity such as vinculin, paxillin and α-actinin; (3) enzymes that effect integrins downstream signalling and regulate cytoskeletal remodelling, cell migration, survival and gene regulation such as tyrosine kinases, serine/threonine kinases and tyrosine phosphatases (Berrier and Yamada, 2007; Prowse *et al.*, 2011).

1.1.7. Focal adhesion - function

FAs sense and respond to variations in the components and properties of the ECM and in force generated by different actin network and adapt cell-matrix adhesion via activation of several pathways that control cellular behaviours (**Figure 1-4**) such as actomyosin-integrin-ABP-ECM pathway (Ciobanasu *et al.*, 2013), extracellular signal-related-kinase/ mitogen-activated protein kinase (ERK/MAPK) pathway and Rho associated protein kinase pathway

(RhoA/ROCK) (Walters and Gentleman, 2015). ERK/MAPK pathway plays important role in cell growth control via connecting the activation of growth factor receptors to the machinery of cell-cycle (Huang and Ingber, 1999). The activation of ERK/MAPK causes the induction of cyclin D1 and triggers a series of nuclear events that leads the cell to pass through the late-G1 restriction point and enter the S phase (Huang and Ingber, 1999). Rho/ROCK pathway is important for the organisation of the actin cytoskeleton and promotes specialised actin structures (stress fibres) that are essential for cell polarity and migration (Brakebusch and Fassler, 2003).

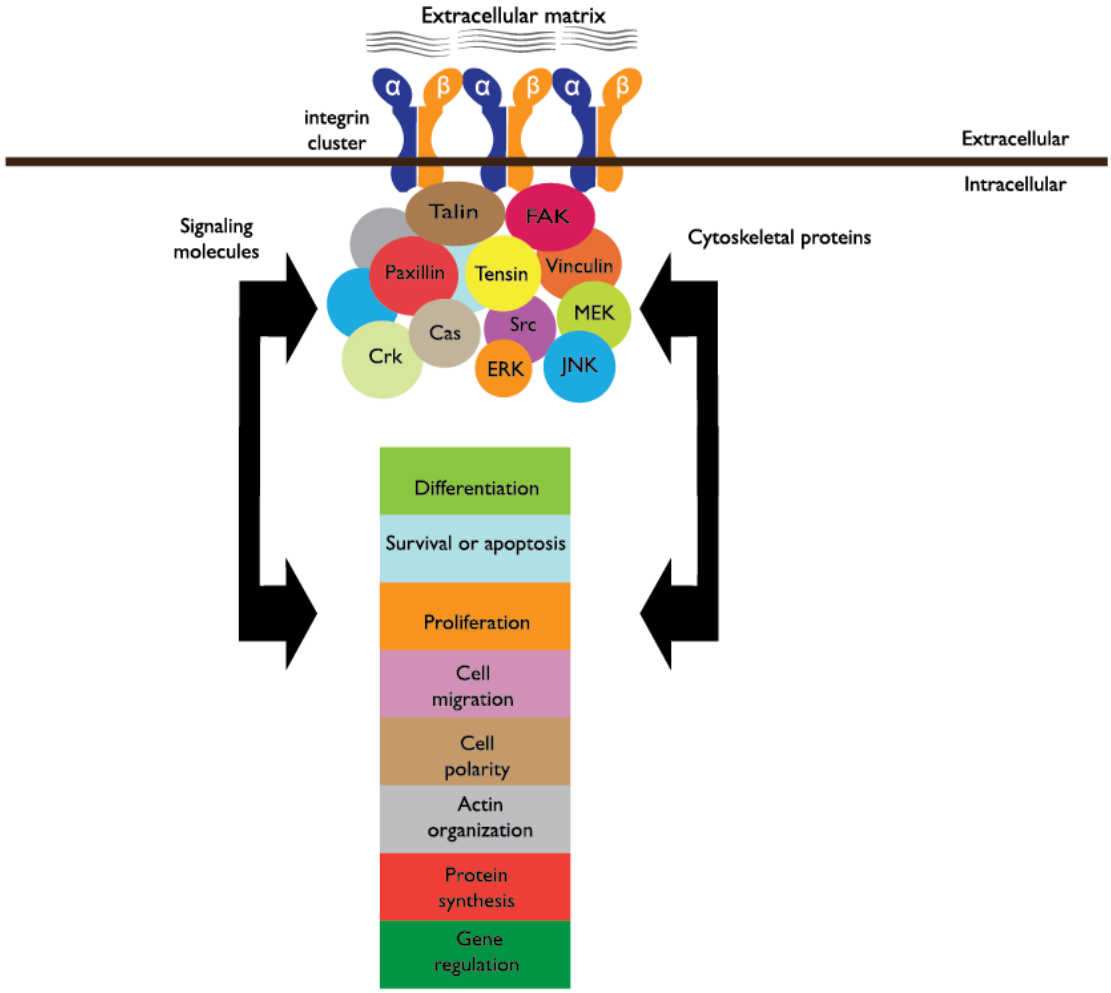

Figure 1-4: A diagram of integrin-mediated cell-ECM adhesion, adapted from reference (Berrier and Yamada, 2007).
Cell-ECM adhesion causes integrin clusters and aggregation of several types of proteins that control various cellular behaviors (Berrier and Yamada, 2007).

1.1.8. ECM remodelling

The ECM is a dynamic structure that constantly changes its composition (remodelled) to control tissue homeostasis (Reinhard *et al.*, 2015). During development, ECM remodelling is an effective mechanism to regulate various cellular functions such as cell shape,

proliferation and migration that are important for tissue morphogenesis (Bonnans *et al.*, 2014). The main process during ECM remodelling is the cleavage of ECM components, which regulates ECM abundance, composition and structure as well as releasing biologically active molecules such as growth factors including fibroblast growth factor (FGF), epidermal growth factor (EGF) and different signalling molecules such as WNTs, amphiregulin and transforming growth factor-β (TGFβ) (Bonnans *et al.*, 2014). Several families of proteases are involved in ECM cleavage including matrix metalloproteinases (MMPs) and adamalysins (**Table 1-6**) (Bonnans *et al.*, 2014).

Around 23 human MMPs have been discovered and these are the main enzymes that degrade ECM (Bonnans *et al.*, 2014). All MMPs share a self-inhibitory prodomain at the amino terminus, and a catalytic domain, flexible hinge motif and hemopexin domain at the carboxyl terminus (Lu *et al.*, 2011). Most of the MMPs contain the basic three-domain structure with certain variations in some enzymes such as MMP-2 and MMP-9 contain fibronectin type II repeats found in the catalytic domain to mediate collagen binding (Lu *et al.*, 2011). Most of the MMPs are secreted molecules except the membrane-type MMPs (MT-MMPs), MMP-14, -15, -23, and -24 that have a transmembrane domain and a short cytoplasmic tail, while MMP-17 and -25 have glycosylphosphatidylinositol (GPI) linkages (Lu *et al.*, 2011). MMPs enzymatic activity is low under normal states but increases during the processes of repair or remodelling as well as in inflamed or diseased tissues (Bonnans *et al.*, 2014). They are activated by proteolytic cleavage (by serine proteases or other MMPs) or via the modification of the thiol group by oxidation (Bonnans *et al.*, 2014). MMPs proteolytic activity on ECM plays crucial roles in organogenesis and branching morphogenesis (Bonnans *et al.*, 2014). MMPs target a broad spectrum of ECM molecules such as MMP-1 targeting collagen III and entactin, whereas MMP-3 and MMP-10 target aggrecan, fibronectin and laminin (Lu *et al.*, 2011). Meprins are part of the astacin family of MMPs and consist of two subunits (α and β) (Bonnans *et al.*, 2014). They can cleave ECM proteins such as collagen IV, nidogen, fibronectin and laminin, and indirectly control ECM remodelling by activating other MMPs (Bonnans *et al.*, 2014). For instance, the activation of MMP9 can be accelerated by meprin-β cleaving ADAM10, and by meprin-α and meprin-β promoting the cleavage of pro-MMP9 by MMP3 (Bonnans *et al.*, 2014). In addition to ECM cleavage, MMPs play important role in cell signalling by proteolytically activating cytokines such as transforming growth factor-*β* (TGF-*β*) by MMP-9 (Sivak and Fini, 2002). Several MMPs have been reported in human vitreous and interphotoreceptor matrix including MMPs 1, 2, 3 and 9 (Sivak and Fini, 2002). Up-regulation of MMPs has been observed with a number of diseases such as age-

related macular degeneration and proliferative diabetic retinopathy (Sivak and Fini, 2002). However, up-regulation of MMPs has also a positive impact on the cell behaviour. For example, up-regulation of MMP-2 has also a beneficiary effect on inhibiting neurocan, an extracellular matrix component which increases the cell mortality and promotes cells migration and integration of retinal progenitor cells into host retina (Jiang *et al.*, 2010).

Table 1-6: Different proteases and their ECM substrates (Lu *et al.*, 2011; Bonnans *et al.*, 2014).

Enzyme	ECM and other substrates
MMP7	Collagen IV, gelatin, fibronectin, laminin, elastin, aggrecan, tenascin, decorin
MMP26	Collagen IV, fibrinogen, fibronectin, gelatin, pro-MMP9
MMP1	Collagens, entactin, aggrecan, entactin, tenascin, perlecan, ovostatin, MMP2, MMP9, pro-MMP9
MMP3	Collagens, gelatin, aggrecan, laminin, elastin, casein, osteonectin, fibronectin, ovostatin, entactin, plasminogen, pro-MMP9
MMP8	Collagens, fibronectin, aggrecan
MMP10	Collagens, gelatin, casein, elastin, fibronectin
MMP12	Collagen IV, elastin, gelatin, casein, fibronectin, vitronectin, laminin, entactin, fibrinogen
MMP13	Collagens, tenascin, plasminogen, aggrecan, fibronectin, osteonectin, MMP9
MMP19	Collagen I and IV, gelatin, fibronectin, laminin
MMP20	Amelogenin
MMP11	Collagens, laminin, elastin, fibronectin, casein, aggrecan
MMP21	N.D.
MMP28	Casein
MMP2	Collagens (IV, V, VII, X), gelatin, elastin, fibronectin
MMP9	Collagens (IV, V, VII, X), gelatin, elastin, fibronectin
MMP17	Gelatin, fibrinogen, pro-MMP2
MMP25	Collagen IV, gelatin, fibronectin, pro-MMP2, pro-MMPp
MMP14	Collagens, gelatin, fibronectin, laminin, vibronectin, entactin,pro-MMP2
MMP15	Fibronectin, gelatin, vibronectin, entactin, laminin, pro-MMP2
MMP16	Collagen III, gelatin, casein, fibronectin, pro-MMP2
MMP24	Fibronectin, pro-MMP2, fibrin, gelatin
MMP23A MMP23B	Gelatin
ADAM9	Fibronectin, gelatin
ADAM12	Collagen IV, gelatin, fibronectin
ADAM15	Collagen IV, gelatin
ADAM10	Collagen IV, gelatin, meprin β
ADAMTs	Aggrecan, versican, brevican, decorin, fibronectin, pro-collagens
Meprin α	Collagen IV, nidogen 1, fibronectin, laminin 111, laminin 332, pro-collagen I, pro-collagen III
Meprin β	Collagen IV, nidogen 1, fibronectin, laminin 111, laminin 332, pro-collagen I, pro-collagen III, pro ADAM10

Adamalysins family include ADAMs (a disintegrin and metalloproteinases) and ADAMs with a thrombospondin motif (ADAMTS) (Bonnans *et al.*, 2014). ADAMs have a disintegrin domain, a cysteine-rich region and a series of epidermal growth factor (EGF)-like repeats (Lu *et al.*, 2011; Khokha *et al.*, 2013; Bonnans *et al.*, 2014). They cleave transmembrane ectodomains that are adjacent to the cell membrane which release cytokines, growth factors, receptors and adhesion molecules (Bonnans *et al.*, 2014). ADAMs bind integrins through the disintegrin domains that mediate cell-ECM interactions (Lu *et al.*, 2011), and interact with HS through Cys-rich domains (Bonnans *et al.*, 2014). Unlike ADAMs, ADAMTS are secreted proteinases that contain thrombospondin type-I repeats in their carboxyl terminus (Lu *et al.*, 2011; Bonnans *et al.*, 2014). ADAMTS cleave PGs, collagens and von Willebrand factor (Bonnans *et al.*, 2014).

There are other enzymes that contribute in ECM modeling such as serine protease plasmin that degrade fibrin, fibrinogen and laminin (Lu *et al.*, 2011; Bonnans *et al.*, 2014). In addition, heparanases and sulphatases can target ECM PGs and modulate their properties (Lu *et al.*, 2011; Bonnans *et al.*, 2014). Sulphatase 1 and 2 are secreted endosulphatases that remove 6-*O*-sulphate from HS and alter HS binding to several cytokines and growth factors including FGF, vascular endothelial growth factor (VEGF) and Wnt (Lu *et al.*, 2011; Bonnans *et al.*, 2014). Heparanases present in several developmental processes and alter the structure of ECM by cleaving HS that release HS-bound growth factors, cytokines and bioactive saccharide fragments (Lu *et al.*, 2011; Bonnans *et al.*, 2014).

Firm regulation of ECM proteolysis is required to avoid excessive and deleterious tissue degradation (Bonnans *et al.*, 2014). The tissue inhibitor of metalloproteinases (TIMP) family is composed of four members (TIMP1-TIMP4) that reversibly inhibit the activities of MMPs, ADAMs and ADAMs except meprins (Bonnans *et al.*, 2014). TIMPs contain two domains: an amino-terminal domain of around 125 amino acid residues that contain most of the MMP inhibitor activity, and carboxy-terminal domain of about 65 residues that facilitates the binding between TIMPs and MMPs (Lu *et al.*, 2011; Khokha *et al.*, 2013). TIMPs bind to MMPs at a 1:1 ratio which regulates their proteolytic activity and each TIMP has special MMP-binding specificity (Lu *et al.*, 2011; Bonnans *et al.*, 2014). TIMPs 12 and 4 are present in soluble form *in vivo* whereas TIMP3 is sequestered in the ECM and the main inhibitor of ADAMs and ADAMTS (Bonnans *et al.*, 2014). In addition, meprins have been found to be naturally inhibited by Cystatin C, elafin and fetuin (Bonnans *et al.*, 2014). Fetuin is a plasma protein that is strongly expressed in developing epithelial and contains three domains

including two N-terminal cystatin-like domain and one C-terminal domain (Hedrich *et al.*, 2010). Cystatin C is a protein that is structurally close to fetuin and both inhibit α-meprin (Hedrich *et al.*, 2010).

1.1.9. ECM and growth factor interaction

ECM interacts with growth factors by binding directly through their domain or cross-talk between integrins and growth factor receptors (GFR) (Taipale and Keski-Oja, 1997). Integrins regulate the activity of GFR either by recruiting adaptor proteins through integrins cytoplasmic domain and concentrating them towards GFR, or by changing their localisation through focal adhesion (Alam *et al.*, 2007). For example, $\beta1_A$ forms a complex with the receptors of insulin growth factor-I (IGF-IR) promoting cellular proliferation while $\beta1_C$ reduces cells proliferation by inhibiting auto-phosphorylation of IGF-IR (Goel *et al.*, 2005). Moreover, ECM acts as a reservoir that retains various growth factors which can be released proteolytically (von der Mark *et al.*, 2010; Kim *et al.*, 2011; Lu *et al.*, 2011; Bonnans *et al.*, 2014). For instance, the PG, perlecan, which is present in basement membranes can bind fibroblast growth factors (FGFs) (von der Mark *et al.*, 2010) which can be cleaved by heparanase and are released as soluble ligands (Kim *et al.*, 2011). HSPGs in the ECM commonly participate in binding, transporting and activating developmental control factors such as Wnt factor and Indian hedgehog (Ihh)(von der Mark *et al.*, 2010). Moreover, fibronectin, vitronectin and HSPGs can bind to hepatocyte growth factor (HGF) and create complexes with Met (HGF receptor) and integrin which positively or negatively control the functions of the diffusible morphogen HGF and promote cell migration (Taipale and Keski-Oja, 1997; Hynes, 2009; Kim *et al.*, 2011). Endothelial growth factor EGF-like motif embedded in several ECM components including laminin, tenascin and fibrillins (Brizzi *et al.*, 2012). The binding of ECM to growth factors usually through specific domains that results in modulation of signalling activities (Kim *et al.*, 2011). For example, fibronectin and tenascin-C bind to vascular endothelial growth factors (VEGF) through FnIII domains and initiate VEGF-mediated signalling through its receptor VEGFR2 and enhance cell proliferation (Hynes, 2009; Kim *et al.*, 2011). In addition, some growth factors depend on heparan sulfate as a cofactor to bind to their signalling receptors (Hynes, 2009). For example, the binding of FGF to FGFR requires heparan sulfate chain that plays crucial role in signalling by acting as a solid-phase ligand (Hynes, 2009).

1.2. Retinal development and the role of ECM components

1.2.1. Structure and function of the human retina

The human eye is a remarkable organ that possesses the ability to perceive vision including shapes, colours, motions and different intensities of light (Sung and Chuang, 2010). The lens transmits and focuses light onto the neural retina which collects and amplifies the signal information before it is transmitted to the midbrain through the optic nerve (**Figure 1-5A**) (Sung and Chuang, 2010). The retina is central nervous tissue (CNS) approximately 0.2 mm thick and it is the first component of the visual system to carry out image processing through the circuits of five main types of cells including the light-sensitive photoreceptors (rods and cones), horizontal, bipolar, amacrine and ganglion cells (Sung and Chuang, 2010). These five cell types are organised in three main layers; the outer nuclear layer (ONL), inner nuclear layer (INL) and ganglion cell layer (GCL) (**Figure 1-5B**) (Nag and Wadhwa, 2006). In addition to these types of cell, Müller cells, specilasied radial glia that spread between the cells through the entire retina from the outer to the inner limiting membrane (Nag and Wadhwa, 2006). Photoreceptors form the outer part of the retina, their cell bodies forming the ONL (Sung and Chuang, 2010) whilst their inner and outer segments reside in the photoreceptor layer (Sung and Chuang, 2010). The retinal pigment epithelium (RPE) lies behind the photoreceptors and captures scattered light and unabsorbed light (Sung and Chuang, 2010). The RPE also has other functions that support the normal function of the photoreceptors including epithelial transport, phagocytosis, visual cycle, immune modulation and secretion (Strauss, 2005). In addition, Bruch's membrane (BrM) is an important pentalaminar structure found between the RPE and the choroidal capillaries of the eye (Booij *et al.*, 2010). BrM plays a crucial role in regulating the exchange of the oxygen, biomolecules, nutrients, fluids and metabolic waste products between the retina and the general circulation as well as cellular communication, differentiation, proliferation or migration (Booij *et al.*, 2010).

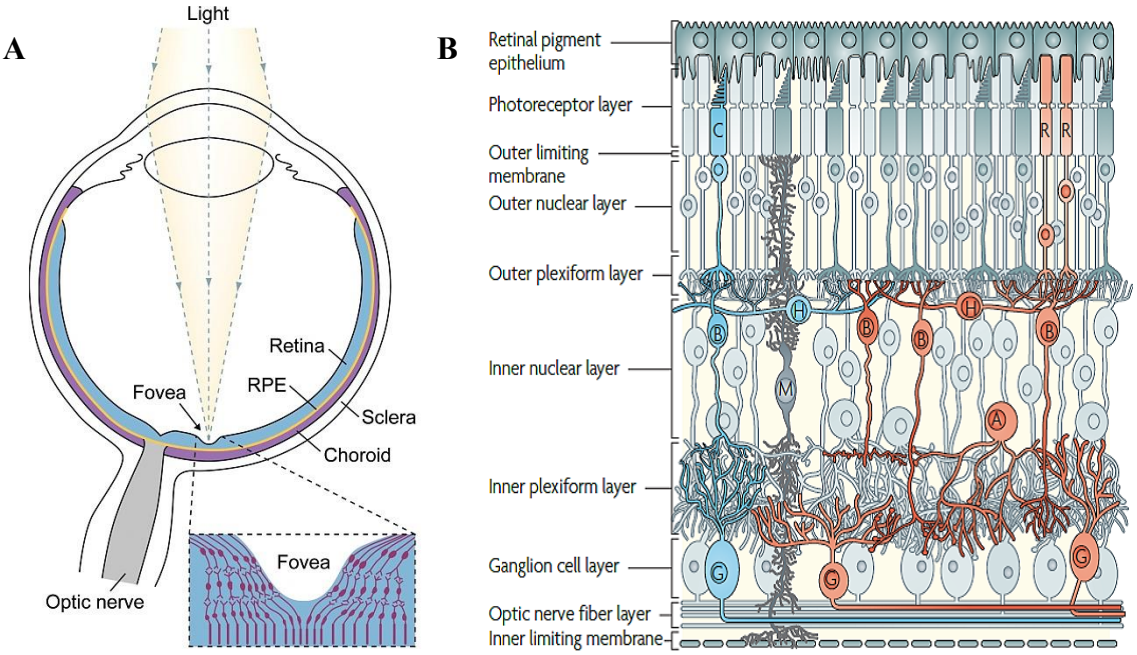

Figure 1-5: (A) Diagram of the human eye with fovea enlarged (Sung and Chuang, 2010). The fovea is a specialised anatomical area of the human retina, around 500 µm in diameter, where the number of photoreceptors (cones) and associated bipolar and ganglion cells are higher than the other parts of the retina (Nag and Wadhwa, 2006). The retina constitutes the inner lining of the posterior part of the eye (Sung and Chuang, 2010). The RPE is located between the retina and the choroid, a vascular connective tissue (Sung and Chuang, 2010). **(B) Diagram shows the laminated structure of the retina** (Swaroop *et al.*, 2010). The ONL contains the somas (cell bodies) of the photoreceptors (R, rods and C, cones) and the INL contains the somas of the horizontal (H), amacrine (A), bipolar (B) and Müller glial (M) cells (Sung and Chuang, 2010; Swaroop *et al.*, 2010). The somas of the ganglion cells constitute the GCL (Sung and Chuang, 2010), and their axons extend toward and form the optic nerve which transmits visual signals to the brain (Swaroop *et al.*, 2010). The processes and synaptic terminals of the photoreceptors, bipolar and horizontal cells are found in the outer plexiform layer (OPL) (Sung and Chuang, 2010; Swaroop *et al.*, 2010). The processes and synaptic terminals of the amacrine, bipolar and ganglion cells are located in the inner plexiform layer (IPL) (Sung and Chuang, 2010; Swaroop *et al.*, 2010). The terminals of the Müller glial cells form the inner and outer limiting membranes (Swaroop *et al.*, 2010).

1.2.2. Development of the human retina

The eye morphogenesis and pattering is highly conserved in vertebrates (Sasai *et al.*, 2012). In human, the eye derived from four tissues in the embryo: the neural ectoderm, the optic neural crest, the surface ectoderm and the mesoderm (O'Rahilly, 1975). The neural ectoderm gives rise to the retina, RPE, optic nerve, ciliary body and iris (O'Rahilly, 1975). The surface ectoderm gives rise to the lens, corneal epithelium and eyelid skin (O'Rahilly, 1975). The neural crest gives rise to the sclera and cornea (endothelium) while the mesoderm gives rise to the vitreous, cornea (stroma) and blood vessels (O'Rahilly, 1975). At 3 weeks of gestations (WG), the neural folds and the optic primordium and optic sulcus appear in the fold of each side of the forebrain at around 22 days of gestation (O'Rahilly, 1975). The optic

sulcus will become the optic vesicle 2 days later (O'Rahilly, 1975) in which retinal neuroepithelium evaginates (expands outwards) bilaterally from the diencephalic wall forming the optic vesicles **(Figure 1-6)** (Sasai *et al.*, 2012). At around 28 days of gestation, the retinal disc appears on in the wall of the optic vesicle (O'Rahilly, 1975; Nag and Wadhwa, 2006). The distal part of the vesicle (in contact with the surface ectoderm) invaginates (folds inward) to produce the bilayered optic cup (Sasai *et al.*, 2012), and the lens are formed once the contact with the surface ectoderm has occurred (O'Rahilly, 1975). The outer layer of the optic cup develops into RPE and the inner layer becomes the neural retina (Sasai *et al.*, 2012). Several major developmental signalling pathways such as FGF, Wnt, TGF-β, Shh, Notch and IGF-1 are essential for the adoption of optic cup to its precise gene expression before the onset of neurogenesis (Kwan, 2014; Mellough *et al.*, 2014).

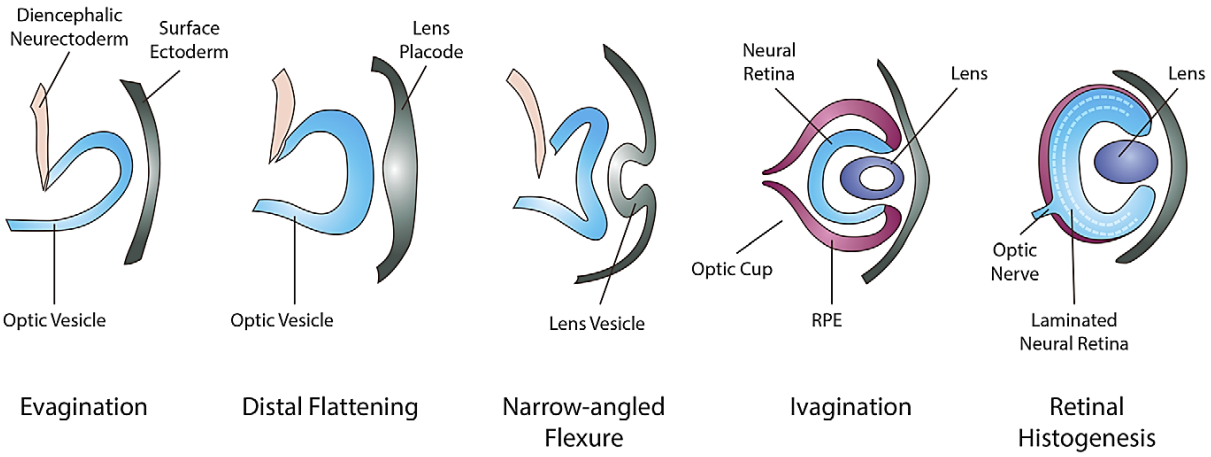

Figure 1-6: Schematic diagram of optic cup morphogenesis (Mellough *et al.*, 2014).

In humans, neural differentiation in the central retina and fovea begins at 6 weeks of gestation and is complete by 19-21 weeks of gestation (midgestation), while neural differentiation in peripheral retina continues until 30 weeks of gestation (Hendrickson and Drucker, 1992; Nag and Wadhwa, 2006). By birth, all neurons and retinal layers become fully mature except in the foveal region where the differentiation of the photoreceptors continues for up to 5 months after birth (Nag and Wadhwa, 2006; Hendrickson and Zhang, 2017). The retina continue to increase in size until the 6th postnatal year (Nag and Wadhwa, 2006). During different stages of differentiation, retinal cells express a wide range of markers such as calcium-binding proteins, amino acid neurotransmitters, nitric oxide, neuropeptides and proteins of the phototransduction pathways (Nag and Wadhwa, 2006; Hoshino *et al.*, 2017).

The functional development of photoreceptor precursors (giving rise to cones and rods) varies between species (Swaroop *et al.*, 2010). For example, the development of

photoreceptors is less advanced in mouse than human at birth (Swaroop *et al.*, 2010). All photoreceptors are generated prenatally in human, whereas in mice they are generated pre- and postnatally (Swaroop *et al.*, 2010). There are also significant differences between the two species in term of the number, ratio and distribution of the photoreceptors (Saghizadeh *et al.*, 2011). The human retina has a larger amount of cone cells (~5%) than the mouse retinal photoreceptors (~3% cone cells) (Fu and Yau, 2007) and it contains the fovea which is not present in the mouse (Sung and Chuang, 2010; Saghizadeh *et al.*, 2011). Moreover, human retina is trichromatic (has three types of cone photoreceptors), whereas mouse retina is dichromatic (Saghizadeh *et al.*, 2011). Therefore, it is important to study the developmental stages of human eye rather than other species in retinal research.

1.2.3. Formation of retinal layers and neurons

Different types of cells are generated at different stages of development (Jean *et al.*, 1998). Retinal ganglion cells are the first cells that appear (Jean *et al.*, 1998). During the early development of the human embryonic eye, the retina starts to differentiate at 6 WG forming its inner neuroblastic zone (INZ) and ganglion cells (GCs) (Nag and Wadhwa, 2006). In addition, the RPE appears in the external layer of the optic cup at 6 WG (O'Rahilly, 1975). Around 7-8 WG, Müller cells appear and are located with the GCs in the INZ (O'Rahilly, 1975; Nag and Wadhwa, 2006). Moreover, horizontal cells appears at this time point in the incipient fovea (Nag and Wadhwa, 2006). The outer neuroblastic zone (ONZ) appears at 9 WG and composed of a heterogeneous population of undifferentiated neuroblasts (Nag and Wadhwa, 2006). ONZ is separated from the INZ by Chievitz layer, a transient fiber layer which will become the IPL (**Figure 1-7A**) (O'Rahilly, 1975; Nag and Wadhwa, 2006; Hendrickson, 2016). Before 9 WG, Ki-67 immuno-labelling shows that the central retina is more proliferative than the peripheral retina (Bozanic and Saraga-Babic, 2004; Nag and Wadhwa, 2006). Ki-67 is a nuclear protein used as a proliferation marker due to its expression in all cell cycle phases except the resting phase (G0) (Bozanic and Saraga-Babic, 2004). The INL starts to differentiate from the ONZ forming amacrine cells at around 11 WG (Rhodes, 1979; Nag and Wadhwa, 2006) and bipolar cells at 15-16 WG (Nag and Wadhwa, 2006). The photoreceptors differentiate from the outer rows of the ONZ, cones born first at 10 WG and rods born at 12 WG (Rhodes, 1979; Nag and Wadhwa, 2006; Hendrickson and Zhang, 2017). The OPL starts to differentiate in the central retina at 11-12 WG and becomes prominent in the central to midperipheral area of the fetal retina by 16 WG (**Figure 1-7B**) (Nag and Wadhwa, 2006; Hendrickson, 2016). The differentiation of most retinal neurons proceeds in a central to peripheral direction and is attained by midgestation (20-21 WG) (**Figure 1-7C**)

(Nag and Wadhwa, 2006; Hendrickson, 2016). At this period, the connection to the visual centers is partially formed via the axons of retinal GCs (Hevner, 2000; Nag and Wadhwa, 2006).

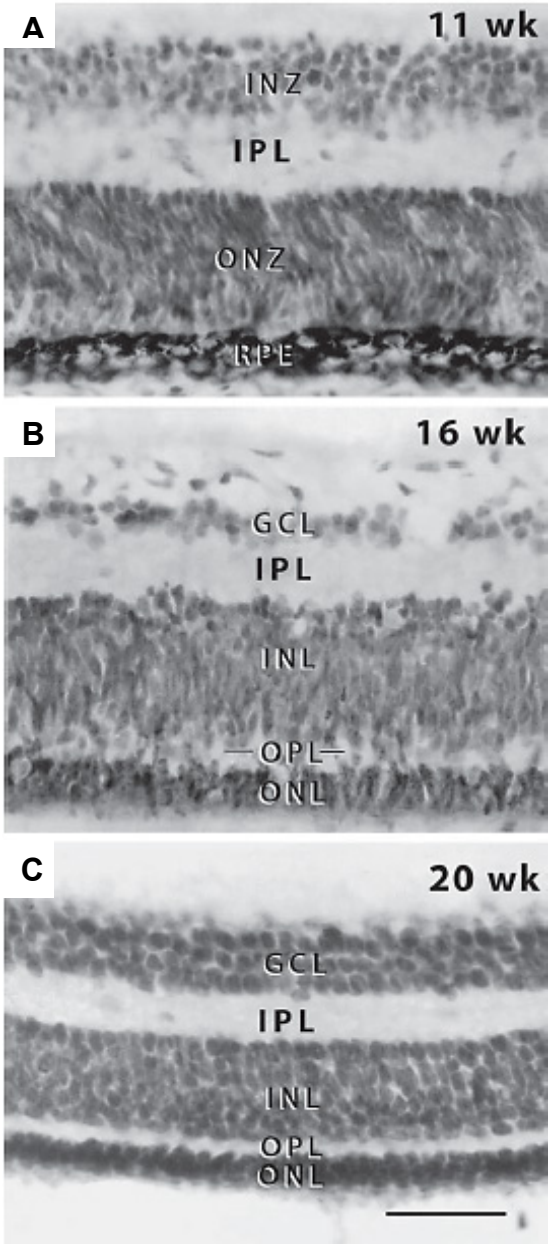

Figure 1-7: Light micrographs of the human fetal retina at different gestational periods (Nag and Wadhwa, 2006).
At 11 WG (a), the RPE and the retina which is composed of ONZ and INZ, separated by the IPL (Nag and Wadhwa, 2006). **At 16 WG (b),** the OPL and GCL are prominent in the central retina while the neurons in the INL are still differentiating (Nag and Wadhwa, 2006). **At 20 WG (c),** all retinal layers are established (Scale bar: 50μm) (Nag and Wadhwa, 2006).

1.2.4. Photoreceptor differentiation

At 15 WG, the cilium develops as a small projection from the apical end of the cone inner segments (Nag and Wadhwa, 2006; Hendrickson and Zhang, 2017). The cone inner segments will be arranged into mosaic patterns at 18-19 WG, where few large cone inner

segments (blue cones) standing out from the mosaic of several small cone inner segments (red/green cones) (Narayanan and Wadhwa, 1998). They elongate and convert from spherical to an oval shape between 19 and 25 WG (Nag and Wadhwa, 2006). The rod inner segments are recognised and show ciliary outgrowths at 18-19 WG (Nag and Wadhwa, 2006). At 24 WG, the rod outer segments start to develop from the distal part of cilia (Narayanan and Wadhwa, 1998; Nag and Wadhwa, 2006). In Fovea, cones start to differentiate in the putative fovea at 13 WG (Yuodelis and Hendrickson, 1986; Nag and Wadhwa, 2006) while rods are not present until 15 WG (Nag and Wadhwa, 2006). Several markers start to be expressed at several time points during the development of the photoreceptors in the human fetal retina that could be critical in their differentiation and maturation (**Table 1-7**) (Nag and Wadhwa, 2006).

Table 1-7: Markers for photoreceptors in developing human retina until birth (Nag and Wadhwa, 2006; Hoshino *et al.*, 2017).

Photoreceptors Markers	Expression starts at gestational week (GW)	Retinal Location
IRBP	9	foveal, peripheral
TULP	9	foveal, peripheral
Phosphodiesterase β	10	foveal
AIPL 1	11	foveal
Short opsin	11	foveal
Long/medium opsin	14	foveal
Taurine	18	central to peripheral
Heat shock protein 70	20	midperipheral
PEDF	21	foveal
Calbindin	24	foveal
Nrl	10	foveal edge, peripheral
S-antigen	13	central, RT
Rod opsin	15	RT, foveal

IRBP = Interphotoreceptor retinal binding protein; **TULP** = Tubby-like protein-1; AIPL 1 = Leber congenital amaurosis protein; **PEDF** = pigment epithelium-derived factor; **Crx** = Cone-rod homeobox; **Nrl** = Neural retina leucine zipper; **RT** = Retinal transplant.

1.2.5. The role of ECM on formation of laminated retina during development

In retina, the ECM divided into two distinct entities including the interphotoreceptor matrix (IPM) and the retinal ECM that surround other cells in the retina (Ishikawa *et al.*, 2015). The IPM surrounds the inner and outer segments of the photoreceptors and plays a significant role in retinal adhesion to the RPE (Hollyfield, 1999), retinoid transport (Hollyfield, 1999), photoreceptor differentiation (Karakousis *et al.*, 2001) and intercellular communication (Beuckmann *et al.*, 1996). During retinal development, the ECM plays major roles in numerous processes including cellular differentiation, proliferation, migration,

maturation, adhesion, guidance and axonal growth (Reinhard *et al.*, 2015). For example, in chick embryos, removing the surface ectoderm and disrupting the surrounding ECM with collagenase resulted in the curvature of the optic vesicle at early stages of invagination and inhibition of subsequent invagination and optic cup formation (Oltean *et al.*, 2016). Another study has demonstrated that blocking the interaction of rat retinal progenitor cells with laminin β2 *in vitro* reduced the fraction of cells that express rhodopsin, suggesting that this laminin could be important for rod photoreceptor differentiation (Hunter *et al.*, 1992). Knockdown of laminin β2 also results in abnormal elongation of photoreceptor outer segments, abnormal electroretinogram, and atypical synaptic formation of rod photoreceptors and apoptosis in mice (Libby *et al.*, 1999). Double knockout of laminin β2 and laminin γ3 in mice resulted in disruption of inner limiting membrane (ILM) and retinal dysplasia (Pinzon-Duarte *et al.*, 2010).

Several ECM components have been studied in the mature and developing retina of many species including rat, mouse, and chicken as well as human adult retina (**Table 1-8**) (Popp *et al.*, 2004; Hausman, 2007; Inoue *et al.*, 2009; Clark *et al.*, 2011; Keenan *et al.*, 2012; Kwan, 2014). The localisation of ECM molecules varies between developmental stages (Keenan *et al.*, 2012) and species (Clark *et al.*, 2011). For example, versican has been identified in the nerve fibres and the inner plexiform layer of the embryonic chicken retina, while in adult chicken it has been found in photoreceptor layer and BrM (Keenan *et al.*, 2012). HA is found only in the photoreceptor layer in the adult retina of chicken (Inoue *et al.*, 2009) but in adult human retina HA is widely distributed throughout the whole retina (Clark *et al.*, 2011).

Aggrecan, brevican, versican and neurocan are members of the CS family that plays an important role in maintaining adhesion between the RPE and neurosensory retina as well as BrM (Keenan *et al.*, 2012). Moreover, they bind to HA from their N-terminal region and are involved in the development of the central nervous system (Popp *et al.*, 2004). HA is another component of the ECM that has a vital role in tissue remodelling during development and normal tissue homeostasis as well as disease (Inoue *et al.*, 2009). HA is expressed in the IPM and creates a scaffold that fills the matrix as well as binding to several proteins of the IPM such as versican, Interphotoreceptor Matrix Proteoglycan 1 (IMPG1) and sialoproteoglycan associated with cones and rods (IMPG2) (Inoue *et al.*, 2009; Mellough *et al.*, 2014). In addition, hyaluronan-binding motifs provide a structural link between the RPE and the neural retina (Ishikawa *et al.*, 2015). HA is secreted from the apical side of the RPE (de *et al.*, 2001) and has a binding affinity to PEDF which is also secreted apically from the

RPE (Becerra *et al.*, 2008; Ishikawa *et al.*, 2015). PEDF is required for avascularity of the IPM and survival of photoreceptors (Becerra, 2006; Broadhead *et al.*, 2010; Ishikawa *et al.*, 2015). Abnormal localisation of HA might result in IPM degeneration, consequently affecting photoreceptor survival (LaVail *et al.*, 1981; Ishikawa *et al.*, 2015).

Table 1-8: Key ECM components

ECM Protein			Tissue Expressed	Developmental Stage	Species Studied	Note	Reference/s
Family	**Class based on GAGs**	**Component**					
Proteoglycans (PGs)	**Chondroitin Sulphate (CS)**	**Aggrecan**	Throughout the retina	Adult	Human	-	(Popp *et al.*, 2004; Hausman, 2007; Keenan *et al.*, 2012)
			Inner retinal layer of the optic cup	Embryo (day 16)	Rat	-	
			Ganglion cell and plexiform layers	Adult	Rat	Weak in nuclear layers	
			Ganglion cell and nuclear layers	Adult	Mouse	Weak in inner plexiform and photoreceptor layers	
		Brevican	- Throughout the retina e.g. Nerve fiber layer & Inner plexiform layer - Bruch's membrane - Choroid - Sclera	Adult	Human	Not studied in perinatal or adult retinal tissues of any vertebrate animal	(Keenan *et al.*, 2012)
		Versican	Bruch's membrane	Adult	Human	Detected in Bruch's/choroid complex	(Popp *et al.*, 2004; Hausman, 2007; Keenan *et al.*, 2012)
			Nerve fiber and inner plexiform layers	Embryo (day 14)	Chicken	-	
			photoreceptor layer and Bruch's membrane	Adult	Chicken	-	
			Inner retinal Layers of the optic cup	Embryo (day16)	Rat	-	
			Ganglion cell and plexiform layers	Adult	Rat	Weak in nuclear layers	
		Neurocan	Inner plexiform and ganglion cell layers.	Neonate	Rat	-	(Popp *et al.*, 2004; Hausman, 2007)
		SPARC	Macroglial Muller cells: INL, IPL, ILM	Adult	Rat	-	(Gilbert *et al.*, 1999)
		IMPG1	Interphotoreceptor matrix	Adult	Human	Binds to HA	(Kuehn and Hageman, 1999)
		IMPG2	Bruch's membrane/choroid complex	Adult	Human	Binds to HA	(Chen *et al.*, 2003; Clark *et al.*, 2011)
			Interphotoreceptor matrix	Embryo (day 15- mouse only) and adult	Human and mouse		
	Polysaccharides	**Hyaluronan**	Widely expressed	Adult	Human	- Binds to Versican, SPACR and SPACRCAN - A major component of the interphotoreceptor matrix	(Hausman, 2007; Inoue *et al.*, 2009; Clark *et al.*, 2011; Mellough *et al.*, 2014)

Table 1-8: Key ECM components, continued.

ECM Protein			Tissue Expressed	Developmental Stage	Species Studied	Note	Reference/s
Family	**Class based on GAGs**	**Component**					
Glycoproteins		**Fibronectin**	Cornea, lens, sclera, trabecular, meshwork and vitreous	Embryo	Chicken, mouse and rat	-	(Hausman, 2007; Kwan, 2014)
		Collagen IV	Bruch's membrane Inner limiting membrane	Embryo	Chicken, mouse and rat	Present in the basement membrane meshwork	(Hausman, 2007; Kwan, 2014)
		Laminins α1	Bruch's membrane	Fetal (9-12 WG)	Human	-	(Bystrom *et al.*, 2006)
		Laminin α5	IPM OPL	adult	Rat, Human	-	(Libby *et al.*, 2000)
		Laminin β1	Bruch's membrane	Fetal (9-20 WG)	Human	-	(Bystrom *et al.*, 2006)
		Laminin β2	IPM OPL	adult	Rat, Human		(Libby *et al.*, 2000)
		Laminin γ1	ILM	adult	Human	-	(Libby *et al.*, 2000)
		Laminin γ2	IPM	adult	Rat, Human	-	(Libby *et al.*, 2000)

IMPG1 & IMPG2 are novel proteoglycans found in the IPM and shown to be involved in the development and maintenance of the photoreceptors, in mice and human (Acharya *et al.*, 1998; Kuehn and Hageman, 1999; Chen *et al.*, 2003). *IMPG1* mutations were reported in Vitelliform macular dystrophies leading to impaired metabolism of the IPM and the accumulation of Vitelliform deposits in the sub-retinal space (Manes *et al.*, 2013). IMPG2 mRNA expression in the developing retina of rat shows that its detected first with time photoreceptors start to extend from the outer retinal surface, suggesting that IMPG2 may contribute in the maturation and maintenance of the photoreceptor outer segments (Foletta *et al.*, 2001). Fibronectin and collagen IV are two mesh-forming glycoproteins of the ECM (Kwan, 2014). Fibronectin is a homodimer and interact with collagens to provide structural support for cell adhesion (Stenzel *et al.*, 2011; Kwan, 2014). The functional importance of fibronectin has been highlighted by the injection of RGD peptides (block fibronectin-integrin interaction) resulting in severe disorganisation of the optic cup in chick (Kwan, 2014). Collagen IV, laminin and fibronectin are the main ECM components of the basement membranes including Bruch's membrane and inner limiting membrane (ILM) (Hausman, 2007; Kwan, 2014). Basement membranes are essential for structural support, cellular adhesion, differentiation, proliferation, migration and intercellular communication (LeBleu *et al.*, 2007). In the case of BrM it is essential for the regulation of the bio-molecules diffusion

between RPE and choroid, RPE cellular adhesion, migration and differentiation, and acting as a division barrier to restrict choroidal and retinal cellular migration (Booij *et al.*, 2010).

The basement membranes of the retina include BrM and the ILM (Reinhard *et al.*, 2015). CSPGs have been found to play an important role in the regulation of synaptic plasticity in CNS and were speculated to have similar role in retinal tissues (Faissner *et al.*, 2010; Reinhard *et al.*, 2015). Moreover, CSPGs are vital for the maintenance of the cellular adhesion between RPE and the neural retina (Lazarus *et al.*, 1993). Lazarus and Hageman (1992) demonstrated that intravitreal injections of xyloside, an inhibitor of CSPG synthesis, in Yucatan micropigs perturb CSPG and induce the degeneration of the cone photoreceptor outer segment and shallow retinal detachment (Lazarus and Hageman, 1992; Ishikawa *et al.*, 2015). This result suggests that adhesion between the PRE and neural retina is dependent on continuous synthesis of cone matrix sheath-associated PGs (Lazarus and Hageman, 1992; Ishikawa *et al.*, 2015). Transmembrane cell-surface HSPGs such as syndecans and glypicans are also present in the retina (Reinhard *et al.*, 2015). For instance, N-syndecan is highly expressed in retinal nerve fiber layer at the beginning of postnatal stage (P0-P14) in human, suggesting that N-syndecan play a role in the formation of the neural network of the retina (Inatani *et al.*, 2002). The inhibition of decorin results in the loss of retinal progenitor polarisation and it serves as neurotrophic factor and participate in cellular differentiation during retinal development (Reinhard *et al.*, 2015). Moreover, the laminins work as mediators of cellular differentiation such as laminins β2 chain that are essential for rod-bipolar cell differentiation and maintenance (Reinhard *et al.*, 2015). In culture, exposing the cells to a laminin β2- rich matrix can promote the production of rods six fold and reduce the bipolar production by 66%, suggesting that laminins may control cells fate between rod photoreceptors and rod bipolar cells (Hunter and Brunken, 1997). Tenascin-C, an extracellular glycoprotein, inhibits cellular proliferation during retinal development (Reinhard *et al.*, 2015). It is mainly expressed in the nerve fiber and plexiform layers of the adult retina (Reinhard *et al.*, 2015). Tenascin-C modulates the responsiveness of growth factors (FGF2 or PDGF) in retinal stem/precursors and supports the de-differentiation ability of Müller glia (Besser *et al.*, 2012).

There has been limited detailed analysis of ECM component distribution throughout retinal development in human and its functional importance is poorly understood (Reinhard *et al.*, 2015). Therefore, studying the distribution of the key ECM component during human embryonic and foetal retinal ontogenesis as well as adult human retina will fill the knowledge gaps existing between the retinal developmental stages in human and other species and may

help to uncover the specific roles of different ECM components on retinal lamination and photoreceptor function in human which will be crucially important for optimising our *in vitro* differentiation protocols. Determining ECM components that expressed in the IPM of the human embryonic and fetal retina may help in selecting the best candidate for enhancing the differentiation of the OS from the hESCs and iPSCs.

1.3. Human pluripotent stem cells

Pluripotent stem cells are remarkable cells that have the ability to differentiate into multiple cell types with the capability of indefinite self-renewal in their undifferentiated form (Ramsden *et al.*, 2013). They can be classified according to their potency which is the range of cell types they may differentiate into (Ramsden *et al.*, 2013). Totipotent stem cells able to differentiate into embryonic and extra-embryonic tissue [tissues that support the embryo such as the placenta and yolk sac (Wang *et al.*, 2017)], pluripotent stem cells have the potential to differentiate into all cell types derived from the three germ layers of embryonic tissue (ectoderm, mesoderm and endoderm), and multipotent stem cells have the ability to differentiate into a limited number of cell types, controlled by the degree of previous differentiation (Ramsden *et al.*, 2013). Pluripotency can be divided into two phases: naïve and primed (Nichols and Smith, 2009). Naïve pluripotent stem cells are embryonic stem cells (ESCs) that are derived from the inner cell mass of a pre-implantation blastocyst (Wu *et al.*, 2015). In human, ESCs are pluripotent cells that are harvested from the inner cell mass of the blastocyst of fresh or frozen embryos produced by *in vitro* fertilisation (IVF) for clinical purposes (**Figure 1-8**) (Thomson *et al.*, 1998; Narsinh *et al.*, 2011; Armstrong *et al.*, 2012; Ramsden *et al.*, 2013). Epiblast stem cells (EpiSCs) are the *in vitro* counterparts of the primed epiblast that established from post-implantations (Nichols and Smith, 2009; Wu *et al.*, 2015). Although both are pluripotent, they have some differenced in term of colony morphology and efficiency, molecular signature, metabolic requirements and epigenetic features (Wu *et al.*, 2015).

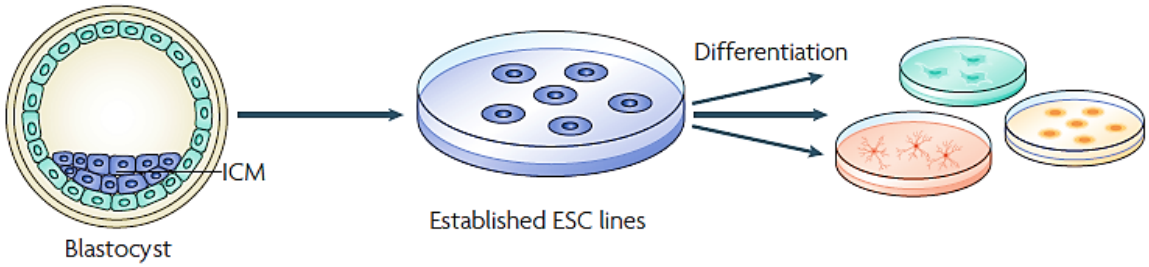

Figure 1-8: Diagram of human embryonic stem cells derivation (Hynes, 2008).
Embryonic Stem cells (ESCs) are harvested from the inner cell mas (ICM) of an early embryo (blastocyst) (Hynes, 2008). ESCs can continuously proliferate under appropriate cultural condition and differentiate into several cell types *in vitro* (Hynes, 2008).

In 2006, Shinya Yamanaka and his group demonstrated that murine fibroblast could be reprogrammed into ESC-like pluripotent stem cells, named as induced pluripotent stem cells (iPSCs) (Takahashi and Yamanaka, 2006; Wiley *et al.*, 2015). Forced expression of four transcription factors including *Oct4, Sox2, Klf4* and *c-Myc* can reprogram differentiated somatic cells into iPSCs (Takahashi and Yamanaka, 2006; Ramsden *et al.*, 2013). Soon after, Yamanaka demonstrated that this reprograming method could be repeated using human fibroblasts, thus making iPSCs relevant to human disease and potential resource for cellular transplantation research (**Figure 1-9**) (Takahashi *et al.*, 2007; Wiley *et al.*, 2015). Moreover, iPSCs derivation can be achieved by using different combinations of transcription factors including Oct4, Sox2, Nanog and Lin28 avoiding the use of c-Myc which is a known proto-oncogene (Yu *et al.*, 2007; Ramsden *et al.*, 2013). Since then, several reprogramming techniques have been developed for iPSCs derivation (**Table 1-9**) (Robinton and Daley, 2012).

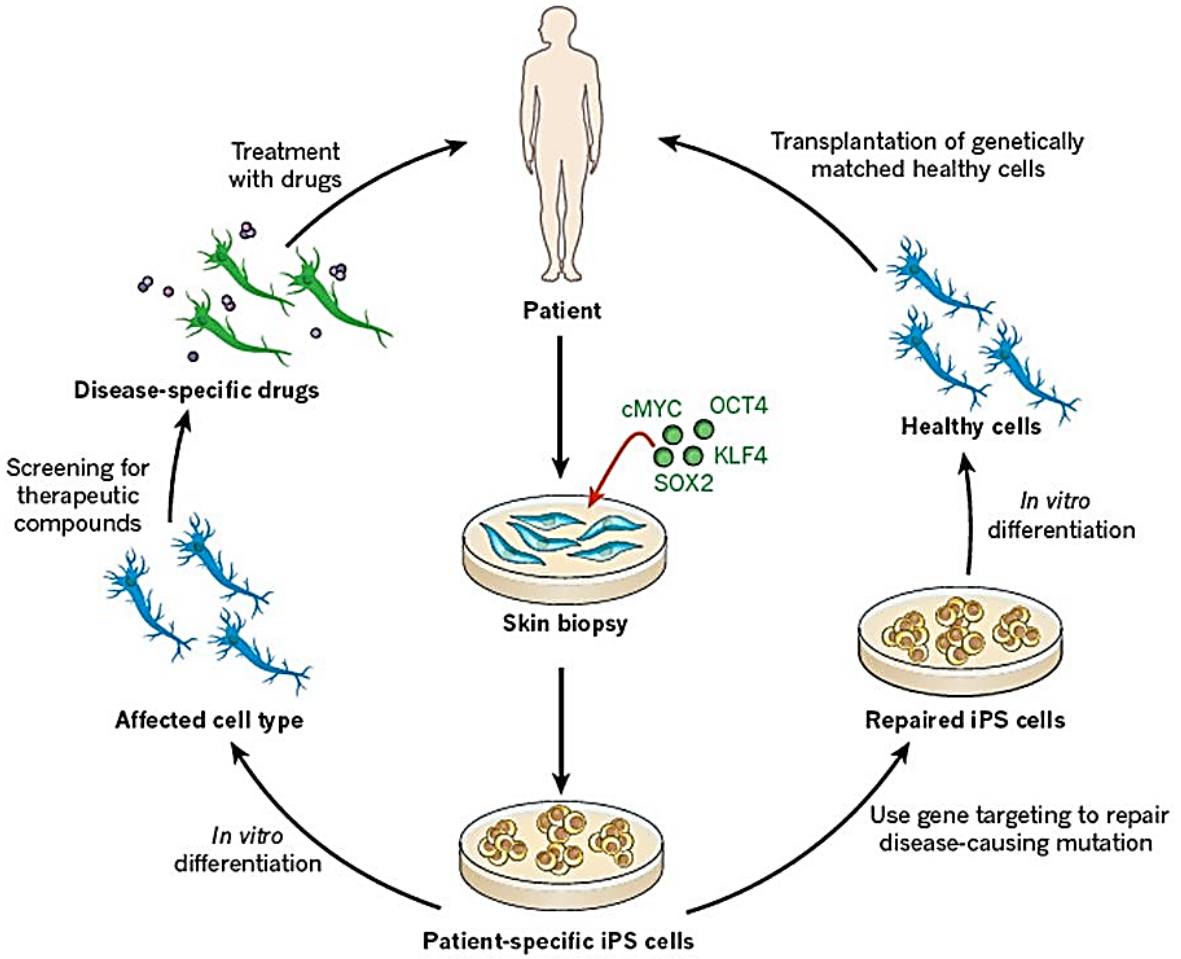

Figure 1-9: Diagram of iPSCs reprograming and their medical application (Robinton and Daley, 2012).

Table 1-9: Techniques for reprograming somatic cells to iPSCs (Robinton and Daley, 2012).

Vector type		Cell types	Factors	Efficiency (%)
Integrating	Retroviral	Fibroblasts, neural stem cells, stomach cells, liver cells, keratinocytes, amniotic cells, blood cells and adipose cells	OSKM, OSK, OSK + VPA, or OS + VPA	~0.001–1
	Lentiviral	Fibroblasts and keratinocytes	OSKM or *miR302/367* cluster + VPA	~0.1–1.1
	Inducible lentiviral	Fibroblasts, β cells, keratinocytes, blood cells and melanocytes	OSKM or OSKMN	~0.1–2
Excisable	Transposon	Fibroblasts	OSKM	~0.1
	loxP-flanked lentiviral	Fibroblasts	OSK	~0.1–1
Non-integrating	Adenoviral	Fibroblasts and liver cells	OSKM	~0.001
	Plasmid	Fibroblasts	OSNL	~0.001
DNA free	Sendai virus	Fibroblasts	OSKM	~1
	Protein	Fibroblasts	OS	~0.001
	Modified mRNA	Fibroblasts	OSKM or OSKML + VPA	~1–4.4
	MicroRNA	Adipose stromal cells and dermal fibroblasts	miR-200c, miR-302s or miR-369s	~0.1

OSKM and similar names represent a group of reprogramming factors: K= KLF4; L= LIN28; M= c-MYC; N= NANOG; O= OCT4; S= SOX2; and VPA= valproic acid.

1.3.1. hESCs and hiPSCs

hESCs and hiPSCs share the important characteristics of self-renewal and pluripotency (Narsinh *et al.*, 2011). hESCs are commonly recognised as a rich biological source of pluripotent cells, and hold an incredible therapeutic potential due to their capability to proliferate, self-renew and differentiate (Ghosh *et al.*, 2010). However, the ethical issues of using human embryo and the limited supply of human embryos may delay the obtaining of hESCs (Narsinh *et al.*, 2011; Armstrong *et al.*, 2012). hiPSCs are a non-controversial different

source of pluripotent human cells that could overcome some of the hESCs difficulties related to immune rejection of the transplanted tissue (Ghosh *et al.*, 2010). hESCs and hiPSCs are similar in term of morphology, surface marker expression and *in vivo* teratoma formation capability (Narsinh *et al.*, 2011). However, they harbour subtle differences due to their origins and ways of derivation (Robinton and Daley, 2012).

1.3.2. Disease modelling and clinical cell transplantation

hESCs and hiPSCs hold great promises for disease modelling and transplantation studies (Ramsden *et al.*, 2013; Wiley *et al.*, 2015). Both cell types have been used in therapeutic application or studies of different retinal diseases such as age-related macular degeneration (AMD) (Ramsden *et al.*, 2013). hESCs have been used to study AMD and propagate RPE-like cells that could replicate the morphology and function of indigenous tissue (Ramsden *et al.*, 2013). Protein and gene expression of hESC-derived RPE *in vitro* demonstrated the expression of RPE65, a specific marker to RPE cells (Ramsden *et al.*, 2013). The derived RPE cells expressed PAX6 at a similar level to foetal RPE cells (Klimanskaya *et al.*, 2004; Ramsden *et al.*, 2013). In addition, hESCs-derived RPE cells show several characteristics of native RPE such as morphology, polarity, tight junction, phagocytosis and retinol cycling (Ramsden *et al.*, 2013). After transplantation of the derived RPE tissue, these cells can rescue visual parameters and might be a potential source for cell therapy for AMD (Ramsden *et al.*, 2013). Recently, transplantation of hESC-derived RPE in 12 Stargardt patients with macular degeneration resulted in subretinal hyperpigmentation indicated the survival of transplanted cells (Mehat *et al.*, 2018).

In advanced AMD, stem cell-choroidal endothelial cells are required in cellular transplantation in order to reconstruct the macula (Wiley *et al.*, 2015). hiPSCs can be used to drive endothelial cells through co-culture with primary endothelial cell lines or conditioned media with endothelial cell-specific factors (Wiley *et al.*, 2015). A recent study has shown the integration of iPSCs-derived endothelial cells with the host vasculature triggers a relatively modest immune response in a murine model of hindlimb ischemia (de Almeida *et al.*, 2014; Wiley *et al.*, 2015), suggesting that autologous endothelial cells may be well tolerated in the choroid (Wiley *et al.*, 2015). Another group successfully transplanted hESC-derived RPE monolayer into the eye subretinal space of two patients with severe AMD which improved their visual acuity (clarity of vision) and reading ability based on letter chart (from being able to read only 10 letters to read 39 and from 8 to 29 letters, respectively) enabling them to read

29 and 21 more letters over 12 months suggesting the feasibility and safety of hESC-derived RPE patch transplantation as a regenerative strategy (da Cruz *et al.*, 2018).

Singh *et al.* used patient specific hiPSCs to model Best disease, an autosomal dominant disorder of the RPE that causes degeneration of the photoreceptors (Singh *et al.*, 2013). Using transmission electron microscopy, all hiPSCs cell lines showed typical RPE features including apical microvilli, intracellular pigment granules and tight-junctional complexes (Singh *et al.*, 2013). hiPSCs modelling of Best disease can provide a platform to explore its pathophysiological mechanism (Singh *et al.*, 2013). Patient-specific hiPSCs have a potential to be as a tool for identification of disease causing mutations, drug screening and source for autologous retinal cell transplantation (Wiley *et al.*, 2015). Recently, Foltz and Clegg reported a rapid (14 days) method to direct the differentiation of hESCs and hiPSCs into RPE with no or minimal dissection required which may provide a platform for pluripotent stem cells to model ocular disease and to generate RPE cells for transplantation (Foltz and Clegg, 2017).

1.4. Human pluripotent stem cell differentiation to retinal lineages and the role of ECM

1.4.1. Differentiations of human pluripotent stem cell into retinal lineages

Researchers have used several growth factors and morphogens including insulin-like growth factor 1 (IGF-1), Wnt inhibitors, activin A and sonic hedgehog (Shh) to differentiate hESCs and hiPSCs as a monolayer (Lamba *et al.*, 2006; Lund *et al.*, 2006; Mellough *et al.*, 2014). However, two-dimensional (2D) culture might not be the ideal method to produce fully mature functional photoreceptors since hESCs-derived photoreceptors fail to develop outer segments (an important cell compartment for phototransduction) *in vitro* (Osakada *et al.*, 2008; Hirami *et al.*, 2009; Lamba *et al.*, 2009), or integrate with low efficiency upon transplantation into adult $Crx^{-/-}$ mice with retinal degeneration (3000 cells $Nr1^{+}$ of human cells) (Lamba *et al.*, 2009). Using three-dimensional (3D) culture system, a number of reports have shown that various aspects of the retinal development can be recapitulated *in vitro* through the differentiation of hESCs and hiPSCs (Rashid and Vallier, 2010; Meyer *et al.*, 2011; Mellough *et al.*, 2012; Nakano *et al.*, 2012; Mellough *et al.*, 2014; Zhong *et al.*, 2014; Gonzalez-Cordero *et al.*, 2017; Welby *et al.*, 2017) into retinal organoids which contain the key retinal cells types and respond to electrophysiological cues. In 2012, Sasai's group reported the generation of 3D optic cup containing typical three layered retinal statures including photoreceptors (Nakano *et al.*, 2012). However, CRX^{+} photoreceptors formed 12-18% of the

total cell numbers at day 126 of the differentiation with some expression of other photoreceptor markers such as NRL (rod specific marker) and RXRγ (marker for cone precursors). Zhong *et al.* supplemented culture media with retinoic acid (RA) that promoted the differentiation of hiPSCs into of photoreceptors by increasing the expression of photoreceptor markers such as RHO, S-opsin and L/M-opsin (Zhong *et al.*, 2014). The retinal organoids from Zhong *et al.* protocol were able to respond to light stimuli but they were from a limited number of photoreceptors (2 out of 13 randomly selected cells) (Zhong *et al.*, 2014). Recently, Hallam *et al.* generated retinal organoids from different patient-specific hiPSCs lines that responded to light similarly to those recoded from neonatal mouse retina (Hallam *et al.*, 2018). However, the differentiation of retinal organoids showed variable efficiency depending on nutrient availability suggesting a possible link between nutrient availability and cell fate (Hallam *et al.*, 2018).

1.4.2. The role of ECM on stem cell differentiation

Stem cells reside in a specialised and dynamic microenvironment known as stem cell niche that provide extracellular cues that control stem cell survival, self-renewal and differentiation (Brizzi *et al.*, 2012). ECM is a major component shaping the stem cell niche and maintain their homoeostasis through integrating signalling emanating from soluble and matrix-bound growth factors as well as cell-matrix interaction (Brizzi *et al.*, 2012). Moreover, ECM regulates stem cell fate through integrin, mainly β1-integrin, that controls the orientation of mitotic spindle and influences symmetric and asymmetric division (Brizzi *et al.*, 2012). Culture conditions for stem cell differentiation might contain soluble factors such as Wnts and FGFs that regulate stem cell self-renewal, membrane associate proteins such as cadherins which form adherens junctions that participate in positioning and anchoring the cells, and integrins that bind to several components of ECM to facilitate cell adhesion and differentiation (Viswanathan *et al.*, 2014). Engineered surfaces with specific ligand affinity and spatial arrangement of surface chemistry, topologies and matrix stiffness can generate cellular responses such as self-renewal and differentiation (Viswanathan *et al.*, 2014).

ECM proteins such as fibronectin and collagen IV can guide the differentiation of stem cell *in vitro* (Votteler *et al.*, 2010). Fibronectin can induce the differentiation of myoblasts into skeletal muscle cells and the differentiation of adipose tissue-derived stem cells into endothelial cells within monolayer cultures (Lan *et al.*, 2005; Heydarkhan-Hagvall *et al.*, 2008; Votteler *et al.*, 2010). In addition, culturing pluripotent stem cells on tissue culture ware coated with collagen IV enhance their differentiation into cardiovascular and

hematopoietic linages (Schenke-Layland *et al.*, 2007; Schenke-Layland *et al.*, 2008; Votteler *et al.*, 2010). A recent study has shown that the addition of heparin to HS–competent ESCs significantly change the differentiation outcomes: the haemopoietic commitment was improved by ~50% at very low level (10 ng/ml), while at high concentration (500 ng/ml) haemopoiesis was reduced (Holley *et al.*, 2014). In contrast, the addition of related sugars CS and DS failed to influence differentiation, suggesting the specific importance of HS in stem cell differentiation (Holley *et al.*, 2014).

1.4.3. The role of ECM on pluripotent stem cell differentiation to laminated retinae

In the human eye, the RPE is essential for normal development *in vivo* and to maintain correct morphogenesis of the neural retina (Gong *et al.*, 2008). Most of the established protocols for the differentiation of hESC and iPSC into RPE cells involve the removal of growth factors from culture medium after the cells have reached confluence (Rowland *et al.*, 2013). Such protocols use animal-derived products including feeder cells (mainly mouse fibroblasts), gelatin and media containing fetal bovine serum (Rowland *et al.*, 2013). Several reports have shown that hESC and iPSC can be differentiated into RPE using purified ECM components such as laminin (Gong *et al.*, 2008; Rowland *et al.*, 2013). In addition, neural progenitor cells can express photoreceptor markers after culture on confluent ARPE19 or laminin (Gong *et al.*, 2008). A recent study has shown that the addition of ECM components to a fully-defined, feeder-free culture system assists the growth of iPSCs and the differentiation of pigmented areas from iPSCs and the maintenance of iPSC-RPE (Rowland *et al.*, 2013). For example, the addition of Matrigel, a complex ECM which is rich in basement membrane components, to the media was shown to promote hESC self-organisation into retinal organoids under 3D culture conditions (Boucherie *et al.*, 2013). Another example, hESC derived neural progenitors express RPE markers when cultured on Matrigel and photoreceptor markers when cultured on laminin coated surfaces respectively (Gong *et al.*, 2008). Matrigel and Laminin-111 also support the highest level of pigmentation frequency in iPSC-derived RPE cells (Rowland *et al.*, 2013). Sasai *et al.* have demonstrated that the addition of laminin and entactin to 3D culture promoted the formation of self-organising optic cups from mouse ESCs (Eiraku *et al.*, 2011; Kuwahara *et al.*, 2015).

Given that human retina develops largely *in utero*, it is imperative to understand the expression of ECM components during retinal ontogenesis, in order to use this knowledge to improve the differentiation of pluripotent stem cells into retinal organoids and understand the role of various ECM components in retinal development and disease (Clark *et al.*, 2011; Keenan *et al.*, 2012).

1.5. Aims of the study

The aims of this project were to:

- Investigate the expression of key ECM components in adult mouse, monkey and human retinae so that important ECM expressions in the IPM and BrM can be identified which may be important for outer retinal development, *in vivo* (Chapter 3). Due to the samples availability of adult human retinae and the ECM composition may change in retinae obtained from elderly as retinal changes occur with aging, there is a need to find animal models such as mouse and monkey that are similar to humans in term of ECM expression. Therefore, the ECM expression was studied in the retinae of the three species.

- Determine the temporal and spatial expression of the ECM components during human retinal morphogenesis in order to identify components associated with the development of the outer retina that could potentially enhance the photoreceptor development, *in vitro* (Chapter 3).

- Investigate the expression of key ECM components (Fibronectin, Collagen IV, Versican, Brevican, IMPG1 and IMPG2) and their functions in the development of retinal organoids generated from hESCs and hiPSCs (Chapter 4).

- Examine the impact of culture supplementation with RPE CM, decellularised ECM from adult bovine neural retina (decel NR) and RPE (decel RPE) on the differentiation of pluripotent stem cells (PSCs) to retinal organoids in order to enhance the current differentiation protocol by manipulating the ECM microenvironment to improve the development of retinal organoids and their responses to electrophysiological stimuli, *in vitro* (Chapter 5).

Chapter 2

Chapter 2. Materials and Methods

2.1. Tissue Preparation

2.1.1. Preparation of retinal sections from mouse and macaque monkey

Eyes were retrieved from post-mortem adult macaque monkeys (aged 9-10 years) which had undergone experiments under terminal anaesthesia as part of an unrelated study into the neural control of movement. That study was carried out under the approval of the Newcastle University Animal Welfare and Ethical Review Board, and appropriate licences from the UK Home Office. Mouse eyes were obtained from wild type mice (C57BL/6 background, 7 months old) from the Functional Genetic Unit, Institute of Genetic Medicine, Newcastle University. Mice were sacrificed humanely via cervical dislocation. Mouse and monkey eyes were dissected from the orbit and immediately transferred to phosphate buffered saline (PBS; Sigma-Aldrich, UK). The anterior portion was removed using micro-scissors and forceps, and fixed in 4% (w/v) paraformaldehyde (PFA; Sigma-Aldrich, UK) at 4°C overnight. Eye fixation was followed by dehydration steps through increasing concentrations of ethanol (50%, 70%, 95% and 100%) before clearing in histo-clear (National Diagnostics, USA) and embedding in paraffin wax (pastillated Gurr wax, VWR, UK) (Hewitson and Darby, 2009). 6 μm thick sections were cut on a microtome and collected onto slides (Superfrost Plus, Thermo Fisher Scientific, UK) then stored at room temperature (RT) and protected from light and dust.

2.1.2. Preparation of retinal sections from adult human eyes

Adult human eyes were obtained from Manchester Eye Bank, Manchester Royal Eye Hospital. Three eyes were collected from adult donors 48 hours after death (a female aged 84 years and two males aged 67 and 88 years). The tissue was stored in organ culture medium at 34°C for 7 days before screening for bacteria and fungi using blood agar plates and liquid microbiological media (Armitage *et al.*, 2014). Organ culture medium was composed of Eagle's Minimum Essential Medium (MEM) containing 26 mM sodium bicarbonate, 20 mM HEPES buffer, 2% Fetal Bovine Serum (FBS; Australian origin, Life Technology Ltd, UK), 2 mM L-glutamine, penicillin (100 U/mL), streptomycin (0.1 mg/mL), and amphotericin B (0.25 mg/mL) (Armitage *et al.*, 2014). All consumables used for storage were from (Sigma-Aldrich, UK) except for FBS. Adult human eyes were fixed, dehydrated and embedded according to the method described above, before 8 μm thick sections were collected.

2.1.3. Human Developmental Tissue

Human embryonic and foetal specimens aged between 6-19 weeks of post-conception (PCW) were obtained from the MRC/Wellcome-Trust funded Human Developmental Biology

Resource at Newcastle University (HDBR; http://www.hdbr.org), with appropriate maternal written consent and approval from the Newcastle and North Tyneside NHS Health Authority Joint Ethics Committee. HDBR is regulated by the UK Human Tissue Authority (HTA; www.hta.gov.uk) and operates in accordance with the relevant HTA Codes of Practice. Ready-prepared 10µm paraffin wax sections were collected from the HDBR and stored at 4°C in slide boxes prior to immunostaining.

2.2. Immunohistochemistry (IHC)

2.2.1. IHC using paraffin sections (adult retina and human developing retina)

Expression of ECM proteins was determined using immunohistochemistry (IHC). Tissue sections were dewaxed by two incubations in histo-clear, each 10 minutes at RT. Histo-clear was removed by placing the tissue in 100% ethanol that was changed every 5 minutes 10 minutes. Then, the samples were rehydrated through several incubations in decreasing concentration of ethanol (90%, 70% and 50%), each 5 minutes. Rehydration of the samples was followed by two washing steps in PBS, each 5 minutes (Hewitson and Darby, 2009). For antigen retrieval, the tissue was placed in citrate buffer (pH 6.3; Sigma-Aldrich, UK) and microwaved at 800 watts for 10 minutes. Afterward, the brim containing the sample was allowed to cool for 10 minutes at RT and for another 10 minutes under tap water. The tissue was rinsed in double-distilled water before being washed three times in PBS, each 5 minutes. Non-specific epitope binding was blocked by incubation at RT for 45 minutes with PBS containing 10% FBS. The slides containing the sections were then placed in a dark humidified chamber before adding the primary antibody.

Primary antibodies were diluted in PBS containing 2% FBS (**Table 2-1**), applied on tissue sections (150 µl/slide) and incubated overnight at 4°C. After several washing steps in PBS (3x5 minutes), appropriate fluorescently-labelled secondary antibodies (**Table 2-2**) diluted in PBS containing 2% FBS were added to each tissue section (150 µl/slide) and incubated at RT for 1.5 hours in a dark humidified chamber. To quench the sample auto-fluorescence, tissue sections were incubated in 0.3 % (w/v) Sudan Black (Sigma-Aldrich, UK) (prepared in 70% ethanol) for 15 minutes at RT (Sun *et al.*, 2011), washed in PBS (4x10 minutes), then mounted with Vectashield (Vector Laboratories, UK) medium containing Hoechst (Life Technologies, UK) as a nuclear counter-stain. Cover-slip was applied on each slide, sealed with nail polish and left to dry in a dark box before storage at 4°C.

Table 2-1: List of antibodies used for labelling cells for immunohistological analysis.

Antibody	Tissue	Cat. No.	Host	Antibody Isotype	Source	Dilution
ACAN	ECM	-	Rabbit	IgG	Gift from Prof Timothy Hardingham	1:100
AP2α	Amacrine cells	sc-12726	Mouse	IgG2b	Santa Cruz	1:200
ARL13B	Connecting cilium	ab83879	Rabbit	IgG	Abcam	1:500
Bassoon	presynaptic protein of ribbon synapses	VAM-PS003	Mouse	IgG2aκ	Stressgen Biotechnologies	1:100
BCAN	ECM	ab111719	Rabbit	IgG	Abcam	1:50
CD44	ECM	ab119348	Rat	IgG2b	Abcam	1:100
Collagen IV	ECM	ab6586	Rabbit	IgG	Abcam	1:100
Cone Arrestin	Cone IS	NBP2-41249	Rabbit	IgG	Novus Biologicals	1:100
CRALBP	RPE & Muller cells	ab15051	Mouse	IgG1	Abcam	1:100
CRX	postmitotic photoreceptors	H00001406-M02	Mouse	IgG2a	Abnova	1:200
CRYAA	Lens	-	Mouse	IgG1	Provided by Prof. Roy Quinlan Durham University, UK	1:50
CtBP2	Synaptic Ribbons	612044	Mouse	IgG1	BD Biosciences	1:100
Donkey anti-goat IgG	*IMPG2*-Isotype Control	705-005-147-JIR	Donkey	IgG	Jackson ImmunoResearch	1:1300
Donkey anti-rabbit IgG	*BCAN*-Isotype Control	711-005-152-JIR	Donkey	IgG	Jackson ImmunoResearch	1:65
	Collagen IV-Isotype Control					1:130
	IMPG1-Isotype Control					1:260
FN1	ECM	sc-8422	Mouse	IgG1	Santa Cruz Biotechnology	1:20
Goat anti-mouse IgG1	*FN1*-Isotype Control	NB7508	Goat	IgG1	Novus Biologicals	1:100
Goat anti-mouse IgM	*VCAN*-Isotype Control	NB7494	Goat	IgM	Novus Biologicals	1:100
Goat anti-rat IgG2b	*CD44*-Isotype Control	NB7127	Goat	IgG2b	Novus Biologicals	1:100
Gαt1	Photoreceptors outer segment	sc-389	Rabbit	IgG	Santa Cruz	1:200
HAPLN1	ECM	9/30/8-A-4 mAb	Mouse	IgG2b	Developmental Studies Hybridoma Bank	1:50
HuC/D	amacrine and retinal ganglion cells	A21271	Mouse	IgG2b	Invitrogen	1:200

Table 2-1: List of antibodies used for labelling cells for immunohistological analysis, continued.

Antibody	Tissue	Cat. No.	Host	Antibody Isotype	Source	Dilution
Hyaluronic Acid	ECM	ab53842	Sheep	IgG	Abcam	1:100
IMPG1	ECM	Ab113493	Rabbit	IgG	Abcam	1:100
IMPG2	ECM	sc-103232	Goat	IgG	Santa Cruz Biotechnology	1:200
KI-67	nuclear expression in proliferative cells during late G1, S, G2 and M phases of the cell cycle	ab15580	Rabbit	IgG	Abcam	1:200
NCAN	ECM	AF6508	Sheep	IgG	R&D Systems	1:100
NRL	post-mitotic rod precursors	sc-374277	Mouse	IgG1	Santa Cruz	1:200
Opsin blue (OPN1SW)	S cone photoreceptors	AB5407	Rabbit	IgG	Millipore	1:200
Opsin red/green (OPN1LW/MW)	L/M cone photoreceptors	AB5405	Rabbit	IgG	Millipore	1:200
Pan Heparan Sulfate	ECM	370255-1	Mouse	IgMκ	Amsbio	1:20
PAX6	neural progenitors, retinal progenitors	ab78545	Mouse	IgG1	Abcam	1:200
PKCα	Bipolar cells	610107	Mouse	IgG2b	BD Biosciences	1:200
PROX1	Horizontal & Amacrine cells	AB5475	Rabbit	IgG	Millipore	1:1000
RBP3	IPM	14352-1-AP	Rabbit	IgG	ProteinTech	1:100
RBPMS	retinal ganglion cells	1830-RBPMS	Rabbit	IgG	PhosphoSolutions	1:1000
Recoverin	photoreceptors and midget OFF bipolar cells	AB5585	Rabbit	IgG	Millipore	1:1000
***RetP1 (*Rhodopsin)**	Rod photoreceptors	O4886	Mouse	IgG1	Sigma	1:200
RPE65	RPE cells	ab13826	Mouse	IgG1	Abcam	1:100
RXRγ	post-mitotic cone precursors	sc-555	Rabbit	IgG	Santa Cruz	1:200
Sox1	neuroectodermal tissue, lens vesicle and neural epithelium of adjacent diencephalon	4194	Rabbit	IgG	Cell Signaling Technology	1:200
SPARC	ECM	ab14174	Rabbit	IgG	Abcam	1:100
Syntaxin	presynaptic plasma membrane	S0664	Mouse	IgG1	Sigma	1:200

Table 2-1: List of antibodies used for labelling cells for immunohistological analysis, continued.

Antibody	Tissue	Cat. No.	Host	Antibody Isotype	Source	Dilution
VCAN	ECM	MABT161	Mouse	IgM	Millipore	1:100
vGlut1	synaptic terminals of photoreceptors and bipolar cells	AB5905	Guinea Pig	N/A	Millipore	1:1000
VSX2	retinal progenitor cells & bipolar cells	HPA003436-100UL	Rabbit	IgG	Sigma	1:50
WGA	inner/outer segments of rods/cones	W11261	N/A	N/A	Invetrogen	1:1000

Table 2-2: List of fluorescently labelled secondary antibodies used for immunohistological analysis.

Antibody	Cat. No.	Host	Antibody Isotype	Source	Dilution
anti-donkey DyLight 488	SA5-10062	Rabbit	IgG	Life Technologies	1:800
anti-goat Cy3	305-165-003	Rabbit	IgG	Jackson ImmunoResearch	
anti-guinea pig Cy3	AP108C	Goat	IgG	Millipore	
anti-mouse Alexa 488	A11001	Goat	IgG	Life Technologies	
anti-rabbit Alexa 488	111-545-003-JIR	Goat	IgG	Jackson ImmunoResearch	
anti-rabbit Alexa 647	111-605-144-JIR	Goat	IgG	Jackson ImmunoResearch	
anti-rabbit Cy3	111-165-003-JIR	Goat	IgG	Jackson ImmunoResearch	
anti-sheep Alexa 488	A-11015	Donkey	IgG	Invitrogen	1:500

2.2.2. IHC using cryostat sections (retinal organoids)

Cryostat frozen sections were rinsed three times (3 minutes each) in PBS and incubated in blocking solution (10 % normal goat serum, 0.3 % Triton-X-100 in PBS) for one hour at RT in a humidified chamber. Antibody diluent solution was prepared (1 % bovine serum albumin (BSA), 0.3 % Triton–X-100 in PBS) and used to dilute all antibodies. Tissue sections were incubated with primary antibodies (**Table 2-1**) overnight at 4°C in a humidified chamber. After three washing steps (7 minutes each) in antibody diluent, sections were incubated with the appropriate fluorescently-labelled secondary antibodies (**Table 2-2**) at RT for 1.5 hours in a dark humidified chamber. Afterwards, sections were washed three times (10 minutes each) in PBS and mounted with Vectashield containing Hoechst. Cover-slip was

applied on each slide, sealed with nail polish and left to dry in a dark box before storage at 4°C.

2.3. RPE conditioned medium

RPE conditioned medium (CM) was collected every day from mature (8 months old) RPE monolayers (Trans-epithelial resistance; TER>250Ω) derived from hESC and hiPSC cultured in DMEM:F12 medium (Life Technologies, UK) supplemented with 2% B27 (Gibco, UK) & 1% N2 (Gibco, UK). The RPE cells density was 100,000 cells/ cm^2 and the cells were provided by Ms. Adriana Buskin and Dr. Dean Hallam (Lako's group, Newcastle University). The collected CM was centrifuged at 1000 rpm for 4 minutes to remove cellular material and prevent mixing between cell lines. Then, CM was diluted in 1:3.5 ratio before being added to the cells and filtered using vacuum filtration kit with pore size of 0.22 μm (TPP, UK).

2.4. Decellularised RPE (dRPE) & neural retina (dRetina)

Master student Martin Kiening has performed the RPE & retinal decellularisation procedures from four bovine eyes following a protocol indicated by Medberry *et al.*, 2013 (Medberry *et al.*, 2013). RPE & neural retina were isolated from four adult bovine eyes freshly collected from the abattoir within one hour after slaughter. Using curved scissors, the muscle surrounding the eye was removed and the eyeball was hemisected to remove the cornea and vitreous humour. The retina was peeled very gently from the RPE using a microspatula and immersed into phosphate buffer saline (PBS, Sigma-Aldrich, UK). Then, the RPE was isolated and transferred into PBS. The isolated tissues (RPE/retina) were washed twice with PBS on orbital shaker at 60 rpm for 5 minutes followed by a decellularisation steps. The RPE and retinal decellularisation procedures were performed following a protocol indicated by Medberry *et al.*, 2013 (Medberry *et al.*, 2013).

2.5. ECMs and DNA quantification

Master student Martin Kiening performed a group of colorimetric assays to quantify the amount of collagen, glycosaminoglycan (GAGs), hyaluronic Acid and DNA content in the decellularised RPE and neural retinae, and compared to the native RPE and neural retinae. The concentration of these components was also determined in the RPE conditioned medium and compared to a control-RPE medium.

2.5.1. Hydroxyproline assay

Hydroxyproline assay kit (BioVision, K555-100) was used to quantify the amount of collagen. Hydroxyproline is a common amino acid found in collagen and formed by post-translational modification of proline. As indicated in manufacturer's protocol, samples

(10µl/sample) were transferred to 96-well plate with flat bottom (TTP, UK) and incubated with Chloramine T reagent (100µl/well) at RT for 5 minutes. Then, 100 µl of p-Dimethylaminobenzaldehyde (DMAB) reagent was added to each reaction well and incubated at 60ºC for 90 minutes before the absorbance was measured at 560 nm in a plate reader (Varioskan LUX, Thermo Fisher Scientific, UK). Each sample was run in triplicate and the average absorbance value was calculated. The background value was corrected against a blank value and the concertation of each sample was determined against a standard Hydroxyproline sample (supplied with kit).

2.5.2. Dimethylmethylene blue assay (DMMB)

GAGs concentration was measured using dimethylmethylene blue assay (DMMB) that involves a changing in the absorbance spectrum after the formation of the GAG-DMMB complex. The DMMB regent was prepared and contained the following: 16 mg DMMB in 1 L double-distilled water containing 3.04 g glycine, 1.6 g NaCl and 95 ml of 0.1 M Acetic Acid. The pH of the solution was 3.0 and all the DMMB components were from (Sigma-Aldrich, UK). 20µl of each sample was transferred to a 96-well plate with flat bottom and incubated with DMMB reagent (200µl/sample) for 5 second. Then, the absorbance value was read immediately at 525 nm using Varioskan LUX plate reader. The average value was calculated, corrected against a blank and the concentration was determined against a standard chondroitin 4-sulfate from bovine (Sigma-Aldrich, UK). The concentration of Hyaluronic acid could not be measured using DMMB assay becaause it only reacts with GAGs chain sulfated group. Therefore, turbidimetric measurement assay was used to measure the concentration of Hyaluronic acid.

2.5.3. Turbidimetric measurement of Hyaluronic Acid

Hyaluronic Acid is another ECM component that was quantified using a turbidimetric protocol indicated by Di Ferrante, 1956 based on the formation of insoluble complex between Cetyltrimethylammonium bromide (CTAB; Sigma-Aldrich, H6269-100G) and the isolated acid mucopolysaccharides (Di Ferrante, 1956). The samples were diluted (1:1 ratio) in acetate buffer (0.2M Acetic acid, 0.15M NaCl, pH 6.0). Then, 100µl of the solution (triplicate/sample) was transferred to 96-well plate and incubated at 37.5^{o}C for 15 minutes. Then, 200µl of CTAB reagent (2.5 g of CTAB dissolved in 100ml of 2% NaOH) was added per well and the plate incubated at RT on a plate shaker (300 rpm) for 30 seconds before the absorbance was read at 405 nm using Varioskan LUX plate reader. The absorbance mean value was calculated and corrected against blank. Then, the concentration of Hyaluronic acid was determined against a standard Hyaluronic acid sodium salt from Streptococcus equi (Sigma-Aldrich, UK).

2.5.4. Laminin Quantification

The quantification of Laminin in the native and decellularised RPE and neural retina was performed using a bovine Laminin enzyme-linked immunosorbent assay (Laminin-ELISA) kit (Amsbio, UK) according to the manufacturer's protocol. In brief, Laminin-ELISA is based on competitive ELISA in which the colorimetric signal is inversely proportional to the concentration of Laminin in the sample. The samples were incubated in 96 well-plate pre-coated with polyclonal anti-Laminin antibody conjugated with horseradish peroxidase (HRP) for one hour followed by five washing steps. Then, the wells were incubated with a substrate for HRP enzyme. The enzyme-substrate reaction formed a blue colour and a stopping solution was added to stop the reaction before spectrophotometrically measuring the colour intensity at 450nm using Varioskan LUX plate reader. The mean absorbance value was calculated and the concentration of Laminin was determined against a standard Laminin (supplied with the kit). Since CM PRE was collected from human cells, Laminin quantification in normal and CM RPE was performed on a different ELISA kit from human (Aviva Systems Biology, UK) following the manufacturer's protocol. The kit principle is based on standard sandwich ELISA in which the colorimetric signal is proportional to the concentration of Laminin in the sample. The absorbance was measured as above.

2.5.5. DNA Quantification

The cellular DNA content was measured using Hoechst fluorometric assay following a protocol indicated by Rago *et al*., 1990 (Rago *et al.*, 1990). The samples were diluted (1:1 ratio) in TNE buffer (10 mM Tris, 2 M NaCl, 1 mM EDTA, pH 7.4) contained 20 µg/ml of Hoechst 33258 (Life Technologies, UK). Then, 200µl of the solution (triplicate/sample) was transferred to 96-well plate. The fluorescence intensity was proportional to the amount of DNA in the sample and was measured at 460 nm using Varioskan LUX plate reader. Then, the concentration was determined against a DNA standard from calf thymes (Sigma-Aldrich, UK).

2.6. Human Pluripotent Stem Cells differentiation to retinal organoids

Retinal organoids were generated from two different cell lines: hiPSCs derived from adult fibroblasts (SB-Ad3) (Melguizo-Sanchis *et al.*, 2018) and human embryonic stem cells (H9, Wicell, USA). Stem Cells were expanded in mTeSR™1 (StemCell Technologies, UK) at 37°C and 5% CO_2 on 6 well plates pre-coated with Low Growth Factor Matrigel (Corning, UK) (**Figure 2-1**). The retinal organoids were generated following the method described in Mellough *et al.,* 2015 (Mellough *et al.*, 2015) with the addition of ROCK inhibitor (Y-27632 dihydrochloride, Sigma, UK) (10 µM) for the first 48 hours of differentiation (**Figure 2-2 &**

Table 2-3). Further modifications include the addition of 10% Fetal Calf Serum (Life Technologies, UK), T3 (40 ng/ml; Sigma-Aldrich UK), Taurine (0.1 mM; Sigma-Aldrich UK) & Retinoic Acid (0.5 µM; Sigma-Aldrich UK) from day 18 of differentiation. After 18 days of differentiation the cells were divided into 4 groups with different cultural conditions: Control, RPE CM, decel NR (10 µg/ml) and decel RPE (10 µg/ml) (**Figure 2-2**). Retinal organoids were collected on day 35, 90 and 150 for qRT-PCR and IHC. For IHC, the organoids were fixed in 4% PFA for 20 minutes, followed by three washes in PBS, then overnight cryoprotection in 30% sucrose (Sigma, UK) in PBS before embedding in Optimal cutting temperature (OCT) medium (Cellpath, UK) and freezing at -20°C. Afterward, 10µm cryostat (Leica Cm1860) sections were collected onto Superfrost Plus slides and stored at -20°C in slide boxes prior to immunostaining. For qRT-PCR retinal organoids were collected, washed with PBS and immediately frozen at -80°C. The total number of retinal organoids with phase bright neuroepithelium, neuroepithelium with RPE or only RPE was counted for each experimental condition using a bright field microscope AxioVert (Zeiss, Germany).

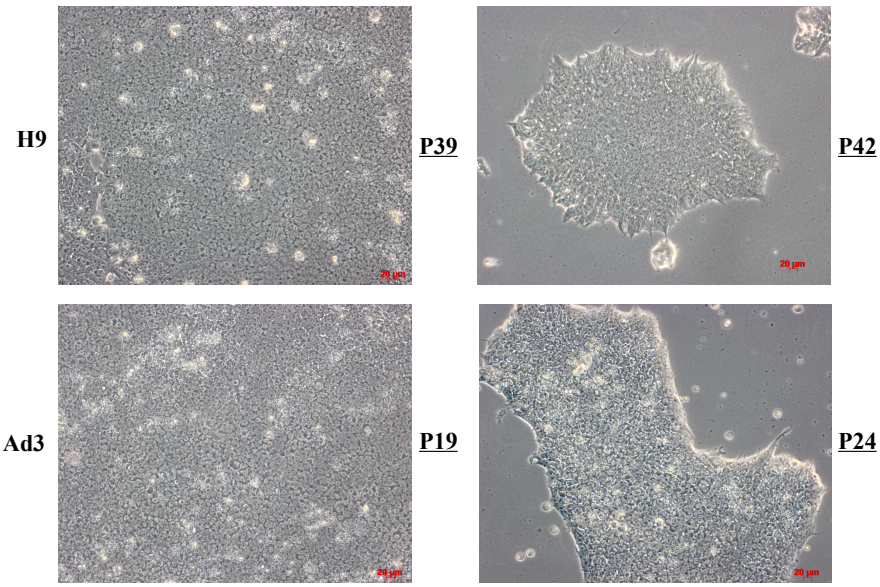

Figure 2-1: Undifferentiated H9 (hESCs) & SB-Ad3 (hiPSCs), cultured on 6-well plate coated with Matrigel. Scale bar =20 µm, (P = passage number).

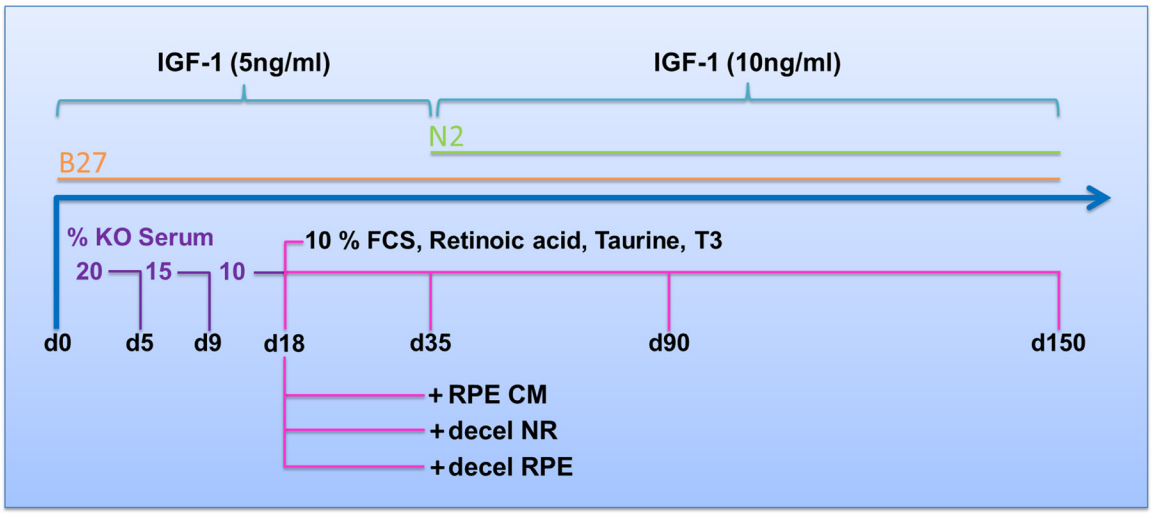

Figure 2-2: Illustrated diagram showing 4 different conditions for differentiating hESCs (H9) & hiPSCs (SB-Ad3) into retinal organoids.

Table 2-3: A list of 4 different cultural conditions for differentiating hESCs (H9) & hiPSCs (SB-Ad3) into retinal linages.

Days of Differentiation	Group	Conditions
0 - 18	All Groups	Basic Medium+ KO serum (Gibco , UK) + IGF-1 (Sigma, UK)
18 - 37	Control	Basic Medium+ FCS+ Retinoic Acid (RA)+ Taurine + T3+ IGF-1
	RPE CM	Basic Medium+ FCS+ RPE condition media+ RA+ Taurine + T3+ IGF-1
	Decel NR	Basic Medium+ FCS+ decellularised neural retina+ RA+ Taurine+ T3+ IGF-1
	Decel RPE	Basic Medium+ FCS+ decellularised RPE + RA+ Taurine + T3 + IGF-1
37 - 150	Control	Basic Medium+ FCS+ RA + Taurine + T3+ IGF-1+ N2 (Gibco , UK)
	RPE CM	Basic Medium+ FCS+ RPE condition media+ RA+ Taurine + T3+ IGF-1+ N2
	Decel NR	Basic Medium+ FCS+ decellularised neural retina+ RA+ Taurine+ T3+ IGF-1+ N2
	Decel RPE	Basic Medium+ FCS+ decellularised RPE + RA+ Taurine + T3 + IGF-1+ N2

Note: Basic Medium include: DMEM:F12 (with L-Glutamine) + B27 supplement (Gibco , UK) + MEM Non-Essential Amino Acids (Gibco , UK) + Penicillin-Streptomycin (100 U/ml, Gibco , UK).

2.7. Blocking IMPG1 and CD44 cellular receptors in retinal organoids

The role of IMPG1 and CD44 in photoreceptor differentiation was investigated using blocking antibodies to IMPG1 (Abcam, UK) and CD44 (Abcam, UK). The antibodies were added (10 μg/ml) to retinal organoid culture medium (Control group) at day 90 and 150 of the differentiation process. After 14 days in culture, the effects of IMPG1 and CD44 receptor inhibition was assessed and compared to a control group which was incubated with (10 μg/ml) non-specific control IgG blocking antibody (Jackson ImmunoResearch, USA). The morphology of the retinal organoids was examined using a bright field microscope AxioVert (Zeiss, Germany).

2.8. Image capture and analysis

Images were captured using an Axio Imager upright microscope with Apotome (Zeiss, Germany) structured illumination fluorescence using 20x objective and 40x oil objective operated with AxioVision software. A range of fluorescent filters were used to cover several dyes including Hoechst, Cy3 and Alexa 488. Tissue sections of two biological replicates of developing human retina and three biological replicates of adult retinae and pluripotent stem cell derived retinal organoids were analysed. Each biological replicate of day 35, 90 and 150 retinal organoids included 10-15 organoids per group. Final images are presented as a maximum projection and adjusted for brightness and contrast in Adobe Photoshop (Adobe Systems).

2.8.1. Image Quantification

Cell image analysis was performed by Dr. Yuchun Ding (Newcastle University, UK) and the cells were quantitatively analysed in the microscopy data using MATLAB software. The data was presented as image segmentation through Hysteresis thresholding technique to segment the cells and filter out any noise background from the images (Zimmer *et al.*, 2002). Furthermore, artefacts were removed manually because they may compromise the accuracy of the analysis. Using measuring property of MATLAB (regionprops), all the pixels of each image were represented as single region in order to extract the information about each cell including the size, average intensity value and length. After obtaining the final segmentation information, the total size and the percentage of the positive cells were calculated and exported as excel file for further analysis.

The quantification and analyses of synaptic markers, Bassoon and CtBP2, were performed by Dr. Birthe Hilgen (Newcastle University, UK) using ImageJ (NIH, Bethesda, MD). For hESCs, 5-7 individual organoids per group and for hiPSCs, 3 individual organoids

per group were analysed. All images were taken with the same exposure time and three squares (500 x 500 pixel) to cover the whole retinal structure were validated in each organoid image. Plaque counts and median intensity were calculated automatically by ImageJ using an intensity threshold (Renyi Entropy) to ensure an accurate count with same conditions for all groups. All results were further analysed using Microsoft Excel and Prism (GraphPad, USA).

2.9. RNA isolation

15-20 retinal organoids were homogenised using Precellys lysing kit (CK28R) (Bertin Technology, UK) and dissociated with RNA lysing buffer provided by RNA extraction kit, RNeasy Plus Mini Kit (Qiagen, UK). Manufacturer's protocol was followed which included passing the cell lysate into two different columns: gDNA eliminator column and RNeasy spin column. The final RNA product were re-suspended in nuclease-free water and stored in -80^{o}C or used for cDNA synthesis, immediately.

2.10. Reverse Transcription

The concentration of RNA samples was measured using NanoDrop 2000 Spectrophotometer (Thermo FisherScientific, UK). Following manufacturer's instructions, 500 ng of extracted RNA was reverse transcribed into cDNA using random primers of Precision nanoScript 2 Reverse Transcription kit (RT-nanoScript2, Primerdesign, UK).

2.11. Quantitative Reverse Transcription Polymerase Chain Reaction (qRT-PCR)

Quantitative reverse transcription polymerase chain reaction (qRT- PCR) was performed on three biological replicates of H9 and SB-Ad3 cell lines and adult human retina as control. Every reaction contained 5 µl of PrecisionPLUS Master Mix with SYBRgreen, 1 µl of cDNA sample, 3 µl of nuclease-free water, 1 µl of primers (10 µM) (**Table 2-4**). 384 wells plates were run on Applied Biosystem Quant Studio 7 Real-Time PCR System (Life Technologies, UK). The cycling protocol consisted of hot-start enzyme activation at 95^{o}C for 2 minutes, followed by 40 cycles of denaturation at 95^{o}C for 15 seconds, annealing/extension at 60^{o}C for 1 minute, and denaturation at 95^{o}C for 1 minute. Following amplification, a melt-curve analysis was performed from 60^{o}C to 90^{o}C with increments every 10 seconds. Each sample was run in triplicate and the average threshold cycle (CT) value was determined. mRNA level was normalised to *GAPDH* using $\Delta\Delta C_T$ method.

Table 2-4: Primers used for qRT-PCR analysis.

Gene	Forward Primer (Sequence (5'->3'))	Reverse Primer (Sequence (5'->3'))	NCBI Reference Sequence
BCAN	AGGAGGCGACAAACTTCGC	AAAAGCGCGGTCCTCTGA	NM_198427.1
FN1	GGTGGAAGTGTGATCCCGTC	CAGGACCACTTGAGCTTGGAT	NM_212482.2
GAPDH	TGCACCACCAACTGCTTAGC	GGCATGGACTGTGGTCATGAG	NM_001256799.2
IMPG1	GCTAGCAGGAAAGTCCCAACT	GTGGAGCTTGAGCCATCTTTT	NM_001563.3
OPSINLW	GCCTACTTTGCCAAAAGTGC	GATGAGACCTCCGTTTTGGA	NM_020061
RBP3	AGATCATGCACACGGATGCC	AGCCATAGCGTTCACCTACA	NM_002900.2
RCVRN	TTCAAGGAGTACGTCATCGCC	GATGGTCCCGTTACCGTCC	NM_002903
RHO	TTTGGAGGGCTTCTTTGCCA	CCTCGGGGATGTACCTGGAC	NM_000539.3
VCAN	TGTTAATCGTGTGGGCCATGA	AGAAGCTGTCTGGCTGGTTG	NM_004385.4
CRX	GTGAGGAGGTGGCTCTGAAG	CTGCTGTTTCTGCTGCTGTC	NM_000554
MATH5	CCCTAAATTTGGGCAAGTGAAGA	CAAAGCAACTCACGTGCAATC	NM_145178

2.12. Electrophysiological recordings

Electrophysiological recordings and analyses of the results were performed by Dr. Gerrit Hilgen (Newcastle University, UK) as follow: 24 hours prior to electrophysiological recordings, 9-cis retinal (10nM; Sigma Aldrich, UK) was added to the incubation medium. Organoids were transferred to 34°C artificial cerebrospinal fluid (aCSF) containing the following (in mM): 118 NaCl, 25 $NaHCO_3$, 1 NaH_2 PO_4, 3 KCl, 1 $MgCl_2$, 2 $CaCl_2$, 10 glucose, 0.5 l-Glutamine and 0.01 9-cis-retinal. Organoids were opened longitudinally and placed, with the presumed RGC layer facing down on the electrodes, onto the 4096 channel multielectrode array (MEA), flattened with a translucent polyester membrane filter (Sterlitech Corp., Kent, WA, USA). The organoids were allowed to settle for at least 2 hours. Recordings were performed on the BioCam4096 MEA platform with BioChips 4096S+ (3Brain GmbH, Lanquart, Switzerland), integrating 4096 square microelectrodes in a 64x64 array configuration.

Light stimuli were projected as described previously (Hilgen *et al.*, 2017a). Broad white (high photopic) light pulses (WLP, 200 ms, 217 µW/cm2 irradiance, 1Hz) were flashed

for 5 min onto the organoids following recording spontaneous activity in the dark for 5 min. Sustained broad blue light stimulation was also used (SBL, 2 min darkness, 2 min SBL, 2 min darkness), same irradiance as WLP), to evoke responses from intrinsically photosensitive RGCs (ipRGCs). The drug cGMP (8-Bromoguanosine 3',5'-cyclic monophosphate, Sigma-Aldrich, MO) was puffed in the recording chamber (final concentration: 100µM) and activity was recorded continuously for 4 minutes, starting at 2 minutes before the puff.

To reliably extract spikes from the raw traces, quantile-based event detection was used (Muthmann *et al.*, 2015). Single-unit spikes were sorted using an automated spike sorting method for dense, large-scale recordings (Hilgen *et al.*, 2017b). Statistical significance (unpaired t-test) and firing rate analyses were evaluated by using MATLAB (Mathworks, MA) and Prism (GraphPad, CA). RGCs were considered responsive if they show at least 25% increase or decrease in spiking activity during 30 seconds after WLP onset compared to a similar time window before the light was turned on. For each cell, all spikes occurring during these two time windows were counted and the mean % change (±SEM) in activity between windows was calculated. All RGCs respond to WLP. To single out ipRGCs, additional analysis of their responses to SBL was performed, taking into account that photoreceptor-driven responses are relatively transient, and therefore stop after a while, whereas intrinsic light responses in ipRGCs are sustained (and generally have a slower onset). Hence, RGCs were classified as ipRGCs if they still exhibited significantly higher firing rate 30-60 s after the onset of the SBL stimulus. All other RGCs were analysed for the WLP protocol (photoreceptor-driven responses).

2.13. Transmission Electron Microscopy

Cells were fixed with 2% glutaraldehyde and kept at 4°C. TEM including all the cell processing was performed at Newcastle University Electron Microscopy Research Services, Ultrathin sections were stained with heavy metal salts (uranyl acetate and lead citrate) and imaged on a Philips CM100 TEM (Philips, Japan).

2.14. Measurements of neuroepithelium thickness

Bright filed images of retinal organoids were taken using a bright field microscope AxioVert (Zeiss, Germany). Morphology of day 90 and 150 retinal organoids were assessed in culture at day 7, 10 and 14 of anti-IMPG1 and anti-CD44 treated groups compared to control. A total

of three biological replicates (n=3) were assessed from each hESCs- and hiPSCs- derived retinal organoids. Measurements of neuroepithelium thickness (a phase bright area typically found at the peripheral side of retinal organoids) were performed using (ImageJ, USA) in day 90 and day 150 retinal organoids (**Figure 2-3**). A scaling system was set for all images of the organoids based on a scaling bar of 100 µm and fine lines were drawn from the apical edge toward the centre of the organoids at different sides to measure the neuroepithelium thickness in µm. A total of 25 measurements (5 measurements / organoid) were taken from each group (control, anti-IMPG1 and anti-CD44) and the neuroepithelium thickness were measured at three time point (day 7, 10 and 14) of the incubation period.

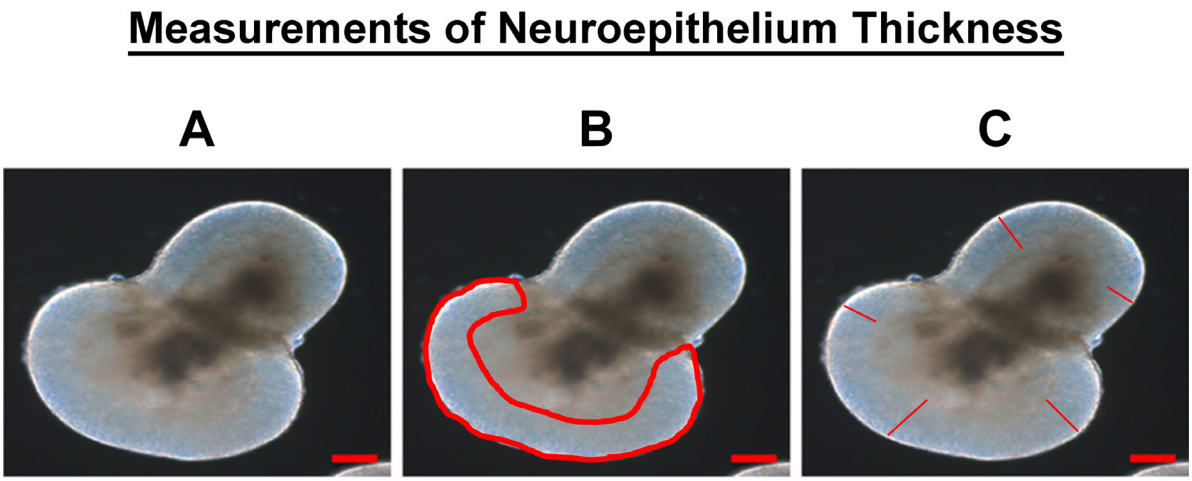

Figure 2-3: Measurements of Neuroepithelium thickness in retinal organoids.
Illustrated figure showing how the thickness of neuroepithelium was measured in the retinal organoids. (A) Bright field images were taken for the retinal organoids and a standard scale was set for measurements based on a 100 µm scale bar. (B) Bright filed Neuroepithelium area was identified on the apical side of the organoids (the area circled in red is an example of the organoid neuroepithelium. (C) 5 measurements were taken per organoid by drawing 5 lines (red) at different areas of the same organoid using (ImageJ, USA).

2.15. Lipofectamine RNAiMAX Transfection

Small interfering RNA (siRNA) studies were performed to validate the specificity of some antibodies used in IHC including fibronectin, brevican versican and IMPG1, where not enough evidence in the literature was found. Lipofectamine RNAiMAX reagent (Invitrogen, UK) was used to transfect stealth siRNA (**Table 2-5**) into undifferentiated hESCs (fibronectin: *FN1*, versican: *VCAN* and brevican: *BCAN*) and hESC- derived retinal organoids at day 150 (*IMPG1*) following the manufacturer's protocol. In brief, Lipofectamine is used for siRNA-mediated gene knockdown experiments on variable types of cells. It is a lipid-based

transfection in which the cationic lipid formulation of Lipofectamine binds to the siRNA and delivers it into the cell cytoplasm. One day before transfection cells were plated on 6-well plate (for qPCR analysis) and 4-well slide chambers (for IHC; Thermo Fisher, UK) coated with Low Growth Factor Matrigel (Corning, UK). The cells were incubated with growth medium without antibiotic and allowed to grow to reach 40-50% confluency at the time of the transfection. Opti-MEM Reduced Serum Medium (Gibco, UK) was used to prepare a mixture of RNAi duplex-Lipofectamine RNAiMAX complex was prepared and a final concertation of 10 nM for each siRNA was added per well/chamber. The cells were incubated 48 hours at 37°C in a CO_2 incubator and medium was changed after 16 hours. Afterward, the medium was removed and the cells were washed in PBS before collection for qPCR and IHC analysis. All siRNA samples were compared to siRNA negative control (Thermo Fisher, UK).

Table 2-5: List of siRNAs used in transfection study

Gene	siRNA Forward Primer (Sequence (5'->3'))	siRNA Reverse Primer (Sequence (5'->3'))	UniGene Reference ID
BCAN	GGGCCAACUGUAUGCAGCCUGGGAU	AUCCCAGGCUGCAUACAGUUGGCCC	Hs.516904
FN1	GCAGUGGCUGAAGACACAAGGAAAU	AUUUCCUUGUGUCUUCAGCCACUGC	Hs.203717
IMPG1	GGUUCCAUAUCUACGAUCCAAUCUU	AAGAUUGGAUCGUAGAUAUGGAACC	Hs.590893
VCAN	CGGAGGCACCUGUUAUCCUACUGAA	UUCAGUAGGAUAACAGGUGCCUCCG	Hs.643801

2.16. Statistical Analyses

All statistical tests were performed using Prism software (GraphPad, USA). The standard errors of all means (SEM) were calculated. Statistical significance of differences was tested with two-tailed Student's t-test for paired samples for neuroepithelium thickness and cell image quantitation or a One-way ANOVA for qRT-PCR and the quantification of synaptic marker proteins. Asterisk = p-value < 0.05, two asterisks = P-value < 0.01, three asterisks = P-value <0.001, four asterisks = P-value <0.0001.

Chapter 3

Chapter 3. Expression of extracellular matrix in adult mouse and monkey retina and adult and developing human retina

3.1. Introduction

The extracellular matrix (ECM) is the non-cellular component of all tissues. It consists of proteins, water and polysaccharides (Frantz *et al.*, 2010) and varies in composition from one tissue to the next (Frantz *et al.*, 2010). The ECM acts as a structural support that facilities cell adhesion via integrins and other adhesion molecules which mediate signalling pathways essential for cell proliferation, migration and differentiation (Streuli, 2009; Fournier *et al.*, 2012; Moreno-Layseca and Streuli, 2014). It also provides biochemical and biomechanical cues that are essential for tissue morphogenesis (Frantz *et al.*, 2010).

Various studies of rat, mouse, chicken and human retina (Popp *et al.*, 2004; Hausman, 2007; Inoue *et al.*, 2009; Clark *et al.*, 2011; Keenan *et al.*, 2012; Kwan, 2014) have shown that the localisation of ECM molecules varies between developmental stages (Keenan *et al.*, 2012) and species (Clark *et al.*, 2011). For example, versican has been identified in the nerve fibres and the inner plexiform layer of the embryonic chicken retina, while in adult chicken it has been found in photoreceptor layer and BrM (Keenan *et al.*, 2012). Hyaluronic acid is found in the IPM of adult chicken retina (Inoue *et al.*, 2009) but in adult human retina hyaluronic acid is widely distributed throughout the whole retina (Clark *et al.*, 2011). During retinal development, different ECM molecules including fibronectin, collagen IV and laminins are required for optic cup morphogenesis (Kwan, 2014). For example, removal of the surface ectoderm and disruption of the surrounding ECM with collagenase resulted in the curvature of the optic vesicle at early stages of invagination and inhibition of subsequent invagination and optic cup formation (Oltean *et al.*, 2016). Another study has demonstrated that blocking the interaction of rat retinal progenitor cells with laminin β2 *in vitro* reduced the fraction of cells that express rhodopsin, suggesting that this laminin could be important for rod photoreceptor differentiation (Hunter *et al.*, 1992). Knockdown of laminin β2 also results in abnormal elongation of photoreceptor outer segments, abnormal electroretinogram, and atypical synaptic formation of rod photoreceptors and apoptosis in mice (Libby *et al.*, 1999).

Collagen IV, laminin and fibronectin are the main ECM components of the basement membranes including BrM and the ILM (Hausman, 2007; Kwan, 2014). Basement membranes are essential for structural support, cellular adhesion, differentiation, proliferation, migration and intercellular communication (LeBleu *et al.*, 2007). Roy *et al.* reported a direct

link between increased expression of fibronectin at the mRNA level and the thickening of BrM in rat animal models of diabetic retinopathy (Roy *et al.*, 2003). Inhibition of fibronectin assembly *in vitro* prevented collagen IV accumulation and thus could be a contributor to the development of fibrotic disease in age-related macular degeneration (Miller *et al.*, 2017). Mutations in collagen IV genes (*COL4A3*, *COL4A4*, or *COL4A5*) were also reported in Alport syndrome (characterised by corneal scarring, temporal retinal thinning, giant macular hole, and maculopathy) patients and mice with ocular anterior segment dysgenesis (Bai *et al.*, 2009; Savige *et al.*, 2015).

The IPM is a highly organised structure that surrounds the inner and outer segments of the photoreceptor cells, and lies between the photoreceptors and the RPE (Ishikawa *et al.*, 2015). It has several prominent functions including: regulating retinoid transport; maintenance of the photoreceptor-specific microenvironment; cellular interactions; and retinal adhesion to the RPE (Ishikawa *et al.*, 2015). A major component of the IPM is hyaluronic acid, a large non-sulfated linear polysaccharide of (1-β-4) D-glucuronic acid and (1-β-3) N-acetyl-D-glucosamine (Ishikawa *et al.*, 2015). Hyaluronic acid is expressed throughout the human retina and is known to bind several other IPM-specific ECM components including hyalectins, IMPG1 and IMPG2, forming a scaffold that fills the IPM (Inoue *et al.*, 2009; Mellough *et al.*, 2014; Mouw *et al.*, 2014; Ishikawa *et al.*, 2015).

Brevican and versican are members of the hyalectins family which has been shown to play an important role in maintaining adhesion between the RPE and neurosensory retina as well as BrM (Keenan *et al.*, 2012). They can bind to hyaluronic acid from their N-terminal region and are involved in the development of the central nervous system (Popp *et al.*, 2004). IMPG1 & IMPG2 are unique proteoglycans found in the IPM and shown to be involved in the development and maintenance of the photoreceptors, in mice and human (Acharya *et al.*, 1998; Kuehn and Hageman, 1999; Chen *et al.*, 2003). *IMPG1* mutations were reported in Vitelliform macular dystrophies leading to impaired metabolism of the IPM and the accumulation of Vitelliform deposits in the sub-retinal space (Manes *et al.*, 2013). A splice mutation in the versican gene (*VCAN,* heterozygous c.9265 + 1G > A nucleotide change in intron 8) was reported in Wagner syndrome patients with retinal detachment (Rothschild *et al.*, 2013), whilst mutations in *IMPG2* cause progressive degeneration of the photoreceptors, leading to autosomal dominant retinitis pigmentosa (Bandah-Rozenfeld *et al.*, 2010; Manes *et al.*, 2013). CD44 acts as the primary receptor for hyaluronic acid and also allows adhesion to other ECMs such as Versican, Brevican and Aggrecan (Brun *et al.*, 2003; Dicker *et al.*, 2014).

It interacts with the glycosaminoglycans (GAGs) of IMPG1 and may participate in retinal adhesion (Kuehn *et al.*, 2000).

Given that human retina develops largely *in utero*, it is imperative to understand the expression of ECM components during retinal ontogenesis, in order to use this knowledge to improve the differentiation of pluripotent stem cells to retinal organoids and understand the role of various ECM components in retinal development and disease (Clark *et al.*, 2011; Keenan *et al.*, 2012). To date, there has been limited detailed analysis of ECM component distribution during human retinal development and so the functional importance of ECM in retinal ontogenesis is poorly understood (Reinhard *et al.*, 2015). Preceding any experiment to study the ECM components during human retinal development, it is important to investigate their expressions in adult human retina. However, the ECM composition may change in retinae obtained from elderly as retinal changes occur with aging. Therefore, there is a need to find animal models such as mouse and monkey that are similar to humans in term of ECM expression.

3.2. Aims

The first aim of this chapter was to investigate the expression of several ECM components (Fibronectin, Collagen IV, Versican, Brevican, Neurocan, Aggrecan, Hyaluronic Acid, HAPLN1, IMPG1, IMPG2, pan-HS and SPARC) in adult mouse, monkey and human retinae so that important ECM expressions in the IPM and BrM can be identified which may be important for outer retinal development, *in vivo*. A further aim was to determine the temporal and spatial expression of these ECM components during human retinal morphogenesis using IHC in order to identify components associated with the development of the outer retina that could potentially enhance the photoreceptor development *in vitro*.

3.3. Results

The expression data obtained from this study are largely IHC and such a validation of antibody specificity is an important consideration. To address this, widely used controls for IHC were employed including: (***i***) omission of primary antibodies (**Figure 3-1**); (***ii***) replacement of primary antibodies with isotype controls (for collagen IV, fibronectin, brevican, versican, IMPG1, IMPG2 and CD44) (**figure 3-2**); (***iii***) usage of antibodies that have been widely published and validated in other studies. For example, the IMPG2 antibody used in this study was validated through incubation with pre-immune serum and shown to be expressed in the IPM of human retina by Acharya *et al.* (Acharya *et al.*, 2000). In addition,

the collagen IV antibody used in this study showed a similar expression in BrM of pig retina (Miura *et al.*, 2010) and the size of CD44 protein detected with the same antibody used in this study was confirmed by western immunoblotting by Enkhjargal *et al.* (Enkhjargal *et al.*, 2017).

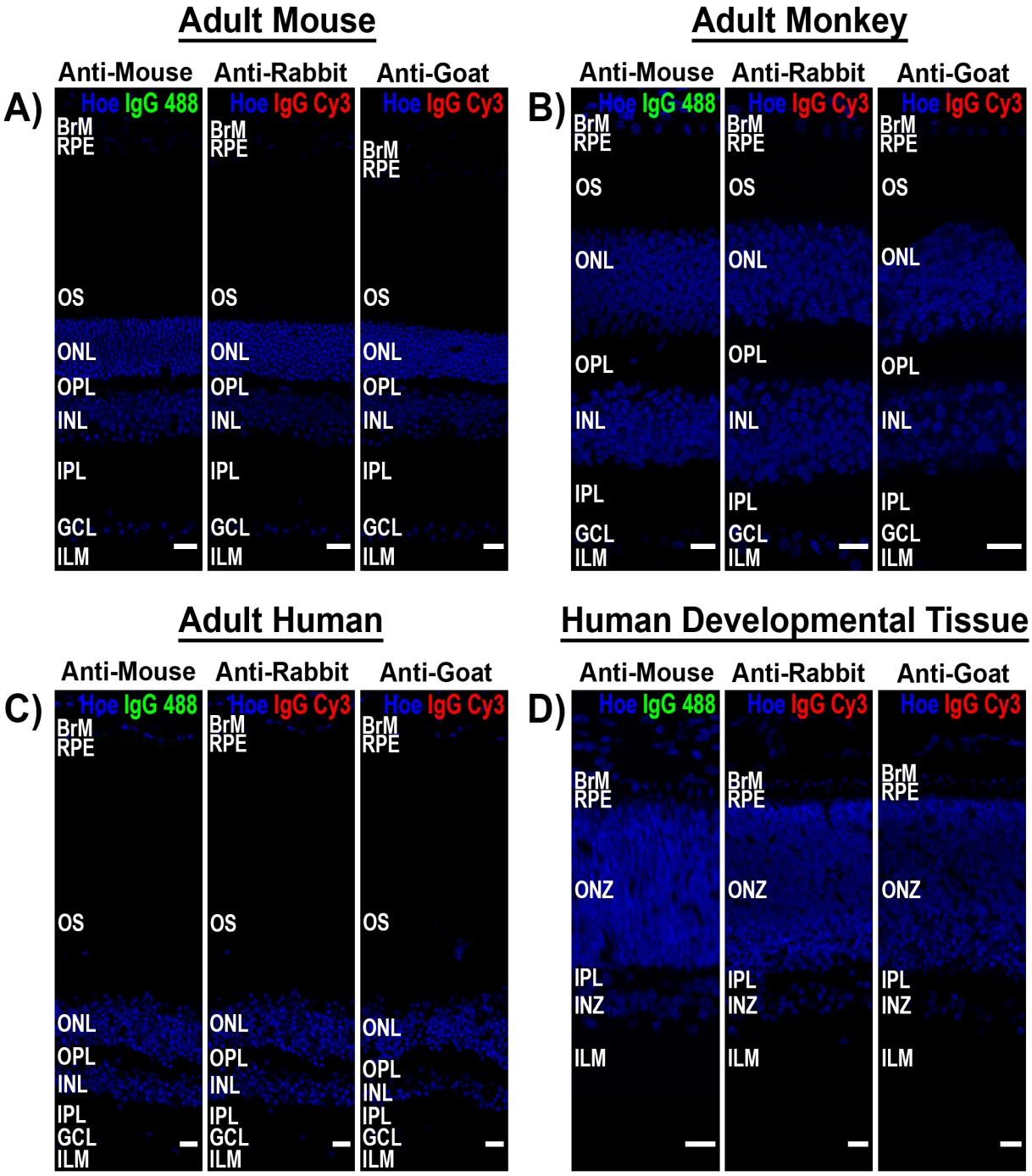

Figure 3-1: Immunostaining of secondary antibody controls in adult mouse and monkey retinae, adult and developing human retinae and retinal organoids derived from hESCs. Different secondary antibodies (anti-mouse (IgG) Alexa Fluor 488, anti-rabbit (IgG) Cy3, and anti-goat (IgG) Cy3) were used to differentiate non-specific background signals in tested tissues: adult mouse retina (A), adult monkey retina (B), adult human retina (C) and human developing retina (19 PCW) (D). Scale bars = 20µm.

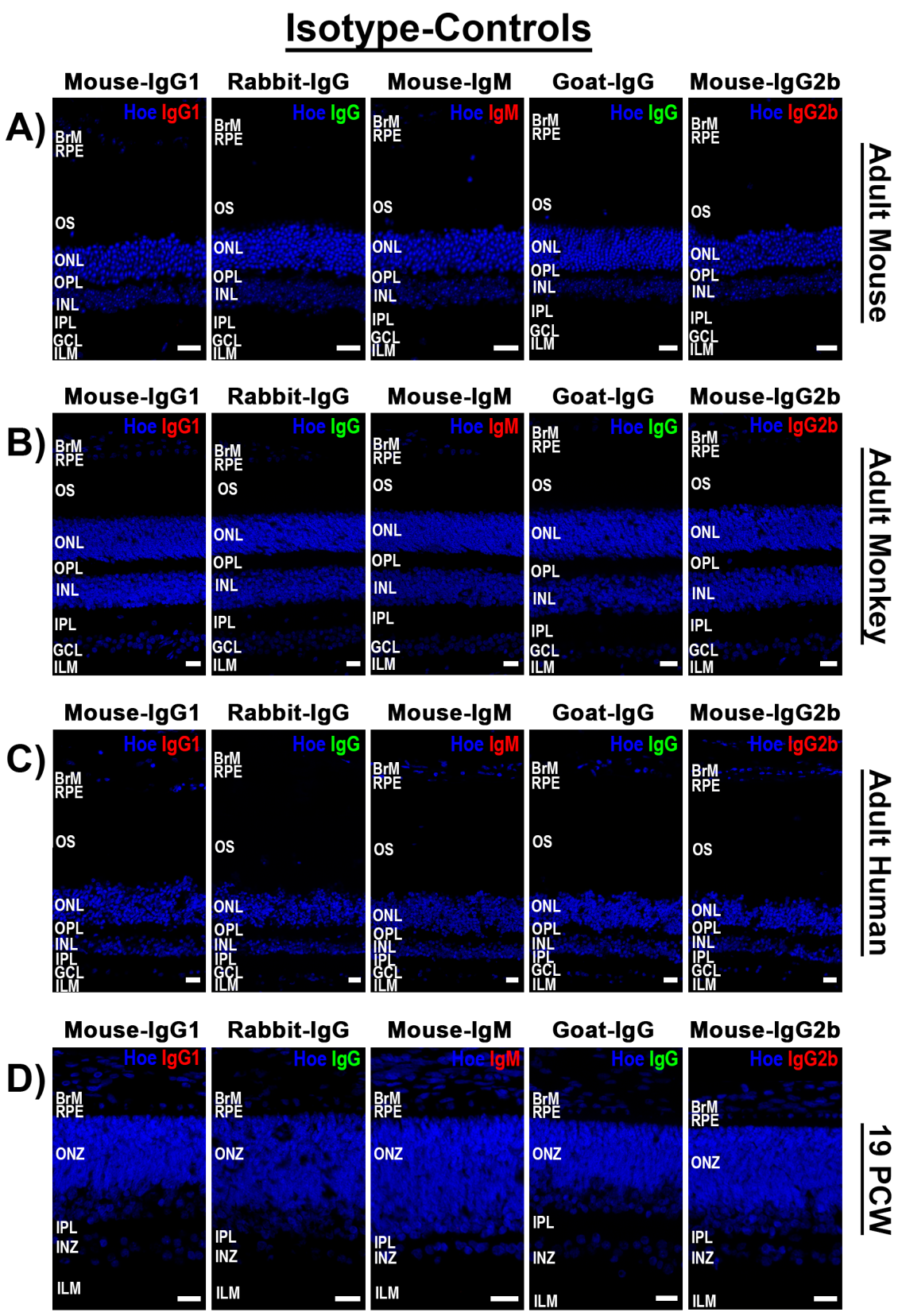

Figure 3-2: Immunostaining of isotype controls to ECM antibodies in adult mouse and monkey retinae, adult and developing human retinae.

Isotype controls matching primary antibodies isotypes were used to differentiate non-specific binding of immunoglobulin to tested tissues: adult mouse retina (A), adult monkey retina (B), adult human retina (C) and human developing retina (19 PCW) (D). Scale bars = 20µm.

3.3.1. Distribution of basement membrane glycoproteins in adult mouse, monkey and human retinae

In order to understand retinal ECM composition in adult retina, IHC was performed on adult mouse, monkey and human retinae. Fibronectin and collagen IV were expressed in BrM in adult mouse, monkey and human retinae (**Figure 3-3**). Fibronectin was also expressed in the ILM in all three species (**Figure 3-3**). Fibronectin and collagen IV expression around blood vessels was also observed in monkey (fibronectin) and human adult retina (collagen IV). Collagen IV has also moderate staining in the INL, IPL and GCL layers in adult human retina (**Figure 3-3**).

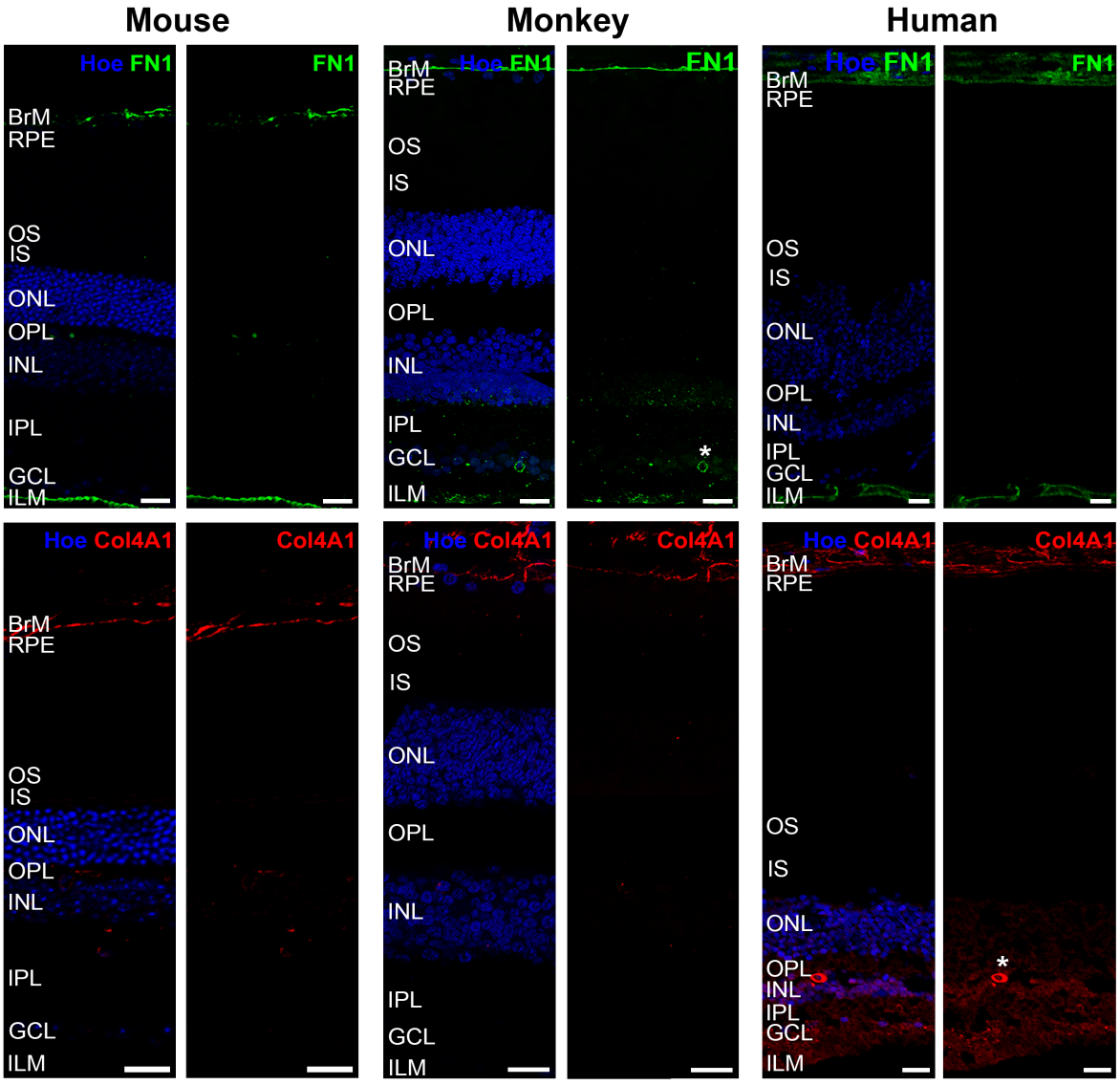

Figure 3-3: Immunostaining of fibronectin (FN1) and collagen IV (Col4A1) in adult mouse, monkey and human retina.
Antibody labelling with and without Hoechst (Hoe) are shown. FN1 and Col4A1 were expressed in BrM in all species. FN1 was also expressed in the ILM. Stars indicate FN1 and Col4A1 expression around blood vessels. Scale bars = 20µm.

3.3.2. Distribution of hyalectins and hyaluronan in adult mouse, monkey and human retinae

Aggrecan, versican, brevican and neurocan are members of the hyalectins family that contain binding domains to hyaluronic acid (Mouw *et al*., 2014). Versican expression was conserved across adult mouse, monkey and human retinae (**Figure 3-4**) with strong expression around the outer segments of the photoreceptors, and partially co-localised with the IPM marker, (Retinol Binding Protein 3) RBP3 (**Figure 3-4**). Versican was faintly expressed in other retinal layers of mouse, monkey and adult human retina (INL and GCL in mouse; ONL and INL in monkey; ONL, INL and GCL in human retina). The expression of Brevican varied between all three species; showing expression in the RPE, around outer and inner segments of photoreceptors, outer plexiform layer, INL and GCL in adult mouse retinae, all retinal layers except outer segment in adult monkey retinae, and the INL, IPL and GCL in adult human retinae (**Figure 3-4**).

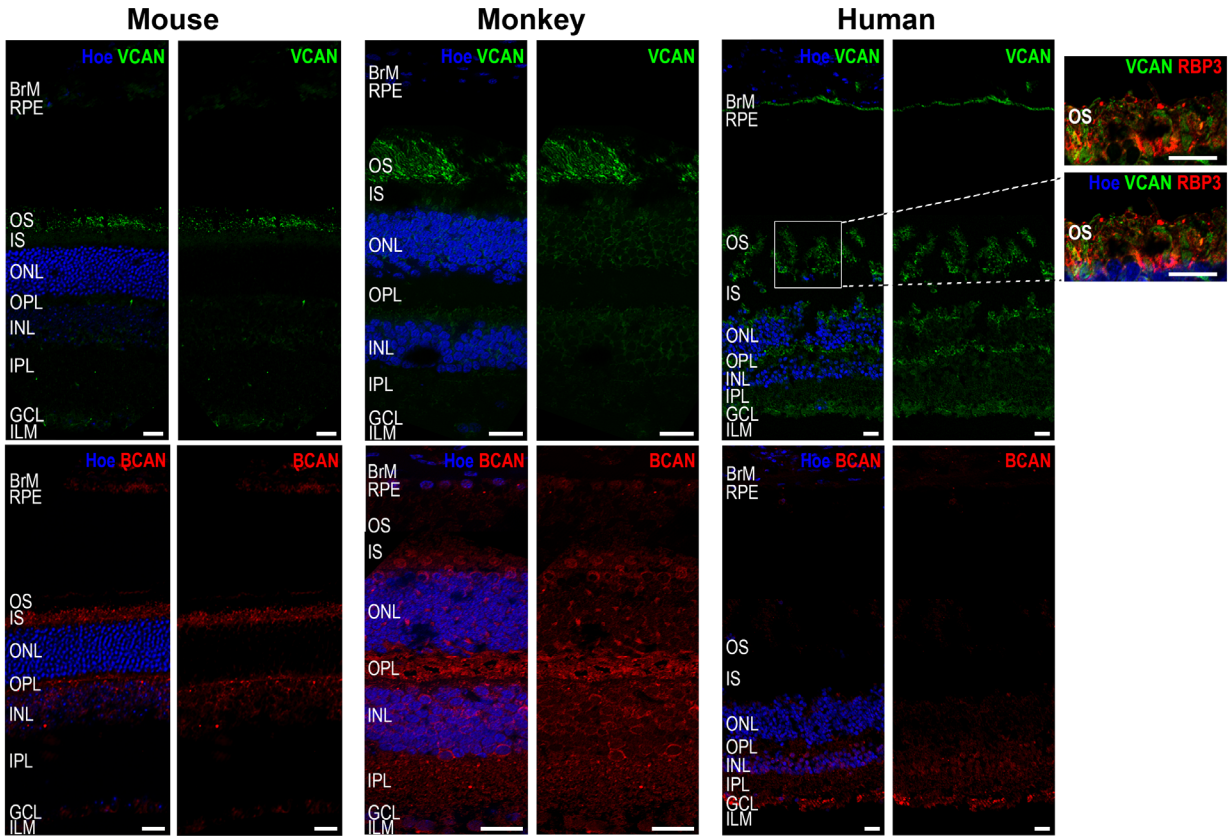

Figure 3-4: Expression of Versican (VCAN) & Brevican (BCAN) in adult mouse, monkey and human retina.
Antibody labelling with and without Hoechst (Hoe) are shown. Smaller boxes show double labelling of Versican with RBP3 in the human retina. Scale bars = 20µm.

Neurocan was expressed in the plexiform layers (OPL & IPL) with moderate expression in the INL and GCL layers in the adult mouse, monkey and human retinae (**Figure**

3-5). Aggrecan expression varied between the three species. It was expressed in several layers including RPE, around IS, INL and GCL in mouse retinae. In monkey retina, aggrecan expression was observed in RPE and all retinal layers (**Figure 3-5**). However, strong immuno-reactivity of aggrecan was only detected in BrM in adult human retinae (**Figure 3-5**).

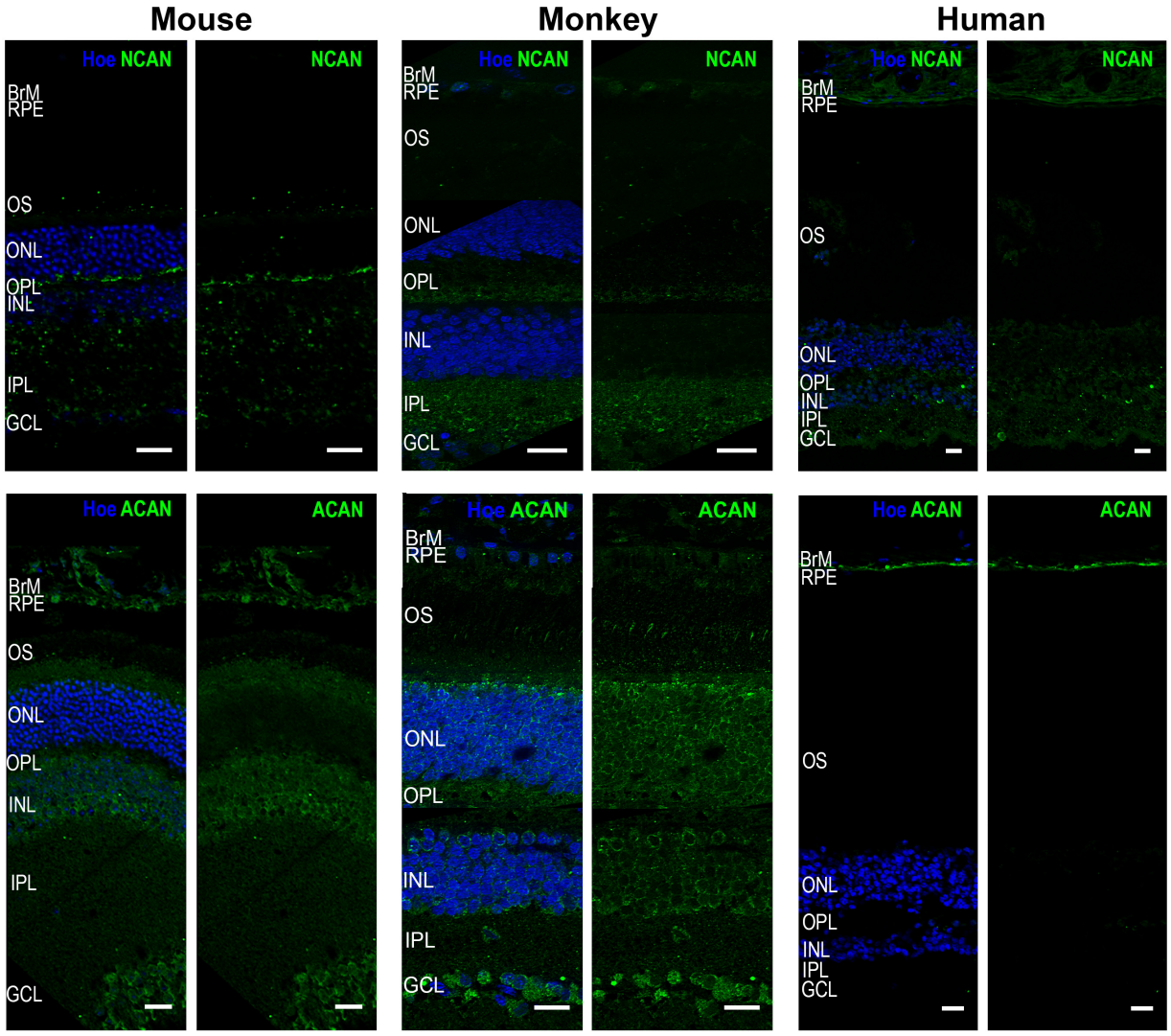

Figure 3-5: Expression of Neurocan (NCAN) & Aggrecan (ACAN) in adult mouse, monkey and human retina.
Antibody labelling with and without Hoechst (Hoe) are shown. Scale bars = 20µm.

The expression of hyaluronic acid was observed throughout the retina of all three species: strong staining was detected in the OPL, INL and GCL and moderate staining in the RPE layer, around IS, and IPL in mouse retinae; moderate staining in the RPE, OPL, INL, IPL and GCL layers in monkey retinae; and strong expression the ONL and moderate staining in the OPL, INL, IPL and GCL layers in human retinae (**Figure 3-6**). HAPLN1 is a cartilage link protein that stabilise the interactions between hyalectins and Hyaluronic Acid (Keenan *et al.*, 2012). Strong immuno-reactivity of HAPLN1 was detected around OS in adult monkey and

human retinae (**Figure 3-6**). HAPLN1 was also expressed in the RPE and GCL in adult human retina. However, different expression of HAPLN1 was detected in adult mouse retina including: strong expression in the INL and GCL; and moderate in the ONL (**Figure 3-6**).

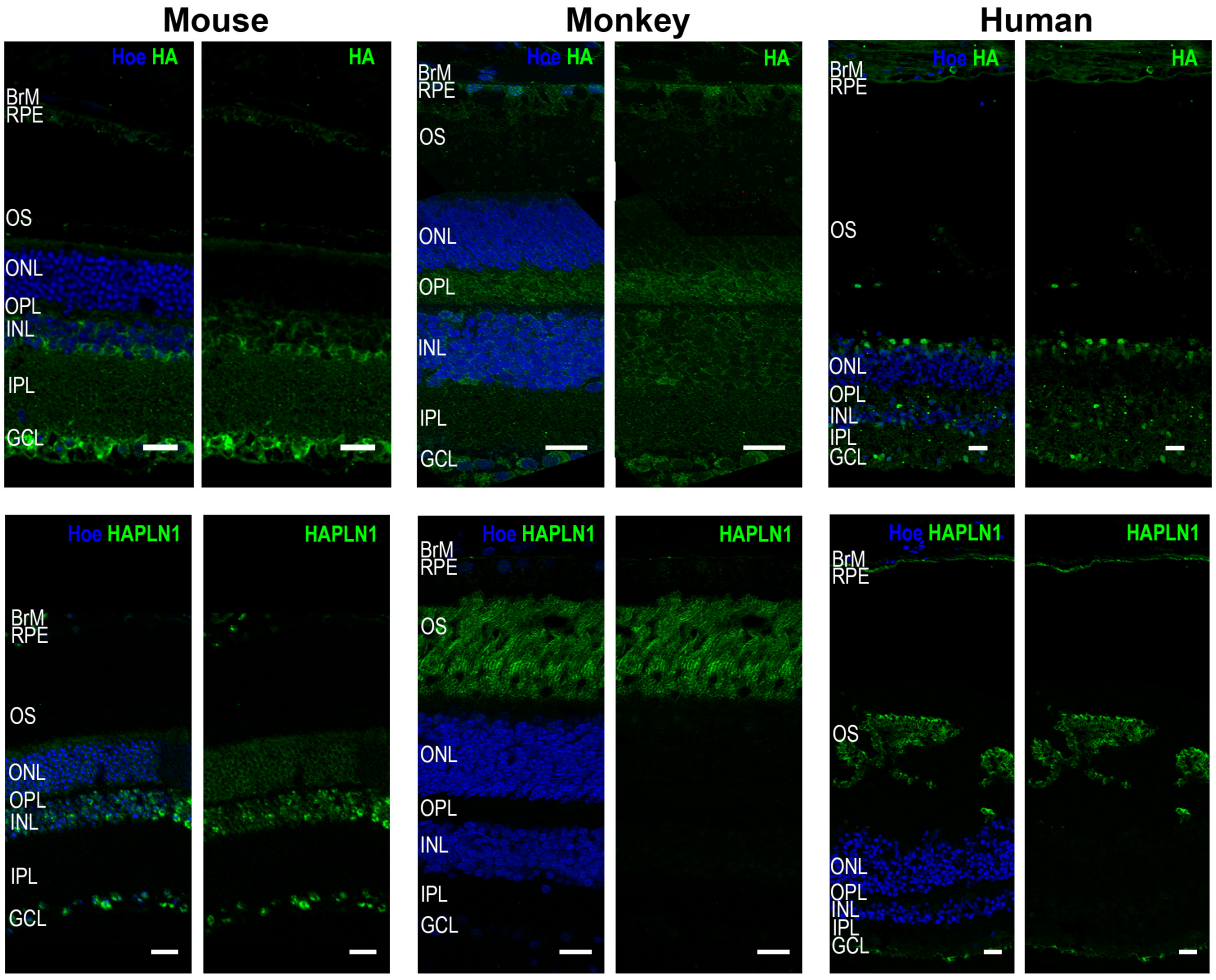

Figure 3-6: Expression of Hyaluronic Acid (HA) & Hyaluronan and proteoglycan link protein 1 (HAPLN1) in adult mouse, monkey and human retina.
Antibody labelling with and without Hoechst (Hoe) are shown. Scale bars = 20µm.

3.3.3. Distribution of photoreceptors specific ECM and other ECM components in adult mouse, monkey and human retinae

The expression profiles of IMPG1 & IMPG2 were conserved across the three species examined (**Figure 3-7**). Remarkably, both IMPG1 and IMPG2 were strongly expressed around the outer segments of the photoreceptors in the adult human and monkey retina (**Figure 3-7**), however, expression around both inner and outer segments was observed in the mouse retina (**Figure 3-7**). In adult human retina, IMPG1 was expressed in the rod photoreceptor outer segments as shown by co-expression with the rod marker Rhodopsin (**Figure 3-7**). It was not possible to perform co-immunostaining of IMPG1 with the cone

markers (OPN1MW/LW) because the antibodies were raised in the same species, however the widespread expression of IMPG1 immunostaining in the outer segments indicates that these may include cone photoreceptors too (**Figure 3-7**). IMPG2 expression did not co-localise with Rhodopsin or opsin staining, thus indicating that IMPG2 is expressed around but not in the outer segments themselves.

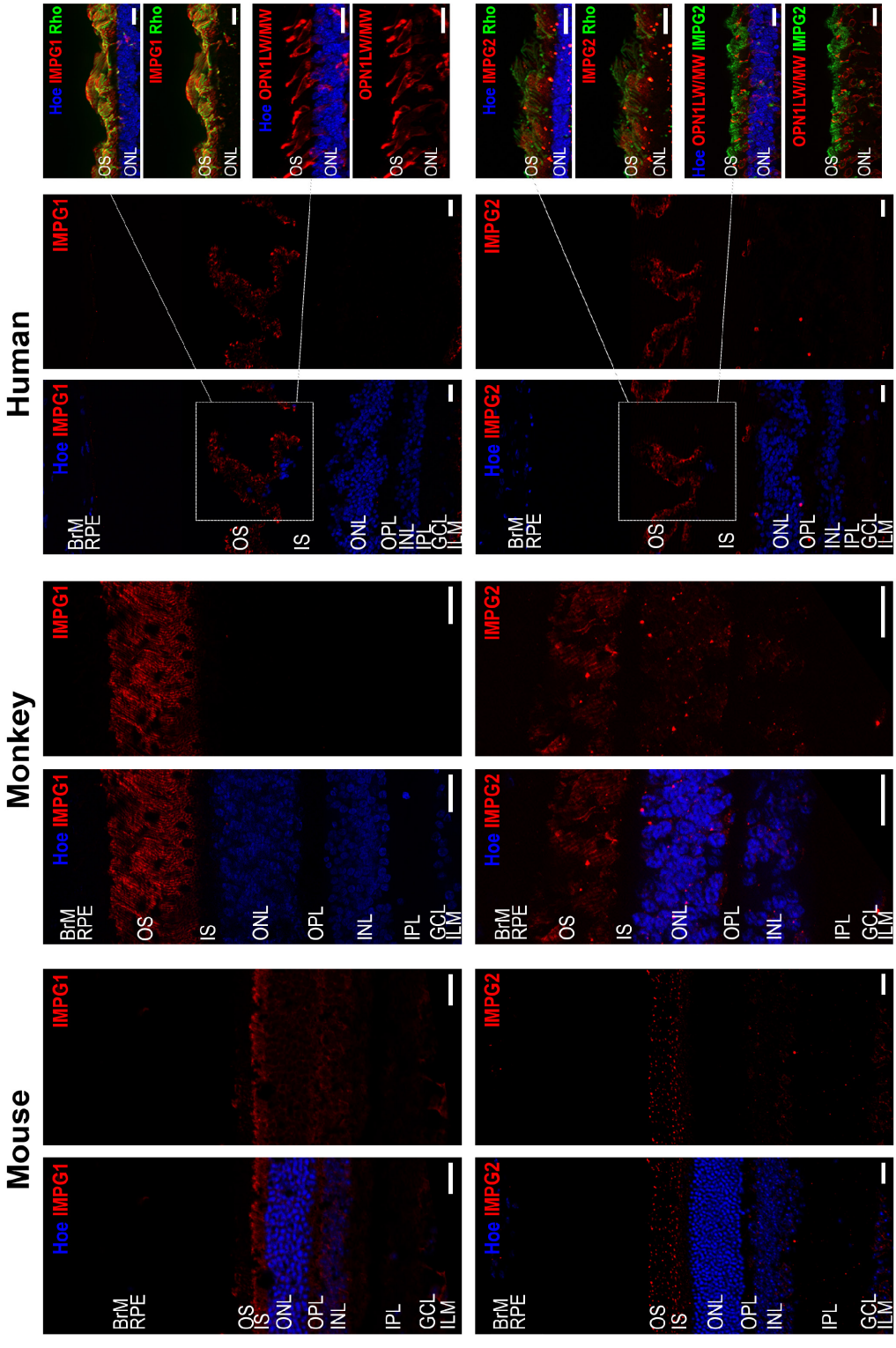

Figure 3-7: Expression of Interphotoreceptor Matrix Proteoglycan 1 (IMPG1) & Interphotoreceptor Matrix Proteoglycan 2 (IMPG2) in adult mouse, monkey and human retina.
Antibody labelling with and without Hoechst (Hoe) are shown. IMPG1 and IMPG2 were expressed around the photoreceptor outer segments in the adult human and monkey retina, and expressed around both inner and outer segments in the mouse retina. Small insets show double labelling of IMPG1 with Rhodopsin and OPN1LW/MW on adjacent sections; and IMPG2 with Rhodopsin and OPN1LW/MW in human retina. Scale bars = 20µm.

The anti-Pan Heparan Sulfate antibody (pan-HS, 10E4) identifies a common N-sulfated epitope within HS that facilitates the determination of the overall distribution of HS in the retina (Clark *et al.*, 2011). Pan-HS expression was differently widespread throughout the retinae of the three species: strong expression in the INL and moderate staining in the RPE, around IS, ONL and GCL layers in mouse retina; strong expression in the RPE and GCL, and moderate staining in the ONL, OPL, INL and IPL layers in monkey retina; RPE, ONL, OPL, INL and GCL layers (strong expression in the GCL) in human retina (**Figure 3-8**). SPARC expression was also different between the three species: strong in the INL and GCL, and moderate in the RPE layer, IS, and OPL in mouse retina; moderate expression in the ONL, INL and GCL layers in monkey retina; and strong expression in the INL and GCL, and moderate in the OPL and IPL in adult human retina (**Figure 3-8**).

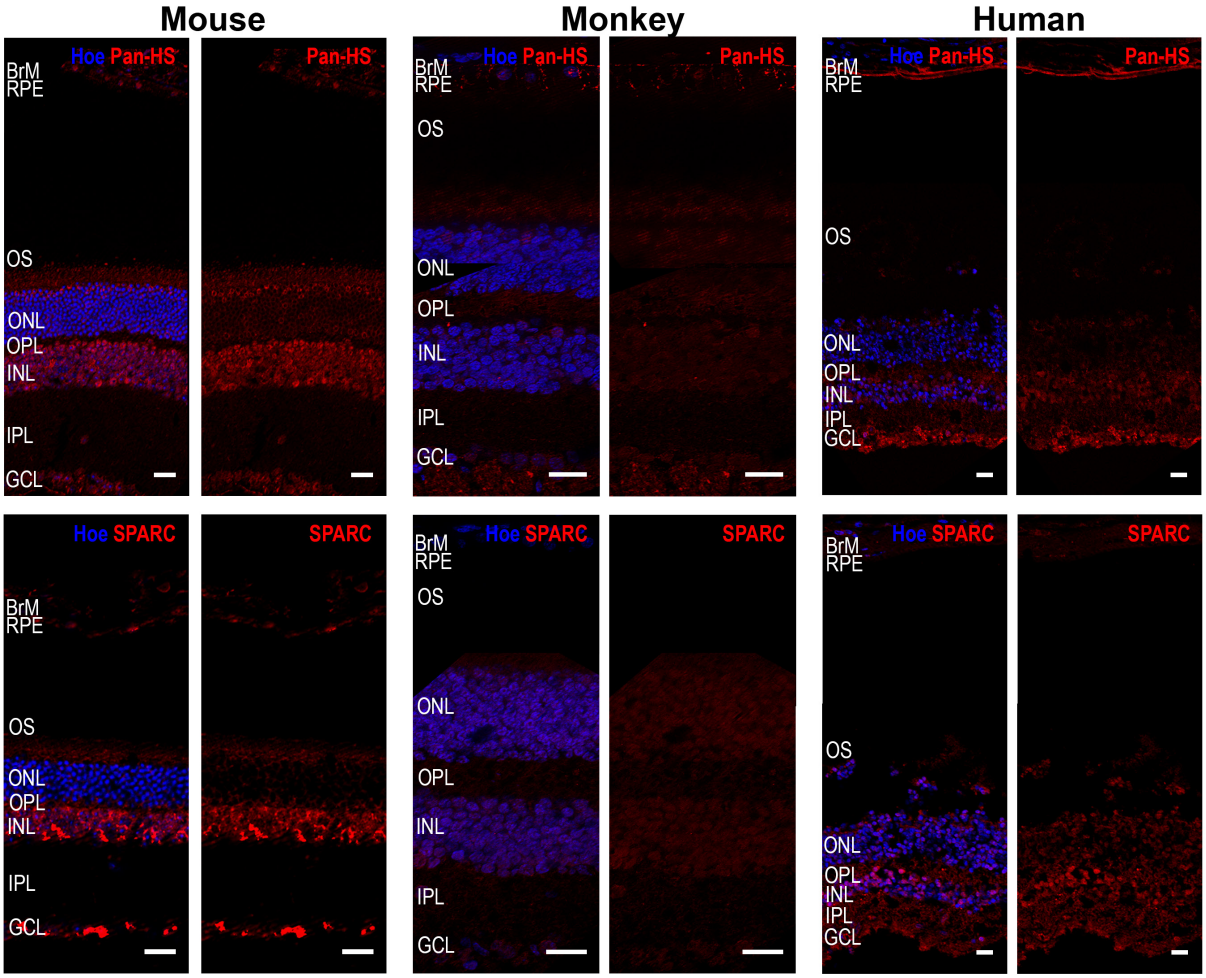

Figure 3-8: Expression of Pan Heparan Sulfate (Pan-HS) & Secreted protein acidic and rich cysteine (SPARC) in adult mouse, monkey and human retina.
Antibody labelling with and without Hoechst (Hoe) are shown. Scale bars = 20µm.

3.3.4. Distribution of basement membrane glycoproteins in developing human retina

Collagen IV and fibronectin are two major components of the basement membranes. Collagen IV was expressed in the choroid and BrM during the 6 -19 PCW (**Figure 3-9A**). This result was further corroborated by adjacent expression of the RPE marker, RPE65 (**Figure 3-9C**). Collagen IV was also expressed in the hyaloid artery and lens capsule during the 6 PCW suggesting that it might play an important role in their development. Faint expression of collagen IV was also detected in the RPE, Outer Neuroblastic Zone (ONZ), Inner Plexiform Layer (IPL) and Inner Neuroblastic Zone (INZ) across all stages (**Figure 3-9A**). The expression pattern of collagen IV was consistent with the expression observed in adult human retina described in the previous section.

Fibronectin was expressed in BrM during the 12-19 PCW (**Figure 3-9B**). In addition, expression was detected in the ILM in the 17 PCW and in the Choroid in 14-19 PCW (**Figure 3-9B**). The expression pattern of fibronectin in BrM and ILM was consistent with the expression observed in adult human retina. Double staining of fibronectin with collagen IV confirmed that both of these ECM components were expressed in BrM, although in different parts with fibronectin localised more basally than collagen IV (**Figure 3-9D**).

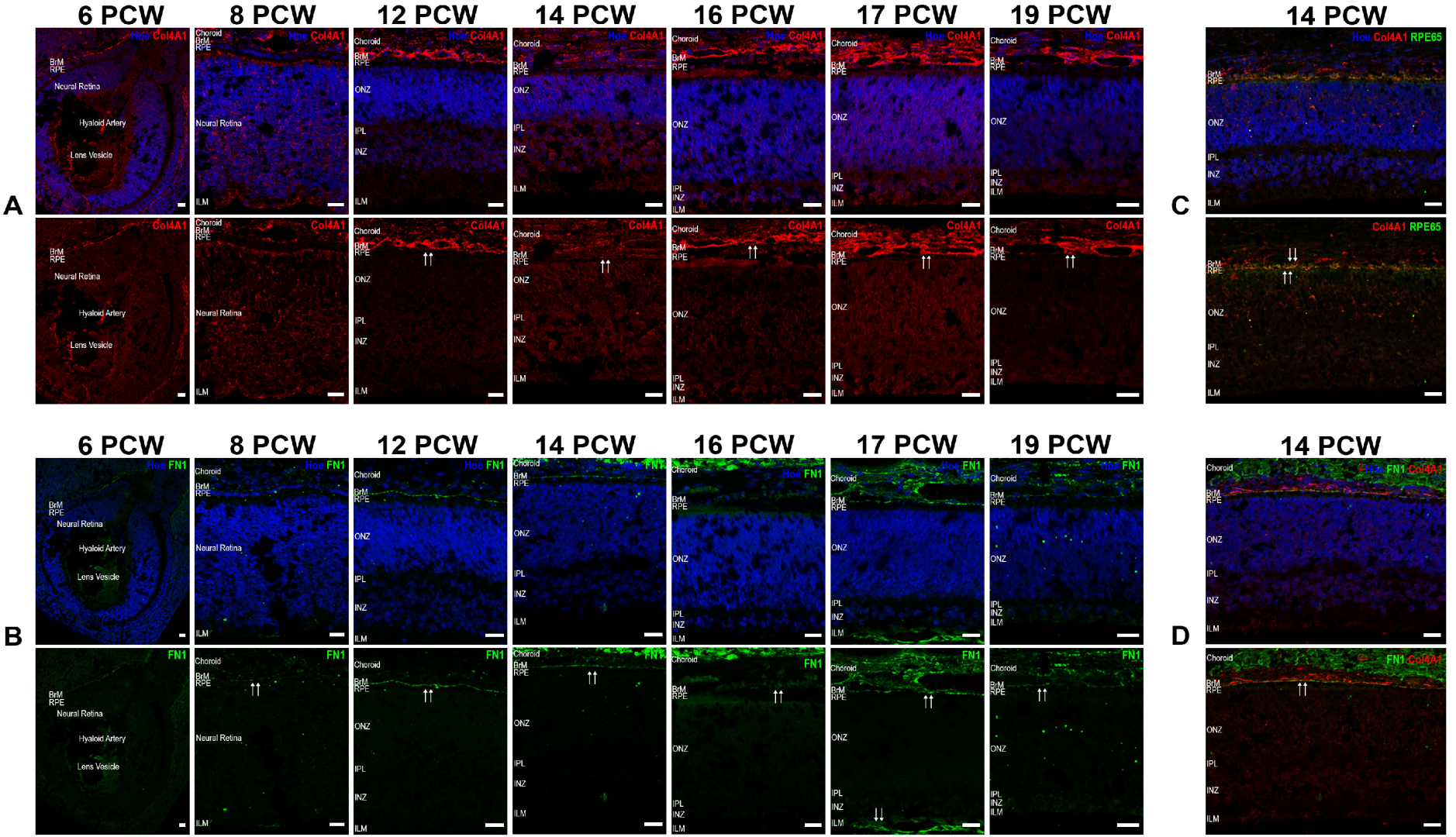

Figure 3-9: Expression of Collagen IV (Col4A1) & Fibronectin (FN1) in the human embryonic and foetal eye.
(A, B) Sagittal sections through the developing human eye showing antibody labelling with and without Hoechst (Hoe) during the 6-19 PCW. Scale bar =20 µm. Arrows indicate Col4A1 expression in BrM, FN1 expression in BrM and ILM.

3.3.5. Distribution of hyalectins and hyaluronan in developing human retina

The expression of brevican was observed throughout the retina (ONZ, IPL and INZ) across all developmental stages (**Figure 3-10A**). Strong expression of brevican was detected around developing photoreceptors (**Figure 3-10C**, inset) and in the emerging space between the RPE and ONZ, often referred as the IPM, during the 12-19 PCW (**Figure 3-10A**). Brevican was also detected in the surface ectoderm in 6 PCW and in the neural retina at 6 and 8 PCW (**Figure 3-10A**). Versican was expressed throughout the retina and strongly expressed around the developing photoreceptors and IPM during the 12-17 PCW (**Figure 3-10B**). Co-expression studies indicated that brevican and versican were both expressed in the developing IPM; however their expression did not overlap entirely **(Figure 3-10C**). Versican expression did, however, overlap with the IPM marker RBP3 and was located above Recoverin-positive labelled photoreceptors (**Figure 3-10D**), thus corresponding with the expression observed in adult human retina.

Neurocan was strongly expressed in the IPL and ILM in 17-19 PCW (**Figure 3-11A**). Neurocan expression was not detected until 12 PCW in the IPL layer (**Figure 3-11A**), and its expression pattern in IPL was consistent with the expression previously observed in adult human retina. Expression of aggrecan was throughout the retina across all developmental stages with stronger expression in INZ than other layers (**Figure 3-11B**). Aggrecan was also expressed in the lens capsule in 6 PCW and dorsal-nasal gradient of the retina in 8 PCW (**Figure 3-11B**).

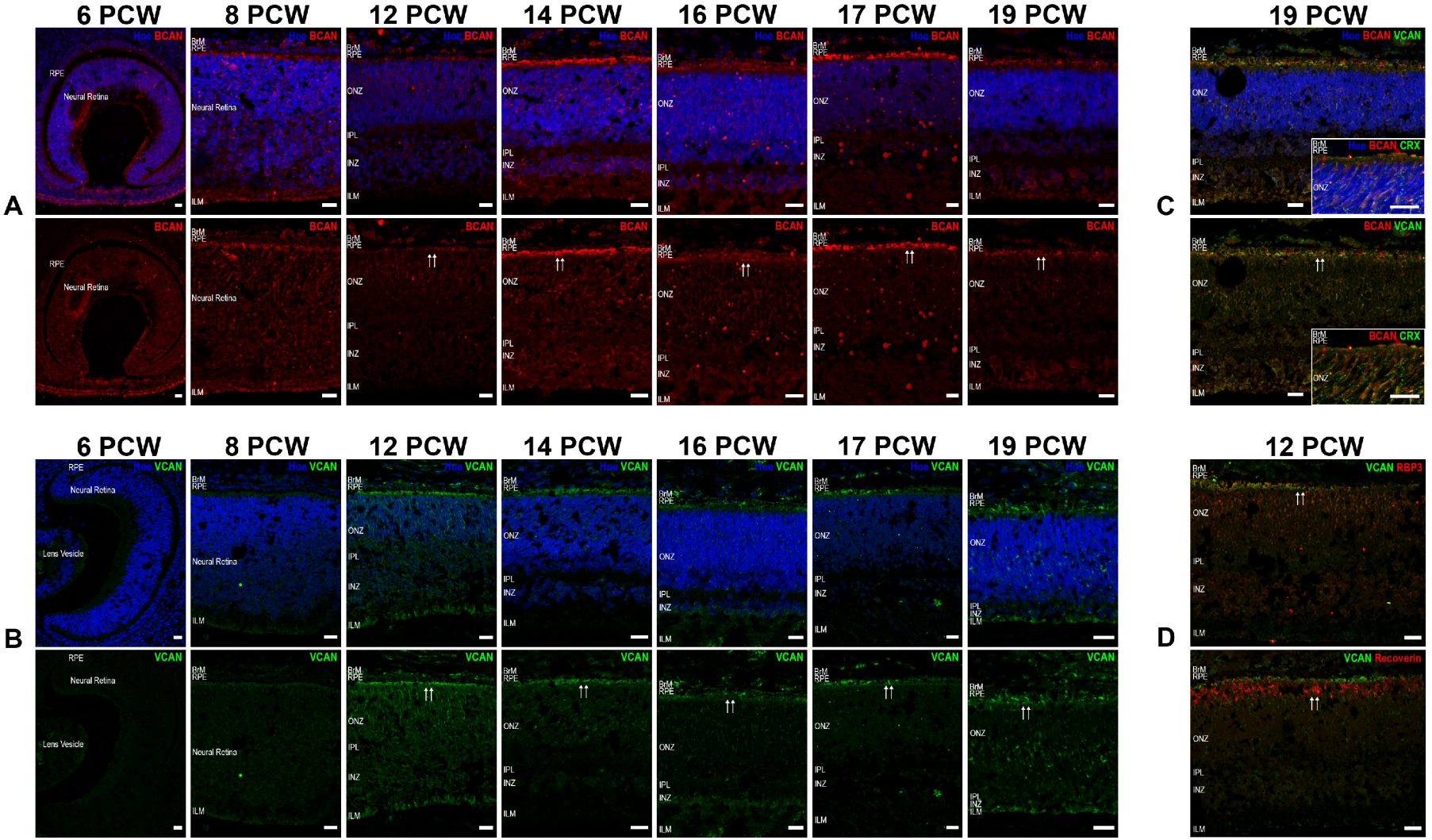

Figure 3-10: Expression of Brevican (BCAN) & Versican (VCAN) in the human embryonic and foetal eye.
(A, B) Sagittal sections through the developing human eye showing antibody labelling with and without Hoechst (Hoe) during the 6-19 PCW. Scale bar =20 µm. Arrows indicate BCAN & VCAN expressions in IPM. Punctate foci visible in the 16 and 17 PCW images in panel A is due to background staining.

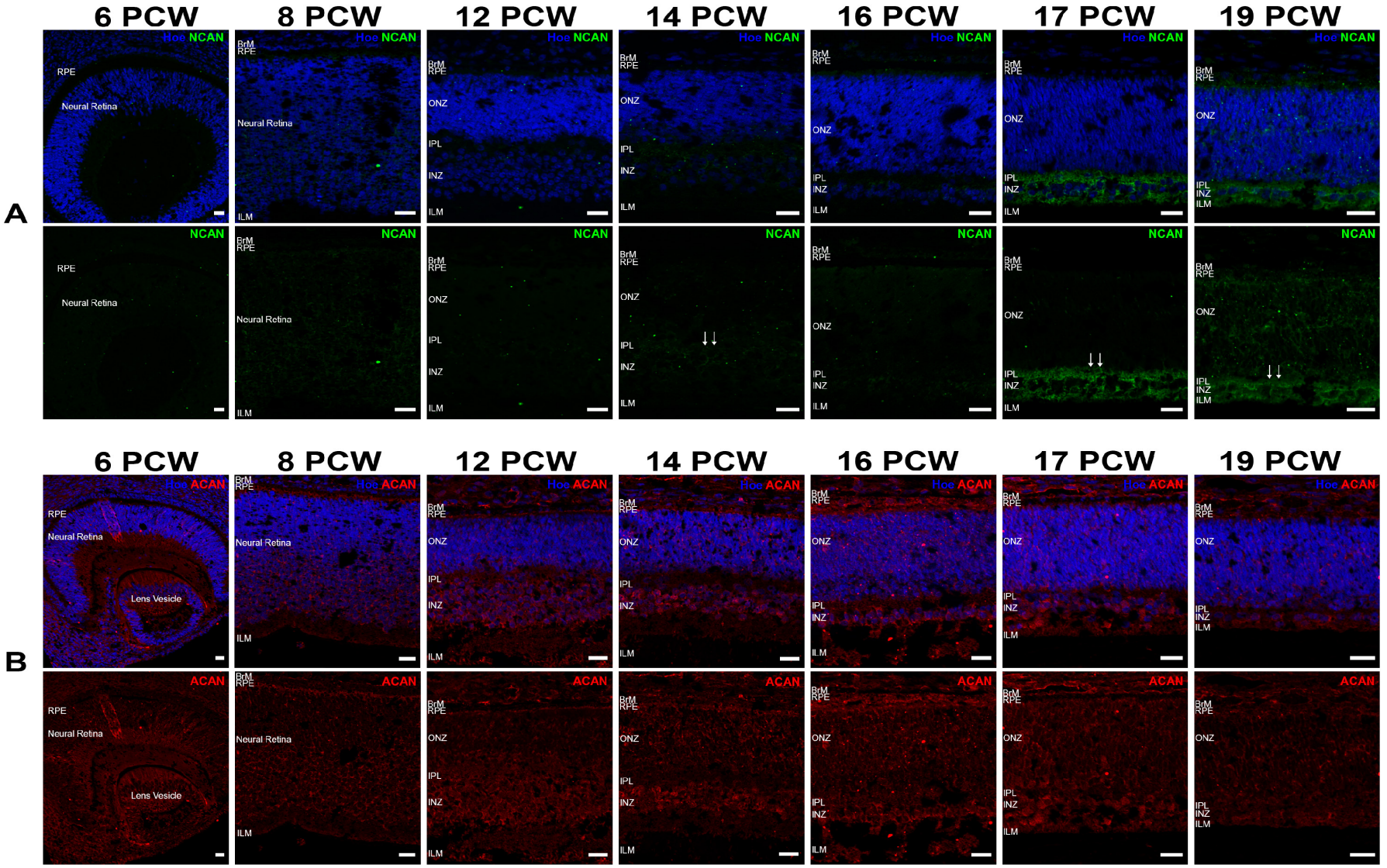

Figure 3-11: Expression of Neurocan (NCAN) & Aggrecan (ACAN) in the human embryonic and foetal eye.
(A, B) Sagittal sections through the developing human eye showing antibody labelling with and without Hoechst (Hoe) during the 6-19 PCW. Scale bar =20 µm. Arrows indicate NCAN expression in IPL and ILM .

The expression of hyaluronic acid was throughout the retina across all developmental stages with stronger expression in the developing IPM (**Figure 3-12A**). Co-expression of hyaluronic acid with RBP3 (IPM marker) was observed in 14 PCW (**Figure 3-12C**). HAPLN1 was strongly expressed in BrM and INZ across all developmental stages (**Figure 3-12B**). It was also expressed in the lens capsule in 6 PCW. As illustrated in **Figure 3-12D**, tissue was double labelled with HAPLN1 and SOX1 (lens marker) or RBPMS (retinal ganglion cells marker) to confirm the localisation of HAPLN1. Co-expression of HAPLN1 with RBPMS was observed in 17 PCW suggesting that HAPLN1 was expressed in retinal ganglion cells (**Figure 3-12D**). Moreover, the distinct lens morphology in 6 PCW and using SOX1 in staining indicated that HAPLN1 was expressed in the lens capsule (**Figure 3-12D**).

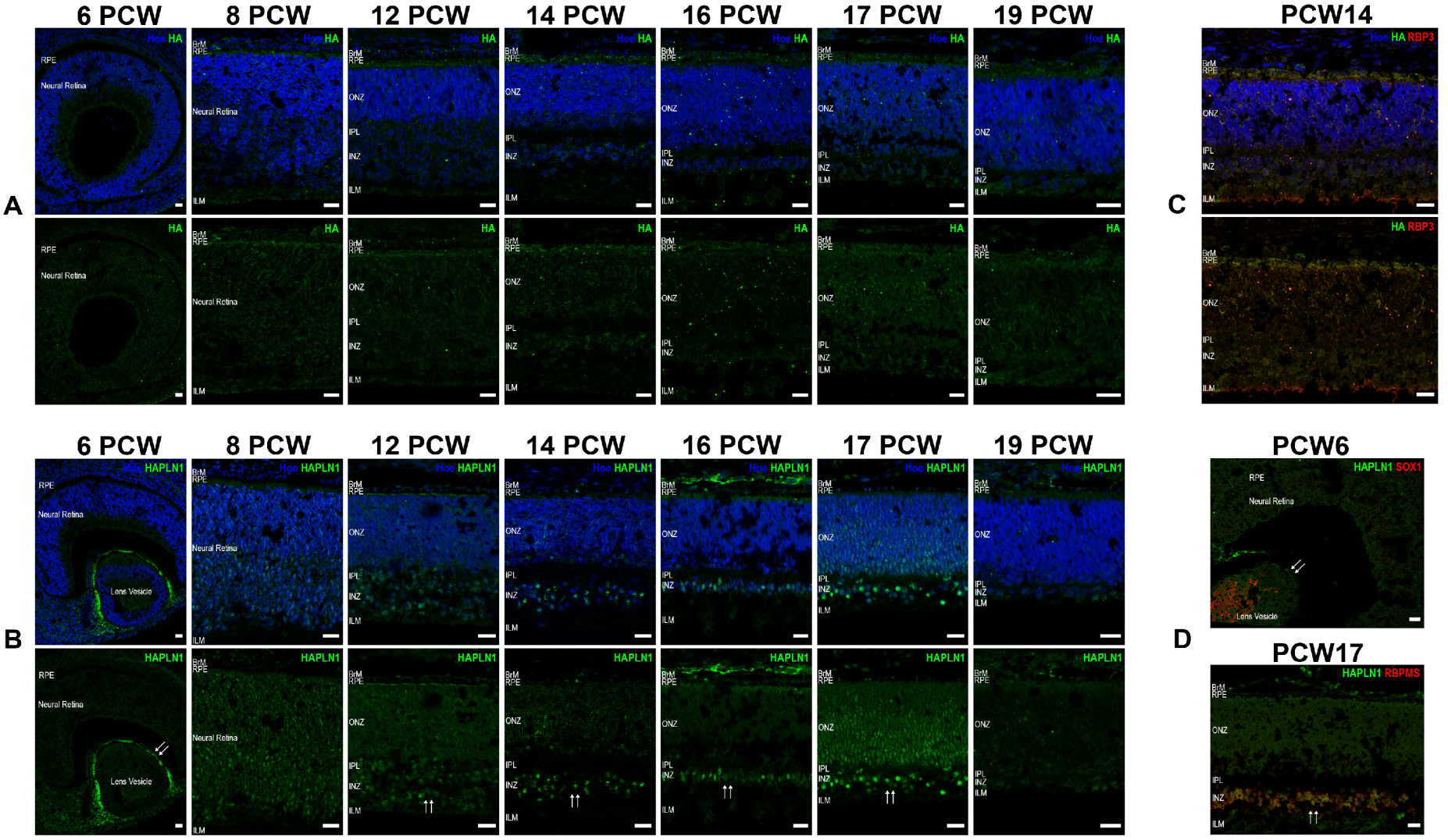

Figure 3-12: Expression of Hyaluronic Acid (HA) & Hyaluronan and proteoglycan link protein 1 (HAPLN1) in the human embryonic and foetal eye.

(A, B) Sagittal sections through the developing human eye showing antibody labelling with and without Hoechst (Hoe) during the 6-19 PCW. Scale bar =20 µm. Arrows indicate HAPLN1 expression in INZ and lens capsule.

3.3.6. Distribution of photoreceptors specific ECM and other ECM components in developing human retina

Strong expression of IMPG1 was observed around the developing photoreceptors and emerging IPM during the 12-19 PCW (**Figure 3-13A**). This was confirmed by the co-expression of IMPG1 with versican (**Figure 3-13C**). IMPG1 expression was also detected across the neural retina from the 6-19 PCW. Co-expression of IMPG1 with CRYAA (a lens-specific marker) was observed in the lens in 6 PCW suggesting that IMPG1 might be important for lens development (**Figure 3-13C**). IMPG2 expression was not detected until the 17 PCW (**Figure 3-13B**). Co-expression of IMPG2 with Recoverin in the ONZ was observed in 19 PCW suggesting that IMPG2 is expressed by the developing photoreceptors (**Figure 3-13D**). Co-expression of IMPG2 with RBP3 was also found in the developing IPM, thus corroborating the expression observed in the adult human retina (data not shown).

Pan-HS was expressed throughout the retina across all developmental stages (**Figure 3-14A**). Pan-HS was also expressed in the lens capsule in 6 PCW. This result was further investigated by double staining Pan-HS with SOX1 (**Figure 3-14C**). The distinct lens morphology in 6 PCW and using SOX1 in staining indicated that Pan-HS was expressed in the lens capsule. SPARC was not expressed until 17 PCW with strong expression in INZ and ILM (**Figure 3-14B**).

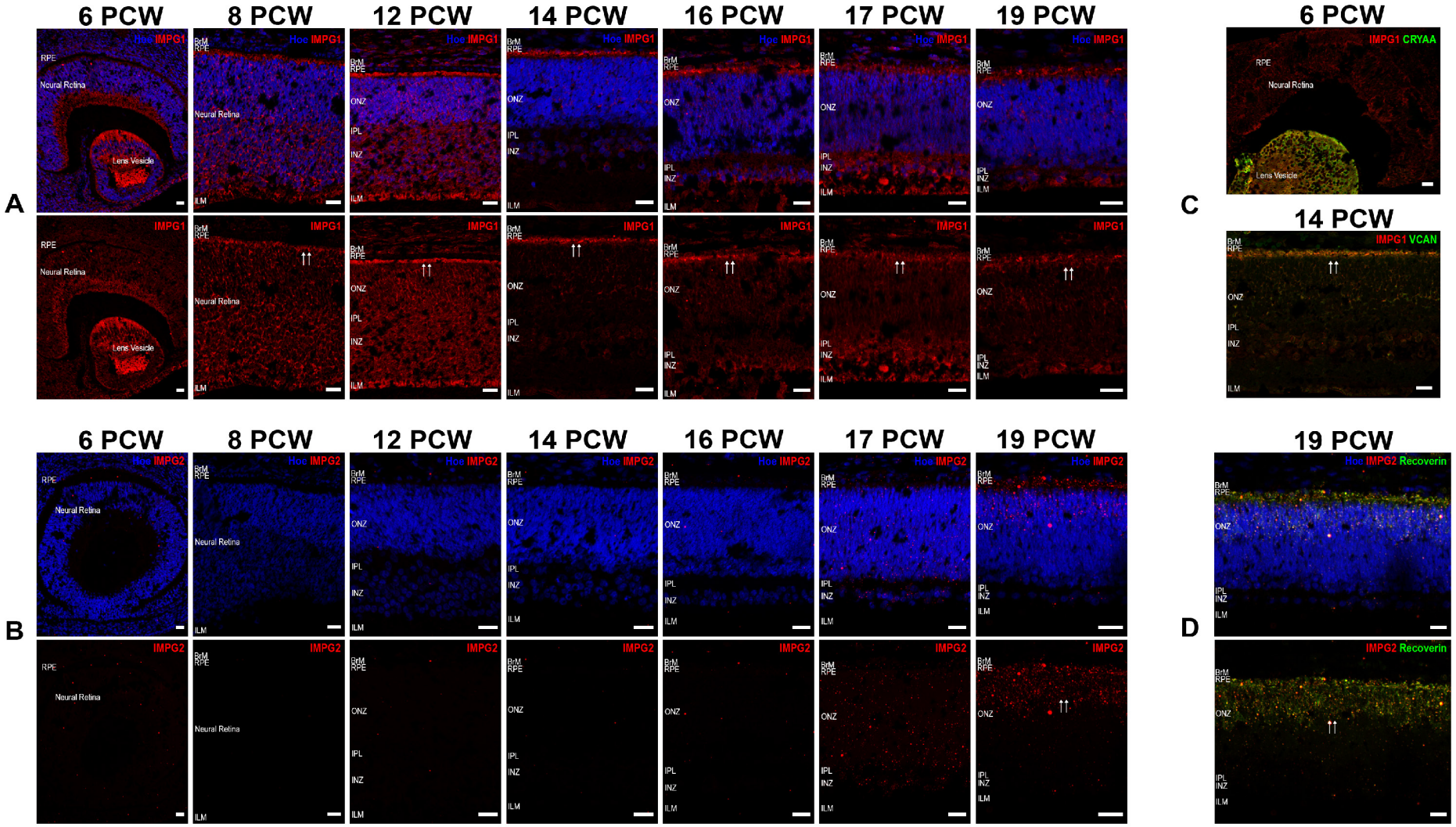

Figure 3-13: Expression of Interphotoreceptor Matrix Proteoglycan 1 (IMPG1) & Interphotoreceptor Matrix Proteoglycan 2 (IMPG2) in the human embryonic and foetal eye.

(A, B) Sagittal sections through the developing human eye showing antibody labelling with and without Hoechst (Hoe) during the 6-19 PCW. Scale bar =20 µm. Arrows indicate IMPG1 & IMPG2 expressions in IPM.

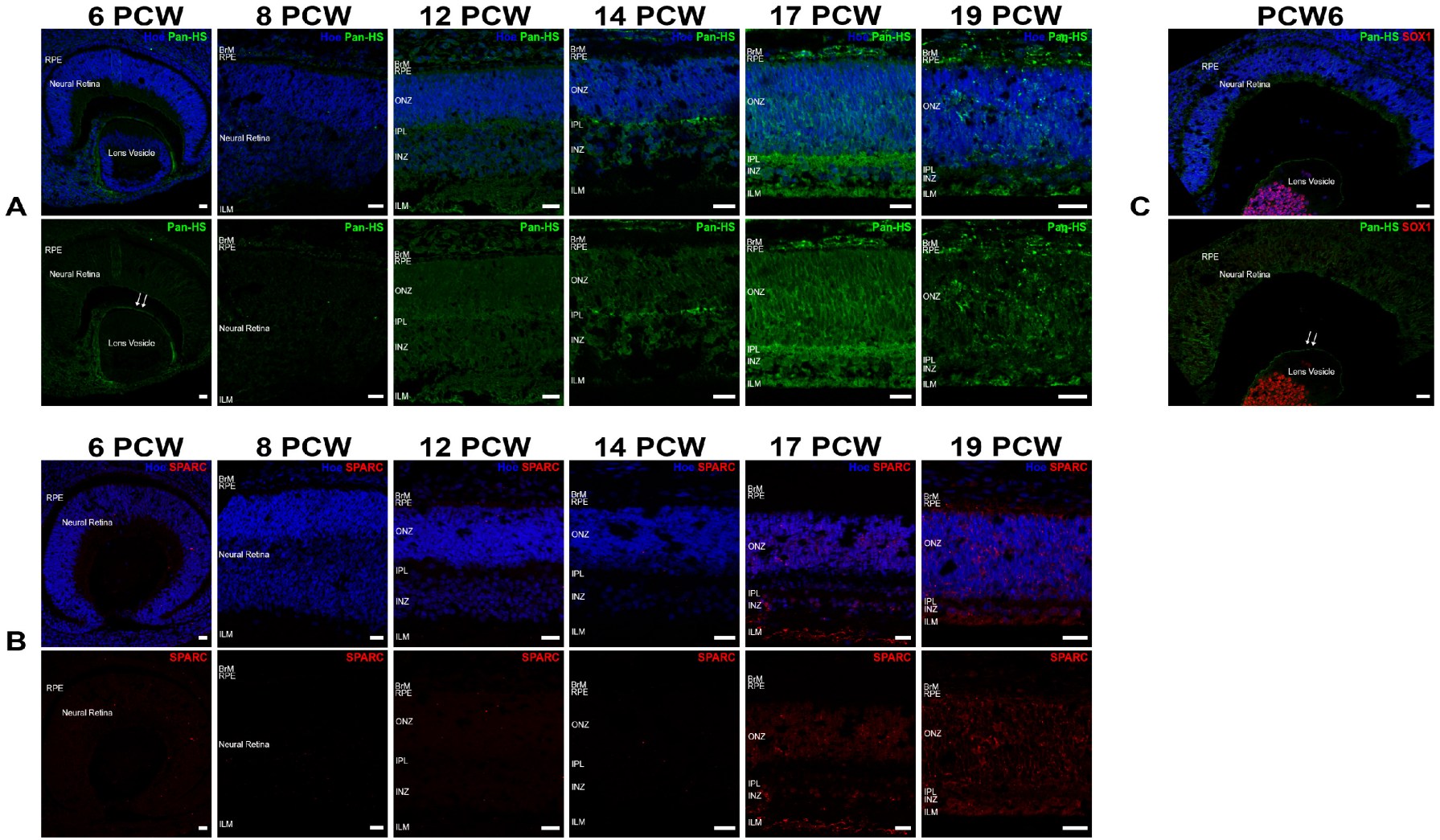

Figure 3-14: Expression of Pan Heparan Sulfate (Pan-HS) & Secreted protein acidic and rich cysteine (SPARC) in the human embryonic and foetal eye.

(A, B) Sagittal sections through the developing human eye showing antibody labelling with and without Hoechst (Hoe) during the 6-19 PCW. (C) Sagittal section showing antibody double staining of Pan-HS and Sox1 with and without Hoechst in PCW6. Scale bar =20 μm. Arrows indicate Pan-HS expression in lens capsule.

3.3.7. Distribution of cluster of differentiation 44 (CD44) in human developing retina

As mentioned previously, CD44 acts as the primary receptor for hyaluronic acid and interacts with other ECMs such as versican, brevican, aggrecan and IMPG1. It was, therefore, important to investigate CD44 expression in the developing human retina. CD44 was found to be expressed in the ONZ & INZ during the later stages of human retinal development studied including 16-19 PCW (**Figure 3-15A**). No immunostaining of CD44 was detected in retinal sections from the 6 until the 14 PCW (**Figure 3-15A**). Strong expression of CD44 was also observed in the developing IPM in 16-19 PCW as revealed by the co-localisation with RBP3 (**Figure 3-15B**).

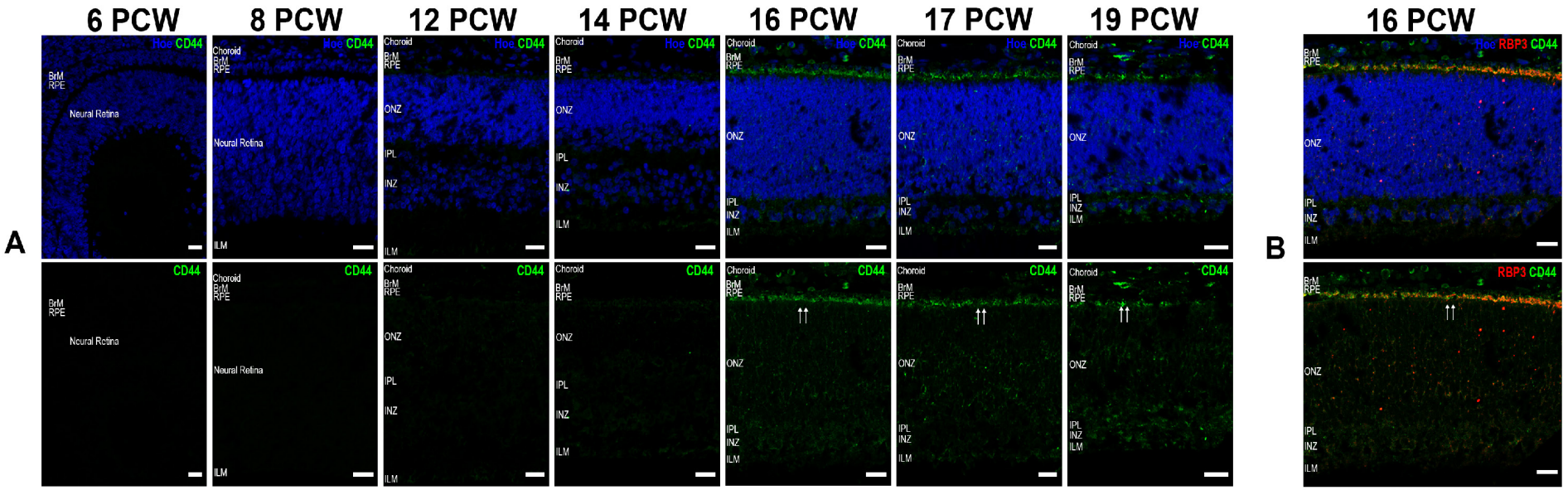

Figure 3-15: Expression of cluster of differentiation 44 (CD44) in the human embryonic and foetal eye.
(A) Sagittal sections through the developing human eye showing antibody labelling with and without Hoechst (Hoe) during the 6-19 PCW. Scale bar =20 µm. Arrows indicate CD44 expressions in IPM. (B) Tissue labelled with CD44 and RBP3 in 16 PCW. Scale bar =20 µm.

3.4. Discussion

In this study the expression of several ECM components in adult mouse and monkey retinae, developing and adult human retinae was investigated (for summary of key ECM expression, please see **Figure 3-16)**. The results of this study demonstrate that different ECM components have distinct distribution patterns throughout the adult retina of different species (Clark *et al.*, 2011). Collagen IV was expressed in BrM, while Fibronectin was expressed in BrM and ILM, consistent with the expression previously observed in adult rat (Chen *et al.*, 2009). Preceding any experimental work to mimic the specific IPM environment, it is essential to understand the composition of the IPM during human retinal organogenesis. Expression studies were performed to map the differential distribution of proteoglycan core proteins and their associated GAGs in sections of adult mouse and monkey retinae, developing and adult human retinae.

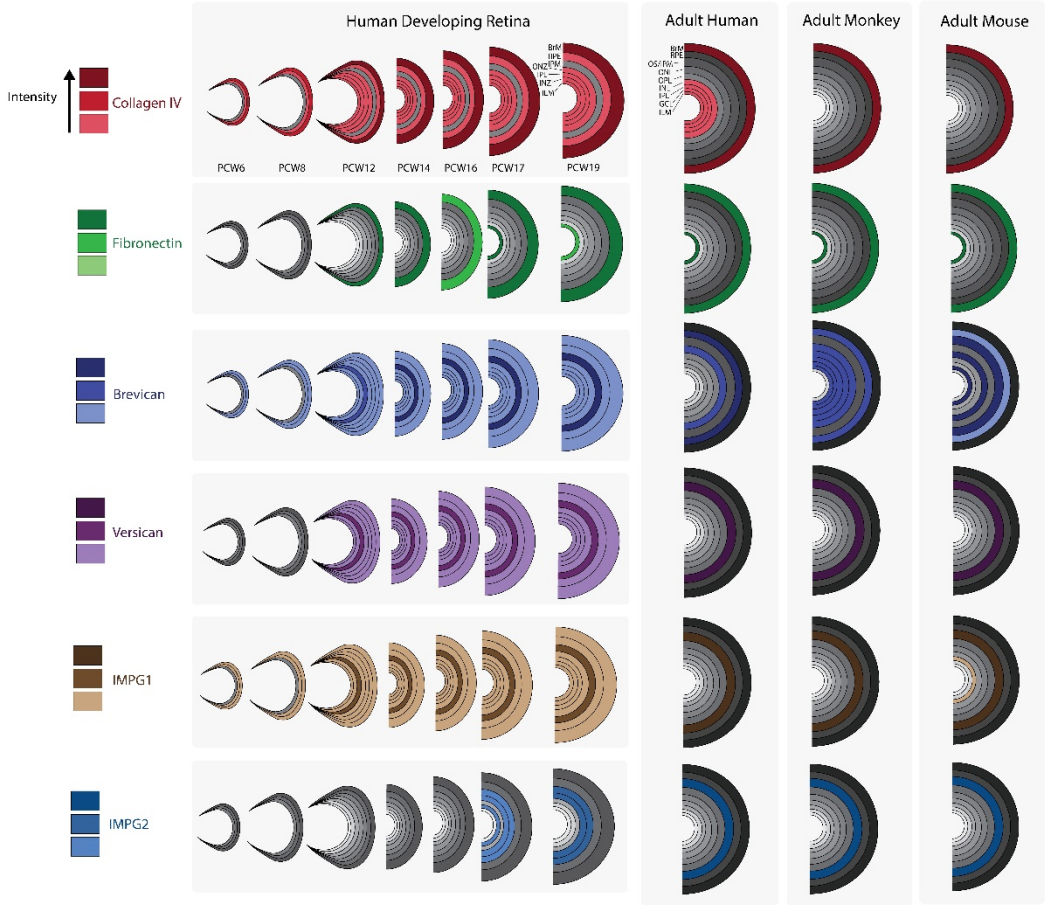

Figure 3-16: Illustrated diagram showing a summary of key ECM expression in human developing retina; and adult human, monkey and mouse retinae.
Colour shades indicate intensity level of fluorescent expression for different ECMs.

Hyaluronic Acid was found to be widely distributed in the human developing retina and the adult retina of mouse, monkey and human. This was consistent with the result reported by Clark et *al.* showing the expression throughout the retina of adult human (Clark *et al.*, 2011). Hyaluronic Acid is secreted from the apical side of the RPE and plays important role in the survival of the photoreceptors by binding to PEDF, a growth factor required for the avascularity of the IPM and survival of photoreceptors (Becerra *et al.*, 2008; Broadhead *et al.*, 2010; Ishikawa *et al.*, 2015). Co-expression study of hyaluronic acid with RBP3 in the IPM of human developing retina suggested that it may play a role in the development of IPM. Versican was previously reported in the IPM in adult chick (Zako *et al.*, 1997). The data obtained in the current study corroborate this published report and also demonstrate conserved expression of versican in the IPM of adult human, mouse and monkey retina. In the developing human retina, versican expression surrounded the developing photoreceptors between the RPE and ONZ, an area which likely develops into the future IPM. The localisation of versican in the IPM was confirmed by co-expression with interphotoreceptor retinoid binding protein (IRBP/ RBP3), the most abundant protein in the IPM (Stenkamp *et al.*, 2005).

Brevican expression was also detected the developing IPM in human developing retina. Although co-expression study showed that brevican and versican expression did not overlap, it indicated that both were expressed in the developing IPM of human developing retina. Brevican expression in the IPM was consistent with data reported by Keenan *et al.* showing it is expressed in the IPM of adult human retina (Keenan *et al.*, 2012). Neurocan expression was detected in the IPL layer of human developing retina, and its expression was consistent with the expression previously observed in postnatal rat retina (Inatani and Tanihara, 2002). Although aggrecan expression varied between the three species studied, it was only detected in BrM of adult human retina. This expression pattern was similar to a result reported by Keenan *et al.* illustrating strong expression of aggrecan in BrM of the adult human retinae (Keenan *et al.*, 2012). Aggrecan was also expressed in the lens capsule and dorsal-nasal gradient in human developing retina, suggesting it might play a role in the development of the lens and retinal ganglion cells during optic cup morphogenesis.

HAPLN1 is a cartilage link protein that maintains the interactions between hyalectins and hyaluronic acid (Keenan *et al.*, 2012). The expression pattern of HAPLN1 in adult human and monkey retina is similar to what Keenan *et al*. reported that it was observed in the IPM of adult human retina (Keenan *et al.*, 2012). HAPLN1 was expressed differently in mouse tissue suggesting that significant species-specific differences exist for this protein, although

expression around the inner segments and in the ONL suggests an important role of HAPLN1 for photoreceptor. HAPLN1 was also expressed in the lens capsule of human developing retina suggesting that it might play an essential role in the lens development.

IMPG1 and IMPG2 are two specific ECM components that are secreted by the photoreceptors into the IPM (Acharya *et al.*, 1998; Acharya *et al.*, 2000). The results of this study demonstrated expression of these two ECMs in the IPM in human developing tissue, with IMPG1 detected earlier and IMPG2 expressed at later stages of development, which may suggest a role for IMPG1 in early photoreceptor development and IMPG2 in photoreceptor maturation. Conserved expression of both ECMs was also detected in the IPM of the adult retinae in the three species studied suggesting an important role in IPM formation and photoreceptors development. Furthermore these data support the clinical phenotype of Vitelliform Macular Dystrophy caused by *IMPG1* mutations and is characterised by impaired metabolism of photoreceptors in the macula region due to the loss of IPM (Manes *et al.*, 2013).

Pan-HS was expressed throughout the retina of all species. This finding is similar to a recent report that demonstrated pan-HS expression throughout the retina of adult human (Clark *et al.*, 2011). SPARC expression varied between the three species studied and was expressed at later stages of human developing retina. Several studies have demonstrated that CD44 is a multi-domain protein that spans the plasma membrane of the cell and acts as a receptor for Hyaluronic Acid and other ECMs such as versican, brevican and aggrecan (Brun *et al.*, 2003; Dicker *et al.*, 2014). CD44 can also interact with the GAGs of IMPG1 and may participate in retinal adhesion (Kuehn *et al.*, 2000). The data obtained in this study indicated that CD44 was expressed in the IPM from the 16 PCW of human development, suggesting that CD44 may play an important role in the development of the photoreceptors. The results of this study and those published by Nishina *et al.*, 1997 indicated that CD44 expression was also found in the longitudinal fibres that extend from the inner to the outer limiting membrane and the surface of Müller cells at later stages of human retinal development (19 PCW) (Nishina *et al.*, 1997).

IHC was the technique for investigating the expression of ECM components. The interpretation of fluorescence microscopy of tissues obtained from elderly individuals might be difficult due to the presence of the auto-fluorescent pigment lipofuscin (Schnell *et al.*, 1999) which is a lipid/protein aggregate resulting from autophagocytosed oxidised cellular components and which accumulates throughout life in the RPE (Boulton and Dayhaw-Barker,

2001; Terman and Brunk, 2004; Petty *et al.*, 2010). The presence of this auto-fluorescence in the visible spectrum can complicate the use of conventional immunofluorescence microscopy to localise molecules in the tissue sections and to distinguish specific labelling from that of lipofuscin (Schnell *et al.*, 1999; Boulton and Dayhaw-Barker, 2001; Petty *et al.*, 2010). Therefore, auto-fluorescence was experienced in most of the tissues used. To overcome this issue, tissue sections were stained with Sudan Black with the aim of quenching and reducing endogenous fluorescence of retinal tissue (Petty *et al.*, 2010). This was successfully achieved in staining most of the tissues used in most mouse, monkey and human embryonic tissue. However, endogenous fluorescence was still present in the RPE of the adult human tissue that could be due to the age of the donors as lipofuscin can occupy up to 19 % of the cells cytoplasmic volume by 80 years of age (Boulton and Dayhaw-Barker, 2001). In addition, based on the fact that human retinal tissue were collected from elderly individuals, there might be changes occur to the ECM composition that in BrM (Booij *et al.*, 2010) and the retina (Al-Ubaidi *et al.*, 2013). To overcome this issue, ECM composition was also investigated in animal models that are similar to human in term of ECM composition and retinal structure.

3.5. Conclusion

In summary, the data presented in this chapter indicate a well conserved expression for Collagen IV and Fibronectin in BrM and BrM/ILM in adult and developing human retinae, and a well conserved expression for Versican, Brevican, IMPG1 and IMPG2 in the IPM of adult and developing human retinae. Therefore, these key ECM components were selected for further experiments described in the following chapter.

Note: The content, data and figures in this chapter were used in a recently published original article (Felemban *et al.*, 2018) published in Acta Biomaterialia Journal (See appendices): "Extracellular matrix expression in human pluripotent stem cell-derived retinal organoids recapitulates retinogenesis in vivo and reveals an important role for IMPG1 and CD44 in the development of photoreceptors and interphotoreceptor matrix".

Chapter 4

Chapter 4. ECM expression in hESC- and hiPSC-derived retinal organoids and the role of IMPG1 and CD44 in the development of photoreceptors and interphotoreceptor matrix

4.1. Introduction

The final impact of many forms of retinal diseases is the loss of photoreceptors, a specialised type of photosensitive neurons that are capable of photo-transduction, and/or the underlying retinal pigmented epithelium (RPE) (Zhong *et al.*, 2014). No treatments currently exist to restore lost photoreceptor cells and the accompanying vision loss which occurs in many retinal diseases. Thus there is a pressing need to generate a source of functional photoreceptors and RPE, the underlying tissue which is essential for photoreceptor function and viability, for disease modelling and transplantation. The retina is a prime system within which to test the development of cell transplantation therapies due to the relative accessibility of the eye that permits local delivery of cells with minimum risk of systemic consequences. Pluripotent stem cells including human embryonic stem cells (hESCs) and induced pluripotent stem cells (hiPSCs) provide great tools for modelling retinal disorders, understanding human fetal ontogenesis or as therapeutic agents; because of their ability to proliferate indefinitely and to differentiate into multiple tissue including retinal linages (Mellough *et al.*, 2014). In the last few years several groups have demonstrated the generation of pluripotent stem cell derived retinal organoids which contain multiple retinal cells types, respond to electrophysiological stimuli (Meyer *et al.*, 2011; Nakano *et al.*, 2012; Zhong *et al.*, 2014; Kuwahara *et al.*, 2015; Mellough *et al.*, 2015; Gonzalez-Cordero *et al.*, 2017; Wahlin *et al.*, 2017; Hallam *et al.*, 2018) and engraft within the degenerate retinae (Shirai *et al.*, 2016; Waldron *et al.*, 2018). Such organoid cultures provide an extremely useful tool for large scale pharmacology and toxicology testing, understanding human retinal development, and dissecting the role of individual genes during this process. As such, it is important to ensure that *in vitro* pluripotent stem cell models are similar counterparts to the retinal tissue *in vivo*.

A number of reports have shown that various aspects of the retinal development can be recapitulated *in vitro* through the differentiation of hESCs and hiPSCs into retinal organoids (Meyer *et al.*, 2011; Mellough *et al.*, 2012; Nakano *et al.*, 2012; Mellough *et al.*, 2014; Zhong *et al.*, 2014; Gonzalez-Cordero *et al.*, 2017; Welby *et al.*, 2017) which contain the key retinal cells types and respond to electrophysiological cues. The ECM plays an important role in controlling the behaviour of stem cells including self-renewal and differentiation (Keung *et al.*, 2012). *In vivo,* the ECM plays major roles in several cellular

processes during retinal development such differentiation, proliferation, migration, adhesion, guidance and axonal growth (Reinhard *et al.*, 2015). This process can be enhanced by ECM supplementation, *in vitro* (Boucherie *et al.*, 2013). For example, the addition of Matrigel, a complex ECM which is rich in basement membrane components, to the media was shown to promote hESC self-organisation into retinal organoids under 3D culture conditions (Boucherie *et al.*, 2013), whilst addition of laminin-111 encouraged differentiation of hESC and iPSC to RPE (Gong *et al.*, 2008; Rowland *et al.*, 2013). Sasai *et al.* have demonstrated that the addition of laminin and entactin to 3D culture promoted the formation of self-organising optic cups from mouse ESCs (Eiraku *et al.*, 2011; Kuwahara *et al.*, 2015).

Given the potential of using pluripotent stem cells to model various aspects of retinal morphogenesis, it is essential to study the expression of ECM components during the differentiation of hESC and hiPSC into retinal organoids and to understand the role of several ECM components in retinal development.

4.2. Aims

In the previous chapter, the expression of several ECM components in adult mouse and monkey retina, developing and adult human retina was studied. The aim of this chapter was to investigate the expression of key ECM components (Fibronectin, Collagen IV, Versican, Brevican, IMPG1 and IMPG2) and their functions in retinal organoids derived from hESCs and hiPSCs.

4.3. Results

In order to validate the antibody specificity used to study the ECM expression in retinal organoids, several approaches was applied including: omission of primary antibodies (**Figure 4-1A**), replacement of primary antibodies with isotype controls (**Figure 4-1B**) and usage of antibodies that have been widely published and validated in other studies. For some antibodies (Fibronectin, Brevican, Versican and IMPG1) where not enough evidence in the literature was found, siRNA studies were performed and showed in all cases a corresponding decrease in gene and protein expression using qRT-PCR and immunocytochemistry (**Figure 4-2**).

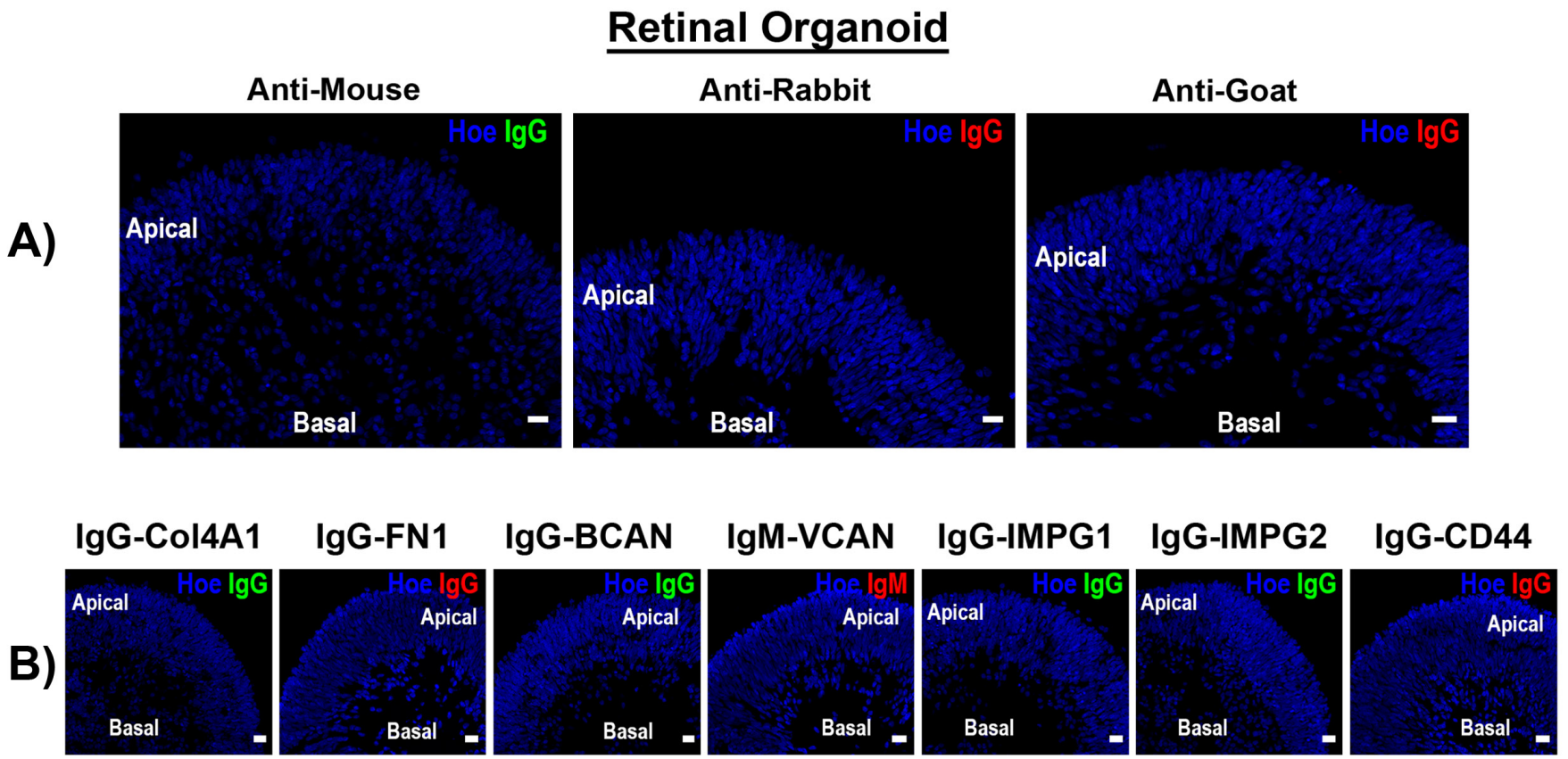

Figure 4-1: Immunostaining of secondary antibody controls and isotype controls to ECM antibodies in retinal organoids derived from hESCs.

(A) Different secondary antibodies (anti-mouse (IgG) Alexa Fluor 488, anti-rabbit (IgG) Cy3, and anti-goat (IgG) Cy3) were used to differentiate non-specific background signals in tested retinal organoids (day 150). (B) Isotype antibodies matching the ECM components (Collagen IV, Fibronectin, Brevican, Versican, IMPG1, IMPG2 and CD44) primary antibodies were used to differentiate non-specific binding of immunoglobulin in tested retinal organoids (day 150). Scale bars = 20µm.

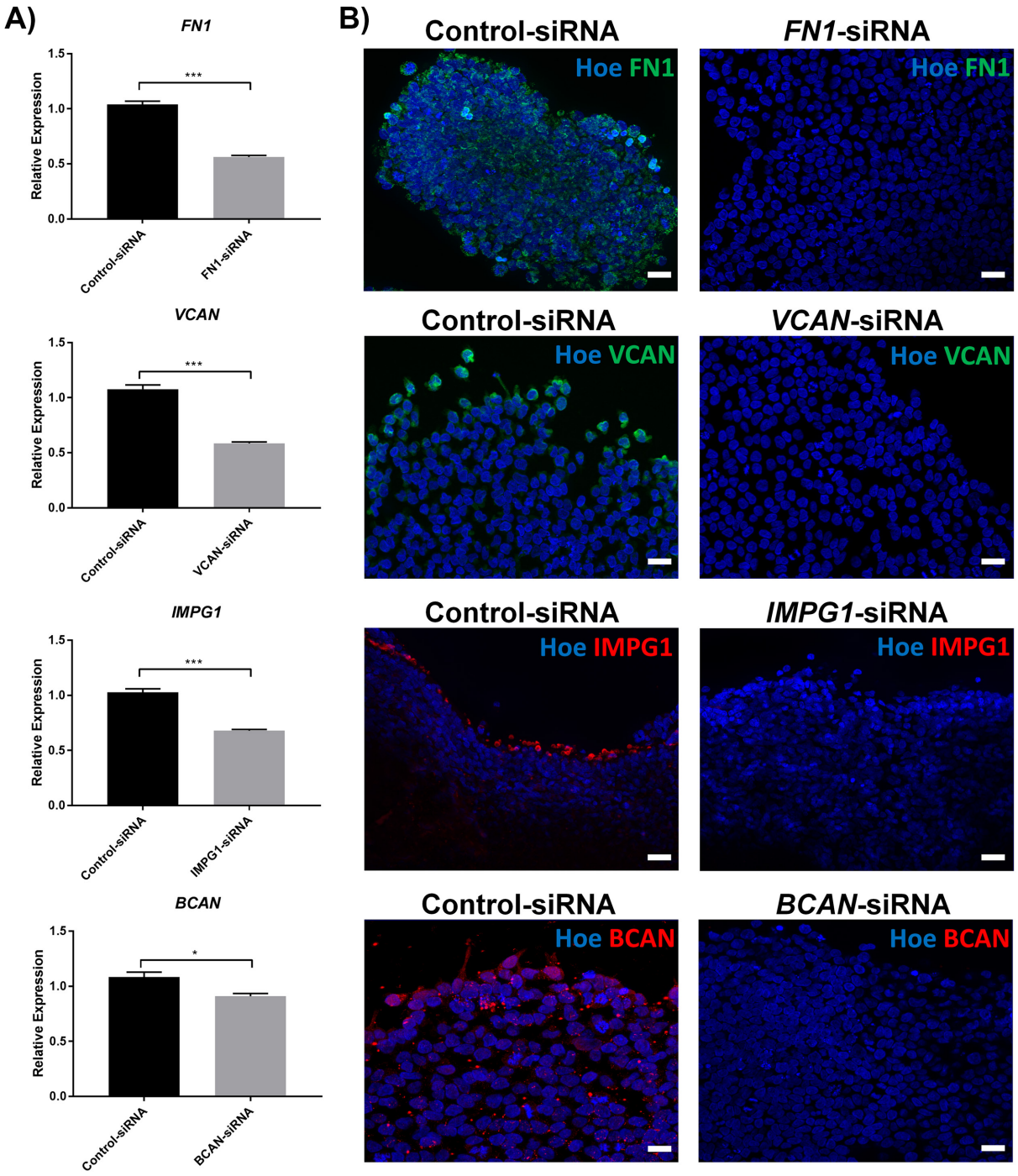

Figure 4-2: siRNA study of ECM protein and gene expression

(A) qRT-PCR study showing a decrease in the mRNA expression upon transfection of (Fibronectin: *FN1*, Versican: *VCAN* and Brevican: *BCAN*) siRNAs in hESCs. *IMPG1* was not expressed in hESCs, hence siRNA was performed in day 90 retinal organoids. (B) Hoechst (Hoe) control and siRNA transfection of FN1, VCAN and BCAN in hESCs, and IMPG1 in day 90 retinal organoids showing a reduction in the ECMs expression after the transfection. *n=3,* error bars = SEM. * p-value < 0.05, *** p-value <0.001.

4.3.1. ECM expression during differentiation of hESC and hiPSC to laminated retina

Retinal organoids were generated from hESCs (H9) and hiPSCs (SB-Ad3) following a differentiation protocol which was previously described (Mellough *et al.*, 2015), with a few modifications (**previously mentioned in Chapter 2, section 2.6**). The development of retinal progenitors and their maturation over time was assessed using a combination of specific markers (**Figure 4-3 and 4-4**). VSX2, a marker of retinal progenitor cells, was expressed in the apical region of retinal organoids of days 35 and 90 of differentiation (**Figure 4-3**). Amacrine and RGCs (detected by the expression of HuC/D) were located in the basal layer (toward the centre of the retinal organoids) (**Figure 4-3**). The development of photoreceptors was assessed using antibodies to CRX and Recoverin. CRX, a post-mitotic photoreceptor marker, was expressed throughout the retinal organoids with strong expression towards the apical region of the organoid as the photoreceptors developed over time (**Figure 4-3**). Strong expression of Recoverin, a photoreceptors and midget OFF bipolar cells, was observed at the most apical side of the organoids at days 90 and 150 (**Figure 4-3**). At day 150, there was no overlap between VSX2 and CRX expression (**Figure 4-3**). PAX6 and VSX2 co-immunostaining showed that bright VSX2 and bright PAX6 expressing cells did not overlap (**Figure 4-4A**), indicating that high VSX2 and high PAX6 expression in the putative inner nuclear layer of day 150 retinal organoids most likely marks the emerging bipolar and amacrine/horizontal cells respectively, corroborating data published by Volkner *et al.* (Volkner *et al.*, 2016). Nonetheless, within the retinal organoids, some cells were found with low PAX6 and low VSX2 expression which most likely mark the remaining proliferating retinal progenitor cells (**Figure 4-4A**), also shown by Ki67 expression (**Figure 4-4A**). At day 150, other cell types including amacrine, horizontal, bipolar and Muller glial cells were observed through immunostaining with AP2α, Prox1, CRLABP (**Figure 4-4A)** in addition to the expression of presynaptic marker (Syntaxin shown to be expressed in the presynaptic terminals of photoreceptor and horizontal cells), vGlut1 (expressed in photoreceptor and bipolar cell terminals) and photoreceptor connecting cilia marker, ARL13B (**Figure 4-4A)**. At day 150, the expression of Rhodopsin was observed in cell bodies and IS/OS like segments (**Figure 4-4A**) in a similar pattern reported by Gonzalez-Cordero *et al.* recently (Gonzalez-Cordero *et al.*, 2017). The expression of cone markers (Cone Arrestin and long/medium wavelength Opsin) was assessed from day 150; however a typical expression pattern in cell bodies and IS/OS like segments was only observed from day 200 onwards (**Figure 4-4B**).

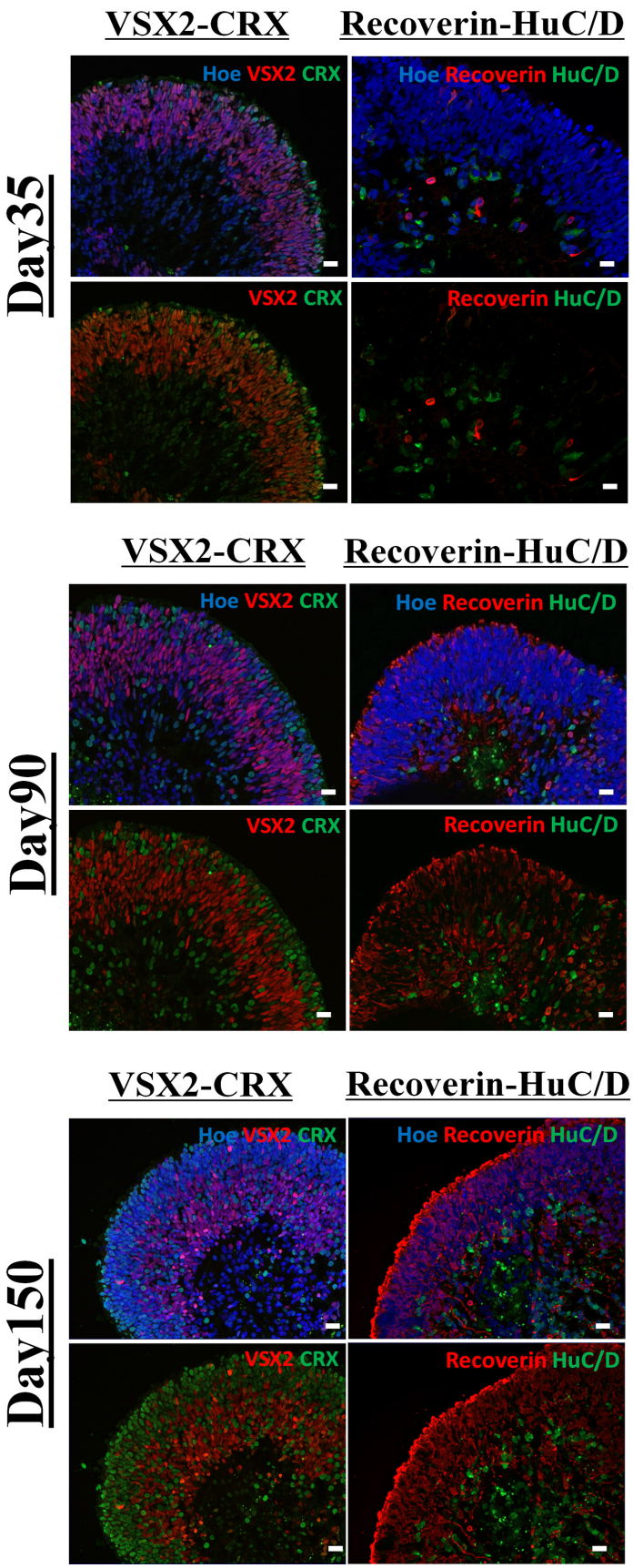

Figure 4-3: Expression of retinal markers during the differentiation of hESC to laminated retina.
H9-derived retinal organoid sections showing the development of retinal progenitors and their maturation over time using retinal markers: VSX2, HuC/D, CRX and Recoverin.

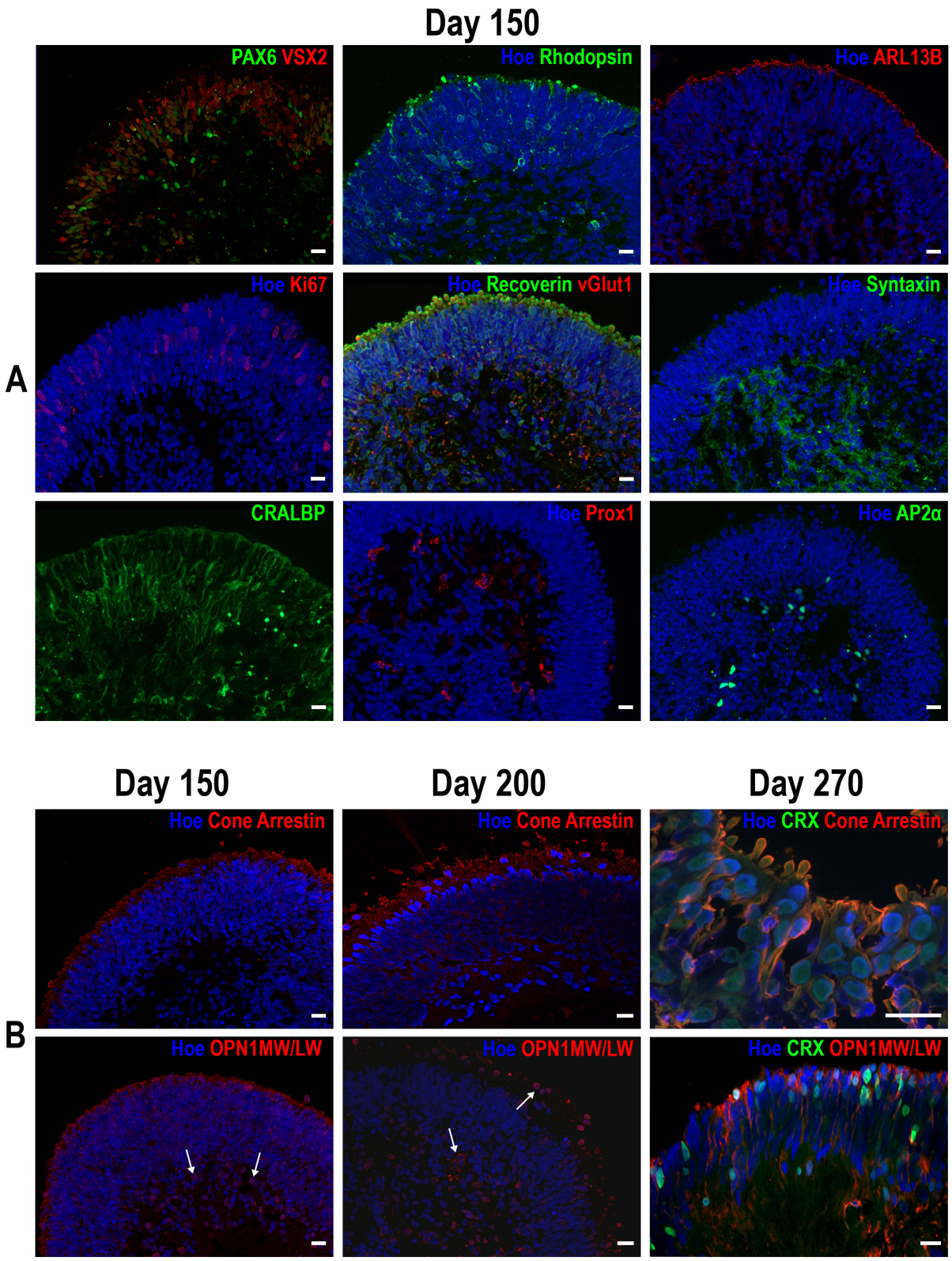

Figure 4-4: Immunostaining of day 150 retinal organoids (hESC) with retinal lineage markers.

(A) Sections through retinal organoids at day 150 showing labelling with retinal markers including: PAX6 & VSX2, Ki67, CRALBP, Rhodopsin, Recoverin & vGlut1, Prox1, ARL13B, Syntaxin, AP2α with or without Hoechst. (B) Sections through retinal organoids showing double labelling of Hoechst with Cone Arrestin, OPN1MW/LW (day 150 & 200) & with Cone Arrestin, OPN1MW/LW & CRX (day 270).

Immunostaining with antibodies against the selected ECM components indicated that Fibronectin was expressed throughout the 3D retinal organoids during the entire period of differentiation in both hESC- and hiPSC-derived retinal organoids (**Figure 4-5** and **Figure 4-6**). On day 35, the strongest expression of Fibronectin was observed on the basal side of the organoids, whilst at day 90 and 150, the strongest expression was at the apical edge. The expression of Collagen IV was detected in the basement membrane on the luminal side of both hESC- and hiPSC-derived retinal organoids (**Figure 4-5** and **Figure 4-6**).

Versican was expressed throughout the retinal organoids with strong apical expression at all stages of differentiation. Furthermore, Versican expression at the most apical edge of the organoid co-localised with RBP3 in both hESC- and hiPSC-derived retinae at day 150 and 120 of differentiation respectively (**Figure 4-5C** and **Figure 4-6C**), indicating expression in the emerging IPM and corroborating data obtained from developing and adult human retinae. A similar analysis in the hESC- and hiPSC-derived retinal organoids showed highest expression of Brevican in the apical layer consisting of photoreceptors marked by the CRX expression at days 90 and 150 of differentiation (**Figure 4-5B, C** and **Figure 4-6B, C**). At day 35, faint expression of Brevican was only detected in hESC-derived retinal organoids (**Figure 4-5A** and **Figure 4-6A**).

The expression of IMPG1 in retinal organoids was first evident on day 90, with strong apical expression at day 150 (around the developing IPM and adjacent to the photoreceptors marked by CRX) suggesting that IMPG1 might have a significant role in the development and maturation of photoreceptors *in vitro* (**Figure 4-5C**). IMPG1 expression in hiPSC-derived retinal sections was only observed from day 120, suggesting potential differences between hESC and hiPSC in the kinetics of differentiation and/or IMPG1 expression (**Figure 4-5** and **Figure 4-6**). In contrast, IMPG2 was not detected at all stages of hESC and hiPSC retinal differentiation tested, suggesting that it might be expressed at later stages of the differentiation process that have not been studied herein. Similar to IMPG1, CD44 expression started at day 90 in the retinal organoids with broad expression throughout neural retinal tissue and a strong punctate-like pattern in the apical layer where Recoverin staining was strongly detected (**Figure 4-7A-C**). Co-immunostaining showed CD44 co-expression with IPM marker RBP3 (**Figure 4-7D**). Collectively, these data indicate that Versican, Brevican, IMPG1 and CD44 were expressed in the IPM of human pluripotent stem cells derived retinal organoids and recapitulate the expression observed in human developing retina.

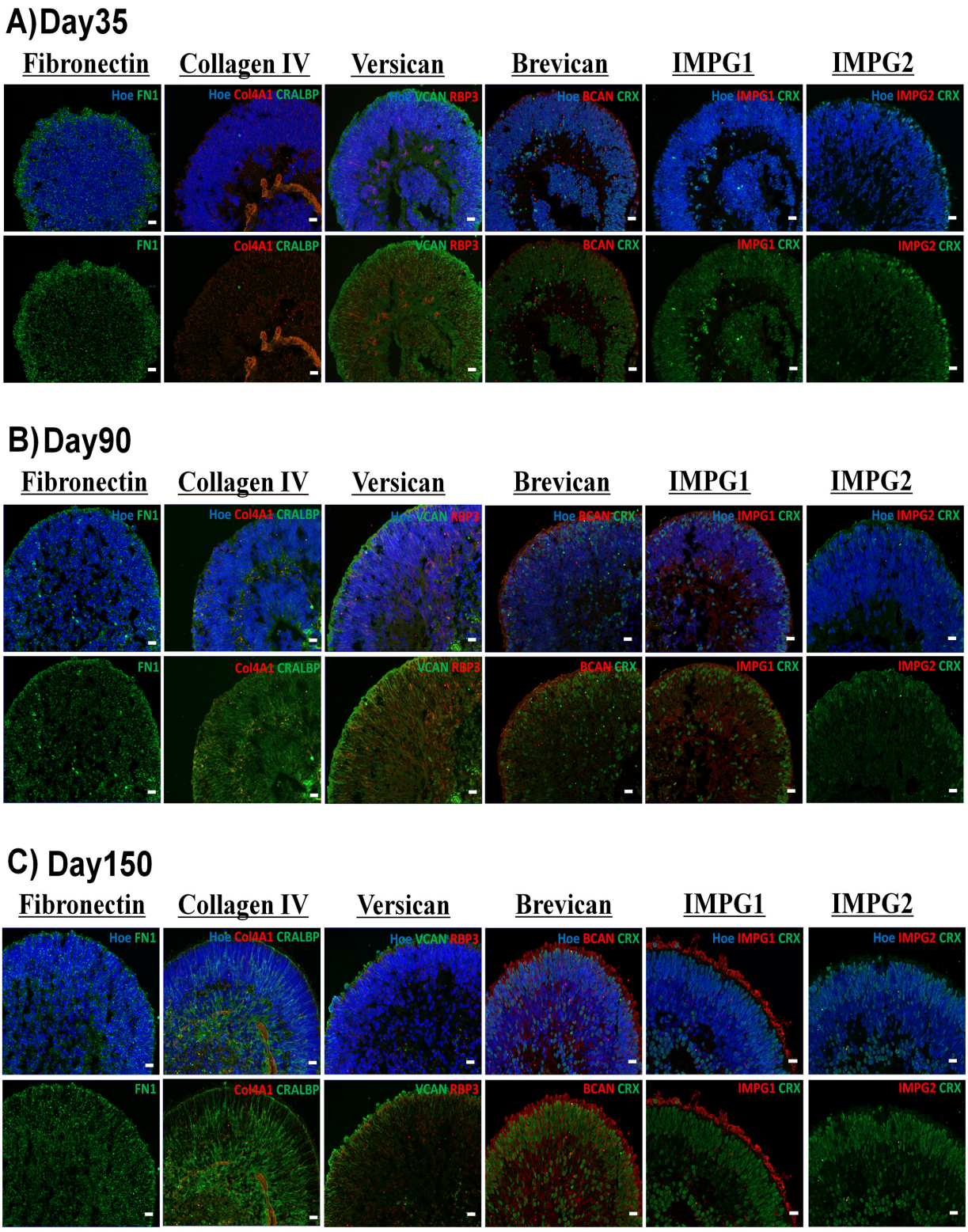

Figure 4-5: Expression of selected ECM components during the differentiation of hESC to laminated retina.

(A-C) H9-derived retinal organoid sections showing Fibronectin, Collagen IV, Versican, Brevican, IMPG1 and IMPG2 antibody labelling with and without Hoechst on day 35 (A), day 90 and (B), day 150 (C). Scale bars =20 µm.

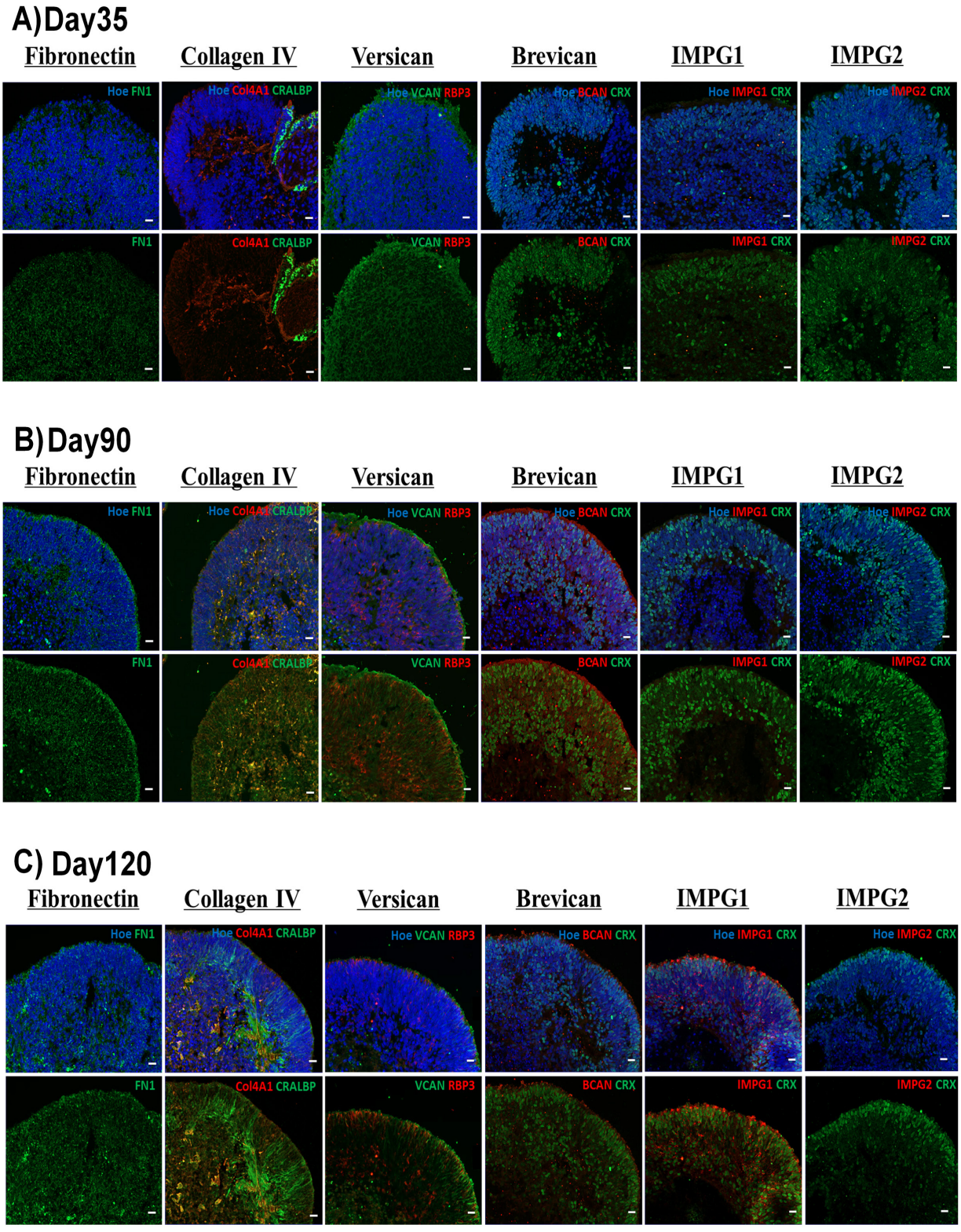

Figure 4-6: Expression of ECM components in hiPSC derived retinal organoids.
(A-C) Sections through retinal organoids showing Fibronectin, Collagen IV, Versican, Brevican, IMPG1 and IMPG2 antibody labelling with and without Hoechst in differentiated SB-Ad3, day 35 (A), day 90 (B), day 120 (C). Scale bars =20 µm.

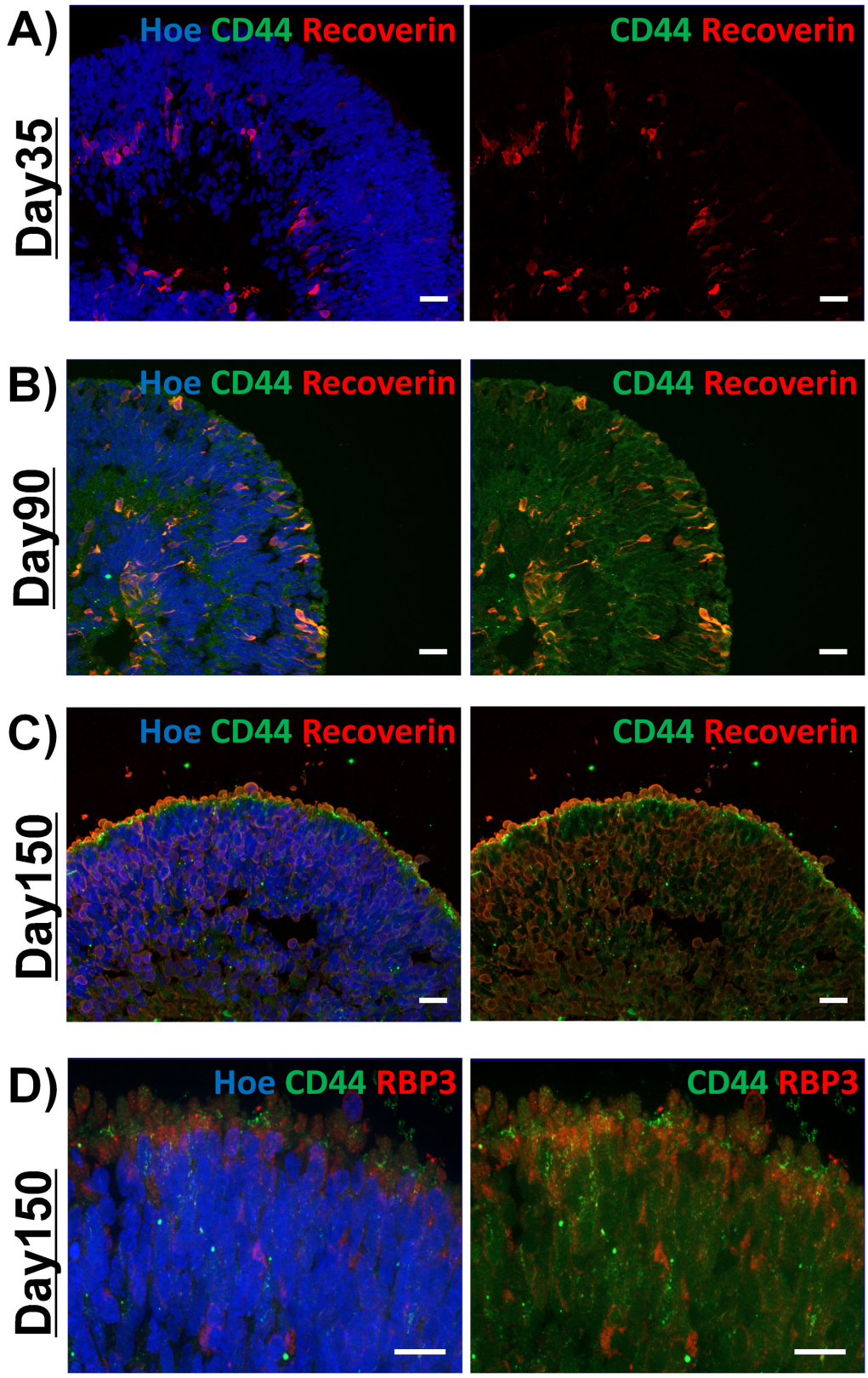

Figure 4-7: Expression of CD44 in human pluripotent stem cell derived retinal organoids.

(A-C) Sections through retinal organoids showing double labelling of CD44 with Recoverin, with and without Hoechst (Hoe) in differentiated H9 (day 35, 90 and150). (D) Double labelling of CD44 with RBP3 in retinal organoid section at day 150 of differentiation. Scale bars =20 µm.

4.3.2. IMPG1 & CD44 receptors mediated effect on photoreceptors development -Day 90 of differentiation

In order to investigate the functional role of IMPG1 and CD44 in photoreceptor differentiation, blocking antibodies to IMPG1 and CD44 were added to retinal organoid culture medium at day 90 and 150 of the differentiation process. IMPG1 antibody blocks the extracellular cell binding domain (SEA domain) of the receptor, while CD44 blocks the LINK domain on the cell membrane (Brun *et al.*, 2003; Vigetti *et al.*, 2008). Treated groups were compared to a control group. After 14 days of incubation of retinal organoids at day 90 of differentiation with IMPG1 and CD44 blocking antibody, thinning of the phase bright neuroepithelium typically found at the periphery of retinal organoids, was observed in the group treated with IMPG1 antibody only (**Figure 4-8**).

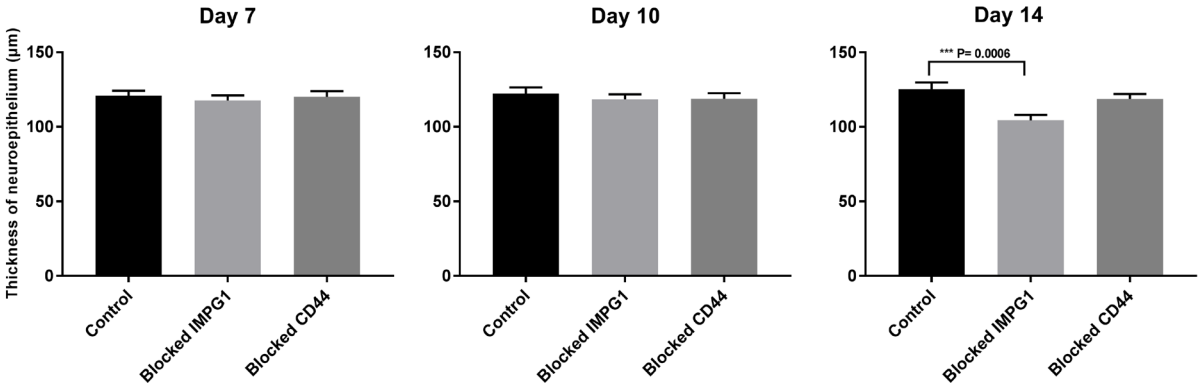

Figure 4-8: Effect of IMPG1 and CD44 blocking on neuroepithelium thickness in day 90 retinal organoids
Measurements of neuroepithelium thickness in retinal organoids at day 7, 10 and 14 of anti-IMPG1 and anti-CD44 treated groups compared to control. *n=3,* error bars = SEM. *** p-value <0.001.

After 14 days in culture, the effects of IMPG1 and CD44 receptor inhibition at day 90 of differentiation were assessed using qRT-PCR and IHC with retinal markers including Recoverin (photoreceptor marker), ARL13B (marker for connecting cilia) and RBP3 (IPM marker) to determine any effect on photoreceptors and/or IPM development (**Figure 4-9** and **4-10**). The expression of *RCVRN* (Recoverin; **Figure 4-9A**) and the number of Recoverin positive cells (**Figure 4-9B** and **Figure 4-10B**) were significantly reduced upon blocking of IMPG1 at day 90 of differentiation. The expression of photoreceptor connecting cilia, ARL13B was also significantly reduced upon blocking of IMPG1 function (**Figure 4-10B**), however no changes in *RBP3* expression were observed (**Figure 4-9A** and **Figure 4-10B**),

suggesting that IMPG1 plays a role in the development and emergence of photoreceptors, but not IPM formation at this developmental time point. Blocking of CD44 had no impact on the gene or protein expression of photoreceptor, connecting cilia or IPM markers at this time point (**Figure 4-9** and **Figure 4-10C**).

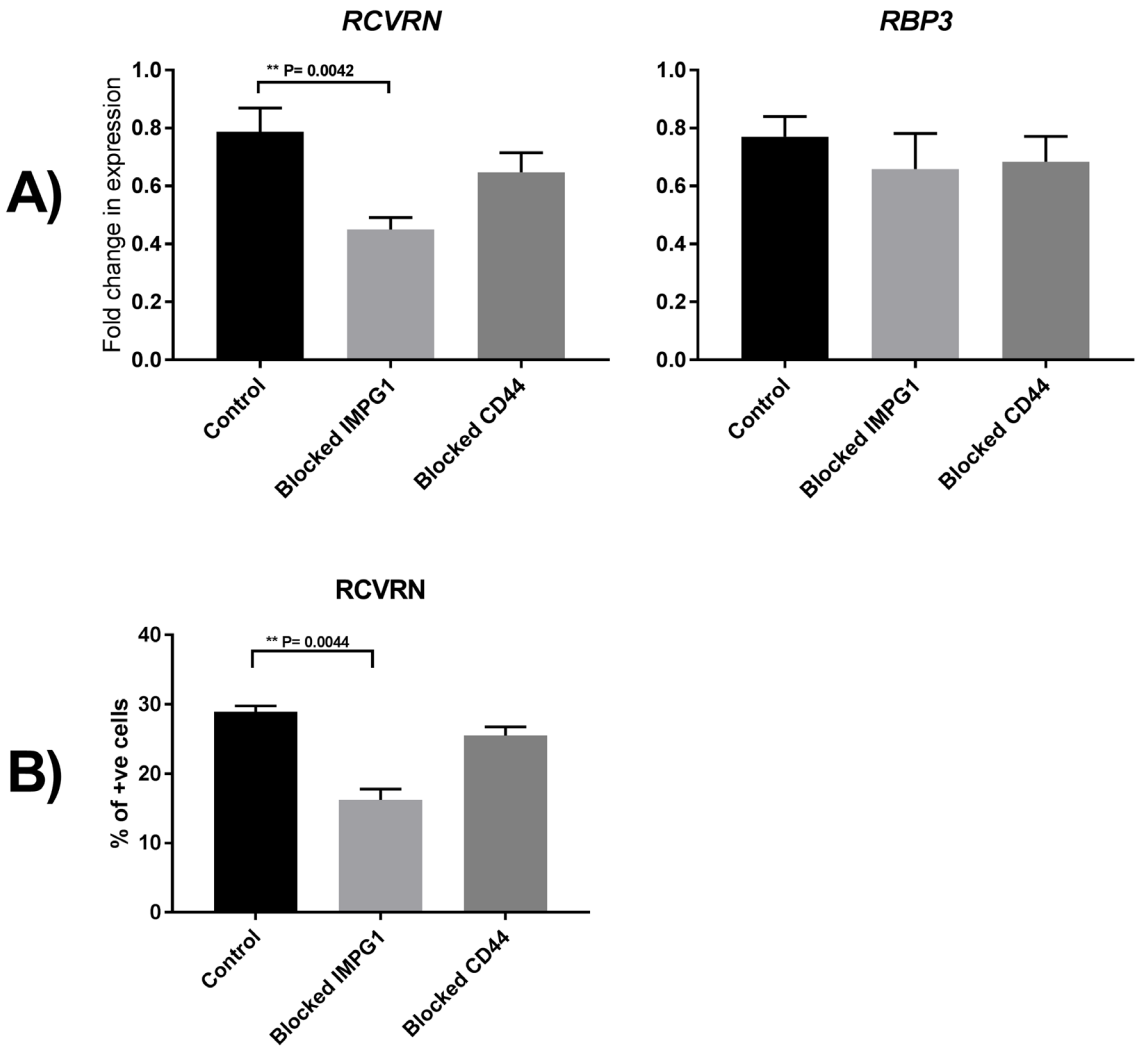

Figure 4-9: Blocking of IMPG1 and CD44 function in retinal organoids (day 90-104). (A) qRT-PCR study showing the expression of *RCVRN* and *RBP3* in blocked retinal organoids (day 104). (B) Quantification of Recoverin immune-positive cells in blocked retinal organoids (day 104). *n*=3, error bars = SEM. ** p-value < 0.01.

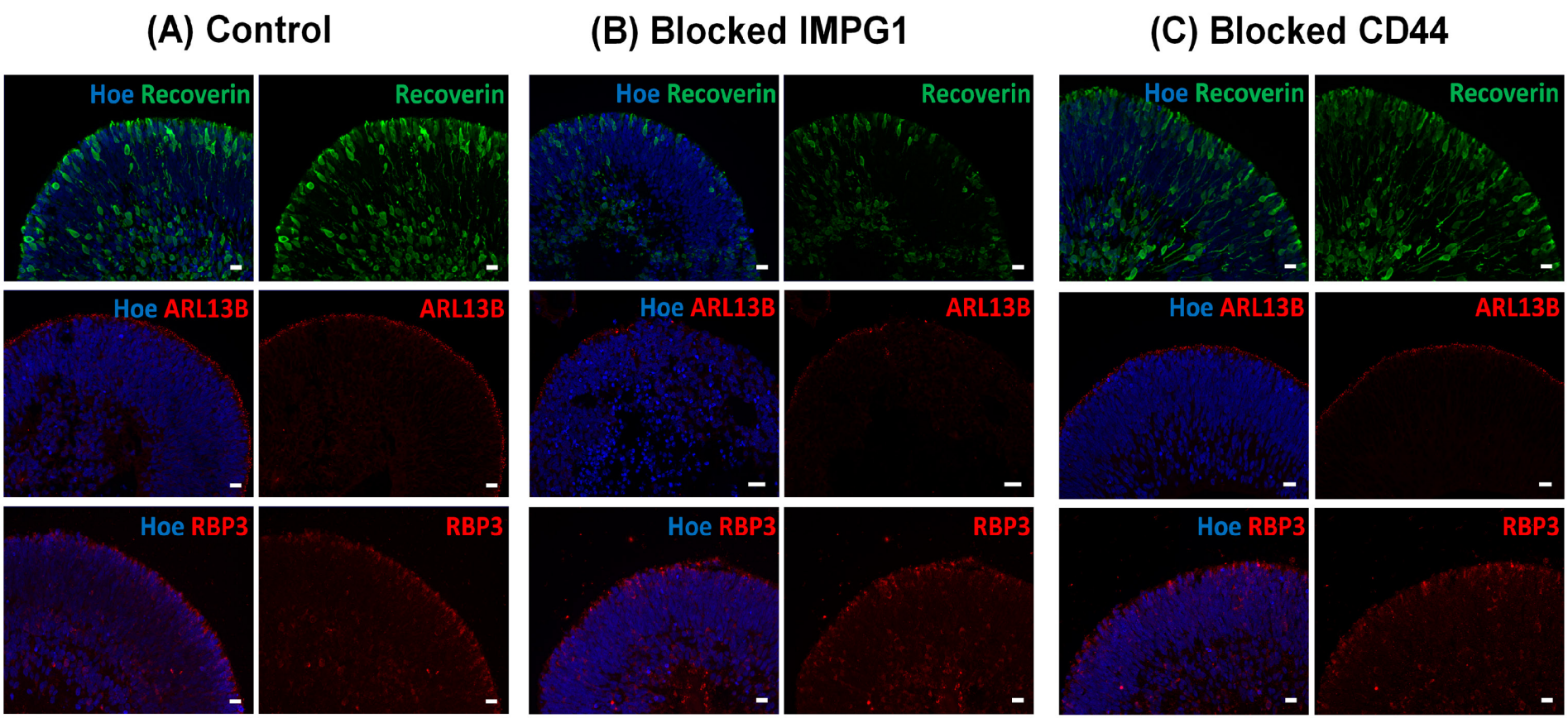

Figure 4-10: Blocking of IMPG1 action affects the development of photoreceptors in retinal organoids (day 90-104).
Retinal organoid sections showing antibody labelling with and without Hoechst (Hoe) in differentiated H9 on day 104 in three different treatment groups: cultures treated with non-specific IgG antibodies (control), cultures blocked with an IMPG1 antibody and cultures blocked with a CD44 antibody. Antibody labelling was performed with Recoverin, ARL13B and RBP3. Scale bars =20 μm.

4.3.3. IMPG1 & CD44 receptors mediated effect on photoreceptors and IPM development - Day 150 of differentiation

At day 150 of differentiation, thinning of the neuroepithelium was observed in both CD44 and IMPG1 treated groups after 14 days of incubation with blocking antibodies (**Figure 4-11**). The effects of IMPG1 and CD44 receptor inhibition at day 150 of differentiation were assessed using qRT-PCR and IHC with retinal markers including Recoverin (photoreceptor marker), Rhodopsin (rod marker), *OPN1LW* (cone marker), WGA (cone and rod inner and outer segment marker), ARL13B (marker for connecting cilia) and RBP3 (IPM marker) to determine any effect on photoreceptors and/or IPM development (**Figure 4-12** and **4-13**). No cone markers for immunostaining analysis were included due to their emergence from day 200 onwards as mentioned previously (**Section *4.3.1.***).

Blocking of IMPG1 action at day 150 led to a significant reduction in the expression of *RCVRN* and the number of Recoverin positive cells within the retinal organoids (**Figure 4-12** and **Figure 4-13B**). The expression of the cone marker (*OPN1LW*) was downregulated only in the IMPG1 blocked group (**Figure 4-12A**), although it was difficult to assess cones expression at the protein level given the later and typical emergence (from day 200) of this cell type. The expression of *Rhodopsin* (*RHO*) and the number of Rhodopsin immune-positive cells were reduced upon IMPG1 and CD44 blocking (**Figure 4-12** and **Figure 4-13B, C**). In addition, the typical pattern of Rhodopsin immunostaining was lost in CD44 and IMGP1 blocked groups (**Figure 4-13B, C**), instead a punctate pattern at the surface of retinal organoids was observed. Immunostaining with the cone and rod inner/ outer segment marker WGA showed a significant reduction in the IMPG1 and less so in the CD44 blocked group, suggesting that blocking the function of these two ECM components interferes with the development of photoreceptor inner/outer segments at different extent (**Figure 4-13B, C**). Furthermore, the expression of photoreceptor connecting cilia (ARL13B) and IPM (RBP3) markers was significantly reduced in the IMPG1 treated group (**Figure 4-13B**), indicating an important role for this protein in cilia and IPM formation. ARL13B and RBP3 immunostaining were also reduced in the CD44 blocked group, but less so when compared to the IMPG1 treated group (**Figure 4-13C**). Collectively, these data suggest that IMPG1 and CD44 play an important role in the development of photoreceptors, their inner and outer segments, connecting cilia and IPM, with IMPG1 having an earlier and more significant impact than CD44.

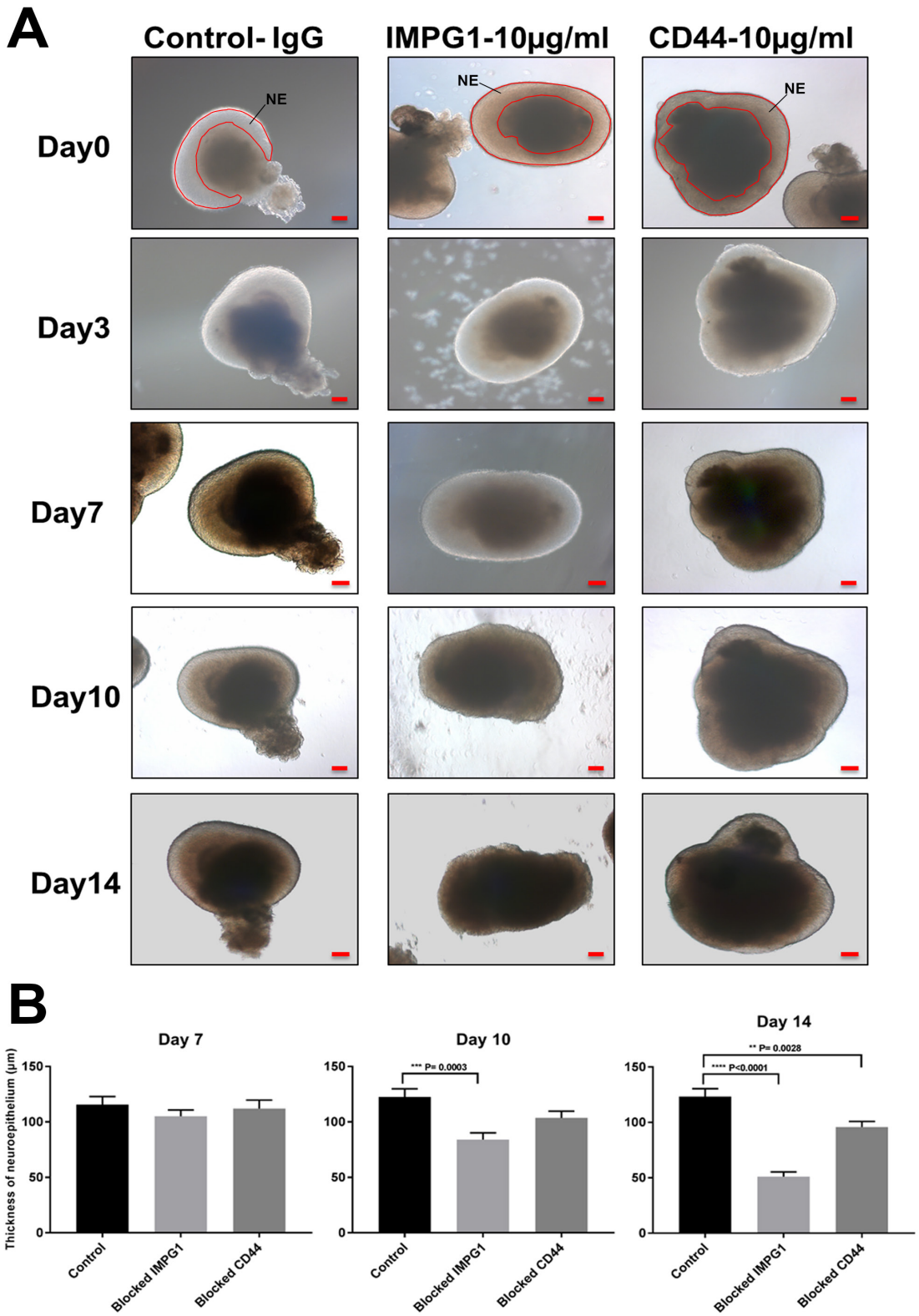

Figure 4-11: Effect of IMPG1 and CD44 blocking on neuroepithelium thickness in day 150 retinal organoids

(A) Bright field images of retinal organoids (day150-164) treated with IMPG1 and CD44 blocking antibodies, compared to treatment with a non-specific IgG antibody control. Scale bars =100 µm. (B) Measurements of neuroepithelium thickness (NE; highlighted by red lines) in retinal organoids (day 150) in culture at day 7, 10 and 14 of anti-IMPG1 and anti-CD44 treated groups compared to control. *n=3,* error bars = SEM. ** p-value < 0.01, *** p-value <0.001, **** p-value <0.0001.

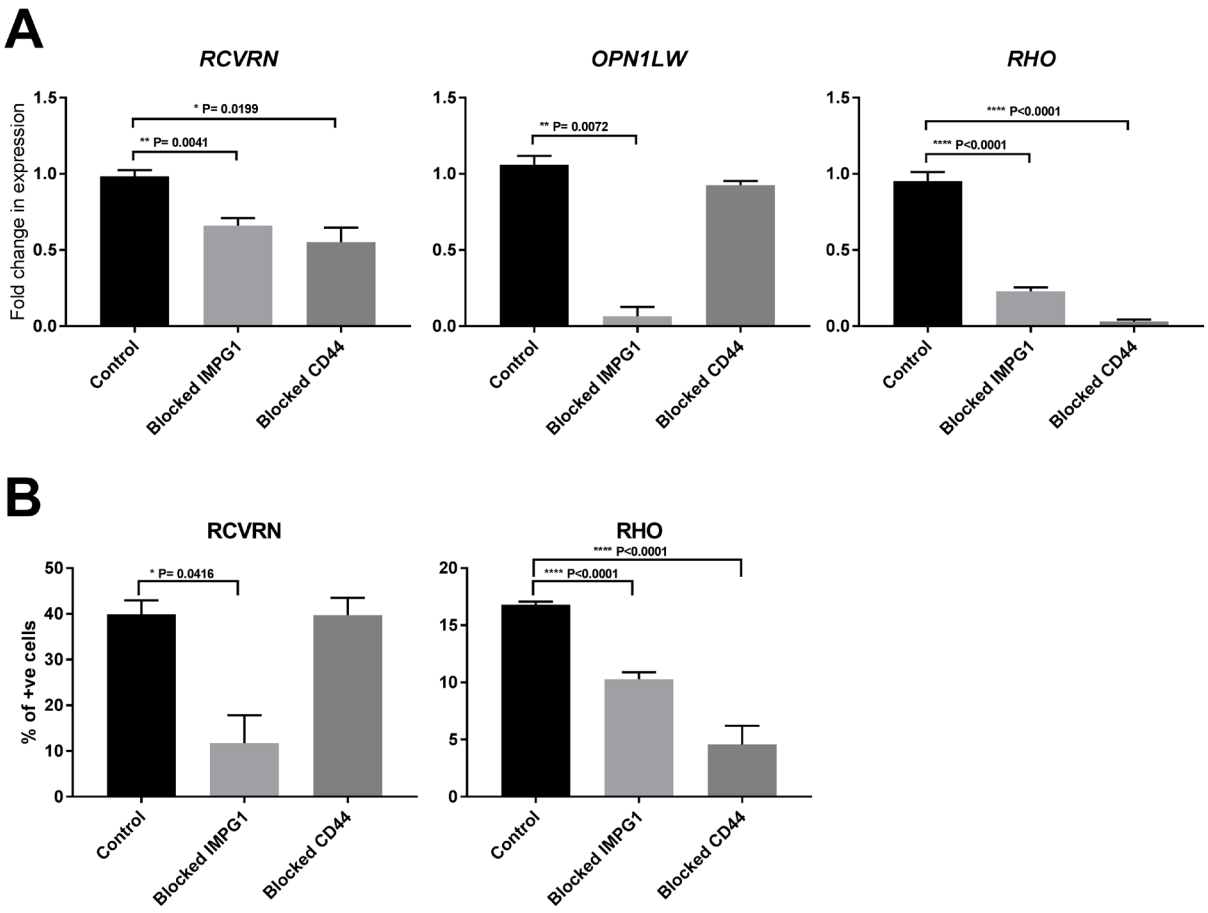

Figure 4-12: Blocking of IMPG1 function in retinal organoids (day 150-164).
(A) qRT-PCR study showing the mRNA expression of *RCVRN, OPN1LW and RHO in* retinal organoids (day 164). (B) Quantification of Recoverin (RCVRN) and Rhodopsin (RHO) immuno-positive cells in blocked retinal organoids (day 164). *n=3,* error bars = SEM. * p-value < 0.05, ** p-value < 0.01, **** p-value <0.0001.

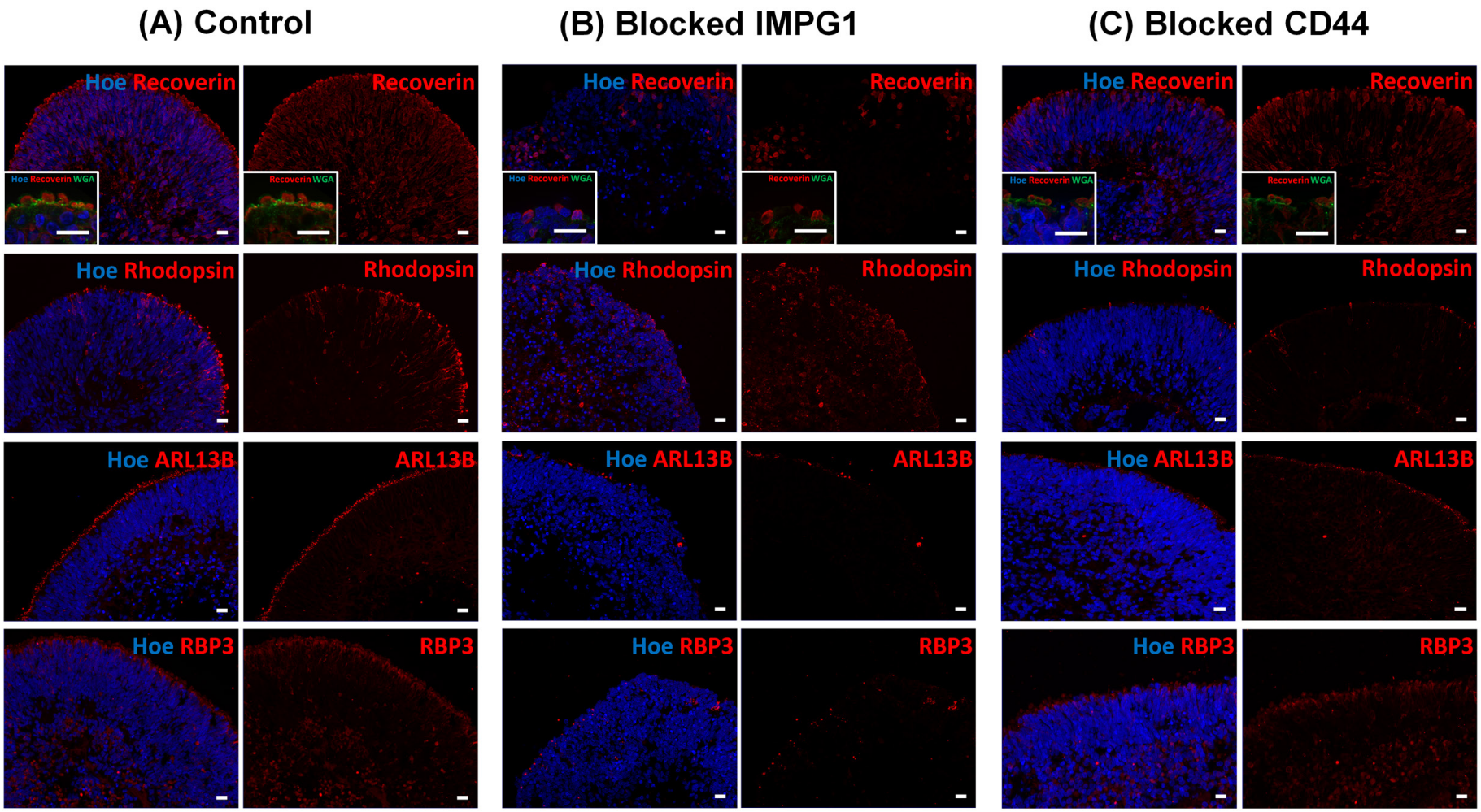

Figure 4-13: Blocking of IMPG1 & CD44 action affected the development of photoreceptors and interphotoreceptor matrix. Sections of retinal organoid derived from H9 showing antibody labelling with and without Hoechst (Hoe) at day 164 in three different treatment groups: cultures treated with a non-specific IgG antibody (control, A), cultures blocked with an IMPG1 antibody (B) and cultures blocked with a CD44 antibody (C). Antibody labelling was performed with Recoverin, Rhodopsin, ARL13B and RBP3. Small insets show higher magnification images of organoid sections double labelled with Recoverin and WGA. Scale bars =20 µm.

4.4. Discussion

Since the seminal discovery of Eiraku and Sasai in 2011 on generation of 3D retinal organoids from mouse ESC, multiple protocols have been developed and optimised for both human and mouse pluripotent stem cells (Jayakody *et al.*, 2015). The initial stages of differentiation protocols that encompass formation of neural progenitors vary between different published methods and include manipulation of IGF-1 and Wnt and TGFβ/activin signalling pathway (Jayakody *et al.*, 2015; Mellough *et al.*, 2015). The second and longer stages of differentiation protocols that encompasses the formation of retinal progenitors, photoreceptor precursors and mature photoreceptors within a laminated structure are more similar to each other and in most cases include the addition of fetal calf serum, taurine and retinoic acid. The differentiation method in this study was based on a previous publication which highlighted enhanced formation of eye and optic cup like structures from hESC by the addition of IGF-1 (Mellough *et al.*, 2015). To obtain laminated retinal organoids with high efficiency from both hESC and hiPSC, this protocol was optimised through the addition of fetal calf serum, retinoic acid, taurine and tri-iodothyronine (T3) from day 18 of differentiation. The data (discussed in more detail in **Chapter 5, sections 5.3 & 5.4**) indicate that this optimised differentiation protocol results in formation of laminated retinal organoids which contain all key retinal cell types, form synaptic connections and respond to light. In view of these results, this differentiation protocol was used for the ECM studies described herein.

In this study the expression of key ECM components in retinal organoids derived from hESC and hiPSC was investigated (for summary of ECM expression, please see **Figure 4-14**). Fibronectin was expressed in the basal layer of the organoids at early stages of differentiation and later the expression changed to become in the apical layer. The expression of Collagen IV was observed in the luminal side of the organoids and corporate a similar result reported by Kuwahara *et al.* showing the formation of Collagen IV in the luminal side of the hESCs-derived retinal epithelium (Kuwahara *et al.*, 2015). In the examined organoids generated from pluripotent stem cells, Versican was expressed in the most apical side of the organoids, an area which likely develops into the future IPM. The localisation of Versican in the IPM was confirmed by co-expression with (IRBP/ RBP3), the most abundant protein in the IPM (Stenkamp *et al.*, 2005). Similarly, Brevican and IMPG1 were also expressed in the apical layer of the organoids. IMPG2 was not expressed in retinal organoids until the last time point examined (day 150). This, however, does correspond well with expression in developing human retina, where IMPG2 expression was observed only from 17 PCW.

The expression of key ECM components was very similar between hESC- and hiPSC-derived organoids (**Figure 4-14**). However, Brevican and IMPG1 were detected earlier (Brevican at day 35 and IMPG1 at day 90) in hESC-derived organoids than hiPSCs, suggesting potential differences between hESC and hiPSC in the differentiation kinetics and/or ECM expression. Moreover, the expression of Versican, Brevican, IMPG1 and CD44 in the apical side of the organoids (developing IPM) was similar to the expression observed in human developing retina. For example, IMPG1 was detected in the developing IPM of human developing retina at 12 PCW which correspond with the expression observed in the apical side (developing IPM) of day 90 retinal organoids. Another example, strong expression of CD44 was detected in the developing IPM at day 150 organoids which recapitulate the expression in human developing retina from 16 PCW.

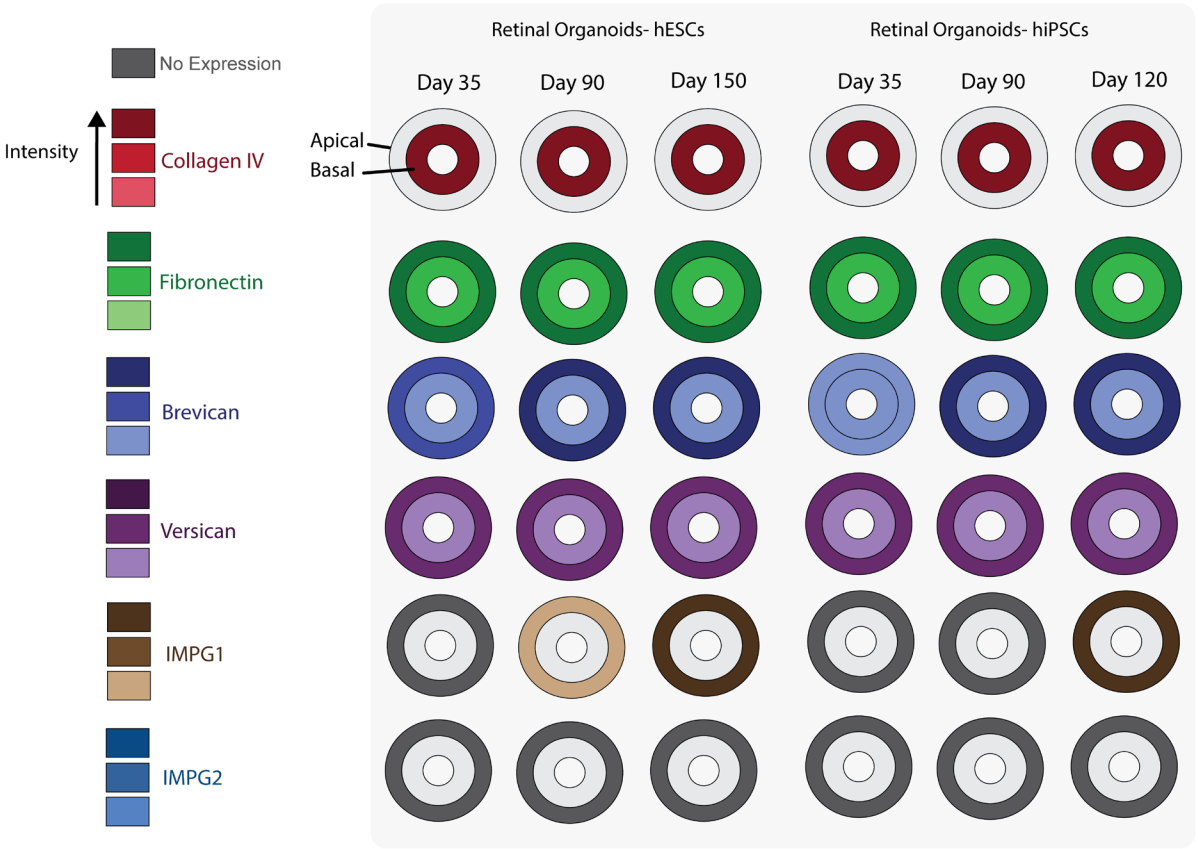

Figure 4-14: Illustrated diagram showing a summary of selected ECM expression during the differentiation of hESCs and hiPSCs to retinal organoids.
Collagen IV was detected in the basal layer (luminal side) of the organoids. Fibronectin was expressed thought the organoids with strong expression toward the apical layer. Brevican, Versican and IMPG1 were strongly expressed in the IPM in the most apical side of the organoids. IMPG2 was not detected until the last time point examined. Colour shades indicate intensity level of fluorescent expression for different ECMs.

Following studying the expression of key ECM components in the retinal organoids, it was clear that their expression in the organoids recapitulates human retinal development *in vivo*. In addition, the expression of IMPG1 and CD44 was first detected in day 90 retinal organoids and became strong in day 150 organoids. Therefore, it was important to perform blocking studies at these time points (day 90 & 150) in order to examine the functional role of these ECMs on retinal development, *in vitro*. At day 90 of differentiation, blocking the action of IMPG1 affected the expression of photoreceptors and connecting cilia but not IPM markers, suggesting important role for IMPG1 in the emergence of the photoreceptors at this time point. Blocking the action of CD44 in day 90 retinal organoids had no impacts on the expression of photoreceptor, connecting cilia and IPM markers. The study also indicated that inhibition of CD44 and IMPG1 in day 150 retinal organoids had a negative impact on the development of photoreceptors and IPM formation (**Figure 4-15**).

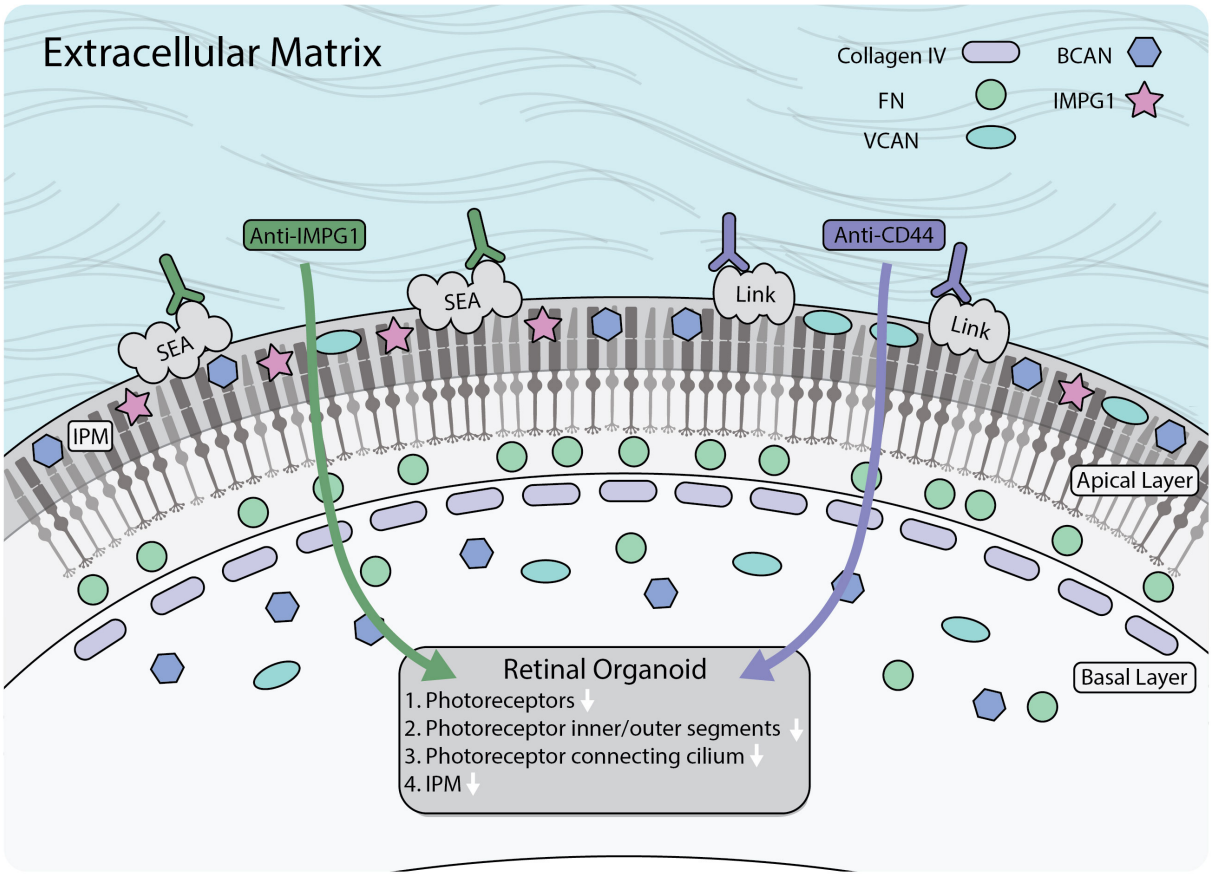

Figure 4-15: Illustrated diagram surmising the effect of blocking IMPG1 and CD44 receptors in retinal organoids.
Blocking antibodies against IMPG1 and CD44 were added to culture medium containing retinal organoid at day 150 of the differentiation process for 14 days. IMPG1 antibody blocked the extracellular cell binding domain (SEA domain) of the receptor, and CD44 blocked the LINK domain on the cell membrane. Inhibition of IMPG1 and CD44 negatively affected photoreceptor development, their inner and outer segments, connecting cilia and IPM formation. Although, IMPG1 acts earlier and having more significant effect on development than CD44.

Blocking the function of IMPG1 in day 150 retinal organoids indicated that IMPG1 plays an important role in the development of photoreceptors as well as formation of their inner/outer segments, connecting cilia and IPM (**Figure 4-15**). Furthermore these data support the clinical phenotype of Vitelliform Macular Dystrophy caused by *IMPG1* mutations and is characterised by impaired metabolism of photoreceptors in the macula region due to the loss of IPM (Manes *et al.*, 2013). Several studies have demonstrated that CD44 is a multi-domain protein that spans the plasma membrane of the cell and acts as a receptor for Hyaluronic acid and other ECMs such as Versican, Brevican and Aggrecan (Brun *et al.*, 2003; Dicker *et al.*, 2014). CD44 can also interact with the GAGs of IMPG1 and may participate in retinal adhesion (Kuehn *et al.*, 2000). In retinal organoids, strong expression of CD44 was observed in the apical layer where the IPM develops, suggesting that CD44 may play an important role in the development of the photoreceptors. The results of this study and those published by Nishina *et al.*, 1997 indicated that CD44 expression was also found in the longitudinal fibres that extend from the inner to the outer limiting membrane and the surface of Müller cells at later stages of human retinal development (19 PCW) (Nishina *et al.*, 1997). Blocking of the CD44 receptor in day 150 retinal organoids resulted in a reduction in the number of rod photoreceptors within the retinal organoids as well as the expression of connecting cilia marker (ARL13B) and IPM marker (RBP3) (**Figure 4-15**). Collectively these data suggest that IMPG1 & CD44 may play an important role in the development of photoreceptors, in addition to being involved in formation of photoreceptor connecting cilia and IPM.

4.5. Conclusion

In summary, Retinal organoids were successfully generated from pluripotent stem cells. The expression of key ECM components (Collagen IV, Fibronectin, Brevican, Versican, IMPG1, IMPG2 and CD44) was examined in the retinal organoids found to recapitulate human retinal development, *in vivo*. Collagen IV and Fibronectin were expressed in Bruch's membrane; whereas Brevican, Versican, IMPG1 and CD44 in the developing IPM. Furthermore, the study highlights an essential role for IMPG1 and CD44 in the development of photoreceptors, their inner and outer segments, connecting cilia and IPM, with IMPG1 having an earlier and more significant impact than CD44. Future work will endeavour to investigate whether manipulation of the ECM can accelerate and enhance retinal development *in vitro* so that effective cell replacement therapies for retinal diseases may be realised.

Note: The content, data and figures in this chapter were used in a recently published original article (Felemban *et al.*, 2018) published in Acta Biomaterialia Journal (See appendices): "Extracellular matrix expression in human pluripotent stem cell-derived retinal organoids recapitulates retinogenesis in vivo and reveals an important role for IMPG1 and CD44 in the development of photoreceptors and interphotoreceptor matrix".

Chapter 5

Chapter 5. Investigating the impact of exogenous ECM manipulation on hESC and hiPSC differentiation towards 3D laminated retina

5.1. Introduction

Human pluripotent stem cells (hPSCs) can be differentiated into retinal organoids to study inherited and age related retinal dystrophies, to screen new drugs and to use them in tissue transplantation. In the last decade, seminal discoveries made by Sasai's group have led to the *in vitro* generation of retinal organoids containing major retinal cell types such as photoreceptors, Muller glia and other retinal neurons organized in laminar structures from murine, primate and human embryonic stem cells and induced pluripotent stem cells (Eiraku and Sasai, 2011; Eiraku *et al.*, 2011; Nakano *et al.*, 2012; Assawachananont *et al.*, 2014; Kuwahara *et al.*, 2015; Takata *et al.*, 2017). Since then, multiple studies modified Sasai's protocol to enhance culturing outcomes (Gonzalez-Cordero *et al.*, 2013; Assawachananont *et al.*, 2014; Völkner *et al.*, 2016). However, current differentiation protocols are impeded by some challenges. For example, the differentiation process is lengthy, requiring 150-300 days and often unable to generate correct proportions of all retinal cell-types especially those located in the inner nuclear layer (Llonch *et al.*, 2018). Other challenges in this field are the failure to establish correct synaptic connections (Llonch *et al.*, 2018), although the expression of some synaptic proteins have been reported (Zhong *et al.*, 2014), inability to maintain mature photoreceptor cells that resemble the native counterparts in both structure and function and light response (Meyer *et al.*, 2011; Nakano *et al.*, 2012; Zhong *et al.*, 2014; Kuwahara *et al.*, 2015; Gonzalez-Cordero *et al.*, 2017; Wahlin *et al.*, 2017). Although light responses were reported by Zhong *et al.*, they were from a limited number of photoreceptors (2 out of 13 randomly selected cells) (Zhong *et al.*, 2014). Another study has reported immature light responses in retinal organoids that resemble early light responses recorded from retinal ganglion cells in mouse developing retina (Hallam *et al.*, 2018). Many groups have also reported the generation of RPE cells (Zhong *et al.*, 2014; Kaewkhaw *et al.*, 2015; Lowe *et al.*, 2016; Wahlin *et al.*, 2017), but not all the cells were able to interact with neural retina (NR) as *in vivo* and were not fully organised on the apical side of the retinal organoid. It has been shown in mouse retina *in vivo* and *in vitro* that the RPE is important for retinal lamination, spatial reorganisation and the differentiation of the photoreceptors (Raymond and Jackson, 1995; German *et al.*, 2008).

In vivo, RPE cells and its associated basement membrane are known to release many extracellular molecules (ECMs) that help to maintain retinal integrity such as laminin,

collagen and hyaluronic acid (Aisenbrey *et al.*, 2006; Clark *et al.*, 2011; Keenan *et al.*, 2012). This is corroborated by *in vitro* proteomic studies which have shown the secretion of numerous trophic factors and ECMs including fibronectin, collagen and laminin (Kolomeyer *et al.*, 2011) from foetal and adult RPE into the culture media. The biological effect of the RPE secreted factors is reflected in enhanced proliferation, neurite outgrowth and differentiation of the photoreceptors isolated from neonatal rat retina and co-cultured with RPE conditioned medium (CM) (Gaur *et al.*, 1992), enhanced RPE differentiation from human embryonic stem cells (hESCs) (Hsiung *et al.*, 2015) and human adipose tissue-derived mesenchymal stromal cells (Zhang *et al.*, 2017). Kolomeyer *et al.* indicated that porcine retina cultured in RPE CM significantly decreases the thinning of outer nuclear layer, photoreceptor axon retraction and retinal death compared to basal medium (Kolomeyer *et al.*, 2013), supporting the presence of key factors in RPE CM which support photoreceptor viability in *in vitro* culture conditions. Another study reported that co-culturing rat neural retina with RPE cells *in vitro* promotes the attachment of the photoreceptors, axon's growth and migration of their cell bodies toward the RPE cells as well as photoreceptors development by increasing the synthesis of rhodopsin (German *et al.*, 2008). Given the close interactions of RPE with NR, co-culture of these two cell types has been used to support the maintenance of neural retina in a novel organotypic culture model (Kaempf *et al.*, 2008). For example, Kaempf *et al.* indicated that co-culture of adult porcine neural retina with choroid-RPE explant *in vitro* enhanced the maintenance of the retina by reducing apoptosis in the all nuclear cell layers, decreasing gliosis and increasing glutamate synthetase compared to retina cultured alone (Kaempf *et al.*, 2008).

In addition to secreted factors provided in CM and direct co-culture of several cell types, tissue decellularisation has been put forward as a useful method for providing the necessary biochemical and biophysical features of cellular niches that are needed to promote progenitor and stem cell differentiation and engraftment (Ott *et al.*, 2008; Ott *et al.*, 2010; Petersen *et al.*, 2010; Baptista *et al.*, 2011; Song *et al.*, 2013; De Waele *et al.*, 2015; Chirco *et al.*, 2017; Sun *et al.*, 2018). Tissue decellularisation is a process of removing the cellular materials from a tissue so that only the extracellular matrix (ECM) components remain (Chirco *et al.*, 2017). This process preserves the architecture and integrity of the ECM which can be used as an additional culture media supplement or as a scaffold to support cell engraftment and differentiation as well as a source of biochemical and biophysical cues for the cells that reside within it (Chirco *et al.*, 2017). To date, decellularised ECM (dECM) has been successfully achieved and utilised from many tissues including heart, liver, lung, kidney

and brain (Ott *et al.*, 2008; Ott *et al.*, 2010; Petersen *et al.*, 2010; Baptista *et al.*, 2011; Song *et al.*, 2013; De Waele *et al.*, 2015; Sun *et al.*, 2018). For example, culturing hESCs on decellularised rhesus monkey kidney and lung sections enhanced the expression of kidney and lung markers, respectively (Agmon and Christman, 2016). *Zhang et al.* has also reported that dECM from rat liver enhanced the differentiation of adipose derived mesenchymal stem cell into hepatic cells (Zhang and Dong, 2015). Several groups have also performed decellularisation of tissues in the eye including cornea, retina, Bruch's membrane and RPE (Tezel *et al.*, 2004; Ponce Márquez *et al.*, 2009; Kundu *et al.*, 2016; Chirco *et al.*, 2017; Ji *et al.*, 2018; Singh *et al.*, 2018). More recently, dECM has been prepared from RPE and neural retina and shown to contain several ECMs [such as collagen, laminin sulfated glycosaminoglycans, hyaluronic acid, and growth factors including basic fibroblastic growth factor (bFGF), epidermal growth factor (EGF), nerve growth factor (NGF) and pigment epithelium derived factor (PEDF)] that play a significant role in the development and maturation of the retina and photoreceptors (Kundu *et al.*, 2016; Chirco *et al.*, 2017). Kundu *et al.* showed that decellularised neural retina from bovine eye promoted the attachment, proliferation and differentiation of human retinal progenitor cells *in vitro* (Kundu *et al.*, 2016).

To investigate whether direct contact or only secreted factors (indirect) were needed to direct differentiation of retinal progenitor cells (RPCs) from hESCs, Amirpour *et al.* compared between direct and indirect RPE co-cultured with hESC-derived retinal progenitor cells differentiation system into photoreceptors (Amirpour *et al.*, 2013) and found that the expression of photoreceptor mature markers like arrestin was only increased in direct co-culture (cell-cell contact) comparing to the indirect system (Amirpour *et al.*, 2013). This result suggests that the expression of late photoreceptor markers can be enhanced through seeding retinal progenitor cells on RPE cells, *in vitro*. However, none of these studies tested the impacts of these supplementations on retinal organoids developed in 3D culture systems which recapitulate retinal development *in vivo*.

5.2. Aims

In the previous chapter, the functional role of key ECM components in the differentiation of hPSC-derived retinal organoids was investigated via blocking the action of CD44 and IMPG1. The aim of this chapter is to investigate the impact of culture supplementation with RPE CM, decellularised ECM from adult bovine neural retina (decel NR) and RPE (decel RPE) on the differentiation of pluripotent stem cells (PSCs) to retinal organoids in order to enhance the current differentiation protocol by manipulating the ECM microenvironment to improve the development of retinal organoids and their responses to electrophysiological stimuli, *in vitro*.

5.3. Results

The work in this chapter was performed jointly with Dr. Birthe Hilgen (Newcastle University, UK).

5.3.1. ECMs composition in CM RPE, decel NR & decel RPE

Engineering a natural substrate that can promote pluripotent stem cells differentiation into retinal cells could be essential for the successful generation of retinal organoids, *in vitro*. The ECM has been shown to provide a biomimetic microenvironment with essential cues for retinal differentiation in culture (Kundu *et al.*, 2016). In order to examine the role of ECM on the differentiation of pluripotent stem cells into retinal organoids, neural retina and RPE tissue were extracted and decellularised by the Master student (Martin Kiening) from adult bovine eye following a protocol reported by Medberry *et al.* (Medberry *et al.*, 2013). The RPE CM was collected from polarised RPE cells (8 months old; TER>250Ω) derived from hESCs. ECM components (collagen, laminin, GAGs and HA) were quantified and compared to RPE medium and native tissue of bovine retina and RPE, respectively (**Table 5-1**).

Table 5-1: DNA and ECM composition in RPE normal and conditioned medium (RPE CM), native and decellularised neural retina and RPE (decel NR) and (decel RPE).

	DNA	Collagen	Laminin	GAGs	Hyaluronic Acid	Ratio (collagen:laminin: GAGs:HA)
RPE Medium (µg/ml)	-	0.5 ± 0.0001767	0.00017 ± 0.00001085	0	2.937 ± 0.04582	2941:1:0:17276
RPE CM (µg/ml)	-	1.7 ± 0.0001146	0.00233 ± 0.00001668	0.06358 ± 0.01387	3.333 ± 0.1212	730:1:27:1430
Native Retina (µg/mg of tissue dry weight)	110.5	1.999 ± 0.4285	0.00327 ± 0.009366	8.667 ± 0.1115	43.43 ± 1.403	611:1:2650:13281
Decel NR (µg/mg of tissue dry weight)	8.5	0.9496 ± 0.1731	0.00051 ± 0.01372	3.661 ± 0.5228	8.81 ± 0.9633	1862:1:7178:17275
Native RPE (µg/mg of tissue dry weight)	21.71	1.999 ± 0.0	0.00547 ± 0.01	21.42 ± 0.1115	32.95 ± 0.001171	365:1:3916:6024
Decel RPE (µg/mg of tissue dry weight)	4.3	0.5998 ± 0.1731	0.00228 ± 0.008868	14.58 ± 0.4238	13.05 ± 0.1315	263:1:6395:5724

To confirm the successes of the decellularisation process, the DNA content was assessed in NR and RPE samples. These results indicated 8.5 and 4.3 µg/mg of initial dry weight of NR and RPE, respectively (**Figure 5-1 and Table 5-1**) which was significantly lower than the amount of DNA in the native tissues (**Figure 5-1 and Table 5-1**) indicating that the bulk of cellular material was removed after the decellularisation process from the native retina (~92%) and RPE (~80.5%). This result was similar to the one reported by Kundu *et al.*, 2016 where (~94%) of cellular material was removed after the decellularisation of NR from bovine eyes (Kundu *et al.*, 2016), but higher than the amount of DNA reported by Medberry and his group (0.0379 µg/mg of initial dry weight of tissue) (Crapo *et al.*, 2012).

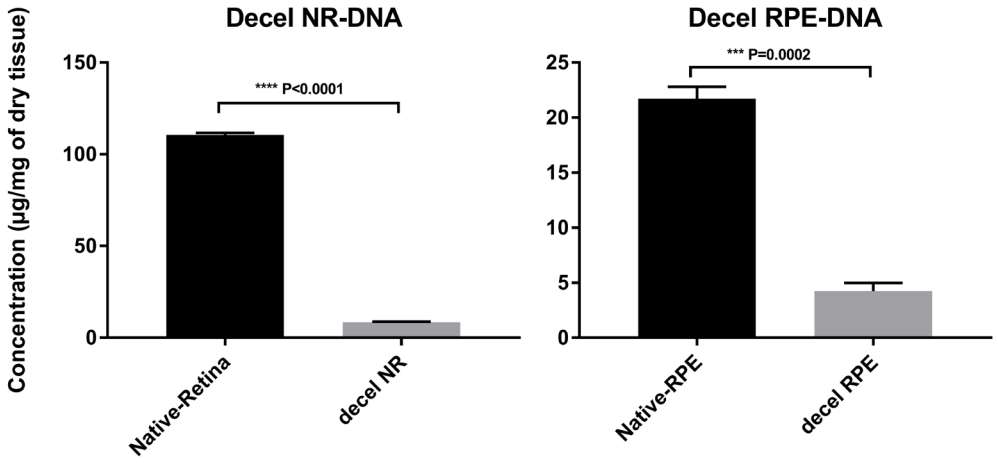

Figure 5-1: Cellular material composition of native and decel NR and RPE.
DNA content (µg/mg of dry tissue). Data is shown as mean ± SEM, $n = 3$. Differences were considered statistically significant at ***$p < 0.001$ and ****$p < 0.0001$.

All analysed ECM components (collagen, laminin, GAGs and HA) significantly increased in the CM RPE compared to the normal RPE medium (**Figure 5-2 and Table 5-1**). Opposite results were found for the native retina after decellularisation, revealing a decrease of all analysed ECM components in the decel NR compared to the native retina (**Figure 5-3 and Table 5-1**). Similar to decel NR, the ECM components in the decel RPE were reduced compared to the native RPE after decellularisation (**Figure 5-4 and Table 5-1**). The ratio between the ECM components before and after the decellularisation was changed for all ECMs except laminin. Together these results indicate that some of the ECM components (collagen, sulfated GAGs & HA) were lost during the decellularisation procedures while removing the majority of cellular material. Kundu *et al.* has also reported that some of the ECMs were lost after the decellularisation procedures and the ECMs concentration in the decel NR was 79 ± 13 µg collagen/mg, 21.3 ± 8 µg sGAG/mg, and 15.14 ± 0.22 µg HA/mg of tissue dry weight (Kundu *et al.*, 2016).

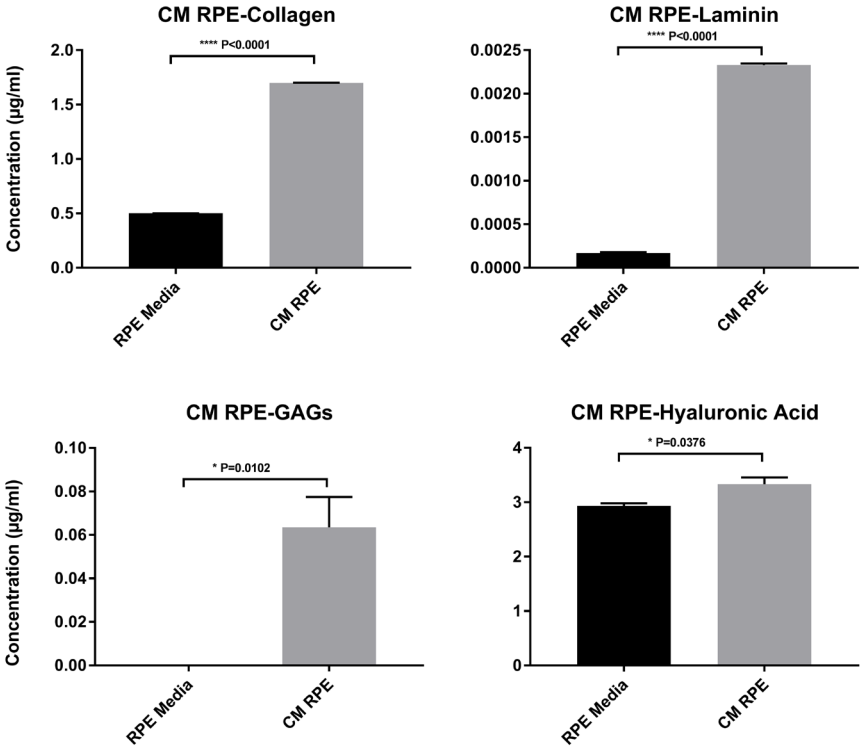

Figure 5-2: ECM composition of RPE normal and conditioned medium (CM RPE). Collagen, laminin, sulfated GAGs and hyaluronic acid content (µg/ml of medium). Data is shown as mean ± SEM, *n* = 3. Differences were considered statistically significant at *p < 0.05 and ****p < 0.0001.

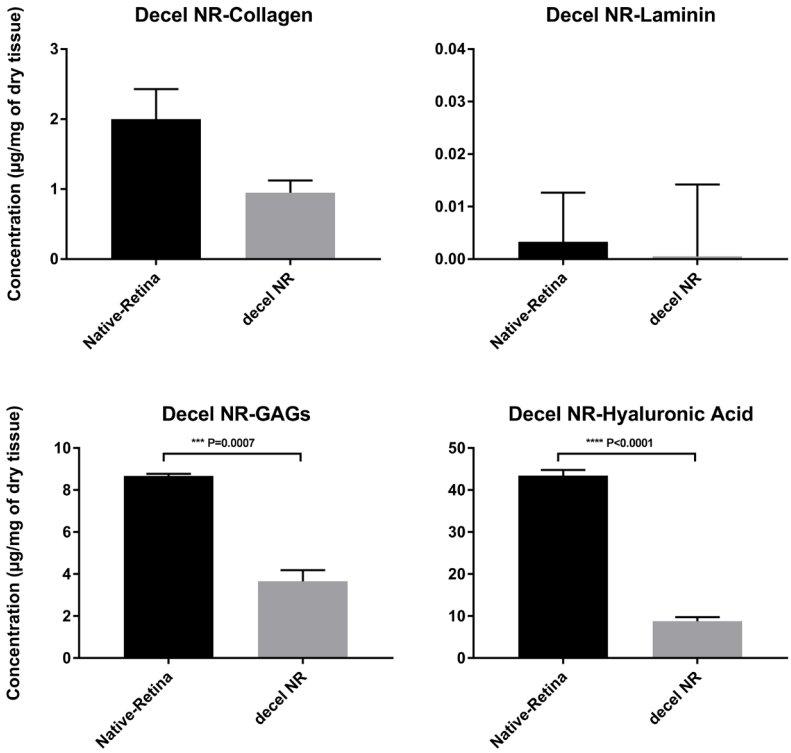

Figure 5-3: ECM composition of native and decellularised neural retina (decel NR). Collagen, laminin, sulfated GAGs and hyaluronic acid content (µg/mg of dry retina). Data is shown as mean ± SEM, *n* = 3. Differences were considered statistically significant at ***p < 0.001 and ****p < 0.0001.

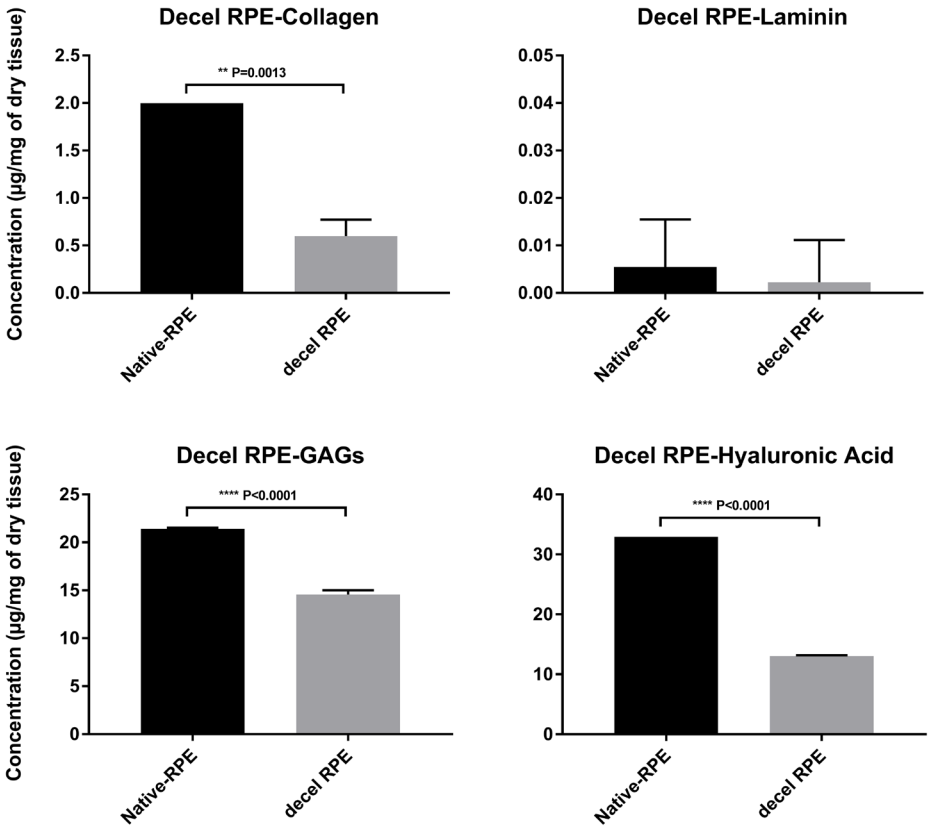

Figure 5-4: ECM composition of native and decellularised RPE (decel RPE).
Collagen, laminin, sulfated GAGs and hyaluronic acid content (µg/mg of dry RPE). Data is shown as mean ± SEM, $n = 3$. Differences were considered statistically significant at **$p < 0.01$ and ****$p < 0.0001$.

5.3.2. Effects of ECM supplementation on early/middle retinal differentiation

Retinal organoids were generated from hESCs and hiPSCs in four culture systems including: control culture system from previously published protocol (Dorgau *et al.*, 2018; Felemban *et al.*, 2018), and media supplemented with CM RPE, decel NR or decel RPE. The impacts of each ECM supplementation were assessed using IHC for specific markers of retinal developmental at three time points during the differentiation process: early (day 35), middle (day 90) and later stages of retinal differentiation (day 150). In addition, semi-quantitative analysis of positive cells for distinct key retinal marker was performed to validate the effect of each ECM supplementation on the differentiation process.

At early stages of differentiation (day 35), a thick layer of retinal progenitor cells, expressing VSX2, was found on the apical edge of retinal organoids generated from hESCs (**Figure 5-5**) and hiPSCs (**Figure 5-6**) in all four culture conditions. Recoverin-positive

photoreceptors and HuC/D- positive amacrine/ganglion cells were observed in the centre region of retinal organoids in all culture conditions (**Figure 5-5** and **Figure 5-6**).

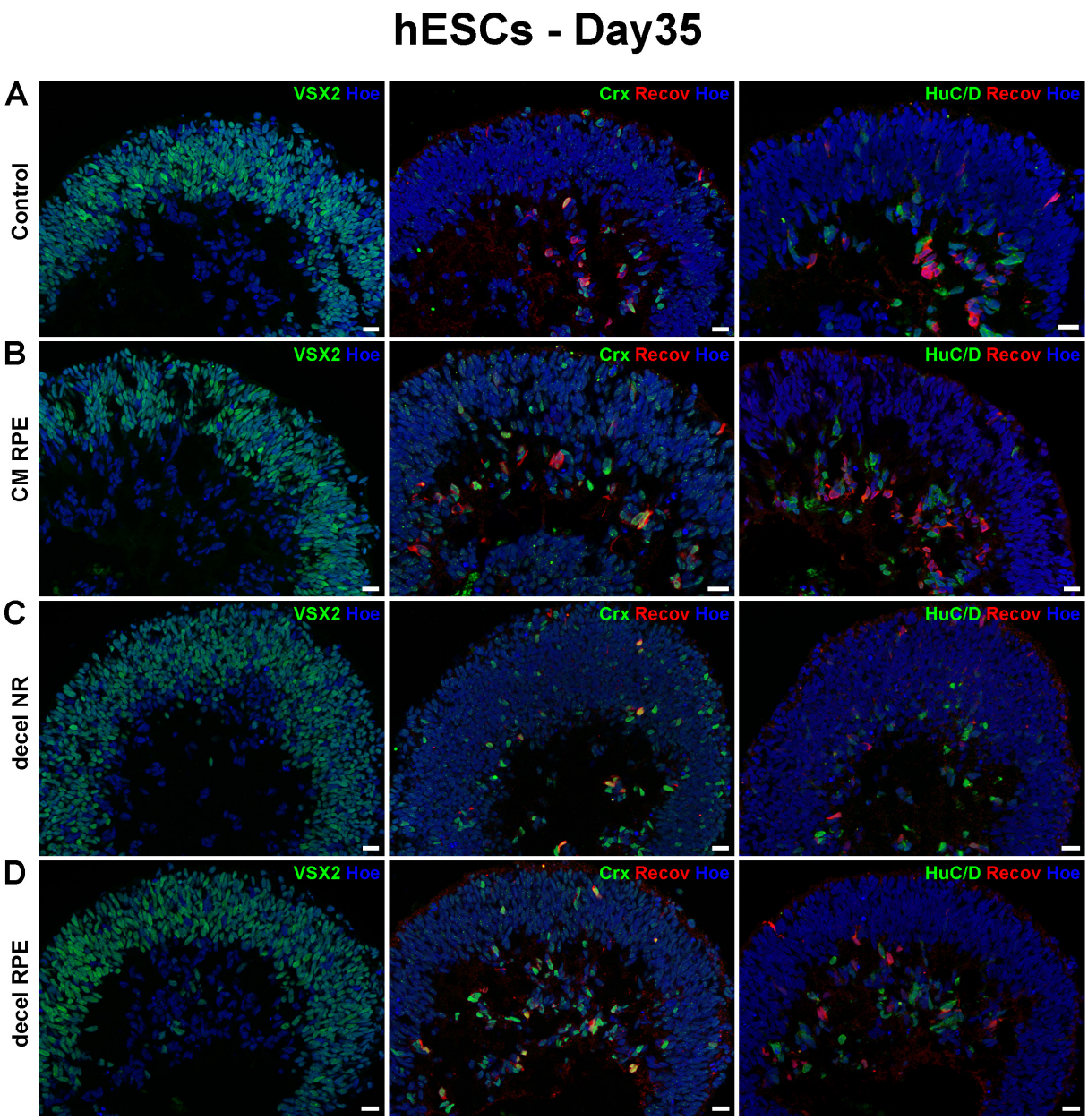

Figure 5-5: Characterisation of hESC-derived retinal organoids at day 35 of differentiation.

(A-D) Sections through retinal organoids at day 35 showing immunofluorescence labelling with retinal markers including: VSX2, CRX, Recoverin (Recov) and HuC/D with Hoechst (Hoe) in four culture systems: control (A), CM RPE (B), decel NR (C) and decel RPE (D). Scale bars =20 μm.

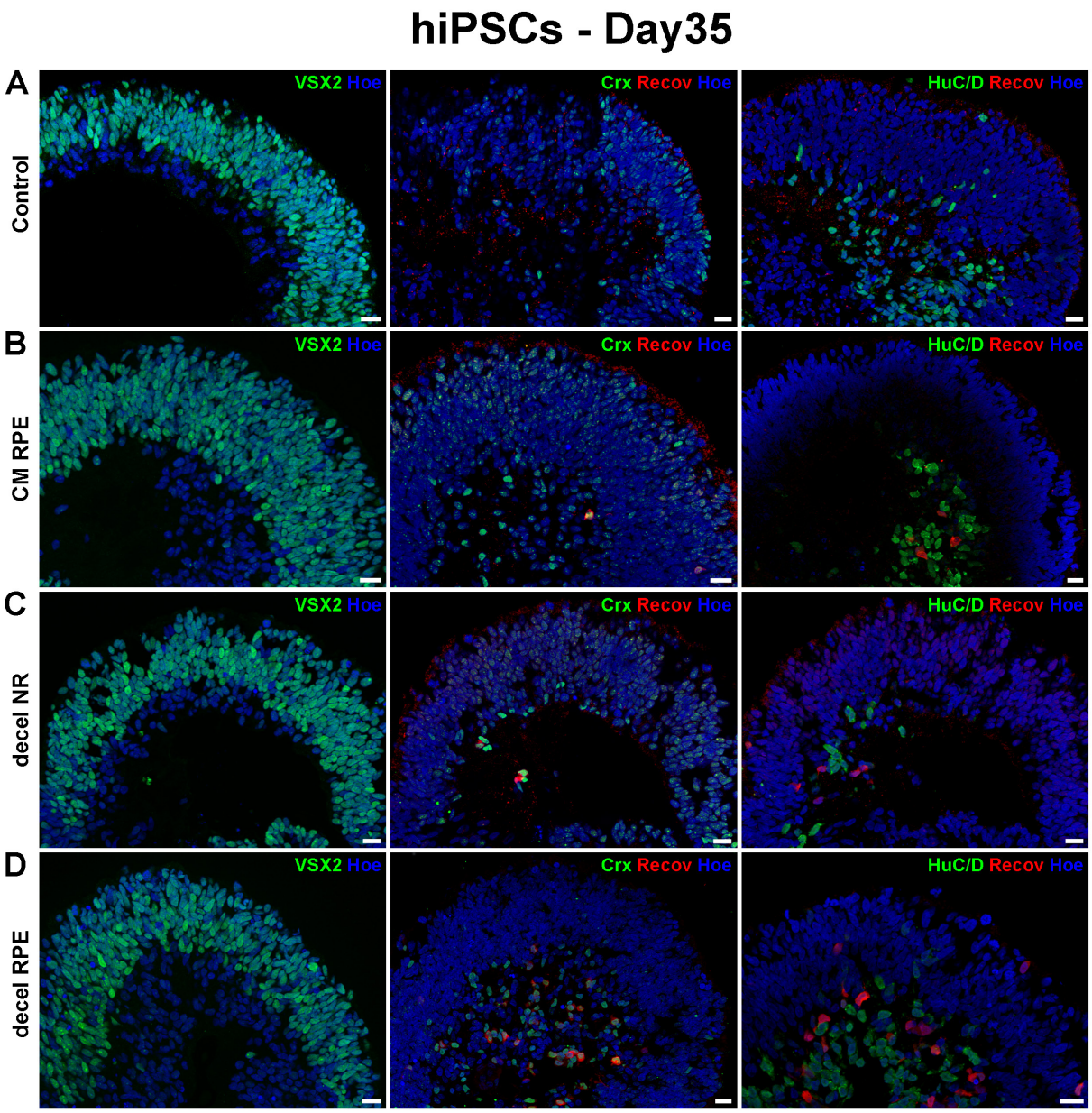

Figure 5-6: Characterisation of hiPSCs-derived retinal organoids at day 35 of differentiation.
(A-D) Sections through retinal organoids at day 35 showing immunofluorescence labelling with retinal markers including: VSX2, CRX, Recoverin (Recov) and HuC/D with Hoechst (Hoe) in four culture systems: control (A), CM RPE (B), decel NR (C) and decel RPE (D). Scale bars =20 μm.

CRX, a marker for post-mitotic photoreceptors, was expressed across the entire neural retina of both cell lines in all culture conditions, marking some positive cells in the centre as well as the apical edge of the organoids where retinal progenitor cells are located (**Figure 5-5** and **Figure 5-6**). Cell quantification analysis of retinal progenitor cells (VSX2), photoreceptors (CRX and Recoverin) and amacrine/ganglion cells (HuC/D) revealed no significant differences between all conditions (**Figure 5-7**). These data correspond with

morphological observations which showed similar percentage of organoids that had developed neural retina with or without RPE (or RPE only) across different culture conditions at day 35 of the differentiation process (**Figure 5-8**).

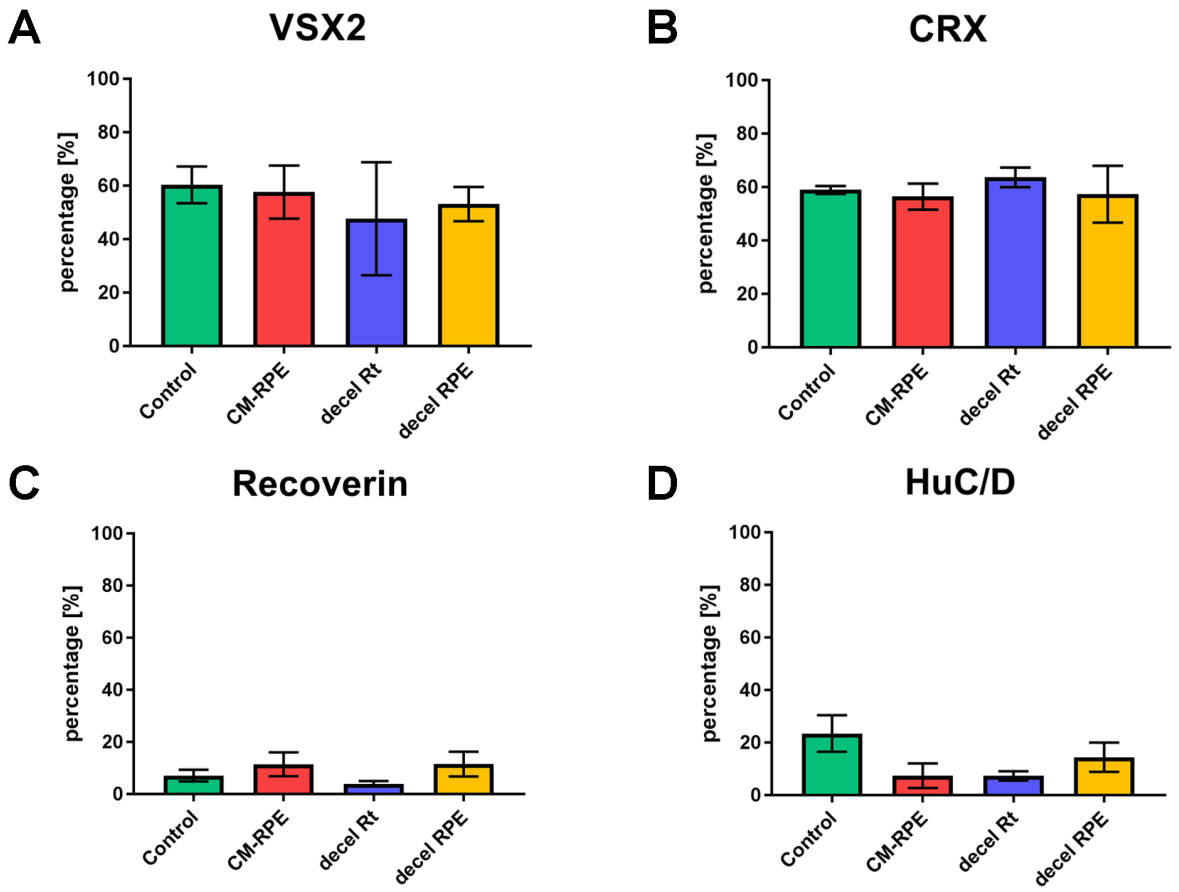

Figure 5-7: Cell quantification of retinal markers in day 35 retinal organoids derived from hESCs & hiPSCs.
(A-D) Schematic charts showing semi-quantitative measurements of the retinal markers: VSX2 (A), CRX (B), Recoverin (C) and HuC/D (D) in day 35 hPSC-derived retinal organoids. Data is shown as mean ± SEM, *n=6-8* (average of hESCs + hiPSCs).

In comparison to day 35, a massive increase in the percentage of retinal organoids containing neural retinal structures with or without RPE was observed at day 90 of differentiation in all conditions of both cell lines, except for decel RPE condition of hESC-derived retinal organoids (**Figure 5-8**). Interestingly, in this culture condition, retinal organoids had developed less structures of neural retina without RPE ($p<0.001$) and more structures of neural retina containing RPE ($p<0.01$) compared to control conditions (**Figure 5-8B**), suggesting that the addition of decel PRE supplementation may have a beneficial effect on the development of neural retina with RPE.

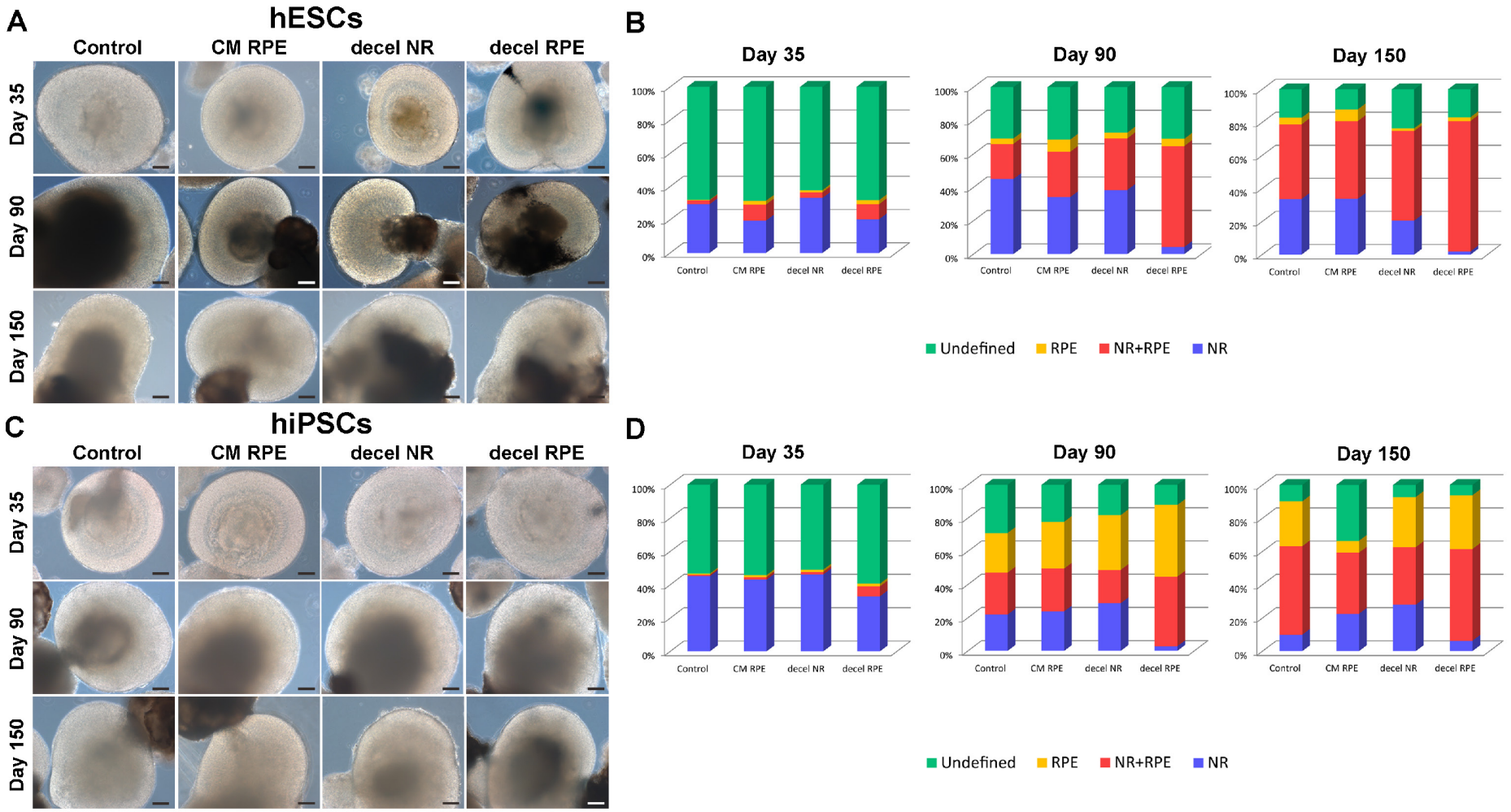

Figure 5-8: Development of hPSC-derived retinal organoids

(A & C) Representative examples of bright field images showing the development of retinal organoids derived from hESCs (A; day 35-150) and hiPSCs (C; day 35-150) in four different culture systems: control, RPE conditioned media (CM RPE), decellularised neural retina (decel NR) and decellularised RPE (decel RPE). Schematic charts showing the development of hESC-derived (B) and hiPSC-derived (D) retinal organoids and RPE, *n= 4-6*. RPE= organoids with RPE spheres only, NR= organoids with neural retina only, NR+ RPE = organoids with neural retina & RPE and undefined= organoids that did not contain any neural retina or RPE cells. Scale bars =100 µm.

At middle stages of retinal differentiation (day 90), a thick layer of VSX2-positive retinal progenitor cells was still found in all culture conditions but a remarkable increase in the number of photoreceptors and amacrine/ganglion cells was observed compared to early stages of differentiation (day 35) in both cell lines and all conditions (**Figure 5-9** and **Figure 5-10**).

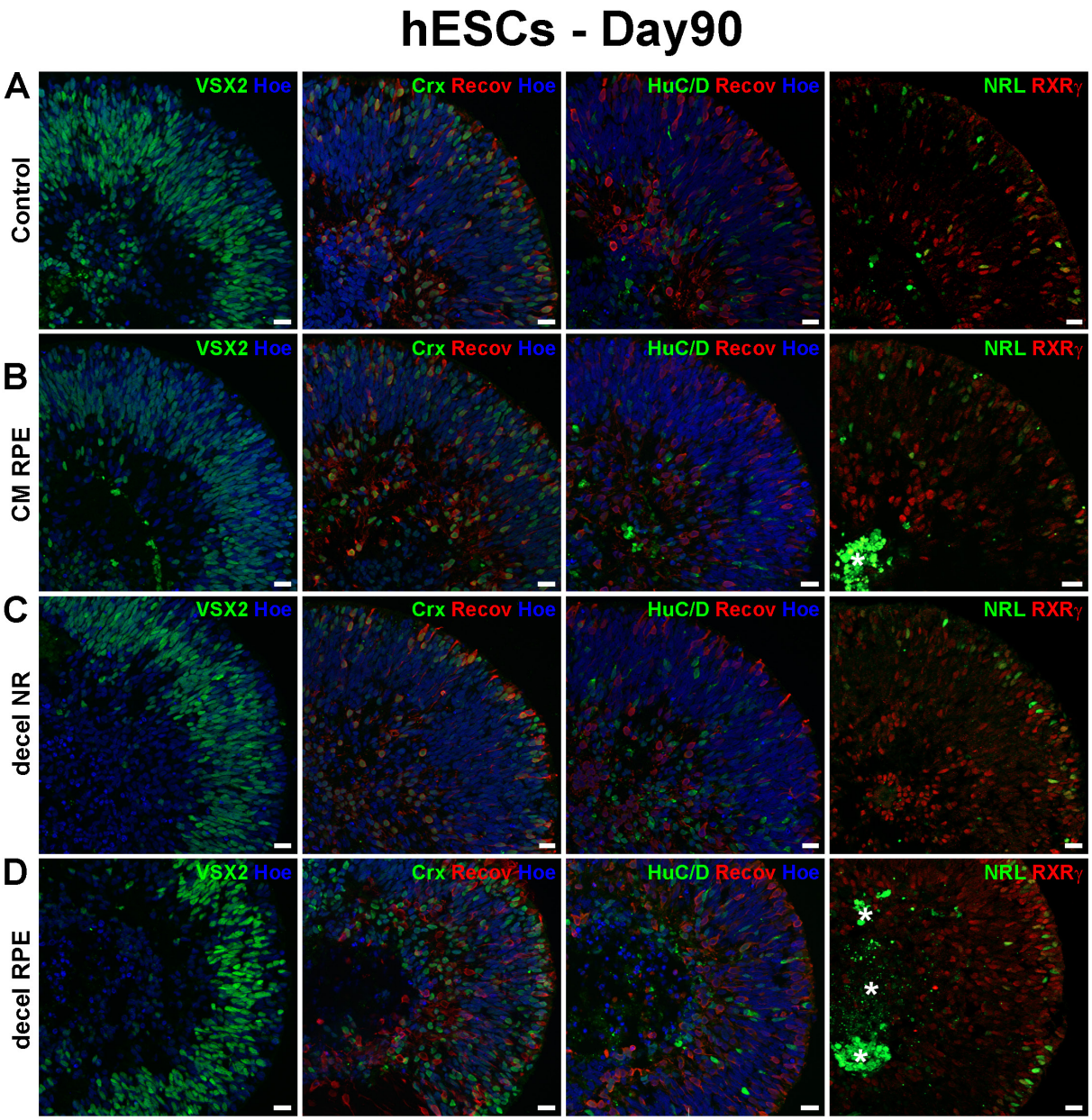

Figure 5-9: Characterisation of hESC-derived retinal organoids at day 90 of differentiation.

(A-D) Sections through retinal organoids at day 90 showing immunofluorescence labelling with retinal markers including: VSX2, CRX, Recoverin (Recov), HuC/D, NRL and RXR with Hoechst (Hoe) in four culture systems: control (A), CM RPE (B), decel NR (C) and decel RPE (D). Stars indicate cellular debris in NRL staining. Scale bars =20 µm.

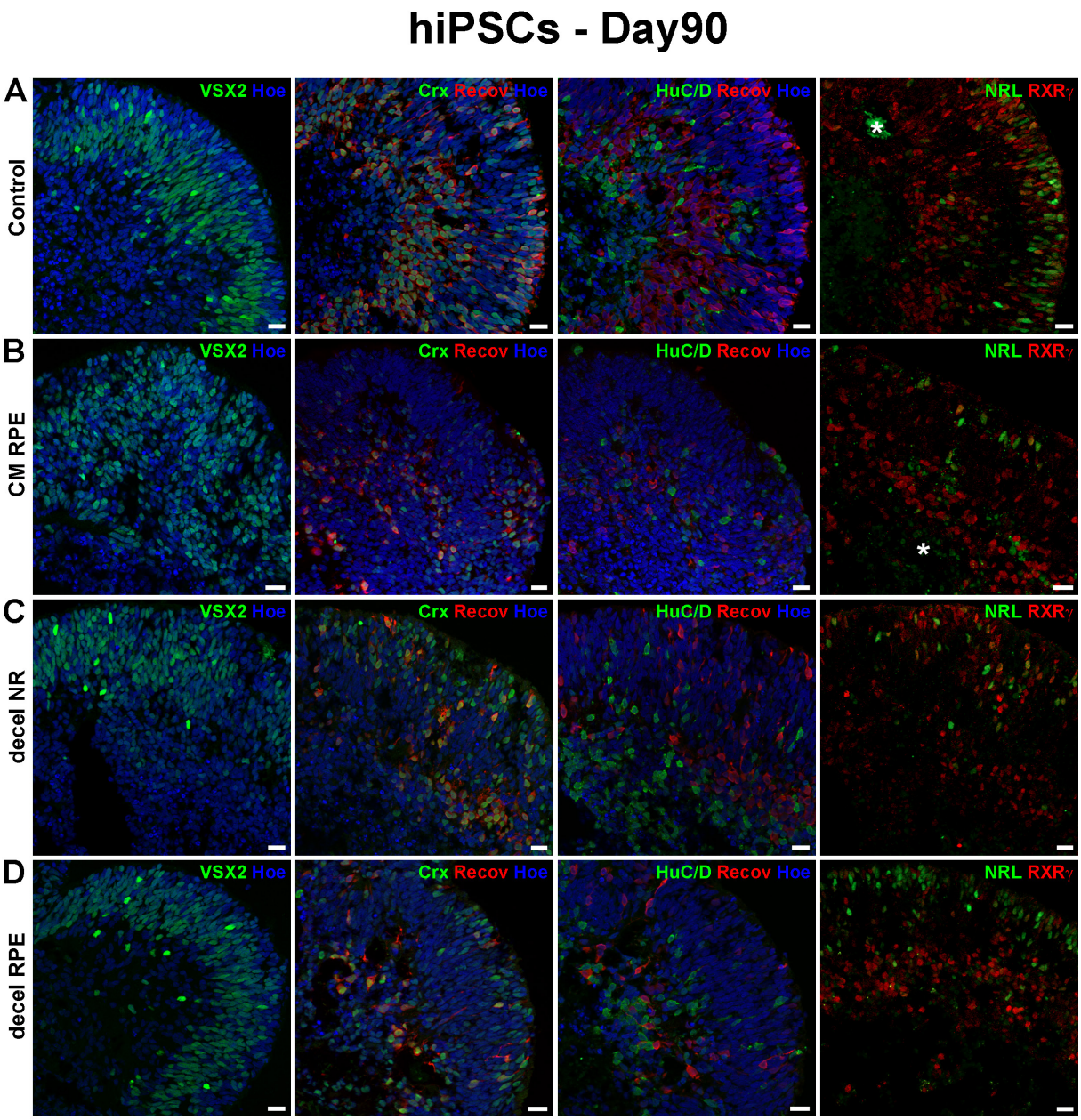

Figure 5-10: Characterisation of hiPSC-derived retinal organoids at day 90 of differentiation.

(A-D) Sections through retinal organoids at day 90 showing immunofluorescence labelling with retinal markers including: VSX2, CRX, Recoverin (Recov), HuC/D, NRL and RXR with Hoechst (Hoe) in four culture systems: control (A), CM RPE (B), decel NR (C) and decel RPE (D). Stars indicate cellular debris in NRL staining. Scale bars =20 µm.

The majority of HuC/D-positive amacrine/ganglion cells were observed in the centre of the retinal organoids rather than across the neural retina in both cell lines (**Figure 5-9** and **Figure 5-10**). A thin layer of photoreceptors, co-expressing CRX and Recoverin, was found at the apical edge of the organoids; however CRX- and Recoverin-photoreceptor precursors were also found across the organoids and accumulated in the centre (**Figure 5-9** and **Figure**

5-10). The expression of NRL and RXRγ, markers for post-mitotic rod and cone precursors respectively, were expressed at day 90 of differentiation with slightly different distribution pattern. NRL-positive cells were mainly located at the apical edge of the organoids whereas RXRγ-expressing cells were found across the neural retina in both cell lines and all conditions (**Figure 5-9** and **Figure 5-10**). In addition, there were less NRL-expressing rod precursors than RXRγ-positive cone precursors which were confirmed by cell quantification analysis (**Figure 5-11**). The cell quantification analysis showed no significant differences in retinal progenitor cells (VSX2), amacrine/ganglion cells (HuC/D), photoreceptors (CRX and Recoverin), rod (NRL) and cone (RXRγ) precursors between all conditions in both cell lines (**Figure 5-11**). In summary, these data indicate that supplementation of CM RPE, decel NR and decel RPE in culture media had no effect on retinal development at early and/or middle stages of the differentiation process.

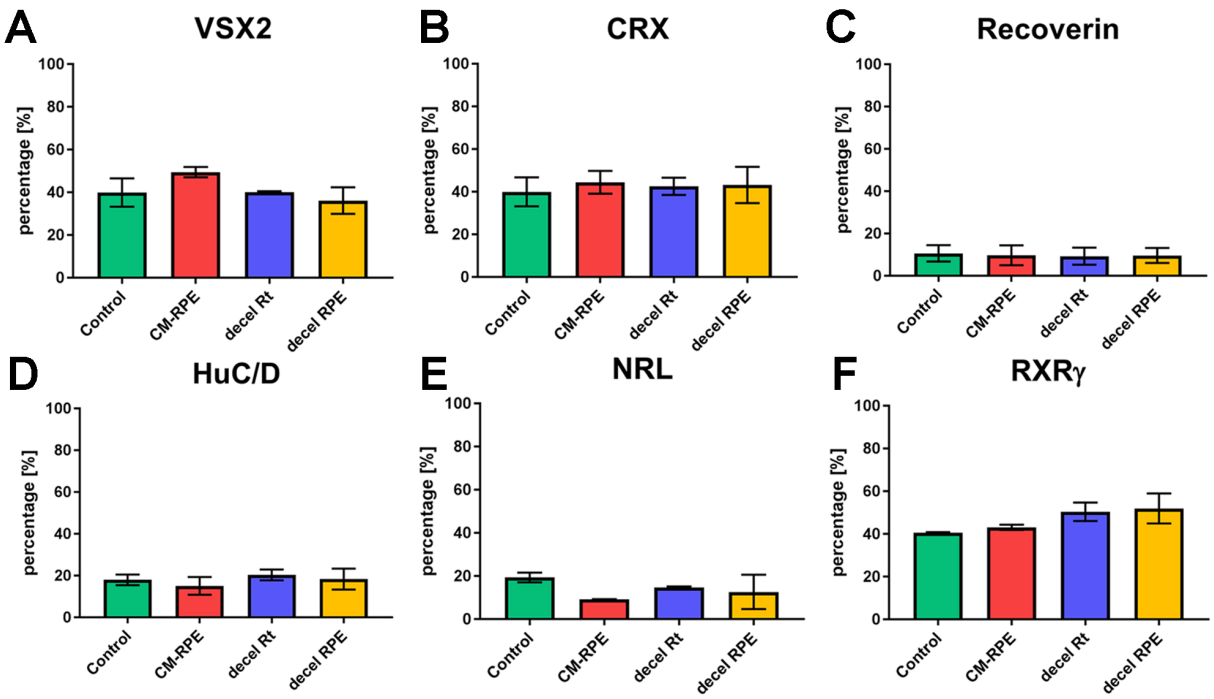

Figure 5-11: Cell quantification of retinal markers in day 90 retinal organoids derived from hESCs & hiPSCs.

(A-F) Schematic charts showing semi-quantitative measurements of the retinal markers: VSX2 (A), CRX (B), Recoverin (C), HuC/D (D), NRL (E) and RXRγ (F) in day 90 hPSC-derived retinal organoids. Data is shown as mean ± SEM, *n=6-8* (average of hESCs + hiPSCs).

5.3.3. ECM supplementation improves retinal differentiation at later stages

To assess the development and confirm that retinal organoids contain all retinal cell-types during later stages of the differentiation process (day 150), more specific retinal markers were used in IHC analysis and TEM was performed in all culture conditions. In addition, cell quantification analysis and qRT-PCR were carried out to evaluate any differences between individual ECM supplementation conditions.

At later stages of retinal differentiation (Day 150), the number of retinal structures, the bright phase neuroepithelium on the apical side of organoids, increased slightly in both cell lines and all conditions compared to day 90 of the differentiation process (**Figure 5-8B,D**). Moreover, a remarkable increase of retinal structures with RPE was observed in all conditions of hESCs in contrast to early stages of differentiation (**Figure 5-8B**). In line with this, there were significantly more retinal structures with RPE ($p<0.05$) and subsequently less without RPE ($p<0.01$) in the decel RPE condition compared to control condition (**Figure 5-8B**).

IHC analysis revealed a thick layer of photoreceptors, detected by CRX and Recoverin, on the apical side of retinal organoids in all conditions (**Figure 5-12, 5-13, 5-14 and Figure 5-15**), indicating the formation of outer nuclear layer (ONL). Moreover, in culture all conditions higher magnifications of Recoverin-positive cells displayed nice morphological features of photoreceptors possessing a connecting cilium, labelled with ARL13B, and developing outer segments (OS) as demonstrated by Gαt1 immunoreactivity (**Figure 5-12, 5-13, 5-14 and Figure 5-15**).

Although qRT-PCR studies and cell quantification analyses failed to show any differences in gene expression of *CRX* and *RCVRN* as well as the number of Crx- and Recoverin-positive photoreceptors in all culture conditions (**Figure 5-16)**, the next step was to examine in more detail the expression of both photoreceptor types, rods and cones, in retinal organoids. In general, the two photoreceptor types were found in all conditions of hPSC-derived retinal organoids at day 150 of differentiation (**Figure 5-12, 5-13, 5-14 and Figure 5-15**). Rods, detected by Rhodopsin, were evenly distributed across the developing ONL of the organoids in all conditions (**Figure 5-12, 5-13, 5-14 and Figure 5-15**). Higher magnifications highlighted typical rod morphology in detail as shown in **Figure 5-12, 5-13, 5-14 and Figure 5-15**.

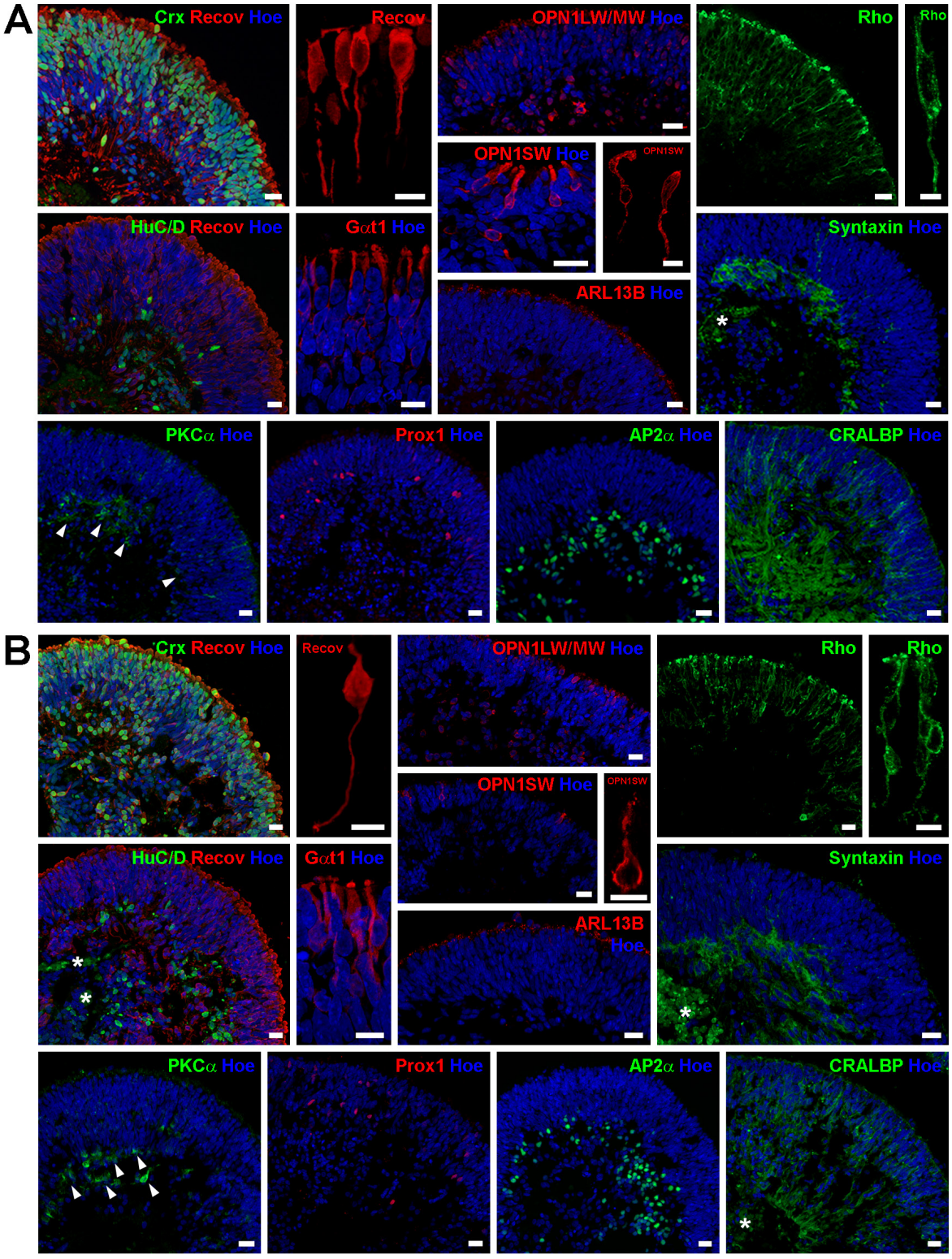

Figure 5-12: Characterisation of hESC-derived retinal organoids at day 150 of differentiation. (A-B) Sections through retinal organoids at day 150 showing immunofluorescence labelling with retinal markers including: CRX, Recoverin (Recov), HuC/D, Gαt1, OPN1LW/MW, OPN1SW, Rhodopsin (Rho), ARL13B, Syntaxin, PKCα, Prox1, AP2α and CRALBP with or without Hoechst (Hoe) in four culture systems: control (A), CM RPE (B). Stars indicate cellular debris in organoids. Scale bars =20 μm.

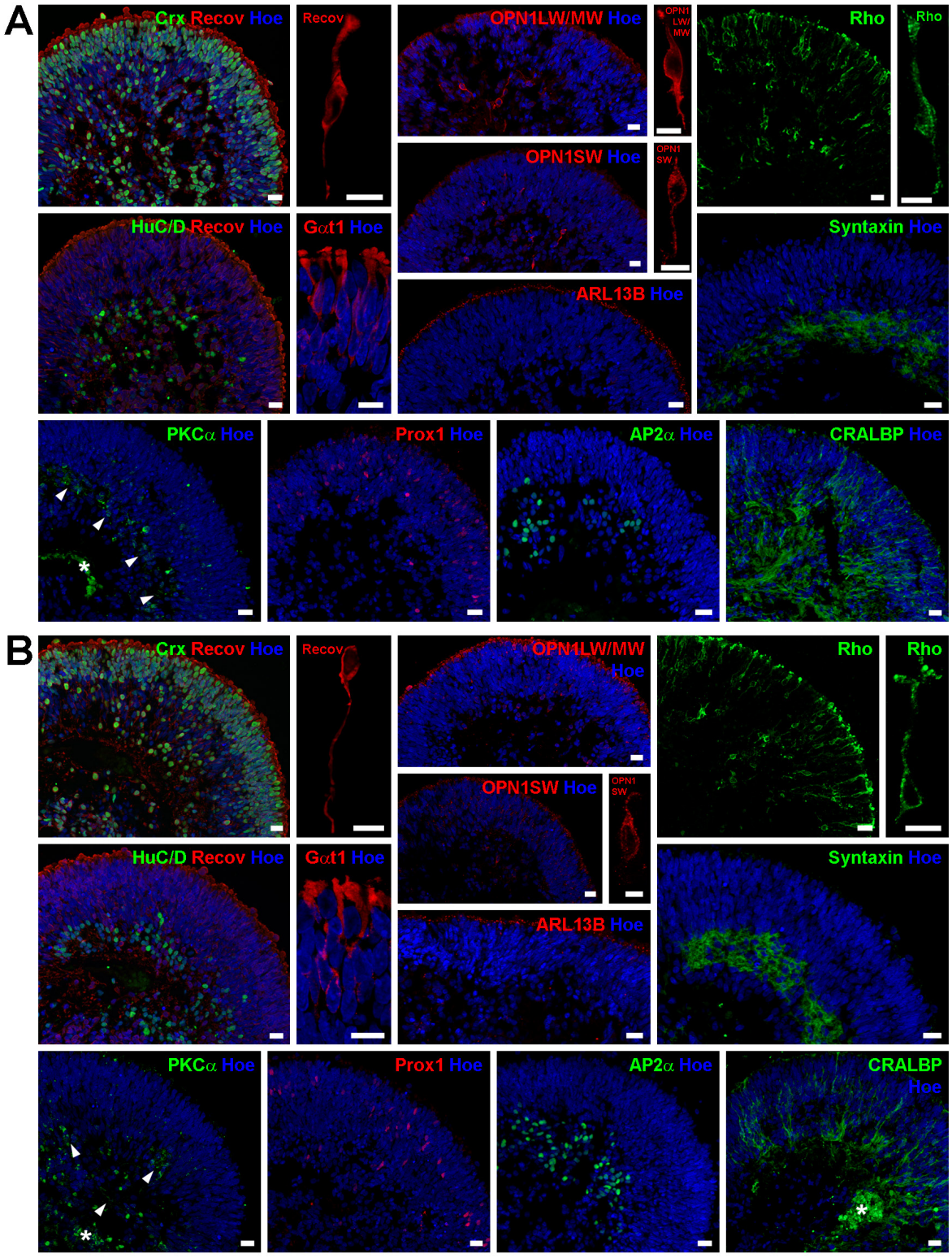

Figure 5-13: Characterisation of hESC-derived retinal organoids at day 150 of differentiation. (A-B) Sections through retinal organoids at day 150 showing immunofluorescence labelling with retinal markers including: CRX, Recoverin (Recov), HuC/D, Gαt1, OPN1LW/MW, OPN1SW, Rhodopsin (Rho), ARL13B, Syntaxin, PKCα, Prox1, AP2α and CRALBP with or without Hoechst (Hoe) in four culture systems: decel NR (A) and decel RPE (B). Stars indicate cellular debris in organoids. Scale bars =20 μm.

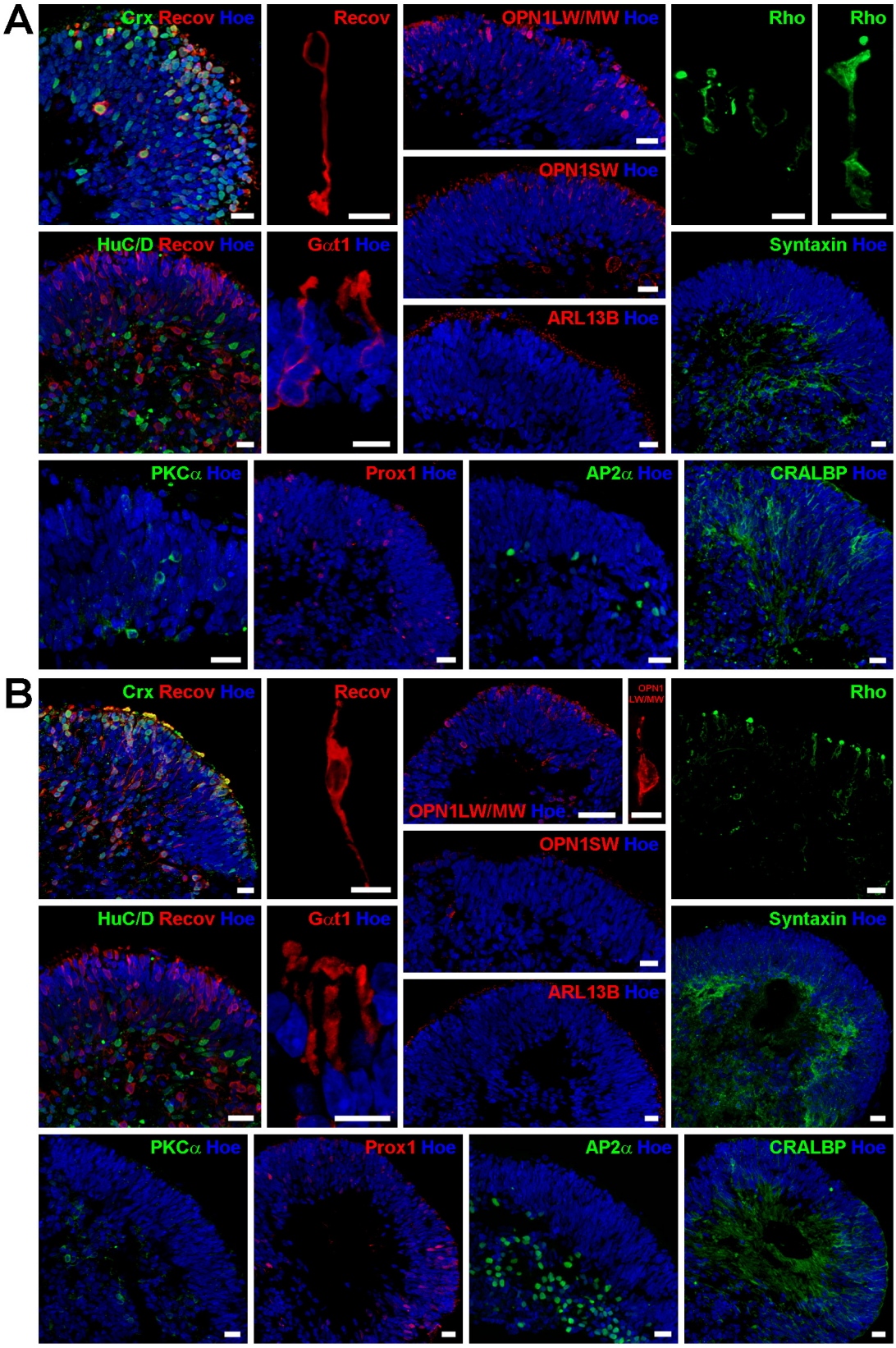

Figure 5-14: Characterisation of hiPSC-derived retinal organoids at day 150 of differentiation. (A-B) Sections through retinal organoids at day 150 showing immunofluorescence labelling with retinal markers including: CRX, Recoverin (Recov), HuC/D, Gαt1, OPN1LW/MW, OPN1SW, Rhodopsin (Rho), ARL13B, Syntaxin, PKCα, Prox1, AP2α and CRALBP with or without Hoechst (Hoe) in four culture systems: control (A), CM RPE (B). Scale bars =20 μm.

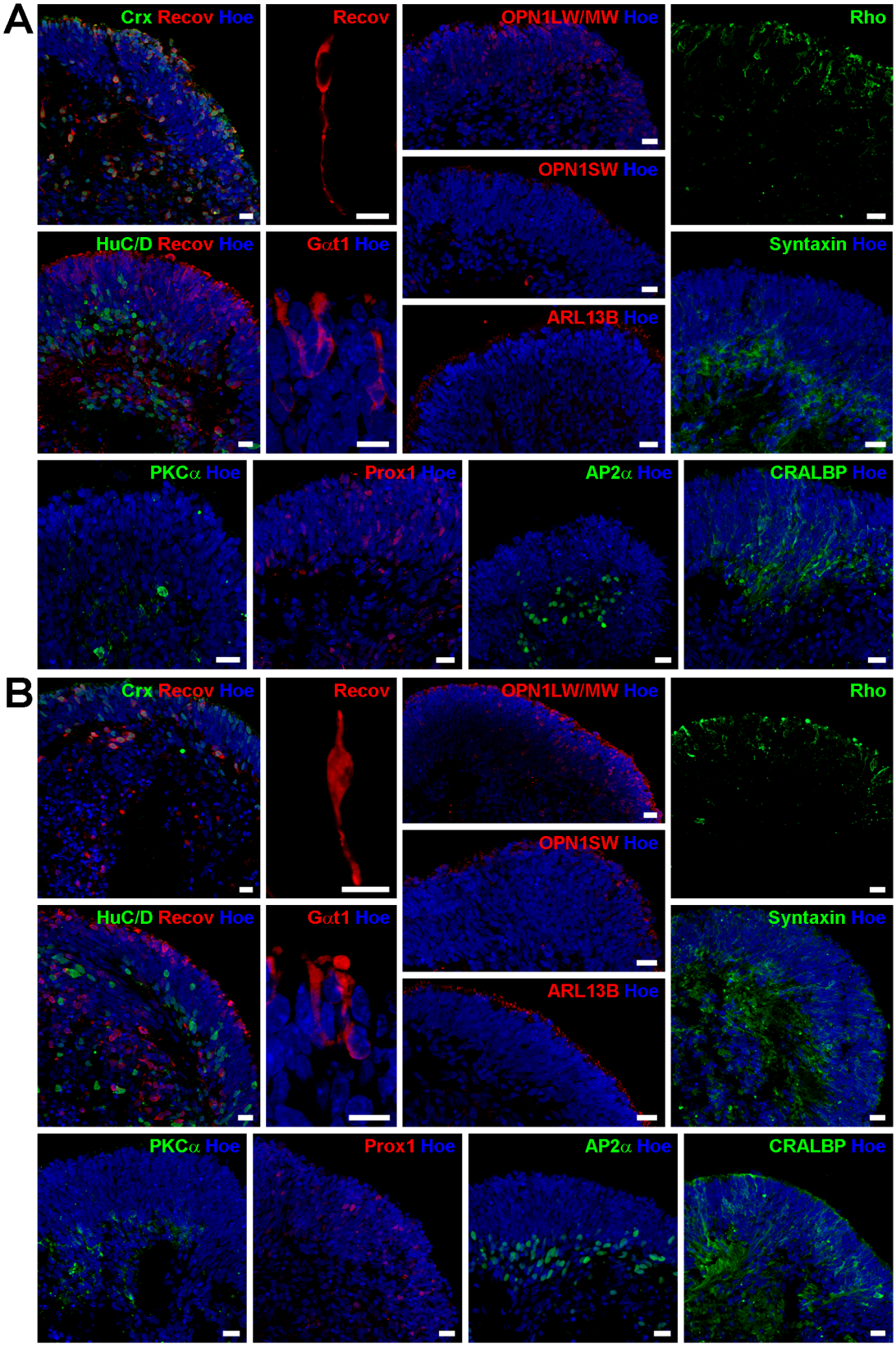

Figure 5-15: Characterisation of hiPSC-derived retinal organoids at day 150 of differentiation. (A-B) Sections through retinal organoids at day 150 showing immunofluorescence labelling with retinal markers including: CRX, Recoverin (Recov), HuC/D, Gαt1, OPN1LW/MW, OPN1SW, Rhodopsin (Rho), ARL13B, Syntaxin, PKCα, Prox1, AP2α and CRALBP with or without Hoechst (Hoe) in four culture systems: decel NR (A) and decel RPE (B). Scale bars =20 μm.

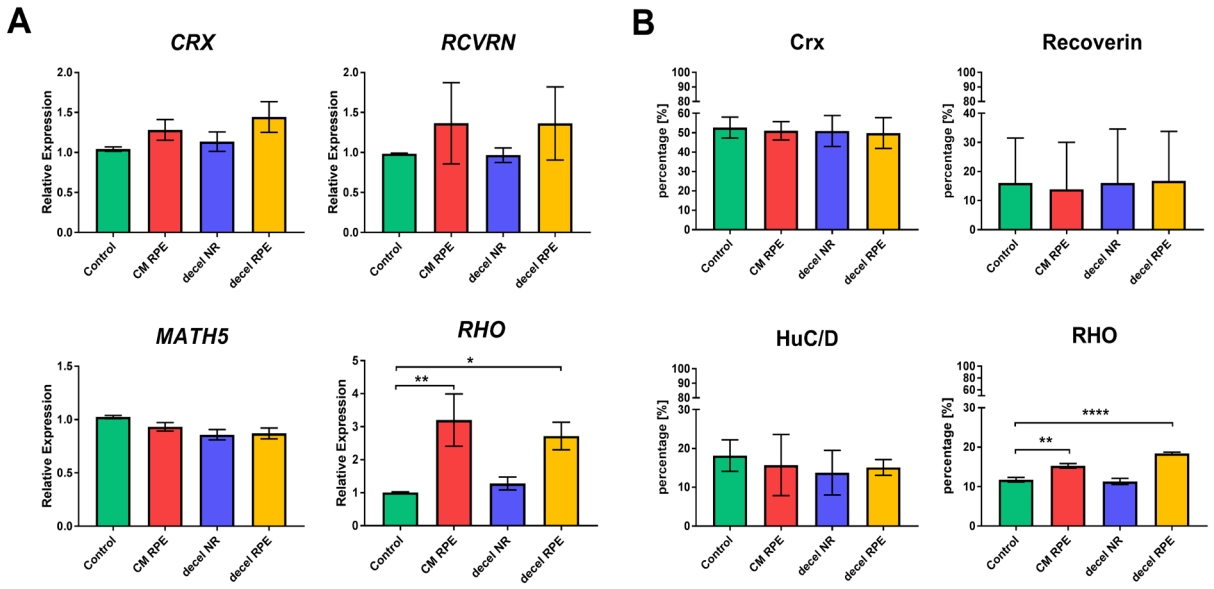

Figure 5-16: Expression of retinal markers in day 150 retinal organoids derived from hESCs & hiPSCs.

(A) Schematic charts showing qPCR study of retinal markers expression: *CRX*, *RCVRN*, *MATH5* and *RHO* in day 150 retinal organoids in four culture systems. (B) Schematic charts showing semi-quantitative measurements of retinal markers: CRX, Recoverin, HuC/D and RHO in day 150 organoids. Data is shown as mean ± SEM, *n=6-8* (average of hESCs + hiPSCs). Differences were considered statistically significant at *p < 0.05, **p < 0.01 and ****p < 0.0001.

qRT-PCR studies indicated a higher expression of *RHO* in the CM-RPE and decel RPE condition when compared to control condition (**Figure 5-16A**). These changes were confirmed by cell quantification analyses which revealed a significant increase in the number of rhodopsin-positive cells in CM-RPE and decel RPE condition when compared to control (**Figure 5-16B**). Furthermore, the higher expression of RHO could also be due to an increase in the production of the protein within the cells. This data suggests that the supplementation of CM-RPE and decel RPE improves the development of rods. In contrast to rod expression, the expression of long/middle wavelength (OPN1LW/MW) and short wavelength (OPN1SW) cones were found more sporadic within retinal organoids (**Figure 5-12, 5-13, 5-14 and Figure 5-15**), suggesting the beginning of opsin expression at this developmental stage. Nevertheless, both OPN1LW/MW and OPN1SW immunoreactivity-positive cells were found either at the apical side or in the centre of retinal organoids. In addition, higher magnifications of both cone types displayed the typical morphology at this time point of the differentiation process (**Figure 5-12, 5-13, 5-14 and Figure 5-15**).

All other retinal cell-types (bipolar, horizontal, amacrine, ganglion and Müller cells) were found at day 150 of differentiation in retinal organoids derived from both cell lines and

in all conditions (**Figure 5-12, 5-13, 5-14 and Figure 5-15**). HuC/D-positive ganglion cells were mostly located in the centre of retinal organoids, forming a ganglion cell layer (GCL) (**Figure 5-12, 5-13, 5-14 and Figure 5-15**). This was seen in all conditions (**Figure 5-12, 5-13, 5-14 and Figure 5-15**) without any differences in the *MATH5* gene expression (**Figure 5-16A)** or the percentage of HuC/D-positive cells as indicated by the cell quantification analysis (**Figure 5-16B**). Interestingly, horizontal cells detected by the marker protein Prox1 were found more towards the apical side of organoids while amacrine cells (Ap2α-labelled) were located more toward the centre of the organoids (**Figure 5-12, 5-13, 5-14 and Figure 5-15**), reflecting correct positions of both cell-types within the retinal organization. In all conditions Müller cells (CRALBP) are spanning through the whole retinal structure like known from the adult retina (**Figure 5-12, 5-13, 5-14 and Figure 5-15**).

The development of mature RPE cells was confirmed by TEM analysis, showing polarized melanosomes [melanosomes are pigment granules where the synthesis, storage and transport of melanin pigments occur (Wasmeier *et al.*, 2008); and called polarized because it is an essential feature for normal function of RPE cells that involve the polarization of Na,K ATPase to the apical membrane domain of RPE cells (Hu and Bok, 2001)] in decel RPE retinal organoids (**Figure 5-17D**). The TEM analysis also revealed the presence of organized photoreceptor-like ultrastructures such as photoreceptor OS, inner segments (IS), connecting cilium (cc) and basal body (bb) in all conditions (**Figure 5-17A-D**). In addition, an outer limiting membrane (OLM) was observed basal to the IS of developing mitochondria-rich photoreceptors in all culture conditions (**Figure 5-17A-D**). The development of other retinal cell types such as amacrine cells and Müller cells (indicated by the formation of neurofilaments) were also confirmed by TEM analysis (**Figure 5-17B**). Taken together, these results suggests that the supplementation of decel RPE has a positive impact on the development of RPE and rods, whereas the development of other retinal cell types including cones was not affected by the supplementation of CM RPE, decel NR or decel RPE at later stages of the differentiation.

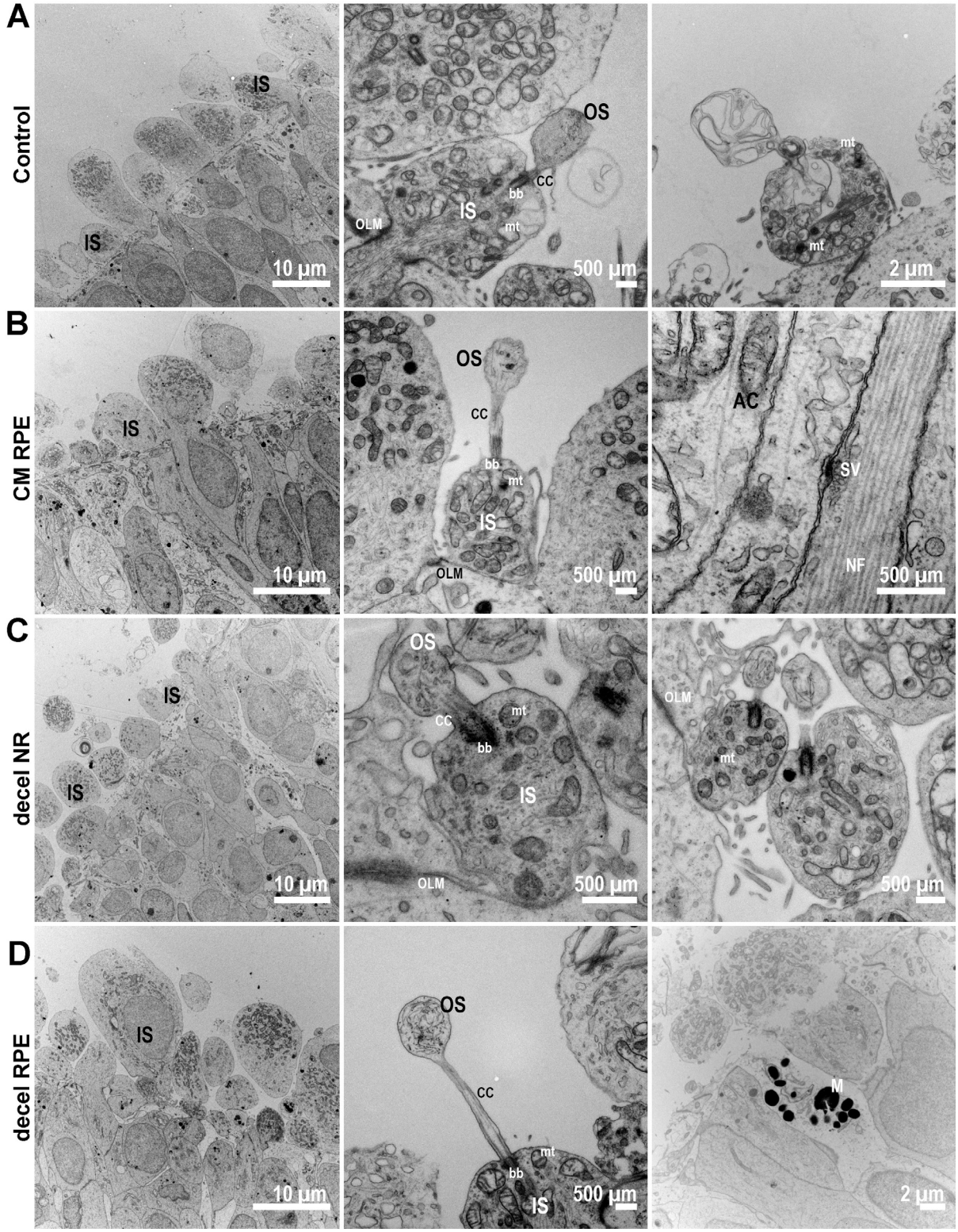

Figure 5-17: Ultrastructural analysis of hPSC-derived retinal organoids using transmission electron microscopy.

(A-D) Sections of retinal organoid derived from hPSCs showing ultrastructural analysis of photoreceptors in four different cultural conditions: control (A), CM RPE (B), decel NR (C) and decel RPE (D). Scale bars: 2µm, 10µm or 500µm. Abbreviations: AC: amacrine cells; bb: basal body; cc: connecting cilium; IS: photoreceptors inner segments; mt: mitochondria; M: melanosomes; NF: neurofilaments; OLM: outer limiting membrane; OS: photoreceptors outer segments; SV: synaptic vesicles.

5.3.4. Effect of ECM supplementation on the development of synapses and electrophysiology light responses

Electrophysiological recordings and analyses of the results were performed by Prof. Evelyne Sernagor and Dr. Gerrit Hilgen (Newcastle University, UK). Also, quantification analyses of synaptic markers were performed by Dr. Birthe Hilgen (Newcastle University, UK).

The previous results demonstrated that the retinal organoids derived from pluripotent stem cells in all culture conditions contained all retinal cell-types, forming different nuclear layers as in adult retina. However, the formation of correct synaptic connections between different cell-types, known as plexiform layers in adult retina (OPL and IPL), is still challenging in the retinal differentiation process (Llonch *et al.*, 2018). IHC study was performed to investigate the effect of different ECM supplementations at day 150 of differentiation using more common synaptic marker proteins as well as ribbon synapse specific marker proteins.

Syntaxin, a marker for the presynaptic plasma membrane, was found underneath the putative ONL of retinal organoids in all culture conditions at day 150 of differentiation (**Figure 5-12, 5-13, 5-14 and Figure 5-15**), indicating the formation of possible photoreceptor synapses. Ribbon synapse marker proteins (Bassoon and CtBP2) in combination with vGlut1, a marker for synaptic terminals of photoreceptors and bipolar cells, and Recoverin for photoreceptors were used to assess this in more detail. Bassoon and CtBP2 puncta immunoreactivity were largely found below photoreceptor nuclei in retinal organoids derived from both cell lines in all conditions (**Figure 5-18**). Co-localisation of Bassoon or CtBP2 respectively with vGlut1 and Recoverin were observed at putative axons/axon terminals as highlighted by higher magnifications (**Figure 5-18**, insets). This suggests that photoreceptors might be able to form synaptic connections with second order neurons like bipolar or horizontal cells. In addition, a quantification of Bassoon and CtBP2 patches as well as the median intensity was performed to validate the impact of different ECM supplementations on the synapse formation.

Bassoon-positive patches were significantly decreased in CM RPE and decel NR in hESC-derived retinal organoids while in hiPSCs they were significantly increased in decel NR compared to control condition (**Figure 5-19A**). This data suggest less putative photoreceptor synapses to be formed in CM RPE condition at day 150 of differentiation and potential differences between hESCs and hiPSCs. In contrast, immunoreactivity-positive

patches for CtBP2 were not affected by the different types of ECM supplementations in hESC-derived retinal organoids while in hiPSC-derived retinal organoids they were significantly increased in decel NR compare to control condition (**Figure 5-19B**), suggesting that decel NR condition promoted the formation of putative photoreceptor synapses and the expression of Bassoon and CtBP2 in hiPSC-derived retinal organoids. The protein expression of Bassoon and CtBP2 analysed by the median intensity quantification revealed an increase in hESC-derived retinal organoids of all culture conditions compared to the control condition (**Figure 5-19C**). This effect was slightly different in hiPSC-derived retinal organoids where the expression of Bassoon and CtBP2 significantly increased in CM RPE and decreased in decel NR and RPE (**Figure 5-19D**). These results indicate a higher protein expression of Bassoon and CtBP2 in both hESC- and hiPSC-derived retinal organoids in response to the three different ECM supplementations but CM RPE condition showed stronger effect.

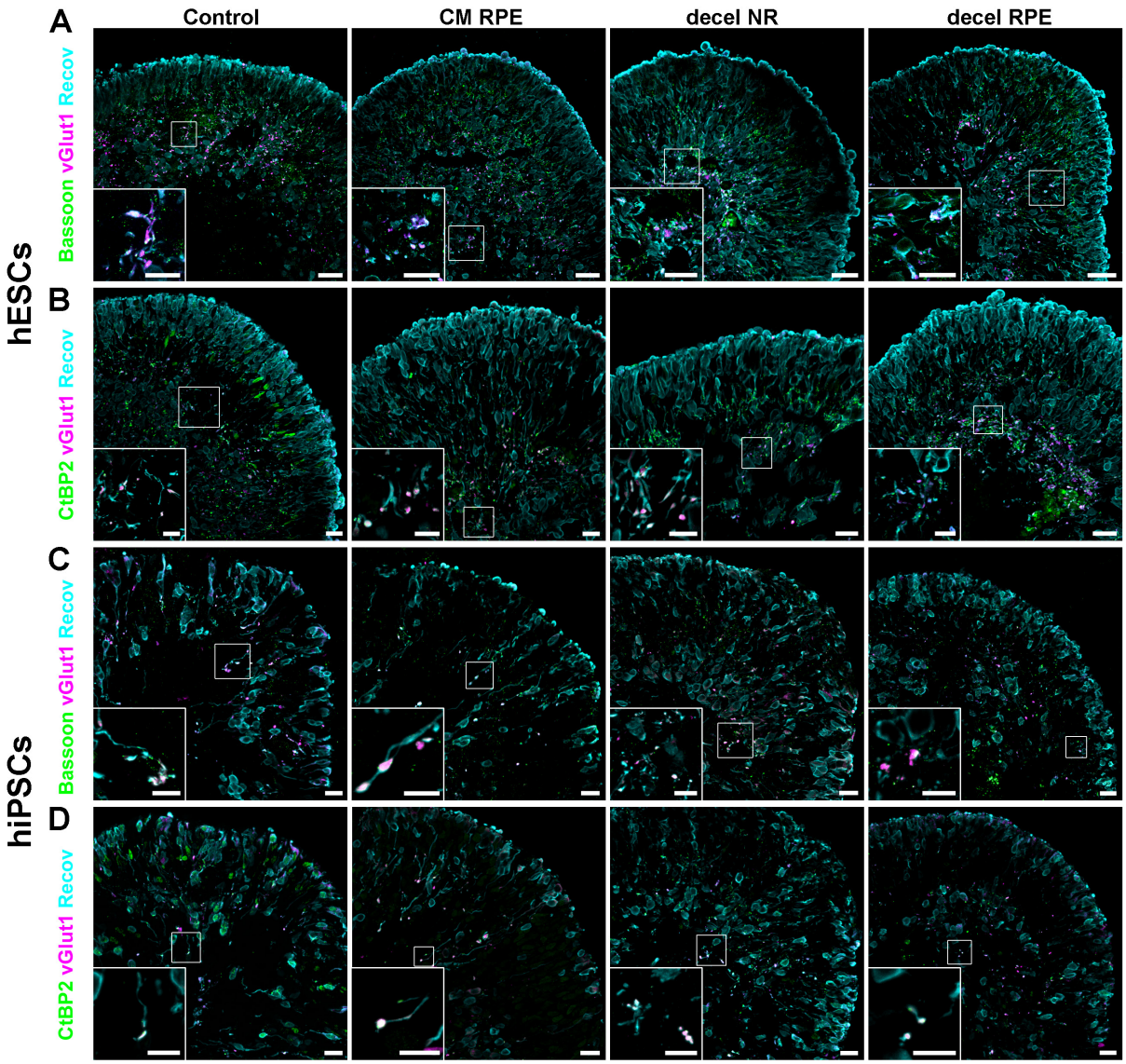

Figure 5-18: Expression of synaptic markers in day 150 retinal organoids.
Sections through day150 retinal organoid derived from hESCs (A-B) & hiPSCs (C-D) showing immunofluorescence labelling of retinal markers (vGlut1 & Recoverin; Recov) with synaptic markers (Bassoon or CtBP2). Small insets show higher magnification images of the organoid. Scale bars =20 µm.

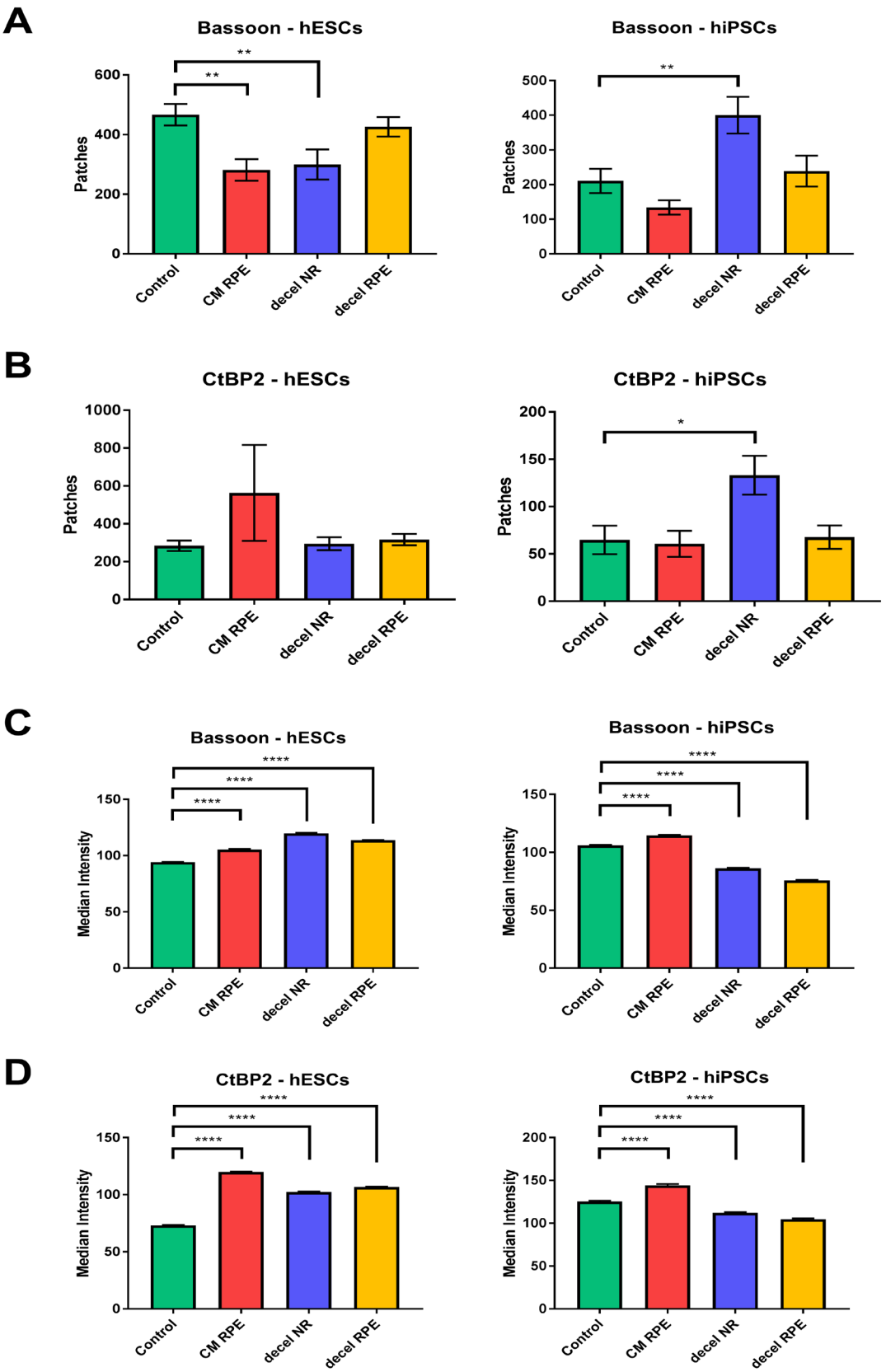

Figure 5-19: Quantification of synaptic markers in day 150 retinal organoids derived from hESCs & hiPSCs.

Schematic charts showing semi-quantitative measurements (A-B) and median intensity (C-D) of synaptic markers: Bassoon & CtBP2 in hPSC-derived day 150 retinal organoids. Data is shown as mean ± SEM, *n=6-8*. Differences were considered statistically significant at *p < 0.05, **p < 0.01 and ****p < 0.0001.

To further investigate the formation of synaptic connections between retinal cell-types in hPSC-derived retinal organoids, Dr. Gerrit Hilgen performed multi-electrode recordings (MEA) for ganglion cells using strong light stimuli as well as the application of cyclic guanosine monophosphate (cGMP). Many presumed ON RGCs in retinal organoids derived from hESC and hiPSCs in control, CM-RPE, decel NR and decel RPE conditions at day 150 of differentiation exhibited an increase in spiking activity when exposed to high intensity WLP stimuli. The spike raster plots (**Figure 5-20A-D**) show all ON responses for RGCS that responded at least with a 25% increase in spiking activity following WLP. **Figure 5-20E** illustrates the normalised mean change of spiking activity in all four conditions with a general increase in responsiveness of hESC- and hiPSC-derived retinal organoids in all conditions compared to their respective controls. However, the only conditions showing statistically significant increases were the decel NR and decel RPE in hiPSC-derived retinal organoids (**Figure 5-20E**).

cGMP is a secondary messenger in the phototransduction cascade that gates Na^+-permeable channels in the outer segments of photoreceptors. Puffing 8-br-cGMP, a membrane permeable analogue of cGMP, in the recording chamber triggers Na^+ influx and depolarises photoreceptors, thus mimicking the dark current. Organoid RGCs responding to the 8-br-cGMP puff with increased spiking activity are thus presumed OFF RGCs (**Figure 5-21A**), whilst those exhibiting a decrease in activity after the puff are presumed ON RGCs (**Figure 5-21B**). RGCs of the hESC-derived retinal organoids in decel NR and decel RPE groups showed the smallest change in activity for OFF (**Figure 5-21A, left**) and ON (**Figure 5-21B, left**) responses. In contrast, RGCs of the hiPSC-derived retinal organoids in control group showed the smallest change in activity for OFF (**Figure 5-21A, right**) and ON (**Figure 5-21 B, right**) responses. In summary, these results show that all four conditions improve the light-driven responses but decel NR and RPE conditions showed stronger effects. In contradiction, the effect of 8-br-cGMP was minimal in these two groups and the control conditions showed higher dynamics than the other conditions.

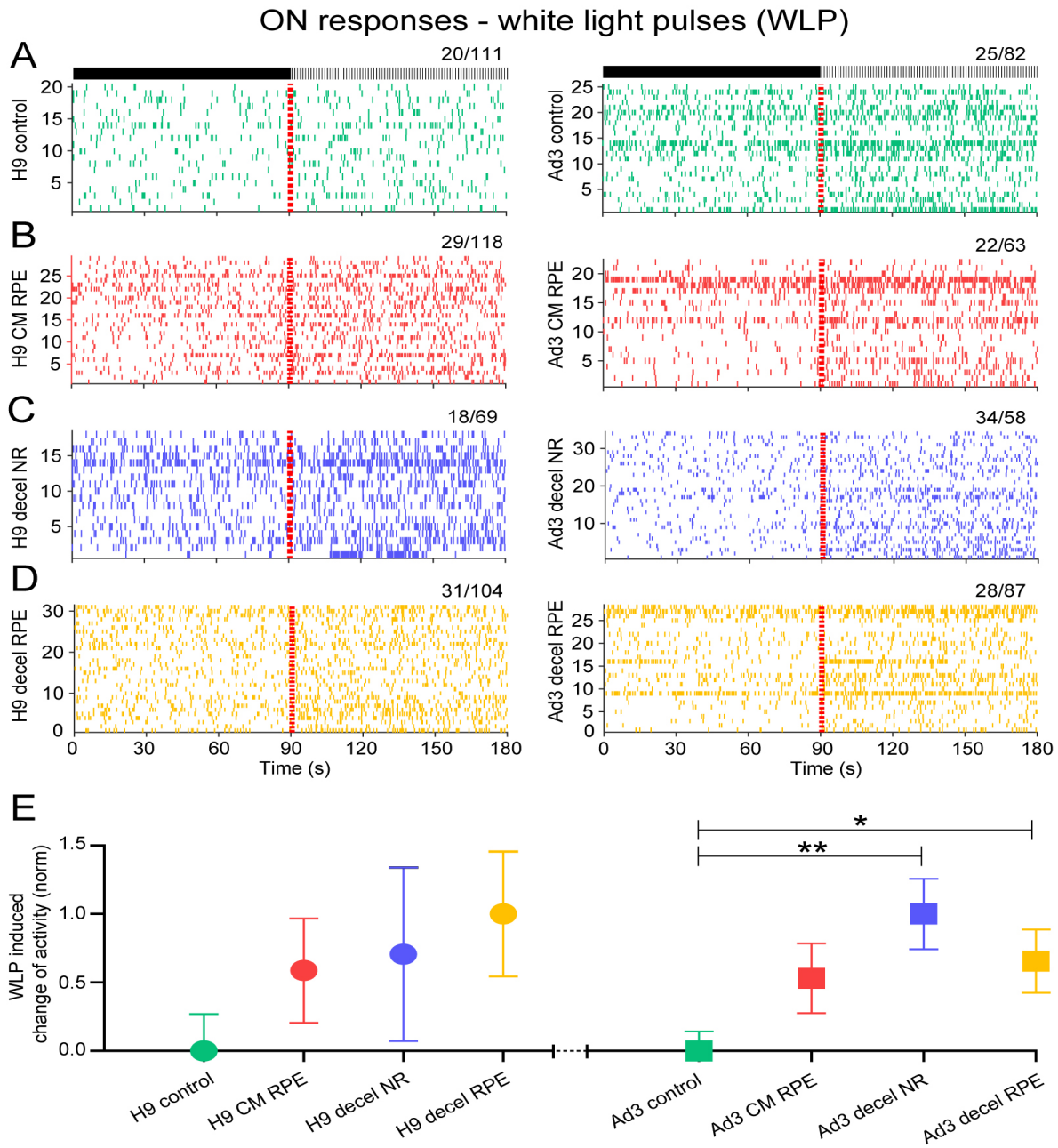

Figure 5-20: Light-driven spiking activity recorded from presumed ON RGCs in four different groups of 3D retinas derived either from hES (H9) or hiPSC (Ad3) cell lines at day 150 of differentiation.

(A-D) Spike raster plots (SRPs) from RGCs of the different groups that showed a 25% increase in spiking activity during pulsed white light (WLP, see methods). In the raster plot, each small vertical bar indicates the time stamp of a spike, where each row represents a different RGC. The left half illustrates the activity before stimulus onset and, separated by the red line, the right half the activity when exposed to WLP. A) SRPs from H9 control group (left) and Ad3 control group (right). B) SRPs from H9 CM RPE group (left) and Ad3 CM RPE group (right). C) SRPs from H9 decel NR group (left) and Ad3 decel NR group (right). D) SRPs from H9 decel RPE group (left) and Ad3 decel RPE group (right). E) The change of activity before and after stimulus onset was calculated for each RGC shown in A-D. An unpaired t-test was applied this data to estimate the difference between the control group to the other three groups. For better visualisation the means (+SEM) were normalised (as a fraction). Differences were considered statistically significant at *$p < 0.05$ and **$p < 0.01$.

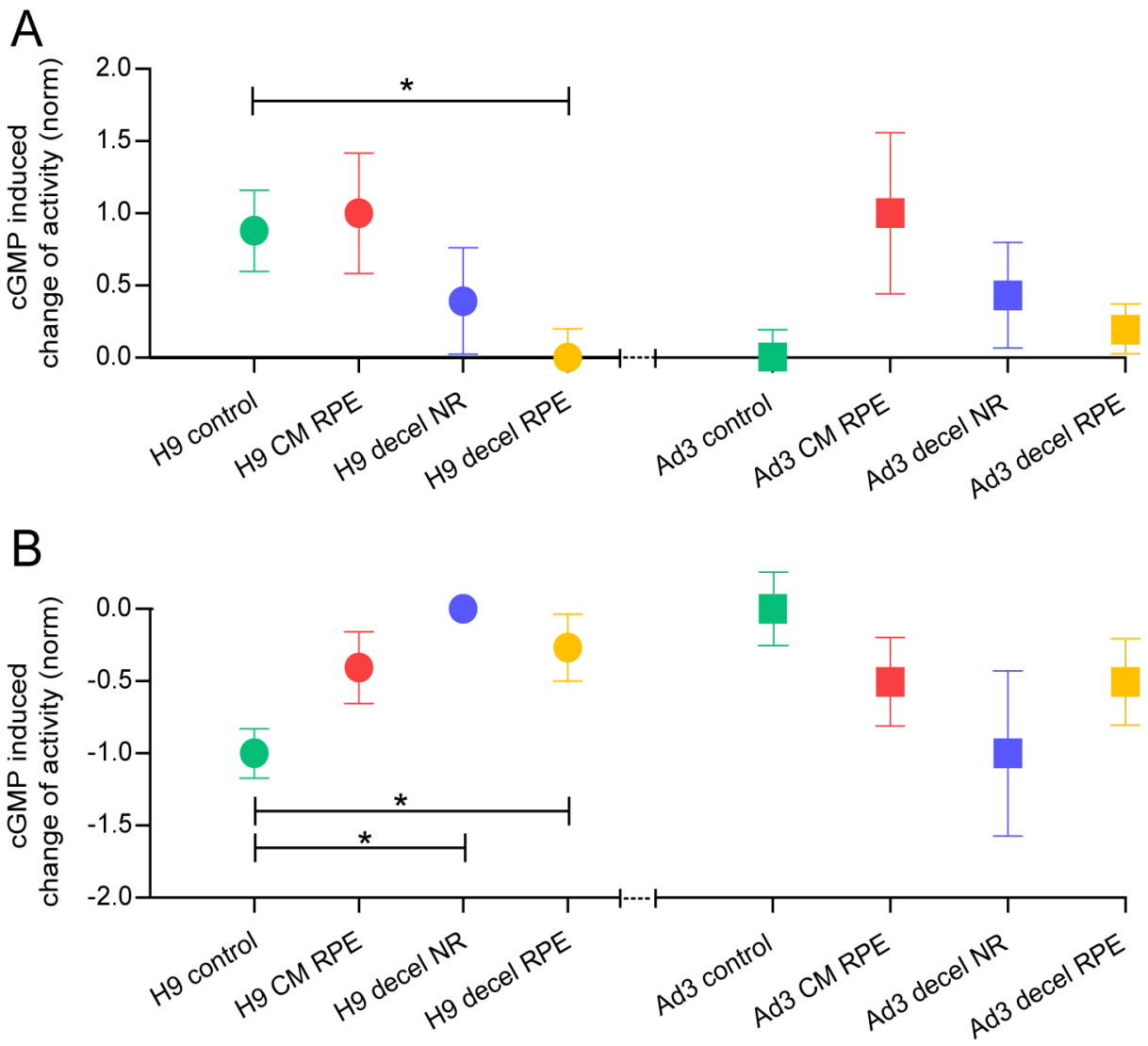

Figure 5-21: Change of RGC spiking activity in four different groups of 3D retinas derived from hESC or hiPSC cell lines at Day 150 of differentiation.

The change of activity after puffing 8-br-cGMP (final concentration 100 µM) compared to the activity before puffing was calculated for each RGC. RGCs that showed either a 25% increase (putative OFF RGCs) or decrease (putative ON RGCs) were considered as responsive. For better visualisation the means (+SEM) were normalised (as a fraction) within each cell line. A) Change of putative OFF RGC activity in H9 (left) and Ad3 (right) cell line groups. B) Change of putative ON RGC activity in H9 (left) and Ad3 (right) cell line groups. An unpaired t-test was applied this data to estimate the difference between the control group to the other three groups, differences were considered statistically significant at *$p < 0.05$.

5.4. Discussion

The ECM of natural organs and tissues represents an essential material formed from highly complex proteins which provide many biological cues known to influence stem cells activity and function as well as differentiation, *in vitro* (Gong *et al.*, 2008; Rowland *et al.*, 2013). Tissue specific ECM biomaterial may also provide micro-environments niches that recapitulate the *in vivo* milieu by possessing distinct properties and therefore provide a potential platform for enhancing tissue engineering and cellular functions in cultures to behave more similar to the original tissue, *in* vivo (Sackett *et al.*, 2018). dECM has been utilised and studied from many tissues such as heart, liver, lung, kidney and brain to improve cellular differentiation (Ott *et al.*, 2008; Ott *et al.*, 2010; Petersen *et al.*, 2010; Baptista *et al.*, 2011; Song *et al.*, 2013; De Waele *et al.*, 2015; Sun *et al.*, 2018). In retina, dECM from bovine eyes promoted the differentiation of human retinal progenitor cells into photoreceptors by enhancing the expression of different markers such as retinal outer membrane-1 (ROM1), NRL and CRX (Kundu *et al.*, 2016). In this study, media supplementations of CM RPE, decel NR and decel RPE containing natural ECM biomaterials was performed and the impacts of these different ECM supplementations on the differentiation of hPSCs into retinal organoids was investigated, *in vitro*. CM RPE and decel RPE media supplementations appear as good candidates to induce photoreceptors differentiation due to the anatomical relationship between the RPE and photoreceptors outer segments in the vertebrate eye (Gong *et al.*, 2008). The data indicated a successful tissue decellularisation process which was achieved by removing the majority of cellular material. However, some of the ECM components were lost during the process which was also observed in other study (Kundu *et al.*, 2016) suggesting that unavoidable reduction in the ECM content may occur during the decellularisation while removing a bulk of the cellular material and maintaining major components of the ECM niche. The ECM niches of the different media supplementations contained essential ECM components such as collagen, laminin, GAGs and hyaluronic acid. For example, Laminin was reported to enhance the differentiation of hPSCs into RPE (Rowland *et al.*, 2013) or retinal progenitors into photoreceptors, in culture (Gong *et al.*, 2008). Clark *et al.* reported that GAGs were major components of the ECM niche in adult human retina (Clark *et al.*, 2011). Thus, each ECM component may have a better effect when it combined with other ECM components in one tissue specific ECM niche used as media supplements.

To examine the effect of different ECM supplementations, retinal organoids from hESCs and hiPSCs were generated and their structural and functional characterisations were assessed in term of containing all retinal layers and cell types, synapses formation and

electrophysiological responses. There was no significance effects of CM RPE, decel NR or decel RPE supplementation found at early and middle stages of retinal differentiation. Although several retinal markers including VSX2, HuC/D, CRX and Recoverin were expressed at early stages (day 35) of differentiation, no significant differences were found between the four culture condition suggesting that it might be early to observe the impact of ECM supplementations at this time point of the differentiation process. This result correspond with data reported by Singh *et al.* showing the expression of retinal marker VSX2, HuC/D and recoverin at day 31 of culturing hESCs on ECM scaffold. At middle stages of the differentiation process, the percentage of retinal organoids containing morphological structures such as neural retina and/or RPE has increased as the organoids developed with time in all culture conditions except in decel RPE condition where the organoids developed more neural retinal structures containing RPE compared to the control condition suggesting a beneficial impact of decel RPE supplementation on the development of neural retina with RPE. This result corresponds with the data reported by McLenachan *et al.* showing that decellularised ECM from ARPE19-PRE cell lines can promote the differentiation of hiPSCs into RPE cells by increasing the number of pigmented colonies and the expression of RPE65, an RPE marker, suggesting that the ECM of decel RPE may contains signals that promote the differentiation of RPE cells from hPSCs (McLenachan *et al.*, 2017). Overall, the result indicated that the impact of different ECM niches in CM RPE, decel NR and RPE started to be observed at middle stages of the differentiation with the ECM niche of decel RPE promoted the differentiation of hPSCs into RPE cells, *in vitro*.

At later stage of the differentiation, the effect of ECM in decel RPE condition continued to promote the characterisation of retinal structures with RPE in the organoids at this stage of development as well. This was in line with the TEM analysis that showed polarized melanosomes in the organoids of decel RPE condition suggesting that the ECM in this supplementation can promote the development of mature RPE cells and correspond with the observation reported by McLenachan *et al.* (McLenachan *et al.*, 2017). More distinct retinal layers such as ONL and GCL started to generate in the organoids in all conditions and morphological features of the photoreceptors maturation were developed such as IS, OS, and CC which were confirmed by IHC and TEM studies. These ultrastructures were similar to the ones reported by other studies (Gonzalez-Cordero *et al.*, 2017; Hallam *et al.*, 2018; Ovando-Roche *et al.*, 2018). qRT-PCR and cell quantification studies indicated that *RHO* expression and the number of RHO-positive cells were higher in CM RPE and decel RPE compared to control condition. This corresponds with the study reported by German *et al.* showing that

RPE cells promoted the synthesis of rhodopsin from photoreceptors in culture (German *et al.*, 2008). Although many reports showed that the ECM of CM RPE or decel RPE can promote the characterisation of RPE cells or proliferation of photoreceptors (Gaur *et al.*, 1992; Hsiung *et al.*, 2015; McLenachan *et al.*, 2017) , these data indicate that for the first time, the ECM of RPE CM and decel RPE promote the differentiation and maturation of hPSCs into rods in culture. All other retinal cell-types (cones, bipolar, horizontal, amacrine, ganglion and Müller cells) were developed and different ECM supplements had no significant effect on their development which was confirmed by IHC and TEM studies.

The generation of retinal organoids containing key retinal cell types from PSCs were reported by several studies (Eiraku and Sasai, 2011; Eiraku *et al.*, 2011; Nakano *et al.*, 2012; Assawachananont *et al.*, 2014; Kuwahara *et al.*, 2015; Takata *et al.*, 2017). However, the formation of correct synaptic connections between different cell-types is still a remaining challenge in the field of retinal differentiation (Llonch *et al.*, 2018). The retinal organoids in this study were able to generate synaptic connections between photoreceptors and second order neurons such as bipolar or horizontal cells. However, variable effects of ECM supplementations on synaptogenesis were observed during retinal organoid development. Less putative photoreceptor synapses, indicated by Bassoon expression, were formed in the CM RPE compared to control condition, while all three media supplementations indicated an increase in the synaptic markers, Bassoon and CtBP2, median intensity compared to control condition with CM RPE condition showed stronger expression. These results suggest that the ECM niches in CM RPE may have better impacts on synaptogenesis than the decel NR and RPE during the differentiation process. To test the impacts of different ECM supplementations on the development of correct synaptic connections, electrophysiological light responses were performed and showed that decel NR and RPE conditions had more mediated the light-driven responses in the retinal organoids than control condition, *in vitro*. This result suggest that the ECM niches of decel NR and RPE may have essential role in mediating the correct synaptic connections and light responses in retinal organoids derived from hPSCs in culture.

Together, the data highlighted a beneficial effect of ECM as a natural biomaterial for efficient generation of retinal organoids in culture. The data observed in this study also suggest an important role for the ECM niches in the RPE CM and decel RPE to promote the differentiation and maturation of hPSCs into rods photoreceptors; as well as a major impact of the ECM niche in the decel RPE to enhance the differentiation of hPSCs into RPE cells and promoting correct synaptic connections and light responses in culture.

5.5. Conclusion

In summary, CM RPE, decel NR and decel RPE containing natural ECM biomaterials were successfully generated and used as media supplements for the development of retinal organoids from hPSCs, *in vitro*. The effects of these supplementations were assessed and found that they had no effect on the differentiation process during early and middle stages. However, at later stages of the differentiation process supplementation with CM RPE and decel RPE promoted the characterisation of RPE cells and maturation of rod photoreceptors. The different ECM supplements had variable effects on synaptogenesis and mediated electrophysiological light responses in retinal organoids *in vitro*. Together, the study highlights an important role for tissue specific ECM supplementation and may provide a potential platform for future studies to test tissue specific ECMs on the development of hPSCs into other various tissue systems so that effective tissue engineering and cell replacement therapies may be achieved.

Chapter 6

Chapter 6. General Discussion & Future Work

6.1. General Discussion

Retinal degeneration is a major cause of blindness in developed countries (Kong *et al.*, 2012). In 2017, world-wide estimates indicated that around 36 million people were blind and around 217 million were visually impaired which may have negative impacts on economy, educational opportunities and public health policies (Bourne *et al.*, 2017). Retinal degenerated diseases are characterised by progressive visual decline that originates from dysfunction and loss of key retinal cells such as RPE (Ovando-Roche *et al.*, 2018) and photoreceptor cells (Oner, 2018) which may leads to total blindness (Köberlein *et al.*, 2013). The most common examples of retinal degeneration are: Age-related macular degeneration which accounts 8.7% of global blindness (Wong *et al.*, 2014) and Retinitis pigmentosa which affects 1 in 4000 individuals (Hamel, 2006). Although animal models may provide several important insights into retinal disorders, they often unable to recapitulate key aspects of human pathophysiology which may obscure full understanding of the molecular mechanisms underlying retinal dystrophy (Ovando-Roche *et al.*, 2018). For example, the development of photoreceptors is less advanced in mouse than human at birth (Swaroop *et al.*, 2010). All photoreceptors are generated prenatally in human, whereas in mice they are generated pre- and postnatally (Swaroop *et al.*, 2010). There are also significant differences between the two species in term of the number, ratio and distribution of the photoreceptors (Saghizadeh *et al.*, 2011). The human retina has a larger amount of cone cells (~5%) than the mouse retinal photoreceptors (~3% cone cells) (Fu and Yau, 2007) and it contains the fovea which is not present in the mouse (Sung and Chuang, 2010; Saghizadeh *et al.*, 2011) . Moreover, human retina is trichromatic (has three types of cone photoreceptors), whereas mice are dichromats (Saghizadeh *et al.*, 2011). Therefore, it is important to study the tissue of human eye rather than other species in retinal research.

hPSCs including hESCs and hiPSCs can be differentiated into retinal organoids which provide a potential tool to study inherited and age related retinal degenration, to screen new drugs and to use them in tissue transplantation (Singh *et al.*, 2018). Several reports have shown that many aspects of the retinal development can be recapitulated *in vitro* through the differentiation of hPSCs into retinal organoids (Meyer *et al.*, 2011; Mellough *et al.*, 2012; Nakano *et al.*, 2012; Mellough *et al.*, 2014; Zhong *et al.*, 2014; Gonzalez-Cordero *et al.*, 2017; Welby *et al.*, 2017) which contain majorretinal cells types and respond to electrophysiological signals. However, current differentiation protocols are impeded by some challenges in term of

the prolong time required for the differentiation, formation of fully mature retinal layers with correct synaptic connections and limited ability to respond to light cues (Llonch *et al.*, 2018; Ovando-Roche *et al.*, 2018). Therefore, to use these advances for optimal retinal disease modelling *in vitro* and cell transplantation, more studies are required to develop differentiation protocols that result in efficient generation of retinal cells and maintaining laminar architecture of the retina (Ovando-Roche *et al.*, 2018).

The ECM plays an important role in controlling the behaviour of stem cells including self-renewal and differentiation (Keung *et al.*, 2012). *In vivo,* the ECM plays major roles in many cellular processes during retinal development such differentiation, proliferation, migration, adhesion, guidance and axonal growth (Reinhard *et al.*, 2015). Given the significant roles of ECM in retinal development, it is important to understand the expression of ECM components during human retinal ontogenesis, in order to utilise this knowledge to improve the differentiation of hPSCs into retinal organoids and understand the role of various ECM components in retinal development and disease (Clark *et al.*, 2011; Keenan *et al.*, 2012). To date, there have been limited detailed studies for the distribution of ECM components during human retinal development and the functional importance of many of them is poorly understood (Reinhard *et al.*, 2015). In this study, the expression of key ECM components was investigated to map the differential distribution of proteoglycan core proteins and their associated GAGs in sections from adult mouse and monkey retina, developing and adult human retina. The results demonstrate that different ECM components have distinct distribution patterns throughout the adult retina of different species and a well conserved expression pattern between adult and developing human retinae. Based on the expression data, ECM components expressed in the BrM or IPM, which play important roles in maintaining health and viability of the photoreceptors (Booij *et al.*, 2010; Ishikawa *et al.*, 2015), in adult and developing human retinae were selected for further studies as important candidates for outer retinal development, *in vitro.* Collagen IV and Fibronectin were conversely expressed in BrM and BrM & ILM respectively which was consistent with the expression previously observed in adult rat (Chen *et al.*, 2009) while Versican, Brevican, IMPG1, IMPG2 and CD44 were expressed in the IPM.

The expression of these key ECM components including Collagen IV, Fibronectin, Versican, Brevican, IMPG1, IMPG2 and CD44 were further studied during the differentiation of retinal organoids which generated form hESCs and hiPSCs, *in vitro*. Collagen IV and Fibronectin were expressed in BrM; whereas Brevican, Versican, IMPG1 and CD44 in the developing IPM. The data indicated that the expression of these ECM components

recapitulates human retinal development, *in vivo*. For example, IMPG1 was detected in the developing IPM of human developing retina at 12 PCW which was in line with the expression observed in the apical side (developing IPM) of day 90 retinal organoids. IMPG2 was not expressed in retinal organoids until the last time point examined (day 150). This, however, does correspond well with expression in developing human retina, where IMPG2 expression was observed only from 17 PCW. Another example, strong expression of CD44 was detected in the developing IPM at day 150 organoids which recapitulate the expression in human developing retina from 16 PCW.

After confirming that the expression of key ECM components in the retinal organoids *in vitro* recapitulates human retinal development *in vivo*, blocking studies were performed in order to examine the functional role of ECM on the differentiation of hPSC into retinal organoids. The action of IMPG1 and CD44 was blocked at day 90 and 150 of the differentiation, as their expression started at these time points, by incubating the organoids with blocking antibodies for 14 days in culture. At day 90 of differentiation, blocking the action of IMPG1 reduced the expression of photoreceptors and connecting cilia but not IPM markers while blocking CD44 had no impacts on the expression of these markers, suggesting important role for IMPG1 in the emergence of the photoreceptors at this time point. At day 150 of differentiation, blocking the action of IMPG1 and CD44 caused changes in the morphological structures of the organoids by thinning of the neuroepithelium structure and disrupted the development of the photoreceptors, their inner and outer segments and IPM formation. Together, these data suggest that IMPG1 and CD44 play an important role in the development of photoreceptors, their inner and outer segments, connecting cilia and IPM. However, IMPG1 acts earlier and has more significant effect than CD44 on retinal development, *in vitro*.

Publishes evidences suggest that the RPE and dECM from the RPE and neural retina contain several ECM components that are important for retinal development and synaptic formation between various retinal cell types (Aisenbrey *et al.*, 2006; Clark *et al.*, 2011; Kolomeyer *et al.*, 2011; Keenan *et al.*, 2012; Kundu *et al.*, 2016). The functional role of ECM on the differentiation of hPSCs into retinal organoids was further investigated via supplementation of culture media with RPE conditioned medium, decellularised ECM of neural retina or RPE. The data indicated that these three ECM supplementations had no impacts on the development of hPSC-derived retinal organoids at early (day 35) and middle stages (day 90) of the differentiation process. However, at later stages of differentiation (day 150) supplementation with decel RPE promoted the characterisation of RPE cells and the

maturation of rod photoreceptors, suggesting that the ECM of this supplement may contain essential cues for the development of these two cell types. This corresponds with the study reported by German *et al.* showing that RPE cells promoted the synthesis of rhodopsin from photoreceptors in culture (German *et al.*, 2008). Supplementation with decel NR and RPE had positive impacts on mediating the light-driven responses in the retinal organoids, *in vitro*. Together, the study highlights an important role for tissue specific ECM supplementation and may provide a potential platform for future studies to test tissue specific ECMs on the development of hPSCs into other various tissue systems so that effective tissue engineering and cell replacement therapies may be achieved.

6.2. General Conclusion

In summary, the study highlights a conserved expression of ECMs between human adult and developing retinae and retinal organoids as well as an important role for IMPG1 and CD44 in the development of photoreceptors, their inner and outer segments, connecting cilia and IPM; with IMPG1 acts earlier and has more significant effect than CD44 on retinal development, *in vitro*. Furthermore, the study identifies important role for ECM supplementation in retinal development *in vitro*.

6.3. Future Work

The work presented here investigated the expression and the functional roles of ECM on the development of retinal organoids, in vitro. However, the experimental approaches used to identify these roles were mainly based on studying the protein and gene expressions of various retinal markers as well as electrophysiological recording. Therefore, it may be important to further study the effect of ECM manipulation on various cellular signalling pathways such as Akt/PKB and the Erk pathways which are essential for cell proliferation (Streuli, 2009; Fournier et al., 2012; Moreno-Layseca and Streuli, 2014); ERK/MAPK pathway which plays important role in cell growth (Huang and Ingber, 1999); and Rho/ROCK pathway which is essential for cell polarity and migration (Brakebusch and Fassler, 2003). Although this study provided evidence that hPSC-derived retinal organoids were able to recapitulate ECM expression in vivo, develop all key retinal cell types in their correcting layers, and electrophysiologically respond to light; it is still not determined whether they able to incorporate in adult mammalian retina which can be examined via dissecting the retinal organoids to prepare a retinal sheet and transplant it in the subretinal space of retinal degenerative animal models as in a recent study by McLelland et al. (McLelland et al., 2018) .

The transplanted retinal sheet was able to integrate and grow within the host retina of retinal degenerative animal model, differentiate into different retinal cell types such as rods and cones as well as show functional connectivity through the formation of active synapses between the donor and host cells within the host IPL layer to improve visual function (McLelland et al., 2018). The improvement in the visual function was confirmed by electrophysiological recording that showed functional connections were made between the cells (McLelland et al., 2018). In summary, transplantation of hPSC-derived retinal organoids could improve visual function in retinal degenerative animal models so that effective retinal cell therapy may be realised.

Appendices

Appendix A: Publication arising from this study.

Acta Biomaterialia 74 (2018) 207–221

Contents lists available at ScienceDirect

Acta Biomaterialia

journal homepage: www.elsevier.com/locate/actabiomat

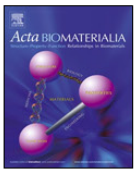

Full length article

Extracellular matrix component expression in human pluripotent stem cell-derived retinal organoids recapitulates retinogenesis in vivo and reveals an important role for IMPG1 and CD44 in the development of photoreceptors and interphotoreceptor matrix

Majed Felemban [a,1], Birthe Dorgau [a,1], Nicola Claire Hunt [a], Dean Hallam [a], Darin Zerti [a], Roman Bauer [b,c], Yuchun Ding [c], Joseph Collin [a], David Steel [a], Natalio Krasnogor [c], Jumana Al-Aama [d], Susan Lindsay [a], Carla Mellough [a,e,f], Majlinda Lako [a,⇑]

[a] Institute of Genetic Medicine, Newcastle University, UK
[b] Institute of Neuroscience, Newcastle University, UK
[c] Interdisciplinary Computing and Complex Biosystems (ICOS) Research Group, Newcastle University, UK
[d] Department of Genetic Medicine and Princess Al-Jawhara Center of Excellence in Research of Hereditary Disorders, Faculty of Medicine, King Abdulaziz University, Saudi Arabia
[e] Lions Eye Institute, 2 Verdun Street, Nedlands, WA, Australia
[f] Centre for Ophthalmology and Visual Science, The University of Western Australia, Crawley, WA, Australia

article info

Article history:
Received 14 December 2017
Received in revised form 7 May 2018
Accepted 15 May 2018
Available online 17 May 2018

Keywords:
Extracellular matrix
Interphotoreceptor matrix
Retinal organoid
Stem cells

abstract

The extracellular matrix (ECM) plays an important role in numerous processes including cellular proliferation, differentiation, migration, maturation, adhesion guidance and axonal growth. To date, there has been no detailed analysis of the ECM distribution during retinal ontogenesis in humans and the functional importance of many ECM components is poorly understood. In this study, the expression of key ECM components in adult mouse and monkey retina, developing and adult human retina and retinal organoids derived from human pluripotent stem cells was studied. Our data indicate that basement membrane ECMs (Fibronectin and Collagen IV) were expressed in Bruch's membrane and the inner limiting membrane of the developing human retina, whilst the hyalectins (Versican and Brevican), cluster of differentiation 44 (CD44), photoreceptor-specific ECMs Interphotoreceptor Matrix Proteoglycan 1 (IMPG1) and Interphotoreceptor Matrix Proteoglycan 2 (IMPG2) were detected in the developing interphotoreceptor matrix (IPM). The expression of IMPG1, Versican and Brevican in the developing IPM was conserved between human developing retina and human pluripotent stem cell-derived retinal organoids. Blocking the action of CD44 and IMPG1 in pluripotent stem cell derived retinal organoids affected the development of photoreceptors, their inner/outer segments and connecting cilia and disrupted IPM formation, with IMPG1 having an earlier and more significant impact. Together, our data suggest an important role for IMPG1 and CD44 in the development of photoreceptors and IPM formation during human retinogenesis.

Statement of Significance

The expression and the role of many extracellular matrix (ECM) components during human retinal development is not fully understood. In this study, expression of key ECM components (Collagen IV, Fibronectin, Brevican, Versican, IMPG1 and IMPG2) was investigated during human retinal ontogenesis.

Abbreviations: BCAN, Brevican; BrM, Bruch's membrane; CD44, cluster of differentiation 44; Col4A1, Collagen IV; ECM, extracellular matrix; FBS, Fetal bovine serum; FN1, Fibronectin; GCL, ganglion cell layer; HDBR, human developmental biology resource; hESCs, human embryonic stem cells; hiPSCs, human induced pluripotent stem cells; Hoe, Hoechst; ILM, inner limiting membrane; IMPG1/2, interphotoreceptor matrix proteoglycan 1/2; INL, inner nuclear layer; INZ, inner neuroblastic zone; IPL, inner plexiform layer; IPM, interphotoreceptor matrix; IRBP, Interphotoreceptor retinoid binding protein; ONL, Outer nuclear layer, ONZ, Outer neuroblastic zone; OPL, outer plexiform layer; OS, outer segment; PBS, phosphate buffered saline; PCW, weeks of post-conception; PFA, paraformaldehyde; RBP3, Retinol Binding Protein 3; RGCs, retinal ganglion cells; RPE, Retinal pigmented epithelium; RT, room temperature; VCAN, Versican.

⇑ Corresponding author at: Prof. of Stem Cell Sciences, Newcastle University, Institute of Genetic Medicine and Institute for Ageing, International Centre for Life, Central Parkway, Newcastle upon Tyne NE1 3 BZ, United Kingdom.
E-mail address: majlinda.lako@ncl.ac.uk (M. Lako).
[1] Both authors contributed equally.

https://doi.org/10.1016/j.actbio.2018.05.023
1742-7061/

Appendix B: Other publications

Dorgau et al. Cell Death and Disease
DOI 10.1038/s41419-018-0648-0

Cell Death & Disease

Laminin γ3 plays an important role in retinal lamination, photoreceptor organisation and ganglion cell differentiation

Birthe Dorgau[1], Majed Felemban[1], Alexander Sharpe[1], Roman Bauer[2], Dean Hallam [1], David H. Steel[1], Susan Lindsay[1], Carla Mellough [1,3] and Majlinda Lako[1]

Abstract

Laminins are heterotrimeric glycoproteins of the extracellular matrix. Eleven different laminin chains have been identified in vertebrates. They are ubiquitously expressed in the human body, with a distinct tissue distribution. Laminin expression in neural retina and their functional role during human retinogenesis is still unknown. This study investigated the laminin expression in human developing and adult retina, showing laminin α1, α5, β1, β2 and γ1 to be predominantly expressed in Bruch's membrane and the inner limiting membrane. Laminin-332 and laminin γ3 expression were mainly observed in the neural retina during retinal histogenesis. These expression patterns were largely conserved in pluripotent stem cell-derived retinal organoids. Blocking of laminin γ3 function in retinal organoids resulted in the disruption of laminar organisation and synapse formation, the loss of photoreceptor organisation and retinal ganglion cells. Our data demonstrate a unique temporal and spatial expression for laminins and reveal a novel role for laminin γ3 during human retinogenesis.

Introduction

The extracellular matrix (ECM) is a non-cellular structure that is present in all tissues and can be divided into two separate types, the connective tissue matrix and the basement membrane[1]. The ECM provides structural support and promotes cellular functions including differentiation, adhesion, migration, proliferation, axonal growth and morphogenesis in many tissues[1–4]. Laminins (Lam) are a family of heterotrimeric glycoproteins and part of the ECM[5]. They are a major component of basement membranes and are important for multiple biological processes[4,5]. Laminins are composed of one α, one β and one γ chain, and at present 11 different laminin chains have been identified in vertebrates: five α, three β and three γ chains[6]. These 11 laminin chains can assemble into at least 16 different laminin isoforms, named according to their trimer composition[7]. All isoforms have a tissue-specific distribution[6]. Mutations in different laminin chains are known to cause several congenital diseases in human including eye abnormalities[8–13].

Laminin functions have often been associated with embryogenesis. For example, laminin-111 has been shown to play an essential role in primitive ectoderm differentiation[14–16] and knockdowns of any individual chain of laminin-111 result in lethality[15,17,18]. Laminin-111 and other laminin chains play an important role during optic cup morphogenesis and retinal histogenesis[19–21], photoreceptor structure and synapse formation[20,22,23], stability of the inner limiting membrane (ILM)[24] and retinal ganglion cell (RGC) axonal growth[25–29].

Correspondence: Majlinda Lako (majlinda.lako@ncl.ac.uk)
[1]Institute of Genetic Medicine, Newcastle University, Newcastle upon Tyne, United Kingdom
[2]Institute of Neuroscience, Newcastle University, Newcastle upon Tyne, United Kingdom
Full list of author information is available at the end of the article.
Edited by A. Verkhratsky

Official journal of the Cell Death Differentiation Association

SPRINGER NATURE
CDDpress

Eye (2018) 32:946–971
https://doi.org/10.1038/s41433-018-0061-z

REVIEWARTICLE

Cellular regeneration strategies for macular degeneration: past, present and future

Valeria Chichagova[1] · Dean Hallam[1] · Joseph Collin[1] · Darin Zerti[1] · Birthe Dorgau[1] · Majed Felemban[1] · Majlinda Lako[1] · David H. Steel[1,2]

Received: 29 November 2017 / Revised: 5 January 2018 / Accepted: 15 January 2018 / Published online: 5 March 2018

Abstract

Despite considerable effort and significant therapeutic advances, age-related macular degeneration (AMD) remains the commonest cause of blindness in the developed world. Progressive late-stage AMD with outer retinal degeneration currently has no proven treatment. There has been significant interest in the possibility that cellular treatments may slow or reverse visual loss in AMD. A number of modes of action have been suggested, including cell replacement and rescue, as well as immune modulation to delay the neurodegenerative process. Their appeal in this enigmatic disease relate to their generic, non-pathway-specific effects. The outer retina in particular has been at the forefront of developments in cellular regenerative therapies being surgically accessible, easily observable, as well as having a relatively simple architecture. Both the retinal pigment epithelium (RPE) and photoreceptors have been considered for replacement therapies as both sheets and cell suspensions. Studies using autologous RPE, and to a lesser extent, foetal retina, have shown proof of principle. A wide variety of cell sources have been proposed with pluripotent stem cell-derived cells currently holding the centre stage. Recent early-phase trials using these cells for RPE replacement have met safety endpoints and hinted at possible efficacy. Animal studies have confirmed the promise that photoreceptor replacement, even in a completely degenerated outer retina may restore some vision. Many challenges, however, remain, not least of which include avoiding immune rejection, ensuring long-term cellular survival and maximising effect. This review provides an overview of progress made, ongoing studies and challenges ahead.

Introduction

Age-related macular degeneration (AMD) is the commonest cause of blindness in the developed world. The number of patients with currently non-treatable AMD is staggering, being responsible for approximately half of the 370,000 people registered as blind or partially sighted in the UK alone [1]. Late-stage AMD affects over 2.4% of the adult population over 50 and 12% of those over 80 years. The number of AMD cases is predicted to rise by one-third over the next decade, totalling nearly 700,000 in the UK by 2020 and 1,300,000 by 2050, with healthcare costs rising to £16.4 billion during 2010–2020 [2]. Each year in the UK, it is estimated that ~70,000 patients present with late AMD; half with wet disease and half with dry [3]. AMD is a worldwide disease and globally it is thought to affect over 8 million people.

AMD is manifested fundoscopically in the early and intermediate stages by the appearance of yellowish sub-retinal deposits, called drusen deep to the retinal pigment epithelium (RPE) in the macular retina. At this stage, the effect on vision is relatively mild, although acuity in low-contrast conditions is frequently affected. At least 15% of patients progress however to the more advanced 'wet' and 'dry' forms of the disease. Dry AMD is characterised by degeneration of the RPE and subsequently the overlying photoreceptors. 'Wet' AMD is characterised by aberrant choroidal blood vessel growth beneath or through the RPE, affecting the function of the overlying neurosensory retina

These authors contributed equally: Valeria Chichagova, Dean Hallam.

* David H. Steel
David.steel@ncl.ac.uk

1 Institute of Genetic Medicine, Newcastle University, Newcastle upon Tyne, UK

2 Sunderland Eye Infirmary, Queen Alexandra Road, Sunderland, UK

References

- Acharya, S., Foletta, V.C., Lee, J.W., Rayborn, M.E., Rodriguez, I.R., Young, W.S., 3rd and Hollyfield, J.G. (2000) 'SPACRCAN, a novel human interphotoreceptor matrix hyaluronan-binding proteoglycan synthesized by photoreceptors and pinealocytes', *J Biol Chem*, 275(10), pp. 6945-55.
- Acharya, S., Rodriguez, I.R., Moreira, E.F., Midura, R.J., Misono, K., Todres, E. and Hollyfield, J.G. (1998) 'SPACR, a novel interphotoreceptor matrix glycoprotein in human retina that interacts with hyaluronan', *J Biol Chem*, 273(47), pp. 31599-606.
- Agmon, G. and Christman, K.L. (2016) 'Controlling stem cell behavior with decellularized extracellular matrix scaffolds', *Curr Opin Solid State Mater Sci*, 20(4), pp. 193-201.
- Aisenbrey, S., Zhang, M., Bacher, D., Yee, J., Brunken, W.J. and Hunter, D.D. (2006) 'Retinal pigment epithelial cells synthesize laminins, including laminin 5, and adhere to them through alpha3- and alpha6-containing integrins', *Invest Ophthalmol Vis Sci*, 47(12), pp. 5537-44.
- Al-Ubaidi, M.R., Naash, M.I. and Conley, S.M. (2013) 'A perspective on the role of the extracellular matrix in progressive retinal degenerative disorders', *Invest Ophthalmol Vis Sci*, 54(13), pp. 8119-24.
- Alam, N., Goel, H.L., Zarif, M.J., Butterfield, J.E., Perkins, H.M., Sansoucy, B.G., Sawyer, T.K. and Languino, L.R. (2007) 'The integrin-growth factor receptor duet', *J Cell Physiol*, 213(3), pp. 649-53.
- Amirpour, N., Nasr-Esfahani, M.H., Esfandiari, E., Razavi, S. and Karamali, F. (2013) 'Comparing Three Methods of Co-culture of Retinal Pigment Epithelium with Progenitor Cells Derived Human Embryonic Stem Cells', *Int J Prev Med*, 4(11), pp. 1243-50.
- Armitage, W.J., Jones, M.N., Zambrano, I., Carley, F. and Tole, D.M. (2014) 'The suitability of corneas stored by organ culture for penetrating keratoplasty and influence of donor and recipient factors on 5-year graft survival', *Invest Ophthalmol Vis Sci*, 55(2), pp. 784-91.
- Armstrong, L., Lako, M., Buckley, N., Lappin, T.R., Murphy, M.J., Nolta, J.A., Pittenger, M. and Stojkovic, M. (2012) 'Editorial: Our top 10 developments in stem cell biology over the last 30 years', *Stem Cells*, 30(1), pp. 2-9.
- Assawachananont, J., Mandai, M., Okamoto, S., Yamada, C., Eiraku, M., Yonemura, S., Sasai, Y. and Takahashi, M. (2014) 'Transplantation of Embryonic and Induced Pluripotent Stem Cell-Derived 3D Retinal Sheets into Retinal Degenerative Mice', *Stem Cell Reports*, 2(5), pp. 662-74.
- Bai, X., Dilworth, D.J., Weng, Y.C. and Gould, D.B. (2009) 'Developmental distribution of collagen IV isoforms and relevance to ocular diseases', *Matrix Biol*, 28(4), pp. 194-201.
- Bandah-Rozenfeld, D., Collin, R.W., Banin, E., van den Born, L.I., Coene, K.L., Siemiatkowska, A.M., Zelinger, L., Khan, M.I., Lefeber, D.J., Erdinest, I., Testa, F., Simonelli, F., Voesenek, K., Blokland, E.A., Strom, T.M., Klaver, C.C., Qamar, R., Banfi, S., Cremers, F.P., Sharon, D. and den Hollander, A.I. (2010) 'Mutations in IMPG2, encoding interphotoreceptor matrix proteoglycan 2, cause autosomal-recessive retinitis pigmentosa', *Am J Hum Genet*, 87(2), pp. 199-208.
- Baptista, P.M., Siddiqui, M.M., Lozier, G., Rodriguez, S.R., Atala, A. and Soker, S. (2011) 'The use of whole organ decellularization for the generation of a vascularized liver organoid', *Hepatology*, 53(2), pp. 604-17.
- Barczyk, M., Carracedo, S. and Gullberg, D. (2010) 'Integrins', *Cell Tissue Res*, 339(1), pp. 269-80.

- Bateman, J.F., Boot-Handford, R.P. and Lamande, S.R. (2009) 'Genetic diseases of connective tissues: cellular and extracellular effects of ECM mutations', *Nat Rev Genet*, 10(3), pp. 173-83.
- Becerra, S.P. (2006) 'Focus on Molecules: Pigment epithelium-derived factor (PEDF)', *Exp Eye Res*, 82(5), pp. 739-40.
- Becerra, S.P., Perez-Mediavilla, L.A., Weldon, J.E., Locatelli-Hoops, S., Senanayake, P., Notari, L., Notario, V. and Hollyfield, J.G. (2008) 'Pigment epithelium-derived factor binds to hyaluronan. Mapping of a hyaluronan binding site', *J Biol Chem*, 283(48), pp. 33310-20.
- Berrier, A.L. and Yamada, K.M. (2007) 'Cell-matrix adhesion', *J Cell Physiol*, 213(3), pp. 565-73.
- Besser, M., Jagatheaswaran, M., Reinhard, J., Schaffelke, P. and Faissner, A. (2012) 'Tenascin C regulates proliferation and differentiation processes during embryonic retinogenesis and modulates the de-differentiation capacity of Muller glia by influencing growth factor responsiveness and the extracellular matrix compartment', *Dev Biol*, 369(2), pp. 163-76.
- Beuckmann, C.T., Gordon, W.C., Kanaoka, Y., Eguchi, N., Marcheselli, V.L., Gerashchenko, D.Y., Urade, Y., Hayaishi, O. and Bazan, N.G. (1996) 'Lipocalin-type prostaglandin D synthase (beta-trace) is located in pigment epithelial cells of rat retina and accumulates within interphotoreceptor matrix', *J Neurosci*, 16(19), pp. 6119-24.
- Bix, G. and Iozzo, R.V. (2008) 'Novel interactions of perlecan: unraveling perlecan's role in angiogenesis', *Microsc Res Tech*, 71(5), pp. 339-48.
- Bonnans, C., Chou, J. and Werb, Z. (2014) 'Remodelling the extracellular matrix in development and disease', *Nat Rev Mol Cell Biol*, 15(12), pp. 786-801.
- Booij, J.C., Baas, D.C., Beisekeeva, J., Gorgels, T.G. and Bergen, A.A. (2010) 'The dynamic nature of Bruch's membrane', *Prog Retin Eye Res*, 29(1), pp. 1-18.
- Boucherie, C., Mukherjee, S., Henckaerts, E., Thrasher, A.J., Sowden, J.C. and Ali, R.R. (2013) 'Brief report: self-organizing neuroepithelium from human pluripotent stem cells facilitates derivation of photoreceptors', *Stem Cells*, 31(2), pp. 408-14.
- Boulton, M. and Dayhaw-Barker, P. (2001) 'The role of the retinal pigment epithelium: topographical variation and ageing changes', *Eye (Lond)*, 15(Pt 3), pp. 384-9.
- Bourne, R.R.A., Flaxman, S.R., Braithwaite, T., Cicinelli, M.V., Das, A., Jonas, J.B., Keeffe, J., Kempen, J.H., Leasher, J., Limburg, H., Naidoo, K., Pesudovs, K., Resnikoff, S., Silvester, A., Stevens, G.A., Tahhan, N., Wong, T.Y. and Taylor, H.R. (2017) 'Magnitude, temporal trends, and projections of the global prevalence of blindness and distance and near vision impairment: a systematic review and meta-analysis', *Lancet Glob Health*, 5(9), pp. e888-e897.
- Bozanic, D. and Saraga-Babic, M. (2004) 'Cell proliferation during the early stages of human eye development', *Anat Embryol (Berl)*, 208(5), pp. 381-8.
- Brakebusch, C. and Fassler, R. (2003) 'The integrin-actin connection, an eternal love affair', *Embo j*, 22(10), pp. 2324-33.
- Brakebusch, C., Seidenbecher, C.I., Asztely, F., Rauch, U., Matthies, H., Meyer, H., Krug, M., Bockers, T.M., Zhou, X., Kreutz, M.R., Montag, D., Gundelfinger, E.D. and Fassler, R. (2002) 'Brevican-deficient mice display impaired hippocampal CA1 long-term potentiation but show no obvious deficits in learning and memory', *Mol Cell Biol*, 22(21), pp. 7417-27.
- Brem, R.B., Robbins, S.G., Wilson, D.J., O'Rourke, L.M., Mixon, R.N., Robertson, J.E., Planck, S.R. and Rosenbaum, J.T. (1994) 'Immunolocalization of integrins in the human retina', *Invest Ophthalmol Vis Sci*, 35(9), pp. 3466-74.
- Brizzi, M.F., Tarone, G. and Defilippi, P. (2012) 'Extracellular matrix, integrins, and growth factors as tailors of the stem cell niche', *Curr Opin Cell Biol*, 24(5), pp. 645-51.

- Broadhead, M.L., Becerra, S.P., Choong, P.F. and Dass, C.R. (2010) 'The applied biochemistry of PEDF and implications for tissue homeostasis', *Growth Factors*, 28(4), pp. 280-5.
- Brun, P., Panfilo, S., Daga Gordini, D., Cortivo, R. and Abatangelo, G. (2003) 'The effect of hyaluronan on CD44-mediated survival of normal and hydroxyl radical-damaged chondrocytes', *Osteoarthritis Cartilage*, 11(3), pp. 208-16.
- Bystrom, B., Virtanen, I., Rousselle, P., Gullberg, D. and Pedrosa-Domellof, F. (2006) 'Distribution of laminins in the developing human eye', *Invest Ophthalmol Vis Sci*, 47(3), pp. 777-85.
- Camenisch, T.D., Spicer, A.P., Brehm-Gibson, T., Biesterfeldt, J., Augustine, M.L., Calabro, A., Jr., Kubalak, S., Klewer, S.E. and McDonald, J.A. (2000) 'Disruption of hyaluronan synthase-2 abrogates normal cardiac morphogenesis and hyaluronan-mediated transformation of epithelium to mesenchyme', *J Clin Invest*, 106(3), pp. 349-60.
- Chen, Q., Lee, J.W., Nishiyama, K., Shadrach, K.G., Rayborn, M.E. and Hollyfield, J.G. (2003) 'SPACRCAN in the interphotoreceptor matrix of the mouse retina: molecular, developmental and promoter analysis', *Exp Eye Res*, 76(1), pp. 1-14.
- Chen, W., Mo, W., Sun, K., Huang, X., Zhang, Y.L. and Song, H.Y. (2009) 'Microplasmin degrades fibronectin and laminin at vitreoretinal interface and outer retina during enzymatic vitrectomy', *Curr Eye Res*, 34(12), pp. 1057-64.
- Chirco, K.R., Worthington, K.S., Flamme-Wiese, M.J., Riker, M.J., Andrade, J.D., Ueberheide, B.M., Stone, E.M., Tucker, B.A. and Mullins, R.F. (2017) 'Preparation and evaluation of human choroid extracellular matrix scaffolds for the study of cell replacement strategies', *Acta Biomater*, 57, pp. 293-303.
- Ciobanasu, C., Faivre, B. and Le Clainche, C. (2013) 'Integrating actin dynamics, mechanotransduction and integrin activation: the multiple functions of actin binding proteins in focal adhesions', *Eur J Cell Biol*, 92(10-11), pp. 339-48.
- Clark, S.J., Keenan, T.D., Fielder, H.L., Collinson, L.J., Holley, R.J., Merry, C.L., van Kuppevelt, T.H., Day, A.J. and Bishop, P.N. (2011) 'Mapping the differential distribution of glycosaminoglycans in the adult human retina, choroid, and sclera', *Invest Ophthalmol Vis Sci*, 52(9), pp. 6511-21.
- Crapo, P.M., Medberry, C.J., Reing, J.E., Tottey, S., van der Merwe, Y., Jones, K.E. and Badylak, S.F. (2012) 'Biologic scaffolds composed of central nervous system extracellular matrix', *Biomaterials*, 33(13), pp. 3539-3547.
- da Cruz, L., Fynes, K., Georgiadis, O., Kerby, J., Luo, Y.H., Ahmado, A., Vernon, A., Daniels, J.T., Nommiste, B., Hasan, S.M., Gooljar, S.B., Carr, A.-J.F., Vugler, A., Ramsden, C.M., Bictash, M., Fenster, M., Steer, J., Harbinson, T., Wilbrey, A., Tufail, A., Feng, G., Whitlock, M., Robson, A.G., Holder, G.E., Sagoo, M.S., Loudon, P.T., Whiting, P. and Coffey, P.J. (2018) 'Phase 1 clinical study of an embryonic stem cell–derived retinal pigment epithelium patch in age-related macular degeneration', *Nature Biotechnology*, 36, p. 328.
- de Almeida, P.E., Meyer, E.H., Kooreman, N.G., Diecke, S., Dey, D., Sanchez-Freire, V., Hu, S., Ebert, A., Odegaard, J., Mordwinkin, N.M., Brouwer, T.P., Lo, D., Montoro, D.T., Longaker, M.T., Negrin, R.S. and Wu, J.C. (2014) 'Transplanted terminally differentiated induced pluripotent stem cells are accepted by immune mechanisms similar to self-tolerance', *Nat Commun*, 5, p. 3903.
- de, S.S.P., Calabro, A., Nishiyama, K., Hu, J.G., Bok, D. and Hollyfield, J.G. (2001) 'Glycosaminoglycan synthesis and secretion by the retinal pigment epithelium: polarized delivery of hyaluronan from the apical surface', *J Cell Sci*, 114(Pt 1), pp. 199-205.

- De Waele, J., Reekmans, K., Daans, J., Goossens, H., Berneman, Z. and Ponsaerts, P. (2015) '3D culture of murine neural stem cells on decellularized mouse brain sections', *Biomaterials*, 41, pp. 122-131.
- Di Ferrante, N. (1956) 'Turbidimetric measurement of acid mucopolysaccharides and hyaluronidase activity', *J Biol Chem*, 220(1), pp. 303-6.
- Dicker, K.T., Gurski, L.A., Pradhan-Bhatt, S., Witt, R.L., Farach-Carson, M.C. and Jia, X. (2014) 'Hyaluronan: a simple polysaccharide with diverse biological functions', *Acta Biomater*, 10(4), pp. 1558-70.
- Dorgau, B., Felemban, M., Sharpe, A., Bauer, R., Hallam, D., Steel, D.H., Lindsay, S., Mellough, C. and Lako, M. (2018) 'Laminin γ3 plays an important role in retinal lamination, photoreceptor organisation and ganglion cell differentiation', *Cell Death & Disease*, 9(6), p. 615.
- Eiraku, M. and Sasai, Y. (2011) 'Mouse embryonic stem cell culture for generation of three-dimensional retinal and cortical tissues', *Nat Protoc*, 7(1), pp. 69-79.
- Eiraku, M., Takata, N., Ishibashi, H., Kawada, M., Sakakura, E., Okuda, S., Sekiguchi, K., Adachi, T. and Sasai, Y. (2011) 'Self-organizing optic-cup morphogenesis in three-dimensional culture', *Nature*, 472(7341), pp. 51-6.
- Enkhjargal, B., McBride, D.W., Manaenko, A., Reis, C., Sakai, Y., Tang, J. and Zhang, J.H. (2017) 'Intranasal administration of vitamin D attenuates blood-brain barrier disruption through endogenous upregulation of osteopontin and activation of CD44/P-gp glycosylation signaling after subarachnoid hemorrhage in rats', *J Cereb Blood Flow Metab*, 37(7), pp. 2555-2566.
- Faissner, A., Pyka, M., Geissler, M., Sobik, T., Frischknecht, R., Gundelfinger, E.D. and Seidenbecher, C. (2010) 'Contributions of astrocytes to synapse formation and maturation - Potential functions of the perisynaptic extracellular matrix', *Brain Res Rev*, 63(1-2), pp. 26-38.
- Felemban, M., Dorgau, B., Hunt, N.C., Hallam, D., Zerti, D., Bauer, R., Ding, Y., Collin, J., Steel, D., Krasnogor, N., Al-Aama, J., Lindsay, S., Mellough, C. and Lako, M. (2018) 'Extracellular matrix components expression in human pluripotent stem cell-derived retinal organoids recapitulates retinogenesis in vivo and reveals an important role for IMPG1 and CD44 in the development of photoreceptors and interphotoreceptor matrix', *Acta Biomaterialia*.
- Foletta, V.C., Nishiyama, K., Rayborn, M.E., Shadrach, K.G., Young, W.S., 3rd and Hollyfield, J.G. (2001) 'SPACRCAN in the developing retina and pineal gland of the rat: spatial and temporal pattern of gene expression and protein synthesis', *J Comp Neurol*, 435(3), pp. 354-63.
- Foltz, L.P. and Clegg, D.O. (2017) 'Rapid, Directed Differentiation of Retinal Pigment Epithelial Cells from Human Embryonic or Induced Pluripotent Stem Cells', *J Vis Exp*, (128).
- Fournier, N.M., Lee, B., Banasr, M., Elsayed, M. and Duman, R.S. (2012) 'Vascular endothelial growth factor regulates adult hippocampal cell proliferation through MEK/ERK- and PI3K/Akt-dependent signaling', *Neuropharmacology*, 63(4), pp. 642-52.
- Frantz, C., Stewart, K.M. and Weaver, V.M. (2010) 'The extracellular matrix at a glance', *J Cell Sci*, 123(Pt 24), pp. 4195-200.
- Fu, Y. and Yau, K.W. (2007) 'Phototransduction in mouse rods and cones', *Pflugers Arch*, 454(5), pp. 805-19.
- Gaur, V.P., Liu, Y. and Turner, J.E. (1992) 'RPE conditioned medium stimulates photoreceptor cell survival, neurite outgrowth and differentiation in vitro', *Exp Eye Res*, 54(5), pp. 645-59.

- George, E.L., Georges-Labouesse, E.N., Patel-King, R.S., Rayburn, H. and Hynes, R.O. (1993) 'Defects in mesoderm, neural tube and vascular development in mouse embryos lacking fibronectin', *Development*, 119(4), pp. 1079-91.
- German, O.L., Buzzi, E., Rotstein, N.P., Rodriguez-Boulan, E. and Politi, L.E. (2008) 'Retinal pigment epithelial cells promote spatial reorganization and differentiation of retina photoreceptors', *J Neurosci Res*, 86(16), pp. 3503-14.
- Ghosh, Z., Wilson, K.D., Wu, Y., Hu, S., Quertermous, T. and Wu, J.C. (2010) 'Persistent donor cell gene expression among human induced pluripotent stem cells contributes to differences with human embryonic stem cells', *PLoS One*, 5(2), p. e8975.
- Gilbert, R.E., Cox, A.J., Kelly, D.J., Wilkinson-Berka, J.L., Sage, E.H., Jerums, G. and Cooper, M.E. (1999) 'Localization of secreted protein acidic and rich in cysteine (SPARC) expression in the rat eye', *Connect Tissue Res*, 40(4), pp. 295-303.
- Ginsberg, M.H., Partridge, A. and Shattil, S.J. (2005) 'Integrin regulation', *Curr Opin Cell Biol*, 17(5), pp. 509-16.
- Goel, H.L., Breen, M., Zhang, J., Das, I., Aznavoorian-Cheshire, S., Greenberg, N.M., Elgavish, A. and Languino, L.R. (2005) 'beta1A integrin expression is required for type 1 insulin-like growth factor receptor mitogenic and transforming activities and localization to focal contacts', *Cancer Res*, 65(15), pp. 6692-700.
- Gong, J., Sagiv, O., Cai, H., Tsang, S.H. and Del Priore, L.V. (2008) 'Effects of extracellular matrix and neighboring cells on induction of human embryonic stem cells into retinal or retinal pigment epithelial progenitors', *Exp Eye Res*, 86(6), pp. 957-65.
- Gonzalez-Cordero, A., Kruczek, K., Naeem, A., Fernando, M., Kloc, M., Ribeiro, J., Goh, D., Duran, Y., Blackford, S.J.I., Abelleira-Hervas, L., Sampson, R.D., Shum, I.O., Branch, M.J., Gardner, P.J., Sowden, J.C., Bainbridge, J.W.B., Smith, A.J., West, E.L., Pearson, R.A. and Ali, R.R. (2017) 'Recapitulation of Human Retinal Development from Human Pluripotent Stem Cells Generates Transplantable Populations of Cone Photoreceptors', *Stem Cell Reports*, 9(3), pp. 820-837.
- Gonzalez-Cordero, A., West, E.L., Pearson, R.A., Duran, Y., Carvalho, L.S., Chu, C.J., Naeem, A., Blackford, S.J., Georgiadis, A., Lakowski, J., Hubank, M., Smith, A.J., Bainbridge, J.W., Sowden, J.C. and Ali, R.R. (2013) 'Photoreceptor precursors derived from three-dimensional embryonic stem cell cultures integrate and mature within adult degenerate retina', *Nat Biotechnol*, 31(8), pp. 741-7.
- Gordon, M.K. and Hahn, R.A. (2010) 'Collagens', *Cell Tissue Res*, 339(1), pp. 247-57.
- Gross, J.M., Perkins, B.D., Amsterdam, A., Egana, A., Darland, T., Matsui, J.I., Sciascia, S., Hopkins, N. and Dowling, J.E. (2005) 'Identification of zebrafish insertional mutants with defects in visual system development and function', *Genetics*, 170(1), pp. 245-61.
- Groulx, J.F., Gagne, D., Benoit, Y.D., Martel, D., Basora, N. and Beaulieu, J.F. (2011) 'Collagen VI is a basement membrane component that regulates epithelial cell-fibronectin interactions', *Matrix Biol*, 30(3), pp. 195-206.
- Hallam, D., Hilgen, G., Dorgau, B., Zhu, L., Yu, M., Bojic, S., Hewitt, P., Schmitt, M., Uteng, M., Kustermann, S., Steel, D., Nicholds, M., Thomas, R., Treumann, A., Porter, A., Sernagor, E., Armstrong, L. and Lako, M. (2018) 'Human induced pluripotent stem cells generate light responsive retinal organoids with variable and nutrient dependent efficiency', *Stem Cells*.
- Hamel, C. (2006) 'Retinitis pigmentosa', *Orphanet J Rare Dis*, 1, p. 40.
- Harburger, D.S. and Calderwood, D.A. (2009) 'Integrin signalling at a glance', *J Cell Sci*, 122(Pt 2), pp. 159-63.
- Hausman, R.E. (2007) 'Ocular extracellular matrices in development', *Prog Retin Eye Res*, 26(2), pp. 162-88.

- Hedrich, J., Lottaz, D., Meyer, K., Yiallouros, I., Jahnen-Dechent, W., Stocker, W. and Becker-Pauly, C. (2010) 'Fetuin-A and cystatin C are endogenous inhibitors of human meprin metalloproteases', *Biochemistry*, 49(39), pp. 8599-607.
- Hendrickson, A. (2016) 'Development of Retinal Layers in Prenatal Human Retina', *Am J Ophthalmol*, 161, pp. 29-35.e1.
- Hendrickson, A. and Drucker, D. (1992) 'The development of parafoveal and mid-peripheral human retina', *Behavioural Brain Research*, 49(1), pp. 21-31.
- Hendrickson, A. and Zhang, C. (2017) 'Development of cone photoreceptors and their synapses in the human and monkey fovea', *J Comp Neurol*.
- Hevner, R.F. (2000) 'Development of connections in the human visual system during fetal mid-gestation: a DiI-tracing study', *J Neuropathol Exp Neurol*, 59(5), pp. 385-92.
- Hewitson, T.D. and Darby, I.A. (2009) *Histology Protocols*. Humana Press.
- Heydarkhan-Hagvall, S., Schenke-Layland, K., Yang, J.Q., Heydarkhan, S., Xu, Y., Zuk, P.A., MacLellan, W.R. and Beygui, R.E. (2008) 'Human adipose stem cells: a potential cell source for cardiovascular tissue engineering', *Cells Tissues Organs*, 187(4), pp. 263-74.
- Hilgen, G., Pirmoradian, S., Pamplona, D., Kornprobst, P., Cessac, B., Hennig, M.H. and Sernagor, E. (2017a) 'Pan-retinal characterisation of Light Responses from Ganglion Cells in the Developing Mouse Retina', *Sci Rep*, 7, p. 42330.
- Hilgen, G., Sorbaro, M., Pirmoradian, S., Muthmann, J.O., Kepiro, I.E., Ullo, S., Ramirez, C.J., Puente Encinas, A., Maccione, A., Berdondini, L., Murino, V., Sona, D., Cella Zanacchi, F., Sernagor, E. and Hennig, M.H. (2017b) 'Unsupervised Spike Sorting for Large-Scale, High-Density Multielectrode Arrays', *Cell Rep*, 18(10), pp. 2521-2532.
- Hirami, Y., Osakada, F., Takahashi, K., Okita, K., Yamanaka, S., Ikeda, H., Yoshimura, N. and Takahashi, M. (2009) 'Generation of retinal cells from mouse and human induced pluripotent stem cells', *Neurosci Lett*, 458(3), pp. 126-31.
- Holley, R.J., Meade, K.A. and Merry, C.L. (2014) 'Using embryonic stem cells to understand how glycosaminoglycans regulate differentiation', *Biochem Soc Trans*, 42(3), pp. 689-95.
- Hollyfield, J.G. (1999) 'Hyaluronan and the functional organization of the interphotoreceptor matrix', *Invest Ophthalmol Vis Sci*, 40(12), pp. 2767-9.
- Hoshino, A., Ratnapriya, R., Brooks, M.J., Chaitankar, V., Wilken, M.S., Zhang, C., Starostik, M.R., Gieser, L., La Torre, A., Nishio, M., Bates, O., Walton, A., Bermingham-McDonogh, O., Glass, I.A., Wong, R.O.L., Swaroop, A. and Reh, T.A. (2017) 'Molecular Anatomy of the Developing Human Retina', *Dev Cell*, 43(6), pp. 763-779.e4.
- Hsiung, J., Zhu, D., Rodriguez, A. and Hinton, D.R. (2015) 'Retinal Pigment Epithelial Cell Conditioned Medium Enhances the Yield of RPE Cells Differentiated from Human Embryonic Stem Cells', *Journal of Clinical & Experimental Pathology*, 5(2), p. 216.
- Hu, J. and Bok, D. (2001) 'A cell culture medium that supports the differentiation of human retinal pigment epithelium into functionally polarized monolayers', *Mol Vis*, 7, pp. 14-9.
- Huang, S. and Ingber, D.E. (1999) 'The structural and mechanical complexity of cell-growth control', *Nat Cell Biol*, 1(5), pp. E131-8.
- Humphries, J.D., Byron, A. and Humphries, M.J. (2006) 'Integrin ligands at a glance', *J Cell Sci*, 119(Pt 19), pp. 3901-3.
- Hunter, D.D. and Brunken, W.J. (1997) 'Beta 2 laminins modulate neuronal phenotype in the rat retina', *Mol Cell Neurosci*, 10(1-2), pp. 7-15.

- Hunter, D.D., Murphy, M.D., Olsson, C.V. and Brunken, W.J. (1992) 'S-laminin expression in adult and developing retinae: a potential cue for photoreceptor morphogenesis', *Neuron*, 8(3), pp. 399-413.
- Hynes, R.O. (2002) 'Integrins: bidirectional, allosteric signaling machines', *Cell*, 110(6), pp. 673-87.
- Hynes, R.O. (2008) 'US policies on human embryonic stem cells', *Nat Rev Mol Cell Biol*, 9(12), pp. 993-7.
- Hynes, R.O. (2009) 'The extracellular matrix: not just pretty fibrils', *Science*, 326(5957), pp. 1216-9.
- Hynes, R.O. and Naba, A. (2012) 'Overview of the matrisome--an inventory of extracellular matrix constituents and functions', *Cold Spring Harb Perspect Biol*, 4(1), p. a004903.
- Inatani, M., Honjo, M., Oohira, A., Kido, N., Otori, Y., Tano, Y., Honda, Y. and Tanihara, H. (2002) 'Spatiotemporal expression patterns of N-syndecan, a transmembrane heparan sulfate proteoglycan, in developing retina', *Invest Ophthalmol Vis Sci*, 43(5), pp. 1616-21.
- Inatani, M. and Tanihara, H. (2002) 'Proteoglycans in retina', *Prog Retin Eye Res*, 21(5), pp. 429-47.
- Inoue, Y., Yoneda, M., Miyaishi, O., Iwaki, M. and Zako, M. (2009) 'Hyaluronan dynamics during retinal development', *Brain Res*, 1256, pp. 55-60.
- Ishikawa, M., Sawada, Y. and Yoshitomi, T. (2015) 'Structure and function of the interphotoreceptor matrix surrounding retinal photoreceptor cells', *Exp Eye Res*, 133, pp. 3-18.
- Jayakody, S.A., Gonzalez-Cordero, A., Ali, R.R. and Pearson, R.A. (2015) 'Cellular strategies for retinal repair by photoreceptor replacement', *Prog Retin Eye Res*, 46, pp. 31-66.
- Jean, D., Ewan, K. and Gruss, P. (1998) 'Molecular regulators involved in vertebrate eye development', *Mech Dev*, 76(1-2), pp. 3-18.
- Ji, J., Zhang, D., Wei, W., Shen, B., Zhang, Y., Wang, Y., Tang, Z., Ni, N., Sun, H., Liu, J., Fan, X. and Gu, P. (2018) 'Decellularized matrix of adipose-derived mesenchymal stromal cells enhanced retinal progenitor cell proliferation via the Akt/Erk pathway and neuronal differentiation', *Cytotherapy*, 20(1), pp. 74-86.
- Jiang, C., Klassen, H., Zhang, X. and Young, M. (2010) 'Laser injury promotes migration and integration of retinal progenitor cells into host retina', *Mol Vis*, 16, pp. 983-90.
- Johnson, M.S., Lu, N., Denessiouk, K., Heino, J. and Gullberg, D. (2009) 'Integrins during evolution: evolutionary trees and model organisms', *Biochim Biophys Acta*, 1788(4), pp. 779-89.
- Kaempf, S., Walter, P., Salz, A.K. and Thumann, G. (2008) 'Novel organotypic culture model of adult mammalian neurosensory retina in co-culture with retinal pigment epithelium', *J Neurosci Methods*, 173(1), pp. 47-58.
- Kaewkhaw, R., Kaya Koray, D., Brooks, M., Homma, K., Zou, J., Chaitankar, V., Rao, M. and Swaroop, A. (2015) 'Transcriptome Dynamics of Developing Photoreceptors in Three‐Dimensional Retina Cultures Recapitulates Temporal Sequence of Human Cone and Rod Differentiation Revealing Cell Surface Markers and Gene Networks', *STEM CELLS*, 33(12), pp. 3504-3518.
- Karakousis, P.C., John, S.K., Behling, K.C., Surace, E.M., Smith, J.E., Hendrickson, A., Tang, W.X., Bennett, J. and Milam, A.H. (2001) 'Localization of pigment epithelium derived factor (PEDF) in developing and adult human ocular tissues', *Mol Vis*, 7, pp. 154-63.

- Keenan, T.D., Clark, S.J., Unwin, R.D., Ridge, L.A., Day, A.J. and Bishop, P.N. (2012) 'Mapping the differential distribution of proteoglycan core proteins in the adult human retina, choroid, and sclera', *Invest Ophthalmol Vis Sci*, 53(12), pp. 7528-38.
- Keung, A.J., Asuri, P., Kumar, S. and Schaffer, D.V. (2012) 'Soft microenvironments promote the early neurogenic differentiation but not self-renewal of human pluripotent stem cells', *Integr Biol (Camb)*, 4(9), pp. 1049-58.
- Khokha, R., Murthy, A. and Weiss, A. (2013) 'Metalloproteinases and their natural inhibitors in inflammation and immunity', *Nat Rev Immunol*, 13(9), pp. 649-65.
- Kim, S.H., Turnbull, J. and Guimond, S. (2011) 'Extracellular matrix and cell signalling: the dynamic cooperation of integrin, proteoglycan and growth factor receptor', *J Endocrinol*, 209(2), pp. 139-51.
- Klimanskaya, I., Hipp, J., Rezai, K.A., West, M., Atala, A. and Lanza, R. (2004) 'Derivation and comparative assessment of retinal pigment epithelium from human embryonic stem cells using transcriptomics', *Cloning Stem Cells*, 6(3), pp. 217-45.
- Kloeckener-Gruissem, B., Neidhardt, J., Magyar, I., Plauchu, H., Zech, J.C., Morle, L., Palmer-Smith, S.M., Macdonald, M.J., Nas, V., Fry, A.E. and Berger, W. (2013) 'Novel VCAN mutations and evidence for unbalanced alternative splicing in the pathogenesis of Wagner syndrome', *Eur J Hum Genet*, 21(3), pp. 352-6.
- Köberlein, J., Beifus, K., Schaffert, C. and Finger, R.P. (2013) 'The economic burden of visual impairment and blindness: a systematic review', *BMJ Open*, 3(11).
- Kolomeyer, A.M., Sugino, I.K. and Zarbin, M.A. (2011) 'Characterization of conditioned media collected from cultured adult versus fetal retinal pigment epithelial cells', *Invest Ophthalmol Vis Sci*, 52(8), pp. 5973-86.
- Kolomeyer, A.M., Sugino, I.K. and Zarbin, M.A. (2013) 'Characterization of the effects of retinal pigment epithelium-conditioned media on porcine and aged human retina', *Graefes Arch Clin Exp Ophthalmol*, 251(6), pp. 1515-28.
- Kong, L., Fry, M., Al-Samarraie, M., Gilbert, C. and Steinkuller, P.G. (2012) 'An update on progress and the changing epidemiology of causes of childhood blindness worldwide', *J aapos*, 16(6), pp. 501-7.
- Kuehn, M.H. and Hageman, G.S. (1999) 'Expression and characterization of the IPM 150 gene (IMPG1) product, a novel human photoreceptor cell-associated chondroitin-sulfate proteoglycan', *Matrix Biol*, 18(5), pp. 509-18.
- Kuehn, M.H., Wietecki, D.T. and Hageman, G.S. (2000) 'Molecular characterization of the murine orthologue of the human retinal proteoglycan IPM 150', *Mol Vis*, 6, pp. 148-56.
- Kundu, J., Michaelson, A., Talbot, K., Baranov, P., Young, M.J. and Carrier, R.L. (2016) 'Decellularized retinal matrix: Natural platforms for human retinal progenitor cell culture', *Acta Biomater*, 31, pp. 61-70.
- Kuwahara, A., Ozone, C., Nakano, T., Saito, K., Eiraku, M. and Sasai, Y. (2015) 'Generation of a ciliary margin-like stem cell niche from self-organizing human retinal tissue', *Nat Commun*, 6, p. 6286.
- Kwan, K.M. (2014) 'Coming into focus: The role of extracellular matrix in vertebrate optic cup morphogenesis', *Dev Dyn*, 243(10), pp. 1242-8.
- Lamba, D.A., Gust, J. and Reh, T.A. (2009) 'Transplantation of human embryonic stem cell-derived photoreceptors restores some visual function in Crx-deficient mice', *Cell Stem Cell*, 4(1), pp. 73-9.
- Lamba, D.A., Karl, M.O., Ware, C.B. and Reh, T.A. (2006) 'Efficient generation of retinal progenitor cells from human embryonic stem cells', *Proc Natl Acad Sci U S A*, 103(34), pp. 12769-74.
- Lan, M.A., Gersbach, C.A., Michael, K.E., Keselowsky, B.G. and Garcia, A.J. (2005) 'Myoblast proliferation and differentiation on fibronectin-coated self assembled

monolayers presenting different surface chemistries', *Biomaterials*, 26(22), pp. 4523-31.
- LaVail, M.M., Pinto, L.H. and Yasumura, D. (1981) 'The interphotoreceptor matrix in rats with inherited retinal dystrophy', *Invest Ophthalmol Vis Sci*, 21(5), pp. 658-68.
- Lazarus, H.S. and Hageman, G.S. (1992) 'Xyloside-induced disruption of interphotoreceptor matrix proteoglycans results in retinal detachment', *Invest Ophthalmol Vis Sci*, 33(2), pp. 364-76.
- Lazarus, H.S., Sly, W.S., Kyle, J.W. and Hageman, G.S. (1993) 'Photoreceptor degeneration and altered distribution of interphotoreceptor matrix proteoglycans in the mucopolysaccharidosis VII mouse', *Exp Eye Res*, 56(5), pp. 531-41.
- LeBleu, V.S., Macdonald, B. and Kalluri, R. (2007) 'Structure and function of basement membranes', *Exp Biol Med (Maywood)*, 232(9), pp. 1121-9.
- Leitinger, B. and Hohenester, E. (2007) 'Mammalian collagen receptors', *Matrix Biol*, 26(3), pp. 146-55.
- Libby, R.T., Champliaud, M.F., Claudepierre, T., Xu, Y., Gibbons, E.P., Koch, M., Burgeson, R.E., Hunter, D.D. and Brunken, W.J. (2000) 'Laminin expression in adult and developing retinae: evidence of two novel CNS laminins', *J Neurosci*, 20(17), pp. 6517-28.
- Libby, R.T., Lavallee, C.R., Balkema, G.W., Brunken, W.J. and Hunter, D.D. (1999) 'Disruption of laminin beta2 chain production causes alterations in morphology and function in the CNS', *J Neurosci*, 19(21), pp. 9399-411.
- Llonch, S., Carido, M. and Ader, M. (2018) 'Organoid technology for retinal repair', *Dev Biol*, 433(2), pp. 132-143.
- Lowe, A., Harris, R., Bhansali, P., Cvekl, A. and Liu, W. (2016) 'Intercellular Adhesion-Dependent Cell Survival and ROCK-Regulated Actomyosin-Driven Forces Mediate Self-Formation of a Retinal Organoid', *Stem Cell Reports*, 6(5), pp. 743-756.
- Lu, P., Takai, K., Weaver, V.M. and Werb, Z. (2011) 'Extracellular matrix degradation and remodeling in development and disease', *Cold Spring Harb Perspect Biol*, 3(12).
- Lund, R.D., Wang, S., Klimanskaya, I., Holmes, T., Ramos-Kelsey, R., Lu, B., Girman, S., Bischoff, N., Sauve, Y. and Lanza, R. (2006) 'Human embryonic stem cell-derived cells rescue visual function in dystrophic RCS rats', *Cloning Stem Cells*, 8(3), pp. 189-99.
- Manes, G., Meunier, I., Avila-Fernandez, A., Banfi, S., Le Meur, G., Zanlonghi, X., Corton, M., Simonelli, F., Brabet, P., Labesse, G., Audo, I., Mohand-Said, S., Zeitz, C., Sahel, J.A., Weber, M., Dollfus, H., Dhaenens, C.M., Allorge, D., De Baere, E., Koenekoop, R.K., Kohl, S., Cremers, F.P., Hollyfield, J.G., Senechal, A., Hebrard, M., Bocquet, B., Ayuso Garcia, C. and Hamel, C.P. (2013) 'Mutations in IMPG1 cause vitelliform macular dystrophies', *Am J Hum Genet*, 93(3), pp. 571-8.
- Margolis, R. and Margolis, R. (1983) 'Glycoproteins and Proteoglycans', in Lajtha, A. (ed.) *Handbook of Neurochemistry*. Springer US, pp. 177-204.
- Matsui, T., Raya, A., Callol-Massot, C., Kawakami, Y., Oishi, I., Rodriguez-Esteban, C. and Izpisua Belmonte, J.C. (2007) 'miles-apart-Mediated regulation of cell-fibronectin interaction and myocardial migration in zebrafish', *Nat Clin Pract Cardiovasc Med*, 4 Suppl 1, pp. S77-82.
- May, C.A. (2012) 'Distribution of nidogen in the murine eye and ocular phenotype of the nidogen-1 knockout mouse', *ISRN Ophthalmol*, 2012, p. 378641.
- McLelland, B.T., Lin, B., Mathur, A., Aramant, R.B., Thomas, B.B., Nistor, G., Keirstead, H.S. and Seiler, M.J. (2018) 'Transplanted hESC-Derived Retina Organoid Sheets Differentiate, Integrate, and Improve Visual Function in Retinal Degenerate Rats', *Investigative Ophthalmology & Visual Science*, 59(6), pp. 2586-2603.

- McLenachan, S., Hao, E., Zhang, D., Zhang, L., Edel, M. and Chen, F. (2017) 'Bioengineered Bruch's-like extracellular matrix promotes retinal pigment epithelial differentiation', *Biochemistry and Biophysics Reports*, 10, pp. 178-185.
- Medberry, C.J., Crapo, P.M., Siu, B.F., Carruthers, C.A., Wolf, M.T., Nagarkar, S.P., Agrawal, V., Jones, K.E., Kelly, J., Johnson, S.A., Velankar, S.S., Watkins, S.C., Modo, M. and Badylak, S.F. (2013) 'Hydrogels derived from central nervous system extracellular matrix', *Biomaterials*, 34(4), pp. 1033-40.
- Mehat, M.S., Sundaram, V., Ripamonti, C., Robson, A.G., Smith, A.J., Borooah, S., Robinson, M., Rosenthal, A.N., Innes, W., Weleber, R.G., Lee, R.W.J., Crossland, M., Rubin, G.S., Dhillon, B., Steel, D.H.W., Anglade, E., Lanza, R.P., Ali, R.R., Michaelides, M. and Bainbridge, J.W.B. (2018) 'Transplantation of Human Embryonic Stem Cell-Derived Retinal Pigment Epithelial Cells in Macular Degeneration', *Ophthalmology*.
- Melguizo-Sanchis, D., Xu, Y., Taheem, D., Yu, M., Tilgner, K., Barta, T., Gassner, K., Anyfantis, G., Wan, T., Elango, R., Alharthi, S., El-Harouni, A.A., Przyborski, S., Adam, S., Saretzki, G., Samarasinghe, S., Armstrong, L. and Lako, M. (2018) 'iPSC modeling of severe aplastic anemia reveals impaired differentiation and telomere shortening in blood progenitors', *Cell Death Dis*, 9(2), p. 128.
- Mellough, C.B., Collin, J., Khazim, M., White, K., Sernagor, E., Steel, D.H. and Lako, M. (2015) 'IGF-1 Signaling Plays an Important Role in the Formation of Three-Dimensional Laminated Neural Retina and Other Ocular Structures from Human Embryonic Stem Cells', *Stem Cells*.
- Mellough, C.B., Collin, J., Sernagor, E., Wride, N.K., Steel, D.H. and Lako, M. (2014) 'Lab generated retina: realizing the dream', *Vis Neurosci*, 31(4-5), pp. 317-32.
- Mellough, C.B., Sernagor, E., Moreno-Gimeno, I., Steel, D.H. and Lako, M. (2012) 'Efficient stage-specific differentiation of human pluripotent stem cells toward retinal photoreceptor cells', *Stem Cells*, 30(4), pp. 673-86.
- Meyer, J.S., Howden, S.E., Wallace, K.A., Verhoeven, A.D., Wright, L.S., Capowski, E.E., Pinilla, I., Martin, J.M., Tian, S., Stewart, R., Pattnaik, B., Thomson, J.A. and Gamm, D.M. (2011) 'Optic vesicle-like structures derived from human pluripotent stem cells facilitate a customized approach to retinal disease treatment', *Stem Cells*, 29(8), pp. 1206-18.
- Miller, C.G., Budoff, G., Prenner, J.L. and Schwarzbauer, J.E. (2017) 'Minireview: Fibronectin in retinal disease', *Exp Biol Med (Maywood)*, 242(1), pp. 1-7.
- Miura, Y., Klettner, A., Noelle, B., Hasselbach, H. and Roider, J. (2010) 'Change of morphological and functional characteristics of retinal pigment epithelium cells during cultivation of retinal pigment epithelium-choroid perfusion tissue culture', *Ophthalmic Res*, 43(3), pp. 122-33.
- Mjaatvedt, C.H., Yamamura, H., Capehart, A.A., Turner, D. and Markwald, R.R. (1998) 'The Cspg2 gene, disrupted in the hdf mutant, is required for right cardiac chamber and endocardial cushion formation', *Dev Biol*, 202(1), pp. 56-66.
- Moreno-Layseca, P. and Streuli, C.H. (2014) 'Signalling pathways linking integrins with cell cycle progression', *Matrix Biol*, 34, pp. 144-53.
- Mouw, J.K., Ou, G. and Weaver, V.M. (2014) 'Extracellular matrix assembly: a multiscale deconstruction', *Nat Rev Mol Cell Biol*, 15(12), pp. 771-85.
- Muthmann, J.O., Amin, H., Sernagor, E., Maccione, A., Panas, D., Berdondini, L., Bhalla, U.S. and Hennig, M.H. (2015) 'Spike Detection for Large Neural Populations Using High Density Multielectrode Arrays', *Front Neuroinform*, 9, p. 28.
- Nag, T.C. and Wadhwa, S. (2006) 'Morphological and Neurochemical Development of the Human Neural Retina', *Neuroembryology and Aging*, 4(1-2), pp. 19-30.

- Nakano, T., Ando, S., Takata, N., Kawada, M., Muguruma, K., Sekiguchi, K., Saito, K., Yonemura, S., Eiraku, M. and Sasai, Y. (2012) 'Self-formation of optic cups and storable stratified neural retina from human ESCs', *Cell Stem Cell*, 10(6), pp. 771-85.
- Narayanan, K. and Wadhwa, S. (1998) 'Photoreceptor morphogenesis in the human retina: a scanning electron microscopic study', *Anat Rec*, 252(1), pp. 133-9.
- Narsinh, K.H., Plews, J. and Wu, J.C. (2011) 'Comparison of human induced pluripotent and embryonic stem cells: fraternal or identical twins?', *Mol Ther*, 19(4), pp. 635-8.
- Nichols, J. and Smith, A. (2009) 'Naive and primed pluripotent states', *Cell Stem Cell*, 4(6), pp. 487-92.
- Nishina, S., Hirakata, A., Hida, T., Sawa, H. and Azuma, N. (1997) 'CD44 expression in the developing human retina', *Graefes Arch Clin Exp Ophthalmol*, 235(2), pp. 92-6.
- O'Rahilly, R. (1975) 'The prenatal development of the human eye', *Exp Eye Res*, 21(2), pp. 93-112.
- Olberding, J.E., Thouless, M.D., Arruda, E.M. and Garikipati, K. (2010) 'The non-equilibrium thermodynamics and kinetics of focal adhesion dynamics', *PLoS One*, 5(8), p. e12043.
- Oltean, A., Huang, J., Beebe, D.C. and Taber, L.A. (2016) 'Tissue growth constrained by extracellular matrix drives invagination during optic cup morphogenesis', *Biomech Model Mechanobiol*, 15(6), pp. 1405-1421.
- Oner, A. (2018) 'Stem Cell Treatment in Retinal Diseases: Recent Developments', *Turk J Ophthalmol*, 48(1), pp. 33-38.
- Osakada, F., Ikeda, H., Mandai, M., Wataya, T., Watanabe, K., Yoshimura, N., Akaike, A., Sasai, Y. and Takahashi, M. (2008) 'Toward the generation of rod and cone photoreceptors from mouse, monkey and human embryonic stem cells', *Nat Biotechnol*, 26(2), pp. 215-24.
- Ott, H.C., Clippinger, B., Conrad, C., Schuetz, C., Pomerantseva, I., Ikonomou, L., Kotton, D. and Vacanti, J.P. (2010) 'Regeneration and orthotopic transplantation of a bioartificial lung', *Nat Med*, 16(8), pp. 927-33.
- Ott, H.C., Matthiesen, T.S., Goh, S.K., Black, L.D., Kren, S.M., Netoff, T.I. and Taylor, D.A. (2008) 'Perfusion-decellularized matrix: using nature's platform to engineer a bioartificial heart', *Nat Med*, 14(2), pp. 213-21.
- Ovando-Roche, P., West, E.L., Branch, M.J., Sampson, R.D., Fernando, M., Munro, P., Georgiadis, A., Rizzi, M., Kloc, M., Naeem, A., Ribeiro, J., Smith, A.J., Gonzalez-Cordero, A. and Ali, R.R. (2018) 'Use of bioreactors for culturing human retinal organoids improves photoreceptor yields', *Stem Cell Research & Therapy*, 9(1), p. 156.
- Petersen, T.H., Calle, E.A., Zhao, L., Lee, E.J., Gui, L., Raredon, M.B., Gavrilov, K., Yi, T., Zhuang, Z.W., Breuer, C., Herzog, E. and Niklason, L.E. (2010) 'Tissue-engineered lungs for in vivo implantation', *Science*, 329(5991), pp. 538-41.
- Petty, H.R., Elner, V.M., Kawaji, T., Clark, A., Thompson, D. and Yang, D.L. (2010) 'A facile method for immunofluorescence microscopy of highly autofluorescent human retinal sections using nanoparticles with large Stokes shifts', *J Neurosci Methods*, 191(2), pp. 222-6.
- Pinzon-Duarte, G., Daly, G., Li, Y.N., Koch, M. and Brunken, W.J. (2010) 'Defective formation of the inner limiting membrane in laminin beta2- and gamma3-null mice produces retinal dysplasia', *Invest Ophthalmol Vis Sci*, 51(3), pp. 1773-82.
- Ponce Márquez, S., Martínez, V.S., McIntosh Ambrose, W., Wang, J., Gantxegui, N.G., Schein, O. and Elisseeff, J. (2009) 'Decellularization of bovine corneas for tissue engineering applications', *Acta Biomaterialia*, 5(6), pp. 1839-1847.

- Popp, S., Maurel, P., Andersen, J.S. and Margolis, R.U. (2004) 'Developmental changes of aggrecan, versican and neurocan in the retina and optic nerve', *Exp Eye Res*, 79(3), pp. 351-6.
- Poschl, E., Schlotzer-Schrehardt, U., Brachvogel, B., Saito, K., Ninomiya, Y. and Mayer, U. (2004) 'Collagen IV is essential for basement membrane stability but dispensable for initiation of its assembly during early development', *Development*, 131(7), pp. 1619-28.
- Prowse, A.B., Chong, F., Gray, P.P. and Munro, T.P. (2011) 'Stem cell integrins: implications for ex-vivo culture and cellular therapies', *Stem Cell Res*, 6(1), pp. 1-12.
- Rago, R., Mitchen, J. and Wilding, G. (1990) 'DNA fluorometric assay in 96-well tissue culture plates using Hoechst 33258 after cell lysis by freezing in distilled water', *Anal Biochem*, 191(1), pp. 31-4.
- Ramsden, C.M., Powner, M.B., Carr, A.J., Smart, M.J., da Cruz, L. and Coffey, P.J. (2013) 'Stem cells in retinal regeneration: past, present and future', *Development*, 140(12), pp. 2576-85.
- Rashid, S.T. and Vallier, L. (2010) 'Induced pluripotent stem cells--alchemist's tale or clinical reality?', *Expert Rev Mol Med*, 12, p. 25.
- Raymond, S.M. and Jackson, I.J. (1995) 'The retinal pigmented epithelium is required for development and maintenance of the mouse neural retina', *Current Biology*, 5(11), pp. 1286-1295.
- Reinhard, J., Joachim, S.C. and Faissner, A. (2015) 'Extracellular matrix remodeling during retinal development', *Exp Eye Res*, 133, pp. 132-40.
- Rhodes, R.H. (1979) 'A light microscopic study of the developing human neural retina', *Am J Anat*, 154(2), pp. 195-209.
- Robinton, D.A. and Daley, G.Q. (2012) 'The promise of induced pluripotent stem cells in research and therapy', *Nature*, 481(7381), pp. 295-305.
- Rothschild, P.R., Audo, I., Nedelec, B., Ghiotti, T., Brezin, A.P., Monin, C. and Valleix, S. (2013) 'De novo splice mutation in the versican gene in a family with Wagner syndrome', *JAMA Ophthalmol*, 131(6), pp. 805-7.
- Rowland, T.J., Blaschke, A.J., Buchholz, D.E., Hikita, S.T., Johnson, L.V. and Clegg, D.O. (2013) 'Differentiation of human pluripotent stem cells to retinal pigmented epithelium in defined conditions using purified extracellular matrix proteins', *J Tissue Eng Regen Med*, 7(8), pp. 642-53.
- Roy, S., Sato, T., Paryani, G. and Kao, R. (2003) 'Downregulation of fibronectin overexpression reduces basement membrane thickening and vascular lesions in retinas of galactose-fed rats', *Diabetes*, 52(5), pp. 1229-34.
- Rozario, T. and DeSimone, D.W. (2010) 'The extracellular matrix in development and morphogenesis: a dynamic view', *Dev Biol*, 341(1), pp. 126-40.
- Sackett, S.D., Tremmel, D.M., Ma, F., Feeney, A.K., Maguire, R.M., Brown, M.E., Zhou, Y., Li, X., O'Brien, C., Li, L., Burlingham, W.J. and Odorico, J.S. (2018) 'Extracellular matrix scaffold and hydrogel derived from decellularized and delipidized human pancreas', *Scientific Reports*, 8(1), p. 10452.
- Saghizadeh, M., Gribanova, Y., Akhmedov, N.B. and Farber, D.B. (2011) 'ZBED4, a cone and Muller cell protein in human retina, has a different cellular expression in mouse', *Mol Vis*, 17, pp. 2011-8.
- Sarrazin, S., Lamanna, W.C. and Esko, J.D. (2011) 'Heparan sulfate proteoglycans', *Cold Spring Harb Perspect Biol*, 3(7).
- Sasai, Y., Eiraku, M. and Suga, H. (2012) 'In vitro organogenesis in three dimensions: self-organising stem cells', *Development*, 139(22), pp. 4111-21.

- Savige, J., Sheth, S., Leys, A., Nicholson, A., Mack, H.G. and Colville, D. (2015) 'Ocular features in Alport syndrome: pathogenesis and clinical significance', *Clin J Am Soc Nephrol*, 10(4), pp. 703-9.
- Schaefer, L. and Schaefer, R.M. (2010) 'Proteoglycans: from structural compounds to signaling molecules', *Cell Tissue Res*, 339(1), pp. 237-46.
- Schenke-Layland, K., Angelis, E., Rhodes, K.E., Heydarkhan-Hagvall, S., Mikkola, H.K. and Maclellan, W.R. (2007) 'Collagen IV induces trophoectoderm differentiation of mouse embryonic stem cells', *Stem Cells*, 25(6), pp. 1529-38.
- Schenke-Layland, K., Rhodes, K.E., Angelis, E., Butylkova, Y., Heydarkhan-Hagvall, S., Gekas, C., Zhang, R., Goldhaber, J.I., Mikkola, H.K., Plath, K. and MacLellan, W.R. (2008) 'Reprogrammed mouse fibroblasts differentiate into cells of the cardiovascular and hematopoietic lineages', *Stem Cells*, 26(6), pp. 1537-46.
- Schmidt, S. and Friedl, P. (2010) 'Interstitial cell migration: integrin-dependent and alternative adhesion mechanisms', *Cell Tissue Res*, 339(1), pp. 83-92.
- Schnell, S.A., Staines, W.A. and Wessendorf, M.W. (1999) 'Reduction of lipofuscin-like autofluorescence in fluorescently labeled tissue', *J Histochem Cytochem*, 47(6), pp. 719-30.
- Schwartz, M.A. (2010) 'Integrins and extracellular matrix in mechanotransduction', *Cold Spring Harb Perspect Biol*, 2(12), p. a005066.
- Shirai, H., Mandai, M., Matsushita, K., Kuwahara, A., Yonemura, S., Nakano, T., Assawachananont, J., Kimura, T., Saito, K., Terasaki, H., Eiraku, M., Sasai, Y. and Takahashi, M. (2016) 'Transplantation of human embryonic stem cell-derived retinal tissue in two primate models of retinal degeneration', *Proc Natl Acad Sci U S A*, 113(1), pp. E81-90.
- Singh, D., Wang, S.B., Xia, T., Tainsh, L., Ghiassi-Nejad, M., Xu, T., Peng, S., Adelman, R.A. and Rizzolo, L.J. (2018) 'A biodegradable scaffold enhances differentiation of embryonic stem cells into a thick sheet of retinal cells', *Biomaterials*, 154, pp. 158-168.
- Singh, R., Shen, W., Kuai, D., Martin, J.M., Guo, X., Smith, M.A., Perez, E.T., Phillips, M.J., Simonett, J.M., Wallace, K.A., Verhoeven, A.D., Capowski, E.E., Zhang, X., Yin, Y., Halbach, P.J., Fishman, G.A., Wright, L.S., Pattnaik, B.R. and Gamm, D.M. (2013) 'iPS cell modeling of Best disease: insights into the pathophysiology of an inherited macular degeneration', *Hum Mol Genet*, 22(3), pp. 593-607.
- Sivak, J.M. and Fini, M.E. (2002) 'MMPs in the eye: emerging roles for matrix metalloproteinases in ocular physiology', *Prog Retin Eye Res*, 21(1), pp. 1-14.
- Smith, M.L., Gourdon, D., Little, W.C., Kubow, K.E., Eguiluz, R.A., Luna-Morris, S. and Vogel, V. (2007) 'Force-induced unfolding of fibronectin in the extracellular matrix of living cells', *PLoS Biol*, 5(10), p. e268.
- Song, J.J., Guyette, J.P., Gilpin, S.E., Gonzalez, G., Vacanti, J.P. and Ott, H.C. (2013) 'Regeneration and experimental orthotopic transplantation of a bioengineered kidney', *Nat Med*, 19(5), pp. 646-51.
- Stenkamp, D.L., Calderwood, J.L., Van Niel, E.E., Daniels, L.M. and Gonzalez-Fernandez, F. (2005) 'The interphotoreceptor retinoid-binding protein (IRBP) of the chicken (Gallus gallus domesticus)', *Mol Vis*, 11, pp. 833-45.
- Stenzel, D., Lundkvist, A., Sauvaget, D., Busse, M., Graupera, M., van der Flier, A., Wijelath, E.S., Murray, J., Sobel, M., Costell, M., Takahashi, S., Fassler, R., Yamaguchi, Y., Gutmann, D.H., Hynes, R.O. and Gerhardt, H. (2011) 'Integrin-dependent and -independent functions of astrocytic fibronectin in retinal angiogenesis', *Development*, 138(20), pp. 4451-63.

- Strauss, O. (2005) 'The retinal pigment epithelium in visual function', *Physiol Rev*, 85(3), pp. 845-81.
- Streuli, C. (1999) 'Extracellular matrix remodelling and cellular differentiation', *Curr Opin Cell Biol*, 11(5), pp. 634-40.
- Streuli, C.H. (2009) 'Integrins and cell-fate determination', *J Cell Sci*, 122(Pt 2), pp. 171-7.
- Sun, D., Liu, Y., Wang, H., Deng, F., Zhang, Y., Zhao, S., Ma, X., Wu, H. and Sun, G. (2018) 'Novel decellularized liver matrix-alginate hybrid gel beads for the 3D culture of hepatocellular carcinoma cells', *International Journal of Biological Macromolecules*, 109, pp. 1154-1163.
- Sun, Y., Yu, H., Zheng, D., Cao, Q., Wang, Y., Harris, D. and Wang, Y. (2011) 'Sudan black B reduces autofluorescence in murine renal tissue', *Arch Pathol Lab Med*, 135(10), pp. 1335-42.
- Sung, C.H. and Chuang, J.Z. (2010) 'The cell biology of vision', *J Cell Biol*, 190(6), pp. 953-63.
- Swaroop, A., Kim, D. and Forrest, D. (2010) 'Transcriptional regulation of photoreceptor development and homeostasis in the mammalian retina', *Nat Rev Neurosci*, 11(8), pp. 563-76.
- Taipale, J. and Keski-Oja, J. (1997) 'Growth factors in the extracellular matrix', *Faseb j*, 11(1), pp. 51-9.
- Takahashi, K., Tanabe, K., Ohnuki, M., Narita, M., Ichisaka, T., Tomoda, K. and Yamanaka, S. (2007) 'Induction of pluripotent stem cells from adult human fibroblasts by defined factors', *Cell*, 131(5), pp. 861-72.
- Takahashi, K. and Yamanaka, S. (2006) 'Induction of pluripotent stem cells from mouse embryonic and adult fibroblast cultures by defined factors', *Cell*, 126(4), pp. 663-76.
- Takata, N., Abbey, D., Fiore, L., Acosta, S., Feng, R., Gil, H.J., Lavado, A., Geng, X., Interiano, A., Neale, G., Eiraku, M., Sasai, Y. and Oliver, G. (2017) 'An Eye Organoid Approach Identifies Six3 Suppression of R-spondin 2 as a Critical Step in Mouse Neuroretina Differentiation', *Cell Reports*, 21(6), pp. 1534-1549.
- Terman, A. and Brunk, U.T. (2004) 'Lipofuscin', *Int J Biochem Cell Biol*, 36(8), pp. 1400-4.
- Tezel, T.H., Del Priore, L.V. and Kaplan, H.J. (2004) 'Reengineering of aged Bruch's membrane to enhance retinal pigment epithelium repopulation', *Invest Ophthalmol Vis Sci*, 45(9), pp. 3337-48.
- Thomson, J.A., Itskovitz-Eldor, J., Shapiro, S.S., Waknitz, M.A., Swiergiel, J.J., Marshall, V.S. and Jones, J.M. (1998) 'Embryonic stem cell lines derived from human blastocysts', *Science*, 282(5391), pp. 1145-7.
- Vigetti, D., Viola, M., Karousou, E., Rizzi, M., Moretto, P., Genasetti, A., Clerici, M., Hascall, V.C., De Luca, G. and Passi, A. (2008) 'Hyaluronan-CD44-ERK1/2 regulate human aortic smooth muscle cell motility during aging', *J Biol Chem*, 283(7), pp. 4448-58.
- Viswanathan, P., Gaskell, T., Moens, N., Culley, O.J., Hansen, D., Gervasio, M.K., Yeap, Y.J. and Danovi, D. (2014) 'Human pluripotent stem cells on artificial microenvironments: a high content perspective', *Front Pharmacol*, 5, p. 150.
- Volkner, M., Zschatzsch, M., Rostovskaya, M., Overall, R.W., Busskamp, V., Anastassiadis, K. and Karl, M.O. (2016) 'Retinal Organoids from Pluripotent Stem Cells Efficiently Recapitulate Retinogenesis', *Stem Cell Reports*, 6(4), pp. 525-538.
- Völkner, M., Zschätzsch, M., Rostovskaya, M., Overall, Rupert W., Busskamp, V., Anastassiadis, K. and Karl, Mike O. (2016) 'Retinal Organoids from Pluripotent Stem Cells Efficiently Recapitulate Retinogenesis', *Stem Cell Reports*, 6(4), pp. 525-538.

- von der Mark, K., Park, J., Bauer, S. and Schmuki, P. (2010) 'Nanoscale engineering of biomimetic surfaces: cues from the extracellular matrix', *Cell Tissue Res*, 339(1), pp. 131-53.
- Votteler, M., Kluger, P.J., Walles, H. and Schenke-Layland, K. (2010) 'Stem cell microenvironments--unveiling the secret of how stem cell fate is defined', *Macromol Biosci*, 10(11), pp. 1302-15.
- Wahlin, K.J., Maruotti, J.A., Sripathi, S.R., Ball, J., Angueyra, J.M., Kim, C., Grebe, R., Li, W., Jones, B.W. and Zack, D.J. (2017) 'Photoreceptor Outer Segment-like Structures in Long-Term 3D Retinas from Human Pluripotent Stem Cells', *Sci Rep*, 7(1), p. 766.
- Waldron, P.V., Di Marco, F., Kruczek, K., Ribeiro, J., Graca, A.B., Hippert, C., Aghaizu, N.D., Kalargyrou, A.A., Barber, A.C., Grimaldi, G., Duran, Y., Blackford, S.J.I., Kloc, M., Goh, D., Zabala Aldunate, E., Sampson, R.D., Bainbridge, J.W.B., Smith, A.J., Gonzalez-Cordero, A., Sowden, J.C., Ali, R.R. and Pearson, R.A. (2018) 'Transplanted Donor- or Stem Cell-Derived Cone Photoreceptors Can Both Integrate and Undergo Material Transfer in an Environment-Dependent Manner', *Stem Cell Reports*.
- Walters, N.J. and Gentleman, E. (2015) 'Evolving insights in cell-matrix interactions: Elucidating how non-soluble properties of the extracellular niche direct stem cell fate', *Acta Biomater*, 11c, pp. 3-16.
- Wang, X., Li, T., Cui, T., Yu, D., Liu, C., Jiang, L., Feng, G., Wang, L., Fu, R., Zhang, X., Hao, J., Wang, Y., Wang, L., Zhou, Q., Li, W. and Hu, B. (2017) 'Human embryonic stem cells contribute to embryonic and extraembryonic lineages in mouse embryos upon inhibition of apoptosis', *Cell Research*, 28, p. 126.
- Wasmeier, C., Hume, A.N., Bolasco, G. and Seabra, M.C. (2008) 'Melanosomes at a glance', *Journal of Cell Science*, 121(24), pp. 3995-3999.
- Watanabe, H., Kimata, K., Line, S., Strong, D., Gao, L.Y., Kozak, C.A. and Yamada, Y. (1994) 'Mouse cartilage matrix deficiency (cmd) caused by a 7 bp deletion in the aggrecan gene', *Nat Genet*, 7(2), pp. 154-7.
- Welby, E., Lakowski, J., Di Foggia, V., Budinger, D., Gonzalez-Cordero, A., Lun, A.T.L., Epstein, M., Patel, A., Cuevas, E., Kruczek, K., Naeem, A., Minneci, F., Hubank, M., Jones, D.T., Marioni, J.C., Ali, R.R. and Sowden, J.C. (2017) 'Isolation and Comparative Transcriptome Analysis of Human Fetal and iPSC-Derived Cone Photoreceptor Cells', *Stem Cell Reports*.
- Wiley, L.A., Burnight, E.R., Songstad, A.E., Drack, A.V., Mullins, R.F., Stone, E.M. and Tucker, B.A. (2015) 'Patient-specific induced pluripotent stem cells (iPSCs) for the study and treatment of retinal degenerative diseases', *Prog Retin Eye Res*, 44, pp. 15-35.
- Wise, S.G. and Weiss, A.S. (2009) 'Tropoelastin', *Int J Biochem Cell Biol*, 41(3), pp. 494-7.
- Wong, W.L., Su, X., Li, X., Cheung, C.M., Klein, R., Cheng, C.Y. and Wong, T.Y. (2014) 'Global prevalence of age-related macular degeneration and disease burden projection for 2020 and 2040: a systematic review and meta-analysis', *Lancet Glob Health*, 2(2), pp. e106-16.
- Wu, J., Okamura, D., Li, M., Suzuki, K., Luo, C., Ma, L., He, Y., Li, Z., Benner, C., Tamura, I., Krause, M.N., Nery, J.R., Du, T., Zhang, Z., Hishida, T., Takahashi, Y., Aizawa, E., Kim, N.Y., Lajara, J., Guillen, P., Campistol, J.M., Esteban, C.R., Ross, P.J., Saghatelian, A., Ren, B., Ecker, J.R. and Izpisua Belmonte, J.C. (2015) 'An alternative pluripotent state confers interspecies chimaeric competency', *Nature*, 521(7552), pp. 316-21.

- Xian, X., Gopal, S. and Couchman, J.R. (2010) 'Syndecans as receptors and organizers of the extracellular matrix', *Cell Tissue Res*, 339(1), pp. 31-46.
- Yu, J., Vodyanik, M.A., Smuga-Otto, K., Antosiewicz-Bourget, J., Frane, J.L., Tian, S., Nie, J., Jonsdottir, G.A., Ruotti, V., Stewart, R., Slukvin, II and Thomson, J.A. (2007) 'Induced pluripotent stem cell lines derived from human somatic cells', *Science*, 318(5858), pp. 1917-20.
- Yuodelis, C. and Hendrickson, A. (1986) 'A qualitative and quantitative analysis of the human fovea during development', *Vision Res*, 26(6), pp. 847-55.
- Zako, M., Shinomura, T., Miyaishi, O., Iwaki, M. and Kimata, K. (1997) 'Transient expression of PG-M/versican, a large chondroitin sulfate proteoglycan in developing chicken retina', *J Neurochem*, 69(5), pp. 2155-61.
- Zhang, X. and Dong, J. (2015) 'Direct comparison of different coating matrix on the hepatic differentiation from adipose-derived stem cells', *Biochem Biophys Res Commun*, 456(4), pp. 938-44.
- Zhang, Y., Zhang, D., Wei, W., Shen, B., Wang, Y., Zhang, Y., Zhang, Y., Ji, J., Sun, H., Luo, M. and Gu, P. (2017) 'Effects of RPE-conditioned medium on the differentiation of hADSCs into RPE cells, and their proliferation and migration', *Exp Ther Med*, 14(4), pp. 3699-3707.
- Zhong, X., Gutierrez, C., Xue, T., Hampton, C., Vergara, M.N., Cao, L.H., Peters, A., Park, T.S., Zambidis, E.T., Meyer, J.S., Gamm, D.M., Yau, K.W. and Canto-Soler, M.V. (2014) 'Generation of three-dimensional retinal tissue with functional photoreceptors from human iPSCs', *Nat Commun*, 5, p. 4047.
- Zhou, X.H., Brakebusch, C., Matthies, H., Oohashi, T., Hirsch, E., Moser, M., Krug, M., Seidenbecher, C.I., Boeckers, T.M., Rauch, U., Buettner, R., Gundelfinger, E.D. and Fassler, R. (2001) 'Neurocan is dispensable for brain development', *Mol Cell Biol*, 21(17), pp. 5970-8.
- Zimmer, C., Labruyere, E., Meas-Yedid, V., Guillen, N. and Olivo-Marin, J.C. (2002) 'Segmentation and tracking of migrating cells in videomicroscopy with parametric active contours: a tool for cell-based drug testing', *IEEE Trans Med Imaging*, 21(10), pp. 1212-21.